

DISSERTATION ZUR ERLANGUNG DES DOKTORGRADES DER FAKULTÄT CHEMIE UND  
PHARMAZIE DER LUDWIG-MAXIMILIANS-UNIVERSITÄT MÜNCHEN

# Chemoselective Silylation of Alcohols Through Lewis Base-catalyzed Reactions

Experimental and Theoretical Studies

Pascal Patschinski

aus

Uelzen, Deutschland

2015



## Erklärung

Diese Dissertation wurde im Sinne von §7 vom 28. November 2011 von Herrn Prof. Dr. Hendrik Zipse betreut.

## Eidesstattliche Versicherung

Diese Dissertation wurde eigenständig und ohne unerlaubte Hilfe erarbeitet.

München, 23.06.2015

Ort, Datum

---

Pascal Patschinski

Dissertation eingereicht am 23.06.2015

1. Gutachter	Prof. Dr. Hendrik Zipse
2. Gutachter	Prof. Dr. Manfred Heuschmann

Mündliche Prüfung am 27.07.2015





*'Either write something worth reading or do something worth writing'*  
(Benjamin Frankling)



## Acknowledgement

Zu Beginn möchte ich Prof. Dr. Hendrik Zipse für die großartige Zeit danken. Er hat es geschafft, neben dem großen chemischen Wissen auch die fundamentalen Techniken im Ringen und Wandern zu vermitteln. Es hat nicht nur viel Spaß gemacht, sondern war im positiven Sinne eine "charakterbildende Maßnahme".

Für die Übernahme des Zweitgutachtens möchte ich mich bei Prof. Dr. Manfred Heuschmann herzlich bedanken.

Ohne Florian Achrainner, Florian Barth, Johnny Hioe, Christoph Lindner, Harish, Julian Helberg, Raman Tandon, Jutta Tumpach, Sandhiya Lakshmanan und Cong Zhang wäre es einfach nur ein Job gewesen, aber ihr habt geschafft, dass ich immer mit Freude ins Labor gekommen bin. Neben den vielen lustigen Momenten in- und außerhalb des Labors und legendären group outings, wird mir vor allem die gute Stimmung während der gesamten Zeit in Erinnerung bleiben. Besonders hervorheben möchte ich hierbei noch die "Zipse residuals", die für fast alle Fragen immer eine mehr oder weniger gute Antwort hatten.

Besonders möchte ich mich bei allen bedanken, die durch Korrekturen und konstruktiver Verbesserungsvorschläge geholfen haben diese Arbeit kontinuierlich zu optimieren. Jutta, Christoph, Stella und Nadja vielen herzlichen Dank für die viele Arbeit, die ihr euch gemacht habt.

Des Weiteren möchte ich mich bei all den Bachelor-Studenten sowie bei den Forschungspraktikanten, namentlich David Voßiek, Angela Metz, Martin Maier, Jutta Tumpach, Sarah Linert, Julia Stanek und Martin Peschel für die gute Arbeit und die lustigen Momente während ihrer Zeit im Labor bedanken.

Ich werde mich immer gerne an die unzähligen Kaffee- bzw. Eispausen mit Veronika Weiß und Gökçen Savaşçı zurückerinnern. Ihr zwei hattet stets ein offenes Ohr für alle wissenschaftlichen Fragen und auch bei den Problemen des Alltags wart ihr immer eine der ersten Anlaufstellen. Für diese Unterstützung und die jahrelange Freundschaft ein herzliches Dankeschön.

Großer Dank geht an meine Eltern Marion und Harald, die mich während des gesamten Studiums unterstützt haben. Ihr habt es geschafft mich davon zu überzeugen, dass ich alles erreichen kann, was ich möchte und diese Arbeit ist damit auch der Beweis dafür, dass ihr recht hattet. Außerdem möchte ich meiner Schwester Stella für das große Interesse und die viele Korrekturen bedanken.

Zu guter Letzt möchte ich mich bei meiner Frau Nadja für die stetige Unterstützung, all die aufmunternden Worte und das riesige Interesse über die letzten Jahre herzlich bedanken. Ohne dich wäre ich nie so weit gekommen und diese Arbeit wäre nicht das, was sie heute ist.



## Publication List

- [1] P. Patschinski, H. Zipse, 'Leaving Group Effects on the Selectivity of the Silylation of Alcohols: The Reactivity-Selectivity Principle Revisited' *Org. Lett.* **2015**, *17*, 3318–3321.
- [2] P. Patschinski, C. Zhang, H. Zipse, 'The Lewis Base-Catalyzed Silylation of Alcohols—A Mechanistic Analysis' *J. Org. Chem.* **2014**, *79*, 8348–8357.
- [3] C. Zhang, P. Patschinski, D. S. Stephenson, R. Panisch, J. H. Wender, M. C. Holthausen, H. Zipse, 'The Calculation of  $^{29}\text{Si}$  NMR Chemical Shifts of Tetracoordinated Silicon Compounds in the Gas Phase and in Solution' *Phys. Chem. Chem. Phys.* **2014**, *16*, 16642–16650.
- [4] H. N. Hunter, N. Hadei, V. Blagojevic, P. Patschinski, G. T. Achonduh, S. Avola, D. K. Bohme, M. G. Organ 'Identification of a Higher-Order Organozincate Intermediate Involved in Negishi Cross-Coupling Reactions by Mass Spectrometry and NMR Spectroscopy' *Chem. Eu. J.* **2011**, *17*, 7845–7851.



# Table of Contents

<b>1</b>	<b>Introduction</b>	<b>3</b>
1.1	Organocatalysis . . . . .	4
1.2	Evolution of the Silylation . . . . .	5
1.3	Recent Discoveries with Silyl Reagents . . . . .	7
1.4	Objectives . . . . .	10
<b>2</b>	<b>Mechanistic Study of the Silylation of Selected Alcohols</b>	<b>13</b>
2.1	General Description of the Experiments . . . . .	13
2.2	Effects of Auxiliary and Catalytic Bases . . . . .	16
2.2.1	Influence of Auxiliary Bases . . . . .	16
2.2.2	The Influence of Lewis Base Catalysts . . . . .	18
2.3	Investigation of a Secondary Alcohol . . . . .	23
2.3.1	Effect of Temperature and Solvent on the Reaction Progress . . . . .	25
2.3.2	Selectivity in the Silylation Reaction . . . . .	27
2.4	Comparison of Primary, Secondary, and Tertiary Alcohols . . . . .	30
2.5	<sup>29</sup> Si NMR – Experiments and Theory . . . . .	32
2.6	Influence of <i>para</i> -Substituted Alcohols . . . . .	38
2.6.1	Synthesis of <i>para</i> -Substituted Secondary Alcohols . . . . .	38
2.6.2	Kinetic Measurements of <i>para</i> -Substituted Secondary Alcohols . . . . .	39
2.7	Alternative Lewis Base Catalysts for Silylation Reactions . . . . .	43
2.7.1	SCA Values for Phosphane Catalysts . . . . .	45
<b>3</b>	<b>Leaving Group Effects on the Selectivity of the Silylation Reaction</b>	<b>51</b>
3.1	Influence of the Leaving Group on the Reaction Rate . . . . .	51
3.2	Determination of Selectivity . . . . .	54
3.2.1	Possible Effects of Autocatalysis . . . . .	58
3.3	Theoretical Studies on the Leaving Group Effect . . . . .	61
<b>4</b>	<b>Theoretical Evaluation of the Silyl Transfer Enthalpy</b>	<b>67</b>
4.1	General Procedure for Calculations . . . . .	67
4.2	SCA Values for Various Pyridine Systems . . . . .	68
4.3	SCA Values for Various Imidazole Systems . . . . .	71
4.4	Silyl Cation Affinity vs. Methyl Cation Affinity . . . . .	75
<b>5</b>	<b>Chemoselectivity Through London Dispersion Forces</b>	<b>79</b>
5.1	Effects of Dispersion Catalysts on the Selectivity . . . . .	81
5.1.1	Synthesis of Dispersion Catalysts . . . . .	82
5.1.2	Selectivity in Acylation and Silylation . . . . .	83
5.1.3	Increase of Selectivity by Enlarged Reagents . . . . .	87

5.2	Does the Size of the Silyl Group Matter? . . . . .	89
<b>6</b>	<b>Summary</b>	<b>95</b>
6.1	General Summary . . . . .	95
6.2	Outlook . . . . .	99
<b>7</b>	<b>Experimental Part</b>	<b>101</b>
7.1	General Information . . . . .	101
7.2	NMR Kinetics . . . . .	101
7.2.1	General Procedure for NMR Kinetics . . . . .	102
7.3	Procedure for the Competition Experiments . . . . .	102
7.3.1	Selectivity of Leaving Groups . . . . .	103
7.3.2	Selectivity of Five Alcohols . . . . .	103
7.4	Synthesis of Starting Materials and Catalysts . . . . .	104
7.4.1	General Procedures . . . . .	104
7.4.2	Starting Materials and Products of Silylation Reactions . . . . .	105
7.4.3	<i>para</i> -Substituted Alcohols and Silylated Products . . . . .	108
7.4.4	Synthesis of the Products of Silylation and Acylation . . . . .	115
7.4.5	Synthesis of Catalysts . . . . .	126
<b>8</b>	<b>Appendix</b>	<b>139</b>
8.1	Methodological Approach . . . . .	139
8.1.1	NMR-Kinetics . . . . .	139
8.1.2	GC Measurements . . . . .	142
8.2	Data of Direct Rate Measurements . . . . .	147
8.2.1	Variation of Auxiliary Base Concentration . . . . .	147
8.2.2	Variation of Lewis Base Catalysts at 4 mol% Catalyst Loading . . . . .	152
8.2.3	Variation of Catalysts and Catalyst Loadings for a Secondary Alcohol . . . . .	166
8.2.4	Silylation with Phosphane Catalysts . . . . .	176
8.2.5	Silylation of <i>para</i> -Substituted Secondary Alcohols . . . . .	179
8.2.6	Variation of Temperature and Solvents . . . . .	183
8.2.7	Variation of Silyl Reagent in CDCl <sub>3</sub> and DMF-d <sub>7</sub> . . . . .	187
8.3	Computational Methods . . . . .	199
8.3.1	Data for SCA and MCA Calculations for Various Catalysts . . . . .	199
8.3.2	Data for the Various Leavings Groups . . . . .	235
8.3.3	Data for the Silyl Group Size . . . . .	238
<b>9</b>	<b>References</b>	<b>257</b>

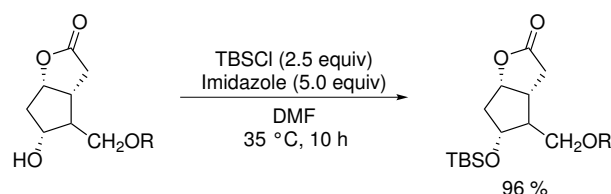






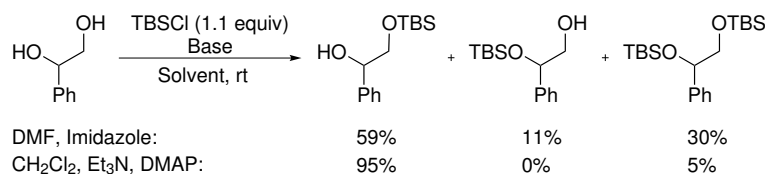
# 1 Introduction

The chemistry of protection groups is one of the commonly used methods in organic chemistry, especially in synthesis, and has been continuously developed ever since it started. Protecting groups are used to avoid unwanted side-reactions with functional groups in a target molecule and can be introduced using a variety of reagents.<sup>[1,2]</sup> For instance, there are more than three methods to protect a hydroxy group by either forming an ether with a protecting group, such as methoxymethyl (MOM), or using acetic anhydride to build acetic ester.<sup>[1,2]</sup> However, the most commonly used protection group for the hydroxy functionality are silyl ethers. Introduced by Corey and Venkateswarlu in 1972, *tert*-butyldimethylsilyl chloride (TBSCl, **1a**) has become one of the most widely used protection reagent. The usefulness of this reaction has been demonstrated using *tert*-butyldimethylsilyl chloride (TBSCl, **1a**) in DMF as solvent and imidazole as base and catalyst for the protection of secondary alcohols (Scheme 1.1). Moreover, they suggest a possible mechanism in which the reaction proceeds via *N*-*tert*-butyldimethylsilylimidazole as a very reactive silylating agent. In the same report, it has been shown that TBS ethers can be cleaved effectively under mild conditions using tetra-*N*-butylammonium fluoride in THF.<sup>[3]</sup> This 'Corey procedure' has been applied to a multitude of substrates containing (mainly) primary and secondary hydroxy groups, thus documenting its general usefulness.<sup>[3]</sup>



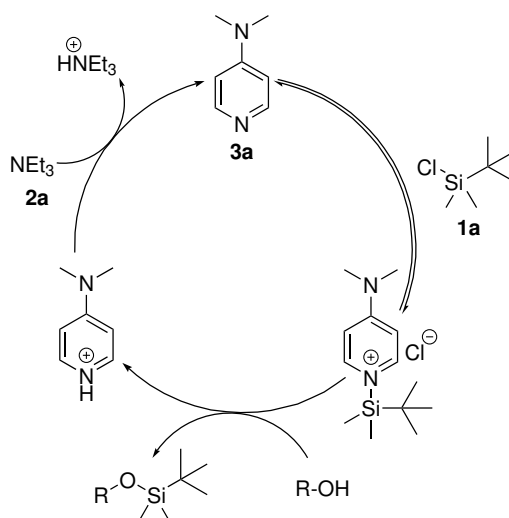
**Scheme 1.1.** Protection of a secondary alcohol using Corey's method.<sup>[3]</sup>

A number of alternative protocols have been developed using different combinations of bases and/or solvents such as those by Hernandez ( $\text{Et}_3\text{N}$ , **2a** / 4-*N,N*-dimethylaminopyridine (DMAP, **3a**),<sup>[4]</sup> Chang ( $\text{Et}_3\text{N}$ , **2a** / 1,1,3,3-tetramethylguanidine and  $\text{Et}_3\text{N}$ , **2a** / DBU),<sup>[5,6]</sup> Weiffen (18-crown-6 /  $\text{K}_2\text{CO}_3$ ),<sup>[7]</sup> Lombardo (*i*- $\text{Pr}_2\text{NEt}$ , **2b**),<sup>[8]</sup> and Fuchs (18-crown-6 / KH).<sup>[9]</sup> The first two of these studies employ catalyst systems closely related to the Corey procedure, as both use nitrogen heterocycles as the actual catalytic base (Scheme 1.2).



**Scheme 1.2.** Selectivity in the silylation of unsymmetric 1,2-diols.<sup>[4]</sup>

Despite this apparent similarity, the reactions catalyzed by DMAP (**3a**) in an apolar, organic solvents show higher selectivities in the transformation of polyol substrates carrying primary and secondary hydroxy groups. As it is shown in Scheme 1.3 for the example of DMAP (**3a**), catalytic Lewis bases are believed to react with silyl chlorides to form silylpyridinium ion pairs, whose subsequent reaction with the alcohol substrate yields the silylether product together with the protonated pyridine base.<sup>[10,11]</sup> Reactivation of the protonated catalyst requires the presence of an auxiliary base such as triethylamine ( $\text{Et}_3\text{N}$ , **2a**) to deprotonate the catalyst and continue the catalytic cycle.



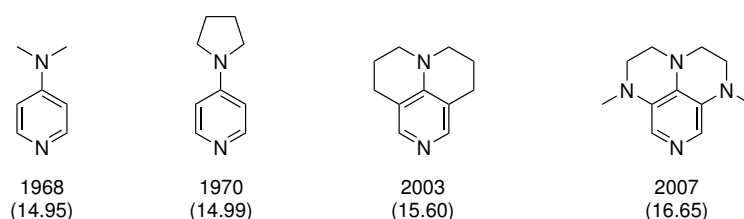
**Scheme 1.3.** Mechanism of the DMAP-catalyzed silylation of alcohols.

This mechanism is practically identical to the well known mechanism for the pyridine-catalyzed acylation of alcohols employing anhydrides as the acylating reagent.<sup>[12–15]</sup> For these acylation reactions more electron-rich pyridines have recently been developed through extension of the DMAP structure and could be observed to be more efficient than DMAP (**3a**). It has been shown that an increase of electron density at the pyridine ring system also increases the rate of the acylation.<sup>[16–18]</sup> In addition to an improved reaction rate, recent research of the acylation reaction showed that enantioselective transformations are feasible and can be performed for a variety of substrates.<sup>[19–22]</sup> Nonetheless, for the similar silylation reaction none of the latter has been reported yet, despite notable efforts in this area of research.<sup>[23–26]</sup>

## 1.1 Organocatalysis

For most reactions in organic synthesis a catalyst is needed, at least in part, to overcome the high barrier by lowering the activation energy. The chemical transformations can be easily performed in nature by specialized enzymes, while in organic chemistry each catalyst has to be designed in order to fit a specific purpose or a reaction.<sup>[27]</sup> A new field of organocatalysis arose within

the last decade with a multitude of applications all over the field of organic chemistry.<sup>[19,28,29]</sup> In order to differentiate between Lewis acids/bases and Brønstedt acids/bases, their mechanisms were studied and compared.<sup>[30]</sup> The biggest benefit in organic synthesis can be observed by Lewis base catalysts such as phosphanes,<sup>[31–33]</sup> sulfides,<sup>[34,35]</sup> or pyridine-based catalysts,<sup>[16,36–39]</sup> because of their high catalytic activity in various reactions.<sup>[40]</sup> The pioneering work in terms of pyridine-based Lewis base catalyst was performed by Steglich and Höfle, who discovered the catalytic potential of DMAP (**3a**) for acylation reactions in 1969.<sup>[36]</sup> A few years later, 4-(1-pyrrolidiny)pyridine (PPY, **3b**) has been discovered with a higher catalytic activity.<sup>[41,42]</sup>



**Figure 1.1.** Development of pyridine-based Lewis base catalysts and the year of discovery in combination with the *N*-parameter in MeCN.<sup>[16,39]</sup>

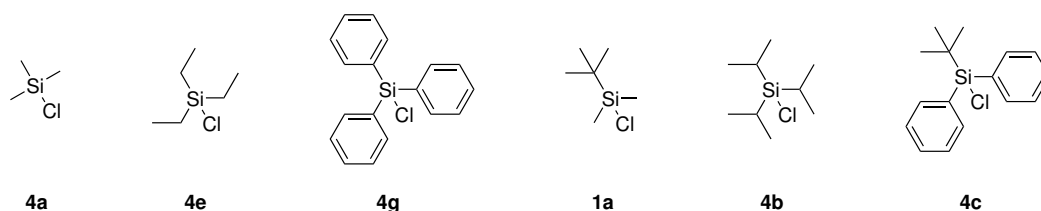
The research in this area was carried on with several new compounds and made another big step with the development of annelated pyridine systems, such as 9-azajulolidine (**3c**) during the last decade.<sup>[37,43]</sup> Recent discoveries by Zipse et al. allow a broad range of modifications on the annelated ringsystem and provide a high catalytic efficiency.<sup>[39]</sup>

## 1.2 Evolution of the Silylation

In contrast to alternative protecting groups for the hydroxyl group, silyl reagents have been developed further since their introduction by Corey and Venkateswarlu. The main goal during this process was to increase the stability towards acidic or basic conditions and to yield higher reactivity of the reagents themselves. The development of other protecting groups started directly after Corey's procedure was published and within a decade four new silicon-based protecting groups have been introduced.<sup>[44–47]</sup> In addition to variations in size of the silyl reagents, the leaving groups were also targeted and led to even more possibilities in this area of research.<sup>[48–51]</sup>

Nowadays, more than hundred different silylation reagents can be purchased and used according to their specific properties. The most commonly used class of silyl chlorides provides a wide range of reagents starting from small compounds such as trimethylsilyl chloride (TMSCl, **4a**)<sup>[52]</sup> to well investigated reagents such as triisopropylsilyl chloride (TIPSCl, **4b**)<sup>[47]</sup> and to the large *tert*-butyldiphenylsilyl chloride (TBDPSCl, **4c**).<sup>[45]</sup> This variability of substituents on the silicon center leads to the benefit that the reactivity (both for formation and for cleavage) can be modified in a suitable way for a particular purpose. The difference in reactivity can be explained by

steric and electronic effects of the substituents and is important for the cleavage of the group. It has been shown that bulkier groups are more stable against acid-catalyzed desilylation which is mostly caused by the higher steric demand. The addition of an electron-withdrawing substituent to the silicon atom increases the susceptibility toward basic hydrolysis, but decrease its sensitivity against acids. Under both conditions the steric effect is similar, while the influence of the electronic environment on the silicon center is much bigger.<sup>[53]</sup> As a conclusion of these effects, the stabilities towards acids and bases are listed below for chosen silyl reagents. The relative stabilities towards acid-catalyzed hydrolysis were obtained in the following order: TMS < triethylsilyl (TES) < triphenylsilyl (TPS) < TBS < TIPS < TBDPS. A small change of positions within the stronger protection groups can be observed for the stabilities towards base-catalyzed hydrolysis: TMS < TES < TPS < TBS  $\approx$  TBDPS < TIPS.<sup>[2]</sup>



**Figure 1.2.** Depiction of typical silylation reagents used in protecting group chemistry.

Furthermore, the leaving groups have been investigated in a similar range in order to increase the reaction rate which has been accomplished with *tert*-butyldimethylsilyl triflate (TBSOTf, **1b**).<sup>[49]</sup> Studies with a similar compound, trimethylsilyl triflate, have shown that triflate reacts  $6.7 \times 10^8$  times faster than the corresponding chloride in their reaction with ketones.<sup>[54]</sup> In addition to the already mentioned leaving groups, an effort has been made to increase the range by the synthesis of various silyl amines, amides, azides, and cyanides.<sup>[51,55–58]</sup>

The difference in reaction rates of various leaving groups can be explained by several factors such as bond energies of the Si–X bond or the polarisation of the Si–X bond depending on the electronegativity of the atom bonded to silicon. In addition, one should also include the steric bulk of the leaving group into this explanation. As shown for the mechanism in Scheme 1.3, it is important that the silicon center can be attacked by a nucleophile. Therefore, the stability of the Si–X bonds can be used as good descriptor since a Si–O bond will be formed during the reaction process. One of the properties that has made silyl groups so popular is the fact that they are easily cleaved by fluoride, which can be provided from compounds such as tetra-*N*-butylammonium fluoride (TBAF).<sup>[3]</sup> The high affinity of silicon to a fluoride ion can also be observed in the bond energies, where the Si–F bond is  $30 \text{ kcal mol}^{-1}$  stronger than the Si–O bond (Table 1.1). When a pyridine-based Lewis base catalyst is used the polarisation of the Si–X bonds is increased in case of TBSCl (**1a**), since the electronegativity for chloride (2.86) is smaller than for nitrogen (3.16). In addition, the silicon atom becomes a strong electrophile based on the positive charge in the activated intermediate.

**Table 1.1.** Average bond energies of silicon with various bonding partners and their relative electronegativities. <sup>[59,60]</sup>

Si–X	Bond Energies [kcal mol <sup>−1</sup> ]	Relative Electronegativities
F	142	4.00
O	112	3.52
Cl	93	2.83
N	75–80	3.16
Br	76	2.52
H	70	2.79
C	69	2.35
Si	54	1.64

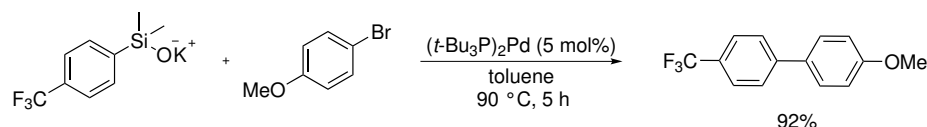
With this information in hand, the class of silyl reagents can be used to fit a specific purpose. While the substituents on the silicon center can be used to form a more stable protecting group, the leaving group provides the means for manipulating reaction rate. Although protecting-group-free synthesis is being described with increasing frequency, the complexity of modern synthetic targets suggests that their synthesis will likely require protecting groups for the foreseeable future. Even though the amount of silyl protection groups and methods for the introduction and removal is already huge, newly developed silyl groups and methods for selective deprotection offer an increased flexibility, especially when unusually challenging examples are encountered. <sup>[23,61]</sup> One of the major advancements of silyl protecting groups lie with the merger of this methodology with other modern techniques such as enantioselective silylation or desilylation.

### 1.3 Recent Discoveries with Silyl Reagents

The chemistry of organosilicon compounds, including silanoles, silyl esters, silyl chloride, silyl hydrides, silenes, and siloles, has found a broad applicability during the last decade in organic synthesis. The large amount of various silicon reagents, suitable for a wide range of possible transformations, changes its role from simple protecting reagents to more broadly used compounds.

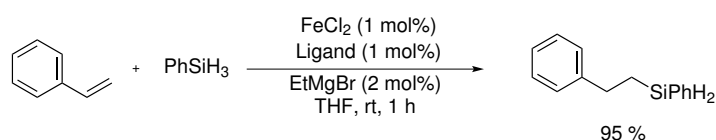
In 1988, it was Hiyama who demonstrated that organosilanes, when suitably functionalized and in the presence of a nucleophilic activator, can undergo cross-coupling reactions with palladium catalysts. However, the conditions were only suitable for a limited scope since a strong fluorine source was used as nucleophilic activator. <sup>[62]</sup> The difficulty for this cross-coupling reaction is caused by the small electronegativity difference between carbon and silicon and therefore a relatively weak reactivity. Within the last decade, Denmark et al. have introduced several

new methods to optimize organosilicon compounds for a higher reactivity and used palladium catalyzed reactions to increase the scope of this reaction.<sup>[63,64]</sup> Further optimization led to the removal of the fluorine-based activator when instead of an silanole a potassium salt is used (Scheme 1.4).<sup>[65–67]</sup>



**Scheme 1.4.** Optimized conditions for a Pd-catalyzed cross-coupling reaction between an organosilicon compound and an arylbromide.

Another well established reaction is the hydrosilylation, which enables the addition of silicon hydrides to C–C multiple bonds. It is an efficient method for the formation of organosilicon compounds and represents one of the most important reactions in silicon chemistry.<sup>[68]</sup> The hydrosilylation can be performed with various transition metal catalysts such as platinum, which is the most commonly used.<sup>[69,70]</sup> By using other late transition metals such as iridium and rhodium, unique chemo- and regioselective hydrosilylations can be achieved.<sup>[71–74]</sup> Furthermore, a significant progress has been achieved in hydrosilylation reactions utilizing cheaper metals (Fe or Ni).<sup>[75,76]</sup> In particular, the precise design of iron catalysts established the systems exhibiting high efficiency and high compatibility towards various functionalized olefins containing epoxide, amide, ester, and keto groups (Scheme 1.5).<sup>[70,77]</sup>



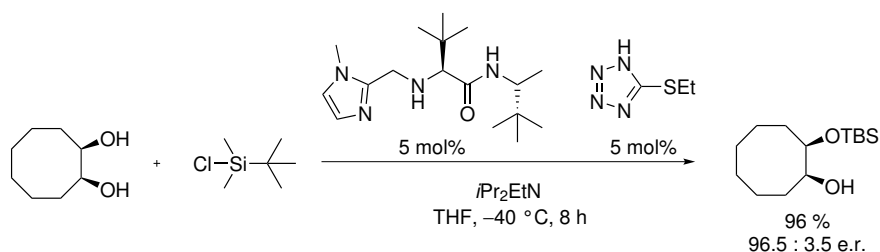
**Scheme 1.5.** Iron-catalyzed hydrosilylation of alkenes.<sup>[77]</sup>

The use of non-transition metal catalysts including early main group metals, Lewis acids and free carbenes have also been studied intensively. Since they follow unique reaction mechanisms, which are different from the well-known mechanisms for the transition metal catalysts, it is expected that the systems could provide a new avenue to hydrosilylation reactions.<sup>[78,79]</sup> Moreover, organosilicon compounds can be used as a traceless direction group for *o*-alkylation of phenols via palladium catalyzed Heck-type reactions.<sup>[80]</sup> The C–H activation using organosilicon compounds in combination with an iridium catalyst has been reported by Hartwig.<sup>[71,81]</sup>

From the synthetic point of view the most promising part is the stereo- and enantioselective protection or deprotection of alcohols in combination with kinetic resolution experiments using the silylation reaction. Since the beginning of protection groups chemistry, selectivity was one of

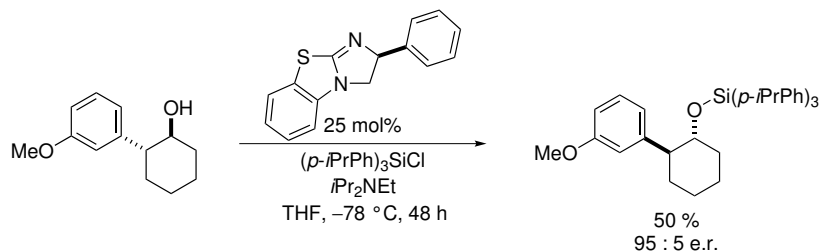


the major issues and has been analyzed first by Westmore et al. who showed that for the deprotection between a primary and secondary center, the silyl group is cleaved first at the primary one.<sup>[82]</sup> In the area of selective cleavage of silyl ethers, the different reactivities of various protection groups are of big importance. Depending on the protection group it is possible to selectively cleave a secondary silyl ether in the presence of a primary one. However, this is not possible if two identical groups are being used for both alcohols.<sup>[53,61]</sup> A big effort has been made to use chiral catalysts for a selective transformation with silyl reagents, which is known for other reactions such as acylation.<sup>[83]</sup> Recently, an enantioselective silyl protection was reported by Snapper et al. by using chiral and achiral Lewis base catalysts, which could be optimized by the use of a co-catalyst.<sup>[84–86]</sup> This intelligent catalyst design can form efficient and selective hydrogen bonds during the transition state to the substrate which leads to high selectivity for the silylation reaction.



**Scheme 1.6.** Enantioselective silylation with TBSCl (**1a**) using a chiral catalyst (5 mol%) and a commercially available co-catalyst (5 mol%) in THF at low temperature.<sup>[86]</sup>

The concept of kinetic resolution experiments has been applied in many reactions for the purification of racemic organic mixtures during the last decades.<sup>[87,88]</sup> The most broadly used reaction in this matter is the acylation of a racemic alcohol mixture with chiral catalysts, as it has been shown by several researchers.<sup>[89–92]</sup> During the last ten years silylation-based kinetic resolution experiments have been studied repeatedly and could be used to resolve a variety of substrates, either through nucleophilic activation of silyl chloride<sup>[93–98]</sup> or dehydrogenative silylation.<sup>[99–101]</sup> The best selectivities so far have been achieved by Wiskur et al. (*S* = 50) by using a modified isothiourea as a chiral catalyst on 2-arylcylohexanols (Scheme 1.7).<sup>[98]</sup> It is worth noting that they used synthesized silyl chlorides as reagents to increase the effect on the reaction.



**Scheme 1.7.** Silylation-based kinetic resolution of trans-2-arylcylohexanols.<sup>[98]</sup>

It has been shown that the possibilities of organosilicon compounds have a huge value for organic synthesis in various directions. They can be used either as specific protection groups, as reagents for cross-coupling reactions, or as compounds for kinetic resolution experiments and therefore can be described as multi-purpose compounds in modern organic chemistry.

### 1.4 Objectives

The aim of this thesis is to gain a better understanding of the silylation reaction in general. In order to achieve this goal, the different reagents, such as Lewis base catalysts, auxiliary bases, and alcohols will be investigated in combination with direct rate kinetic measurements. In addition, the silyl reagents will be studied regarding to their leaving group as well as the size of the protecting group either by experiments or by theoretical evaluation. Furthermore, modifications on Lewis base catalysts will be performed, aiming for a gain in selectivity within competition experiments between various alcohols. Moreover, this thesis aims to provide a broader understanding of protection groups chemistry for the sake of using optimized conditions for organic synthesis.



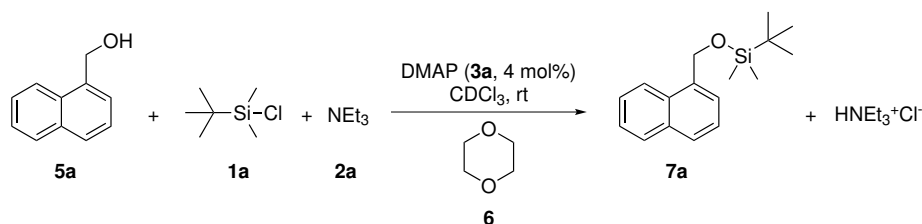


## 2 Mechanistic Study of the Silylation of Selected Alcohols

The silylation of alcohols has been an important topic in organic chemistry since Corey introduced an approach to protect and deprotect secondary alcohols in 1972. In this chapter the reactivity of primary, secondary, and tertiary alcohols in silylation reactions will be compared as well as several reaction parameters such as temperature, choice of catalyst, auxiliary base, and the effect of solvents. The reaction half-life time will be used as a descriptor to compare all reaction parameters with each other. In order to gather this data,  $^1\text{H}$  NMR direct rate kinetic measurements have been used as the method of choice.

### 2.1 General Description of the Experiments

Initial silylation experiments have been performed for the reaction of naphthalen-1-ylmethanol (**5a**) with *tert*-butyldimethylsilyl chloride (TBSCl, **1a**, 1.2 equiv) as reagent and triethylamine ( $\text{Et}_3\text{N}$ , **2a**, 1.2 equiv) as auxiliary base in  $\text{CDCl}_3$  using *N,N*-dimethylaminopyridine (DMAP, **3a**, 4 mol%) as a nucleophilic catalyst (Scheme 2.1). Reaction progress of the silylation reaction has been followed by  $^1\text{H}$  NMR spectroscopy with Dioxane (**6**) as an internal reference.

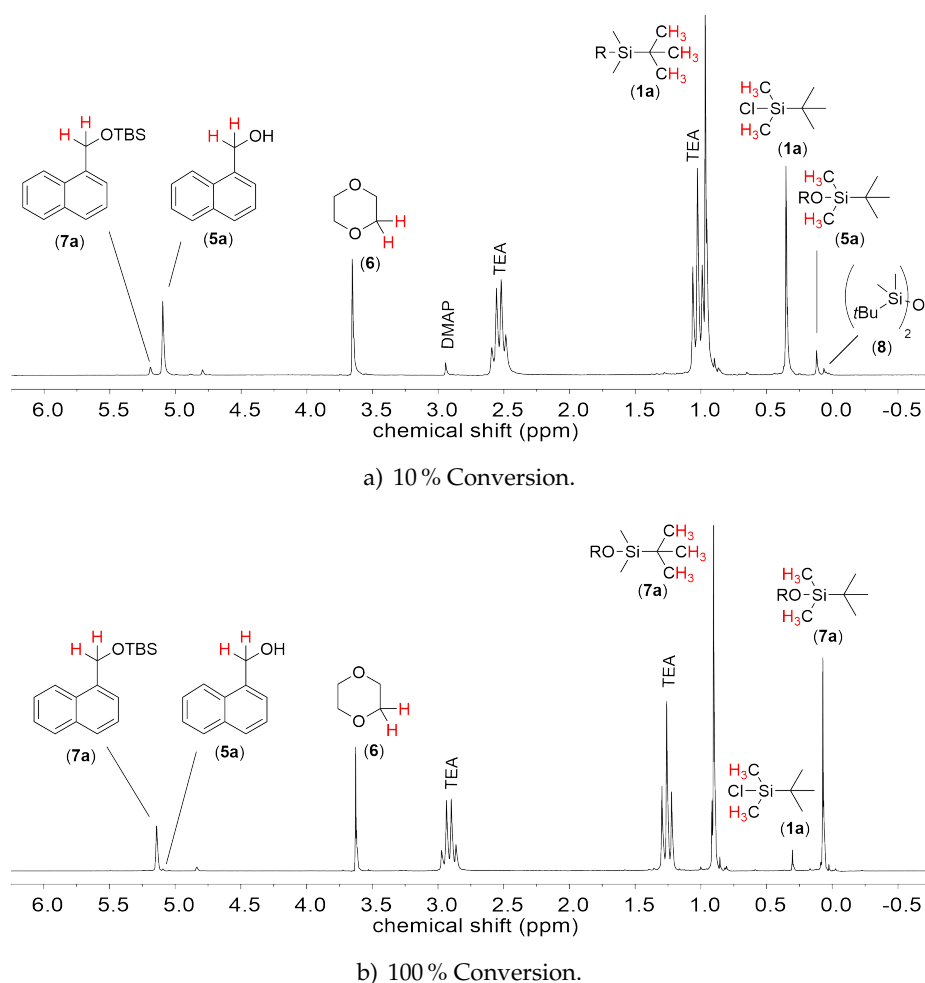


**Scheme 2.1.** Silylation of naphthalen-1-ylmethanol (**5a**) with TBSCl (**1a**) and  $\text{Et}_3\text{N}$  (**2a**) in  $\text{CDCl}_3$  using DMAP (**3a**, 4 mol%) as catalyst.

Initial attempts for determining the reaction rate involved the signals of alcohol **5a** and the resulting silyl ether **7a**. The signals of the respective  $\text{CH}_2$  groups of the alcohol are, however, found to shift in an unfavorable manner as the reaction progresses, which made them unsuitable for full kinetic analysis. The silyl group signals are found to be more useful in this respect. Nonetheless, the *tert*-butyl group can not be used due to overlapping signals with  $\text{Et}_3\text{N}$  (**2a**) at the beginning of the reaction. To illustrate this issue two NMR spectra at 10 % and 100 % conversion are shown in Figure 2.1. The overlapping of the *tert*-butyl can be observed in Figure 2.1a while the unfavorable shifting of the product signals is shown in Figure 2.1b. The most reliable indicator to follow reaction progress to full completion are the two methyl groups attached to the silicon center. The chemical shifts of reagent and product are in good distance in order to perform a full kinetic analysis.

## 2.1 General Description of the Experiments

On closer inspection all  $^1\text{H}$  NMR spectra obtained under reaction conditions indicate the presence of small amounts of bissilylether (**8**) with a chemical shift of 0.06 ppm. It is known that silylchloride is reacting very fast with  $\text{H}_2\text{O}$  to form silylethers. In experiments with defined amounts of added water (10 mol% and 20 mol%) it can be shown that silylether **8** is generated rapidly under reaction conditions from two equivalents of TBSCl (**1a**) and one equivalent of water. The resulting bissilylether (**8**) can be found in an amount of 40.8 % (for 20 mol%) and 18.7 % (for 10 mol%) of additional  $\text{H}_2\text{O}$  relative to the starting material (based on NMR data).



**Figure 2.1.**  $^1\text{H}$  NMR spectra under reaction conditions. Alcohol **5a** reacts with TBSCl (**1a**) and  $\text{Et}_3\text{N}$  (**2a**) in  $\text{CDCl}_3$  using DMAP (**3a**) as catalyst with 4 mol% catalysts loading.

Even though an effort has been made to exclude humidity, final reaction samples may include traces of water. With this information in hand, it can also be shown that the following mechanistic studies involve reaction mixtures containing no more than 2 % of residual water (relative to silyl reagents) which can be determined based on the amount of formed bissilylether (**8**). The residual water is responsible for some conversion data higher than 100 %. The conversion of

TBSCl (**1a**) follows an effective rate law involving first-order behavior of all reactants and the catalyst, and zero order behavior of the auxiliary base. Conversion of silyl chloride and appearance of the silylated alcohol **7a** can be fitted using an effective second-order rate law (Equation 2.1). Here,  $y_0$  is the conversion at infinite time of reaction,  $t_0$  is the starting point of the reaction, and  $k_{eff}$  the effective rate of the reaction.

$$y = y_0 \cdot \left( 1 - \frac{0.2}{1.2 e^{k_{eff} \cdot (0.2) \cdot (t-t_0)} - 1} \right) \quad (2.1)$$

The corresponding effective rate constant  $k_{eff}$  can be used to characterize the reaction in terms of its reaction half-life  $t_{1/2}$  (Equation 2.2).

$$t_{1/2} = \frac{\ln(1.166)}{0.2 \cdot k_{eff}} \quad (2.2)$$

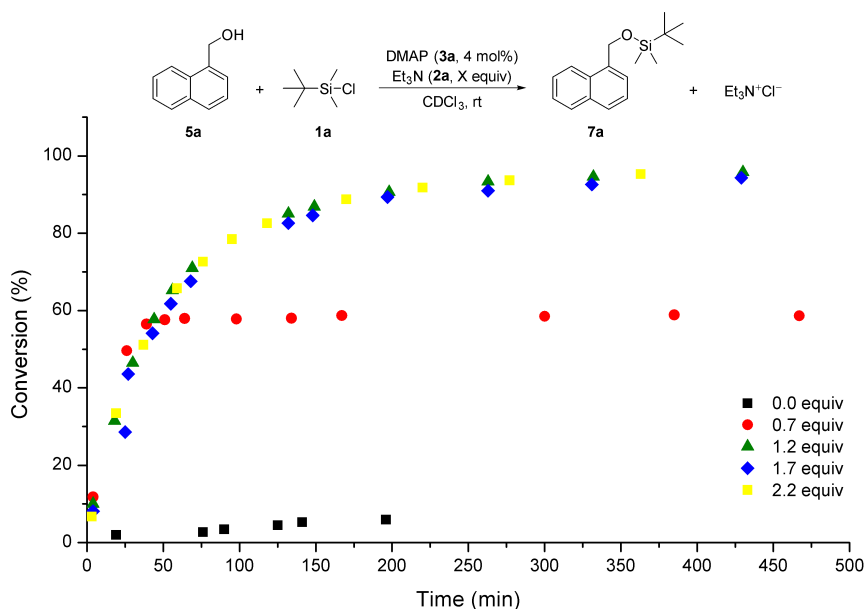
Further information and a full derivation of these equations can be found in the appendix (Chapter 8.1).

## 2.2 Effects of Auxiliary and Catalytic Bases

### 2.2.1 Influence of Auxiliary Bases

In 1979 Hernandez and Chaudhary described the Lewis base-catalyzed silylation of alcohols using DMAP (3a) as catalyst in methylene chloride.<sup>[4]</sup> According to their approach, there is an auxiliary base involved in the reaction for reactivating the catalyst. This leads to two interesting questions: Firstly, how much of an auxiliary base is needed for the reaction and secondly which auxiliary base is the best in terms of reaction rate. It has recently been shown for acylation reactions that the auxiliary base plays an important role in maintaining catalyst activity over many turnover cycles.<sup>[12–14]</sup>

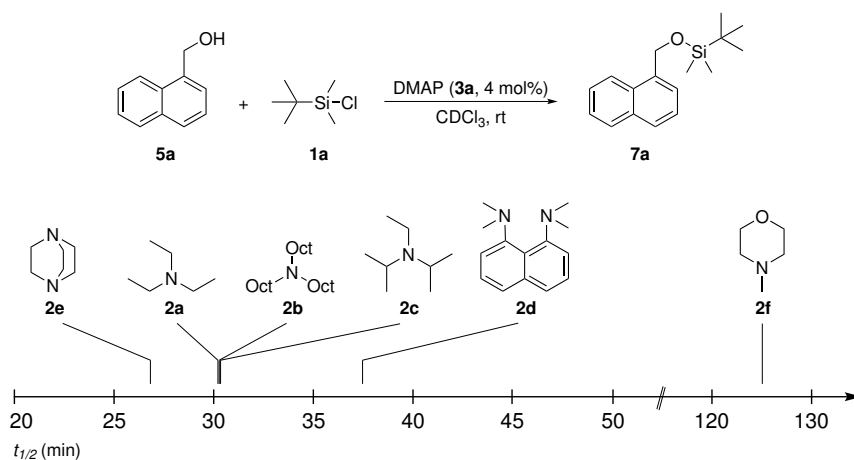
This aspect has been therefore investigated for the silylation reaction shown in Scheme 2.1 through performing the reaction catalyzed by 4 mol% DMAP (3a) in the presence of different amounts of auxiliary base. As can be seen from the turnover curves in Figure 2.2 the rate of silylation is practically identical for the reactions involving 2.2, 1.7, or 1.2 equivalents (relative to alcohol 5a) of Et<sub>3</sub>N (2a) as auxiliary base. This implies that the auxiliary base is not directly involved in the rate determining step, but merely needed to regenerate the catalyst. In case too little auxiliary base is present for this latter task, the reaction slows down dramatically after a certain percentage of turnover (as is visible from the turnover curve for 0.7 equivalents of Et<sub>3</sub>N, 2a). In the absence of an auxiliary base the reaction is extremely slow and cannot be easily analyzed in terms of a second-order rate law. Therefore, it can be concluded that silylation reactions, such as the one described in Scheme 2.1, work best in the presence of 1.2 equivalents of an auxiliary base.



**Figure 2.2.** Turnover curves for the silylation of alcohol 5a catalyzed by 4 mol% DMAP (3a) in the presence of variable concentrations of Et<sub>3</sub>N (2a) in CDCl<sub>3</sub>.



Whether triethylamine ( $\text{Et}_3\text{N}$ , **2a**) is the most suitable auxiliary base for the silylation reaction, has been subsequently explored by rerunning the benchmark reaction (Scheme 2.1) in the presence of other auxiliary bases such as trioctylamine (TOA, **2c**), *N,N*-diisopropylethylamine (DIPEA, **2b**), 1,8-bis(dimethylamino)naphthalene (Proton Sponge, **2d**), 1,4-diazabicyclo[2.2.2]octane (DABCO, **2e**), and *N*-methylmorpholine (NMM, **2f**). While some of these auxiliary bases have already been used in silylation reactions (with different conditions), others have been chosen based on their properties.<sup>[8,102,103]</sup> The results are listed in Table 2.1 and show nearly no variation in half-life times for bases with similar  $\text{pK}_\text{a}$  values like DIPEA (30.7 min), TOA (30.5 min), and  $\text{Et}_3\text{N}$  (30.2 min). As the reaction half-life times are all comparable, the true advantage of TOA (**2c**) over the other two bases lies in its much better solubility in organic solvents (Figure 2.3). By using a weaker base like DABCO (**2e**) or a stronger one like Proton Sponge (**2d**) a change in the reaction rate is observed. In contrast to  $\text{Et}_3\text{N}$  (**2a**) or DIPEA (**2b**), DABCO (**2e**) and Proton Sponge (**2d**) have two nitrogen atoms instead of just one. However, Proton Sponge (**2d**) showed a slower reaction time than **2a** or **2b** as the reaction speed drops from 30.2 min to 37.4 min in case of Proton Sponge. This can be explained by the bigger steric demand of Proton Sponge (**2d**), compared to  $\text{Et}_3\text{N}$  (**2a**).<sup>[104]</sup> A noticeable speed up to a half-life time of 26.5 min can be observed with DABCO (**2e**), which might be caused by its dual role as auxiliary and catalytic base.<sup>[105]</sup>

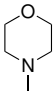
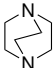
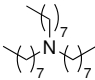
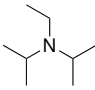
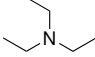
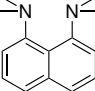


**Figure 2.3.** Reaction half-lives for the silylation of alcohol **5a** with TBSCl (**1a**, 1.2 equiv) catalyzed by 4 mol% DMAP (**3a**) in the presence of various auxiliary bases (1.2 equiv) in  $\text{CDCl}_3$ .

Insufficiently basic amines such as *N*-methylmorpholine (**2f**) lead to a significantly extended reaction half-life of 127.7 min. Under these conditions the regeneration of the catalytic base DMAP (with  $\text{pK}_\text{a} = 9.7$ ) is not effective anymore, which leads to a decrease of the catalyst concentration with increasing conversion (Table 2.1).<sup>[106]</sup>

## 2.2 Effects of Auxiliary and Catalytic Bases

**Table 2.1.** Half-life times  $t_{1/2}$  for the silylation of alcohol **5a** using DMAP (**3a**, 4 mol%) as catalyst with various auxiliary bases (1.2 equiv) in  $\text{CDCl}_3$  and their  $\text{pK}_a$  values.

Auxiliary Base	No.	$\text{pK}_a^{25}(\text{H}_2\text{O})$	$k_{\text{eff}}^{\text{a}}$	$t_{1/2}^{\text{b}}$
no base			$4.10 \cdot 10^{-03}$	187.3 <sup>c</sup>
	<b>2f</b>	7.80 <sup>[107]</sup>	$6.01 \cdot 10^{-03}$	127.7
	<b>2e</b>	8.70 <sup>[108]</sup>	$2.90 \cdot 10^{-02}$	26.5
	<b>2c</b>	11.19 <sup>[109]</sup>	$2.52 \cdot 10^{-02}$	30.5
	<b>2b</b>	11.44 <sup>[110]</sup>	$2.50 \cdot 10^{-02}$	30.7
	<b>2a</b>	11.58 <sup>[111]</sup>	$2.54 \cdot 10^{-02}$	30.2
	<b>2d</b>	12.10 <sup>[112]</sup>	$2.05 \cdot 10^{-02}$	37.4

<sup>a</sup>  $k_{\text{eff}}$  in  $\text{L mol}^{-1} \text{s}^{-1}$ .

<sup>b</sup> Half-life time in min.

<sup>c</sup> Only 7 % conversion.

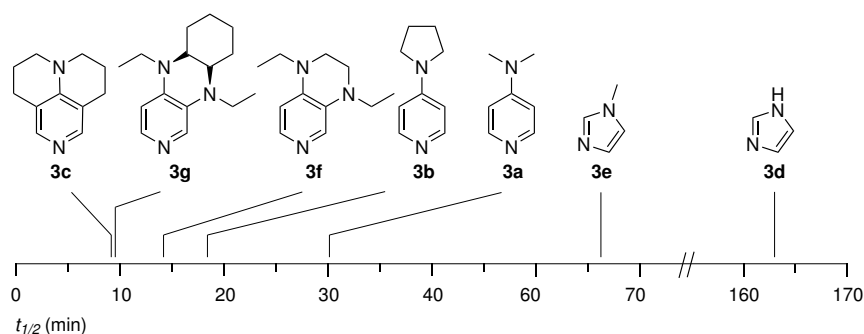
For the choice of auxiliary base it is advisable to take the  $\text{pK}_a$  value of the corresponding catalytic base into account. In this case it can be stated, that the reaction speed is almost not changing between auxiliary bases when the  $\text{pK}_a$  value of the auxiliary base is about two units higher than the one of the catalytic base.

### 2.2.2 The Influence of Lewis Base Catalysts

Regarding the effect of nucleophilic heterocyclic catalysts two major questions appeared during this study. Firstly, which nucleophilic catalyst performs best in the silylation reaction and secondly how much catalyst loading is needed to bring the reaction to full conversion in an acceptable half-life time. In order to answer these questions the benchmark reaction (Scheme 2.1) has been performed with different catalysts at a catalyst loading of 4 mol%. The reaction half-life  $t_{1/2}$  is considered the most relevant kinetic parameter and has been examined for all catalysts shown in Figure 2.4, including DMAP (**3a**), PPY (**3b**), imidazole (**3d**), *N*-methylimidazole (**3e**) as well as two electron-rich pyridines 1,4-diethyl-1,2,3,4-tetrahydropyrido[3,4-*b*]pyrazine (**3f**) and 5,10-diethyl-5,5a,6,7,8,9,9a,10-octahydropyrido[3,4-*b*]quinoxaline (**3g**), which have been recently

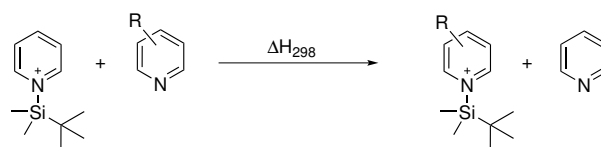
developed for acylation reactions. In addition, the commercially available 9-azajulolidine (**3c**), which has performed very well in acylation reactions, has been included (Table 2.2).<sup>[18,38,43]</sup>

For imidazole (**3d**), which has been used in large excess in the original 'Corey procedure', a reaction half-life of 163.9 min at a catalyst loading of 4 mol% has been obtained and is therefore five times slower than DMAP (**3a**, 30.2 min) and about sixteen times slower than catalyst **3g** (9.4 min). The fastest catalyst has been found to be 9-azajulolidine (**3c**) with 9.0 min half-life time. The range of reaction half-lives among the fast catalysts at 4 mol% is rather small. Half-life times for the reaction with strong nucleophilic catalysts such as PPY (**3b**), **3c**, **3f**, and **3g** are all below 20 minutes and these catalysts are thus well suited for the silylation of primary alcohols. Furthermore, *N,N*-dimethylaminoformamide (DMF, **3h**), which is used as solvent in the 'Corey procedure', has also been investigated as a catalyst under identical conditions (that is, at 4 mol% catalyst loading) and led to a reaction half-life of 955.1 min. This has been the slowest performance observed during this study, but explains in part, why the reaction in DMF (**3h**) as a solvent is so fast. The effects of various solvents, including DMF (**3h**), will be discussed in Chapter 2.3.1 in more detail.



**Figure 2.4.** Reaction half-lives of various catalysts **3a–g** with a catalyst loading of 4 mol%, achieved by kinetic measurements of the reaction of **5a** with TBSCl (**1a**) in  $\text{CDCl}_3$ .

In addition to the kinetic measurement of various catalysts, the catalytic efficiency can also be determined by quantum chemical calculations (Scheme 2.2). In Chapter 4, the silyl cation affinity value (SCA value) will be used to describe the Lewis basicity of various catalysts.

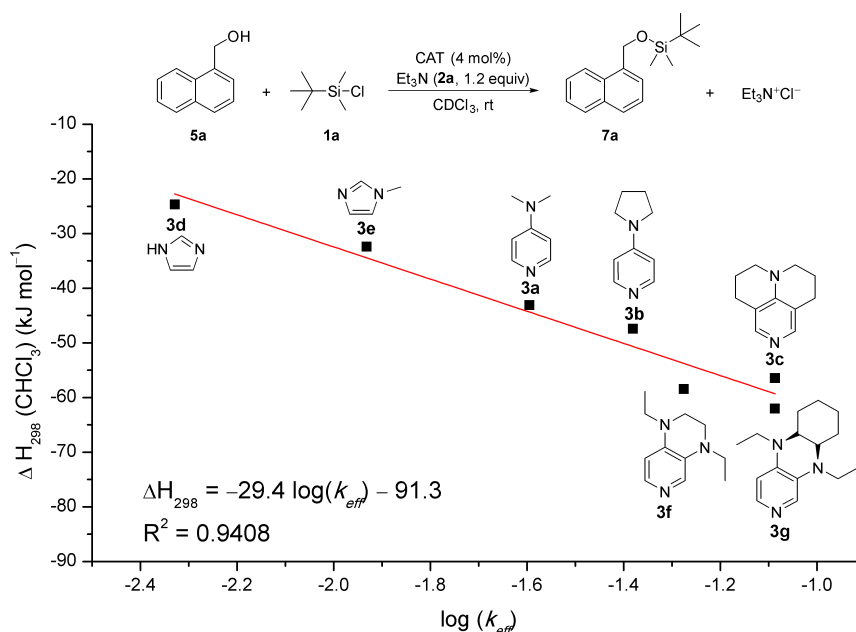


**Scheme 2.2.** Definition of silyl cation affinities (SCA) via an isodesmic silyl group transfer reaction.

By plotting the SCA values against the experimentally obtained rate data ( $k_{\text{eff}}$ ), a good linear correlation ( $R^2 = 0.9408$ ) is obtained, which allows to estimate the effectivity of a catalyst based on its Lewis basicity. The silyl cation affinity of  $-24.7 \text{ kJ mol}^{-1}$  for imidazole (**3d**) implies that the

## 2.2 Effects of Auxiliary and Catalytic Bases

*tert*-butyldimethylsilyl group attaches to imidazole  $24.7 \text{ kJ mol}^{-1}$  more strongly as compared to pyridine. The lowest affinity values have been obtained for the slowest catalysts **3d** and **3e**, while higher values can be found for the more efficient catalysts DMAP (**3a**) and PPY (**3b**). The highest affinity values can be obtained for the diaminopyridines **3f** and **3g** with  $-58.5$  and  $-62.0 \text{ kJ mol}^{-1}$ , both of which count among the most active catalysts (Figure 2.5).



**Figure 2.5.** Rate constants for the silylation of alcohol **5a**  $\log(k_{\text{eff}})$  vs. silyl cation affinities (SCAs) of the respective catalysts (relative to the reference base pyridine) in CHCl<sub>3</sub>.

A low SCA value describes a stabilized intermediate between catalyst and silyl group, which is needed for the first step of the catalytic cycle and can therefore be used as a descriptor for a good catalyst. All results for the reaction with primary alcohol **5a**, including the SCA values, are displayed in Table 2.2.

**Table 2.2.** Reaction half-lives of alcohol **5a** with various catalysts based on  $^1\text{H}$  NMR data in  $\text{CDCl}_3$  at 4 mol% catalyst loading and silyl cation affinities (SCAs) relative to pyridine.

Catalyst	No.	SCA (gas) <sup>a</sup>	SCA (sol) <sup>b</sup>	$k_{\text{eff}}$ <sup>c</sup>	$t_{1/2}$ <sup>d</sup>
	<b>3h</b>	+4.8	−17.5	$8.04 \cdot 10^{-04}$	$955.1 \pm 12.4$
	<b>3d</b>	−20.0	−24.7	$4.69 \cdot 10^{-03}$	$163.9 \pm 2.3$
	<b>3e</b>	−36.4	−32.4	$1.17 \cdot 10^{-02}$	$65.9 \pm 3.3$
	<b>3a</b>	−57.0	−43.1	$2.54 \cdot 10^{-02}$	$30.2 \pm 1.4$
	<b>3b</b>	−64.8	−47.4	$3.90 \cdot 10^{-02}$	$19.7 \pm 0.4$
	<b>3f</b>	−83.4	−58.5	$5.30 \cdot 10^{-02}$	$14.5 \pm 0.3$
	<b>3g</b>	−93.2	−62.0	$8.18 \cdot 10^{-02}$	$9.4 \pm 0.6$
	<b>3c</b>	−75.6	−56.5	$8.49 \cdot 10^{-02}$	$9.0 \pm 0.5$

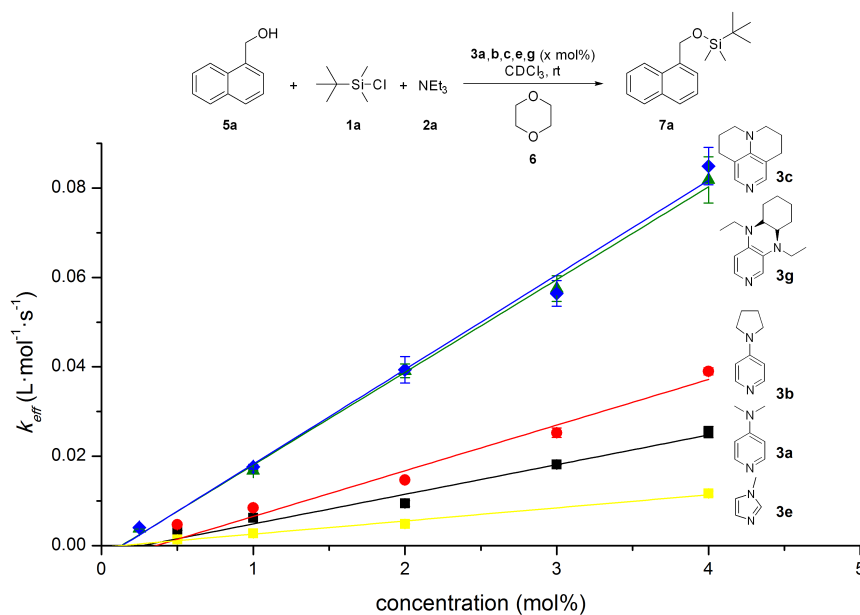
<sup>a</sup> SCA values at 298.15 K (in  $\text{kJ mol}^{-1}$ ) have been calculated at the MP2(FC)/G3MP2large//MPW1K/6-31+G(d) level.<sup>b</sup> Solvation energies (in  $\text{kJ mol}^{-1}$ ) have been calculated at PCM/UAHF/MPW1K/6-31+G(d) level for  $\text{CHCl}_3$ .<sup>c</sup>  $k_{\text{eff}}$  in  $\text{L mol}^{-1} \text{s}^{-1}$ .<sup>d</sup> Half-life time in min.

For five of the catalysts (DMAP (**3a**), PPY (**3b**), **3c**, **3e**, and **3g**) reaction rates have been measured at different catalyst concentrations. A linear correlation between the rate constant  $k_{\text{eff}}$  and the catalyst loading can be observed in all cases (Figure 2.6). A similar correlation can also be found in other Lewis base-catalyzed reactions, such as the *aza*-Morita-Baylis-Hillman reaction and in acylation reactions<sup>[15,39,113,114]</sup>, which implies that only one catalyst molecule participates in the rate limiting step. The slope of the correlation line  $k'_{\text{eff}}$  reflects the intrinsic catalytic efficiency of the catalysts, while the intercept  $b$  represents the background reaction rate in the absence of

catalysts (Equation 2.3).

$$k_{\text{eff}} = k'_{\text{eff}} [\text{cat}] + b \quad (2.3)$$

The reaction rate is already very fast at 4 mol% catalyst loading for all five catalysts, making the accurate determination of half-life times difficult for the fastest two catalysts **3c** and **3g**.

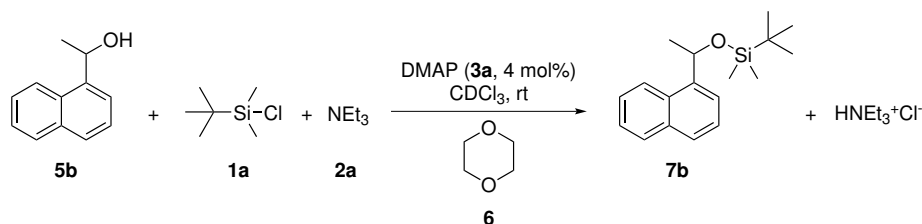


**Figure 2.6.** Correlation of catalyst concentration vs. rate constant  $k_{\text{eff}}$  for the silylation of alcohol **5a** using DMAP (**3a**), PPY (**3b**), **3c**, **3e** and **3g** as catalysts.

Measurements performed at 1 mol% catalyst loading thus yield significantly more accurate half-life times, which has been determined as 283.9 min in for **3e**, 123.9 min for DMAP (**3a**), 90.8 min for PPY (**3b**), 45.7 min for **3g** and 43.6 min for **3c**. Furthermore, these kinetic studies also document that the silylation reaction of alcohol **5a** has nearly no background reaction according to the very small intercept of the y-axis for all five catalysts. In a silylation experiment without any catalyst a conversion below 1 % has been determined after 36 h in CDCl<sub>3</sub>. The background reaction is thus too slow to compete with the catalytic reaction.

## 2.3 Investigation of a Secondary Alcohol

Reaction rates for secondary alcohol 1-(naphthalen-1-yl)ethanol (**5b**) have been determined under identical conditions as those for primary alcohol **5a**. As expected the reaction rate for the silylation of **5b** to the silylated product **7b** is much slower than for primary alcohol **5a**.



**Scheme 2.3.** Silylation of 1-(naphthalen-1-yl)ethanol (**5b**) with TBSCl (**1a**) and Et<sub>3</sub>N (**2a**) in CDCl<sub>3</sub> using DMAP (**3a**, 4 mol%) as catalyst.

Using DMAP (**3a**) at a catalyst loading of 4 mol%, a reaction half-life of 30.2 min has been determined for primary alcohol **5a**, while for the secondary alcohol **5b** it amounts to 3165.6 min. This reduction of the reaction rate of approx. two orders of magnitude is also observed for the other Lewis base catalysts investigated in this chapter (Table 2.3). PPY (**3b**) and *N*-methylimidazole (**3e**) react almost as fast as DMAP (**3a**). A faster reaction has been observed by using more nucleophilic catalysts like **3c** (2034.5 min) and **3g** (1457.8 min). Throughout all measurements with secondary alcohol **5b** a higher deviation has been observed, which might be caused by much longer reaction times and much higher catalyst concentrations.

**Table 2.3.** Reaction half-lives of **5b** with heterocyclic catalysts based on <sup>1</sup>H NMR data in CDCl<sub>3</sub> at 4 mol% catalyst loading and silyl cation affinities (SCA) for the used catalysts relative to pyridine.

Catalyst	No.	SCA (sol) <sup>a</sup>	$k_{\text{eff}}$ <b>5b</b> <sup>b</sup>	$t_{1/2}$ <sup>c</sup>
	<b>3e</b>	−32.4	$2.12 \cdot 10^{-04}$	$3620.8 \pm 9.8$
	<b>3a</b>	−43.1	$2.43 \cdot 10^{-04}$	$3165.6 \pm 33.1$
	<b>3b</b>	−47.4	$2.41 \cdot 10^{-05}$	$3182.0 \pm 85.9$

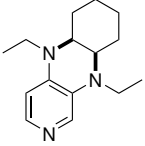
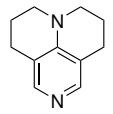
<sup>a</sup> Solvation energies (in kJ mol<sup>−1</sup>) have been calculated at PCM/UAHF/MPW1K/6-31+G(d) level for CHCl<sub>3</sub>.

<sup>b</sup>  $k'_{\text{eff}}$  in L mol<sup>−1</sup> s<sup>−1</sup>.

<sup>c</sup> Half-life time in min.

## 2.3 Investigation of a Secondary Alcohol

**Table 2.3.** Continuation.

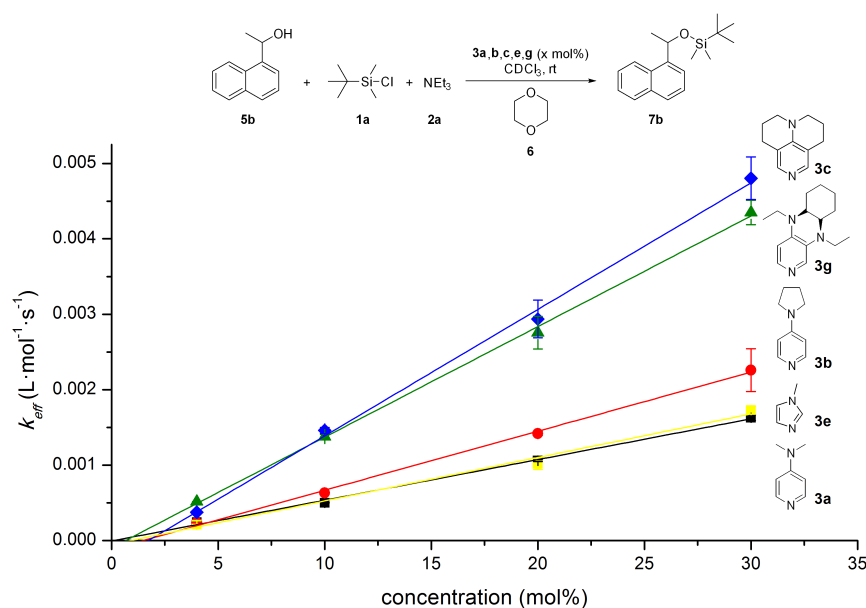
Catalyst	No.	SCA (sol)	$k_{eff}$ <b>5b</b>	$t_{1/2}$
	<b>3g</b>	−62.0	$5.27 \cdot 10^{-04}$	$1457.8 \pm 35.5$
	<b>3c</b>	−56.5	$3.77 \cdot 10^{-04}$	$2034.5 \pm 7.5$

<sup>a</sup> Solvation energies (in  $\text{kJ mol}^{-1}$ ) have been calculated at PCM/UAHF/MPW1K/6-31+G(d) level for  $\text{CHCl}_3$ .

<sup>b</sup>  $k'_{eff}$  in  $\text{L mol}^{-1} \text{s}^{-1}$ .

<sup>c</sup> Half-life time in min.

Kinetic measurements have been repeated at various catalyst loadings for chosen catalysts (**3a**, **3b**, **3c**, **3e**, and **3g**) and lead to similar results as for primary alcohol **5a**. A linear correlation between the concentration of the catalysts and  $k_{eff}$  can be observed for secondary alcohol **5b**. As mentioned before, the deviations in the series of measurements are larger than for the primary alcohol especially at higher catalyst loadings (Figure 2.7).

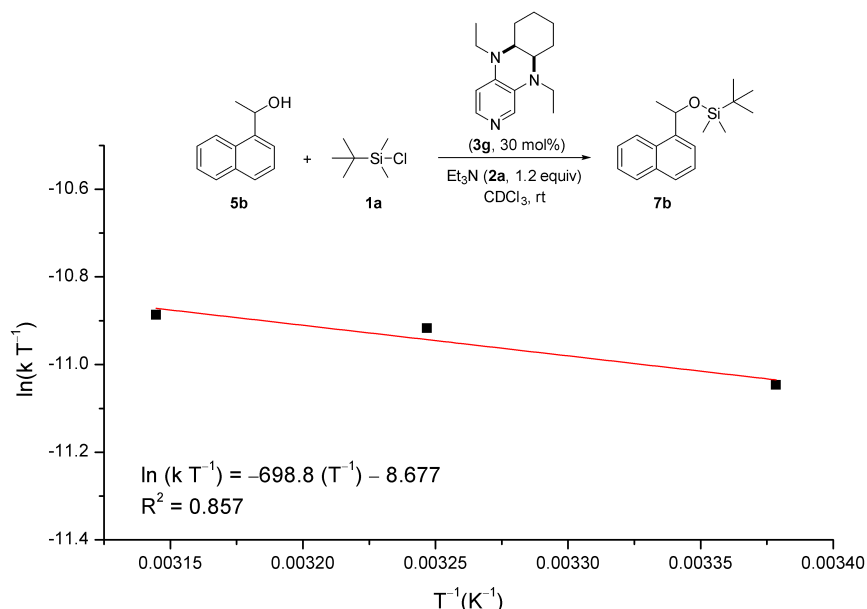


**Figure 2.7.** Correlation of catalyst concentration vs. rate constant  $k_{eff}$  for the silylation of alcohol **5b** using DMAP (**3a**), PPY (**3b**), **3c**, **3e** and **3g** as catalysts.



### 2.3.1 Effect of Temperature and Solvent on the Reaction Progress

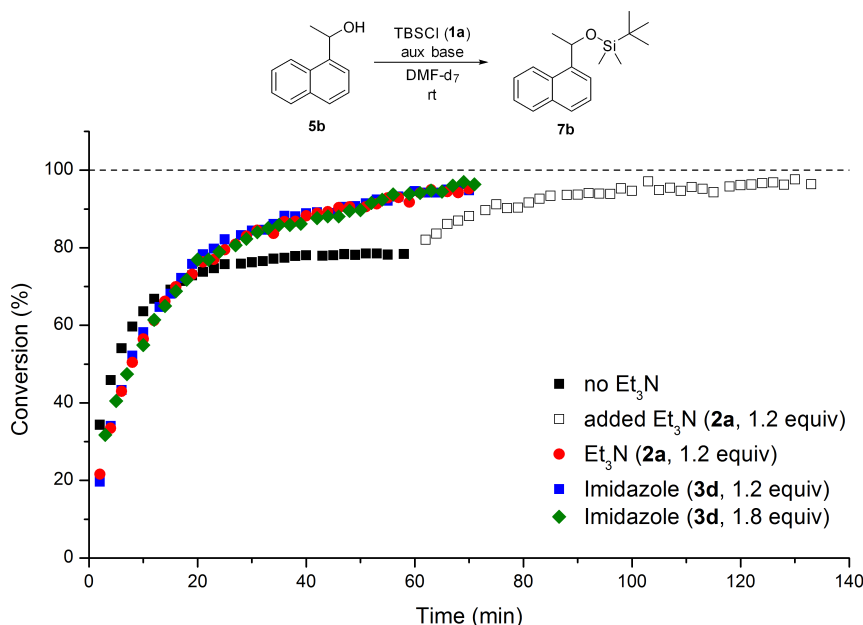
The 'Corey procedure' mentioned earlier uses a reaction temperature of 35 °C in order to increase both the solubility of all reagents and the reaction rate. The silylation reaction of secondary alcohol **5b** has therefore been repeated using catalyst **3g** at 30 mol% catalyst loading at different reaction temperatures in CDCl<sub>3</sub>. Increasing the reaction temperature might change the overall concentration in the reaction mixtures due to solvent evaporation, especially when low boiling solvents such as CDCl<sub>3</sub> or CD<sub>2</sub>Cl<sub>2</sub> are used. In order to avoid this effect in these measurements, the NMR tubes have been flame-sealed. As expected the reaction rates increase at higher temperatures, providing reaction half-lives of 162.7 min at 23 °C and 129.1 min at 45 °C. This rather moderate reduction in reaction half-lives implies that, from a synthetic point of view, elevated temperatures are mainly beneficial for solving solubility problems. Formal analysis of the rate data using an Eyring plot leads to an activation enthalpy ( $\Delta H^\ddagger$ ) of +5.8 kJ mol<sup>-1</sup> and an activation entropy ( $\Delta S^\ddagger$ ) of -269.7 J K<sup>-1</sup> mol<sup>-1</sup> (Figure 2.8). The value obtained for the activation enthalpy is quite small for a reaction in solution, whereas the negative value obtained for the activation entropy is typical for an effective trimolecular reaction. Similar results of  $\Delta H^\ddagger = +12.8$  kJ mol<sup>-1</sup> and  $\Delta S^\ddagger = -240.0$  J K<sup>-1</sup> mol<sup>-1</sup> have recently been determined for the PPY-catalyzed isobutyrylation of secondary alcohol **5b**.<sup>[83,115]</sup> Even though the Eyring plot is only based on three measurements, it is still remarkable that similar results have been obtained for the silylation as for the acylation.<sup>[83]</sup> It can be stated that both mechanisms are related in terms of the necessity of a nucleophilic catalyst and an auxiliary base.



**Figure 2.8.** Eyring plot based on kinetic measurements of **5b** with catalyst **3g** (30 mol%) in CDCl<sub>3</sub> at various temperatures.

### 2.3 Investigation of a Secondary Alcohol

Silylation reactions are often performed in polar aprotic solvents such as DMF or dimethylsulfoxide.<sup>[3,116,117]</sup> The influence of solvent polarity on reaction rates has therefore been studied for the silylation of secondary alcohol **5b** with TBSCl (**1a**) in CD<sub>2</sub>Cl<sub>2</sub>, CDCl<sub>3</sub>, and DMF-d<sub>7</sub>. Using catalyst **3c** at 30 mol% catalyst loading and Et<sub>3</sub>N (**2a**, 1.2 equiv) as the auxiliary base the reaction has first been studied in CDCl<sub>3</sub> and found to proceed with a half-life time of 176.3 min. Repeating the reaction in CD<sub>2</sub>Cl<sub>2</sub> under otherwise identical conditions yields in a slightly faster reaction with a half-life time of 115.4 min. The reaction in DMF-d<sub>7</sub>, in contrast, has been found to be so much faster that accurate rate data could hardly be determined under these conditions. Repeating the reaction without catalyst and auxiliary base allowed accurate measurements, but reaches a plateau at 80 % conversion. For the experiment in DMF-d<sub>7</sub> <sup>29</sup>Si NMR spectra shows signals of starting materials as well as product (Figure 2.9) which support the fact that the reaction really stopped at this point. After adding Et<sub>3</sub>N (**2a**) to the reaction mixture only the product signal appears in <sup>29</sup>Si-NMR measurements, which is an indication for full conversion of the reaction. Therefore, the role of the auxiliary base during the reaction in DMF-d<sub>7</sub> must be important. Adding Et<sub>3</sub>N (**2a**) as auxiliary base right from the start full conversion can be observed and a half-life time of 6.7 min has been determined in DMF-d<sub>7</sub>. Furthermore, these results imply that the reaction is inhibited by hydrogen chloride generated during the reaction process without an auxiliary base. Only after the acid is removed from the reaction mixture by adding a auxiliary base the reaction can continue to full conversion (Figure 2.9).



**Figure 2.9.** <sup>1</sup>H NMR kinetic measurement of **5b** in DMF-d<sub>7</sub> with no catalyst and various amounts of auxiliary base.

After these experiments the question of the role of imidazole (**3d**) in the 'Corey procedure' arose. The experiment in DMF-d<sub>7</sub> has been repeated with 1.2 and 1.8 equivalents of imidazole (**3d**) in order to observe any effect on the reaction rate. If imidazole (**3d**) acts as a catalytically active Lewis base in this reaction an increase of the rate would be expected. However, an effect on the half-life time can not be observed which leads to the conclusion that imidazole is acting exclusively as an auxiliary base in the 'Corey procedure' (Figure 2.9).

Using DMF-d<sub>7</sub> as a solvent leads to an impressive reaction rate due to the amount of Lewis base catalyst which is the solvent DMF (**3h**) itself. The enormous speedup of the reaction in DMF-d<sub>7</sub> as compared to the two halogenated solvents cannot be rationalized with common solvent parameters such as  $E_T(30)$  values or Gutman donor numbers, and may better be understood as the direct involvement of DMF-d<sub>7</sub> as a Lewis base catalyst.<sup>[118,119]</sup> Other solvents such as THF, acetone, and acetonitrile have also been tested, but a full analysis by <sup>1</sup>H NMR has been impeded by formation of inhomogenous reaction mixtures (most likely due to precipitation of Et<sub>3</sub>NH<sup>+</sup>Cl<sup>-</sup>).

### 2.3.2 Selectivity in the Silylation Reaction

Within the last chapter the direct rate measurements for different Lewis base catalysts have been performed for primary and secondary alcohols. The obtained reaction rates can be compared for each catalyst to achieve the selectivity between primary alcohol (**5a**) and secondary alcohol (**5b**). The silylation of primary alcohol **5a** has been repeated in DMF-d<sub>7</sub> in order to include the selectivity ratio of DMF. A very fast reaction with a half-life time of 0.3 min can be observed for primary alcohol **5a**, compared to 6.7 min for secondary alcohol **5b**. The selectivities have been obtained by comparing the  $k'_{eff}$  values of investigated catalysts for both alcohols, which can be seen as independent of the catalyst concentration, as described earlier (Equation 2.3). The selectivity for each catalyst is determined as  $S$ , which is the ratio between the reaction rate  $k'_{eff}$  for **5a** and **5b** (Equation 2.4). Since in DMF-d<sub>7</sub> only two measurements have been performed, those will be compared. The selectivity ratio for DMF-d<sub>7</sub> can only be seen as an estimate, but leads to a plausible results. Comparing the values of  $k'_{eff}$  for the primary as well as for the secondary alcohol, it can be stated that catalysts **3c** and **3g** have similar catalytic efficiency in both cases. PPY (**3b**) performs with a  $k'_{eff}$  of  $7.83 \cdot 10^{-05}$  in the reaction with secondary alcohol (**5b**) better than DMAP (**3a**) with  $5.39 \cdot 10^{-05}$  and therefore supports the results already seen for primary alcohol **5a**. The speedup by a factor of 1.45 from DMAP (**3a**) to PPY (**3b**) is comparable to that found for the primary alcohol before (1.53). **3c** and **3g** show an increase in reaction rate by a factor of 2.7 for **5b** and 3.2 for **5a** in comparison to DMAP (**3a**).

$$S = \frac{k'_{eff}(\mathbf{5a})}{k'_{eff}(\mathbf{5b})} \quad (2.4)$$

A comparison of the  $k'_{eff}$  values for all pyridine-based catalysts indicates that the reaction of a

## 2.3 Investigation of a Secondary Alcohol

secondary alcohol (**5b**) is at least two orders of magnitude slower than the reaction of a primary alcohol (**5a**) (Table 2.4). It is known for simple systems such as diols that a selective silylation (primary over secondary) is already achievable by using DMAP (**3a**).<sup>[4]</sup> These results might become handy when more complex systems, such as carbohydrates, are under investigation for a selective transformations.<sup>[120]</sup>

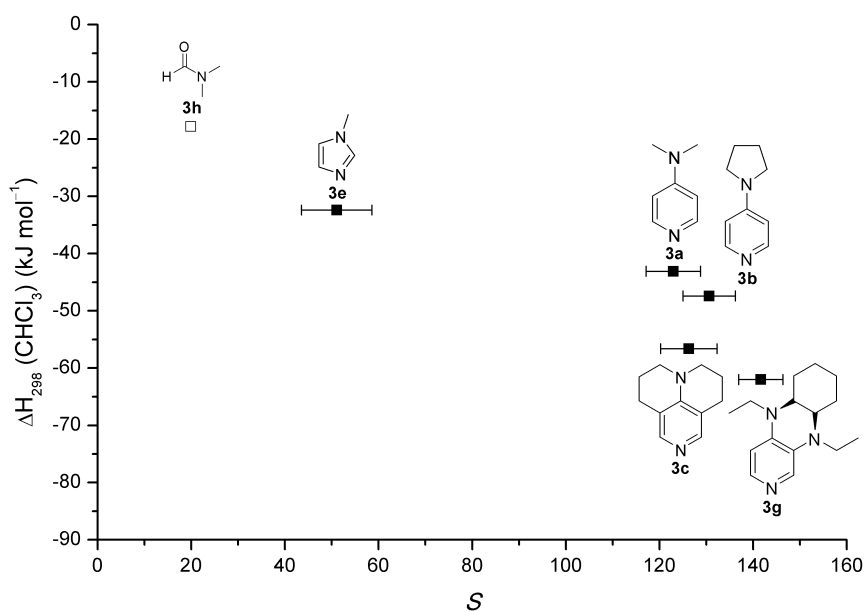
**Table 2.4.**  $k'_{eff}$  values for the silylation of primary (**5a**) and secondary (**5b**) alcohol for different catalysts in combination with the SCA values and the obtained selectivity *S*.

Catalyst	No.	SCA (sol) <sup>a</sup>	$k'_{eff}$ <b>5a</b> <sup>b</sup>	$k'_{eff}$ <b>5b</b> <sup>b</sup>	<i>S</i>
	<b>3h</b>	−17.8	2.85	$1.43 \cdot 10^{-01}$	19.9
	<b>3e</b>	−32.4	$2.94 \cdot 10^{-03}$	$5.76 \cdot 10^{-05}$	51.0
	<b>3a</b>	−43.1	$6.63 \cdot 10^{-03}$	$5.39 \cdot 10^{-05}$	123.0
	<b>3b</b>	−47.4	$1.02 \cdot 10^{-02}$	$7.83 \cdot 10^{-05}$	130.3
	<b>3c</b>	−56.5	$2.12 \cdot 10^{-02}$	$1.68 \cdot 10^{-04}$	126.2
	<b>3g</b>	−62.0	$2.08 \cdot 10^{-02}$	$1.47 \cdot 10^{-04}$	141.5

<sup>a</sup> Solvation energies have been calculated at PCM/UAHF/MPW1K/6-31+G(d) level for CHCl<sub>3</sub>.

<sup>b</sup>  $k'_{eff}$  in L mol<sup>−1</sup> s<sup>−1</sup>.

Even though the reaction for the primary alcohol **5a** in DMF-d<sub>7</sub> is faster by a factor of 30, compared to catalyst **3c** in CDCl<sub>3</sub>, for a selective transformation of primary over secondary alcohol the situation is different. The reactivity difference of primary and secondary alcohols amounts to 19.9 under DMF conditions and can be increased to 51.0 for *N*-methylimidazole (**3e**) in CDCl<sub>3</sub>. The best values of 120 – 145 are obtained for electron-rich pyridines such as **3c** and **3g** in CDCl<sub>3</sub>. When these ratios are plotted against the silyl cation affinity values of the respective Lewis bases, it becomes apparent that the stability of the Lewis base-silyl cation adducts may be responsible for the observed selectivities (Figure 2.10).

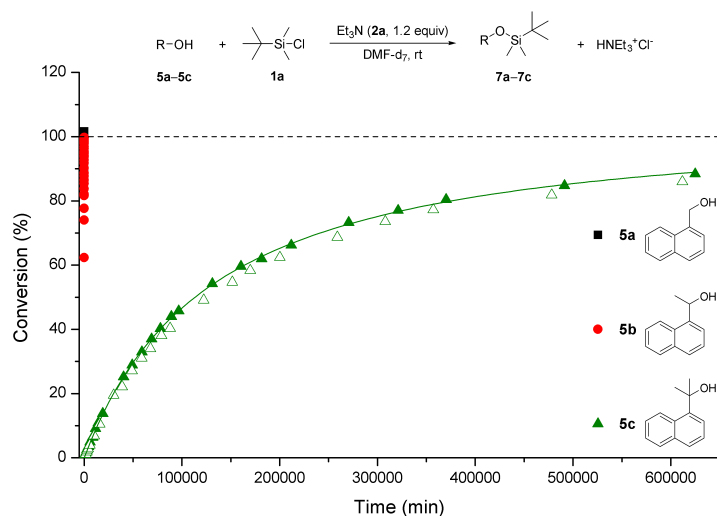


**Figure 2.10.** Calculated silyl cation affinities ( $\Delta H_{298}$ ) vs. selectivity  $S$  for chosen catalysts. The ratio for DMF has been determined from the measurements of **5a** and **5b** in DMF- $d_7$  as a solvent.

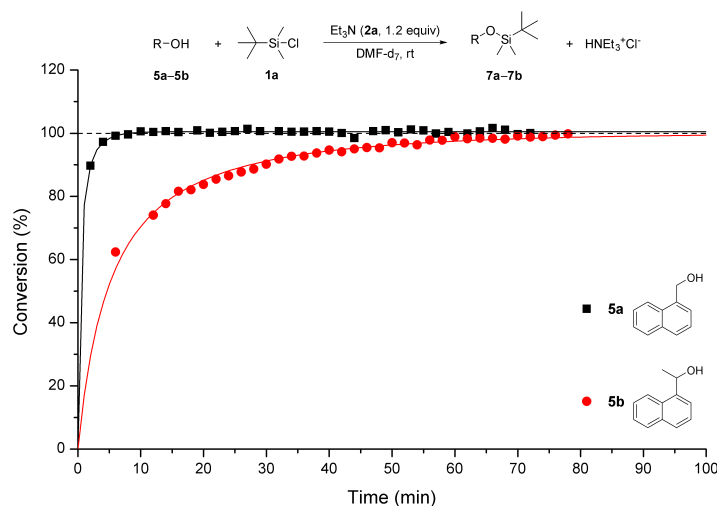
The least stable intermediate (silylated DMF) provides the lowest selectivities, while the much more stable silyl-pyridinium intermediates all yield selectivities  $>100$  in this specific matter. In conclusion, higher SCA values should provide an even better selectivity for the silylation reaction. When a selective silylation is the goal, it is highly advisable to avoid the 'Corey procedure' and use a nucleophilic Lewis base catalyst in a polar, aprotic solvent instead.

## 2.4 Comparison of Primary, Secondary, and Tertiary Alcohols

Reaction rates have also been determined for the silylation of 2-(naphthalen-1-yl)propan-2-ol (**5c**) with TBSCl (**1a**) using exactly the same conditions as shown before in DMF- $d_7$  with Et<sub>3</sub>N (**2a**, 1.2 equiv) as auxiliary base and no catalyst. Reaction progress is very slow under these conditions. While full conversion is reached after several minutes for primary and secondary alcohols **5a** and **5b**, the first product signals for the reaction with **5c** can only be observed after several hours of reaction time. The reaction half-life has been determined to be 112 700 min or approx. 78 days for the tertiary alcohol **5c** in DMF- $d_7$  (Figure 2.11a).



a) Comparison of **5a**, **5b**, and **5c** without any catalyst. Hollow triangles depict reaction with 30 mol% of catalyst **3c** in DMF- $d_7$ .



b) Primary (**5a**) and secondary alcohol (**5b**) in DMF- $d_7$  without any catalyst.

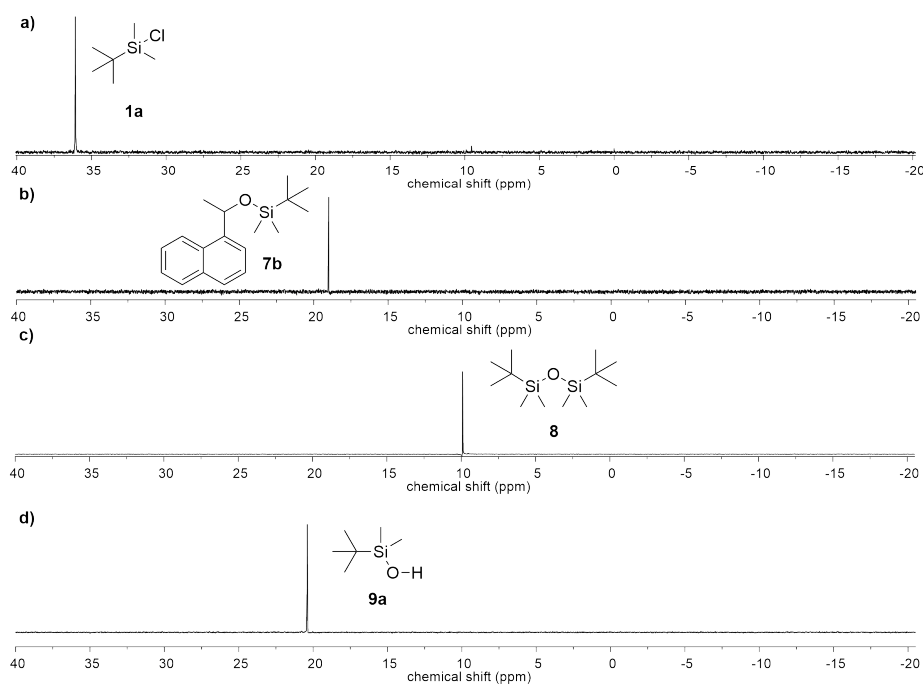
**Figure 2.11.** Time vs. conversion plot for primary (**5a**), secondary (**5b**), and tertiary (**5c**) alcohol in DMF- $d_7$  with TBSCl (**1a**) and Et<sub>3</sub>N (**2a**, 1.2 equiv) as auxiliary base.

The kinetic data available for alcohols **5a–c** can be combined to extract relative reactivities of 418182 (**5a**) : 20925 (**5b**) : 1 (**5c**) for these three substrates under otherwise identical conditions (DMF- $d_7$ , rt, Et<sub>3</sub>N as auxiliary base, no catalyst). The reactivity difference between secondary alcohol **5b** and tertiary alcohol **5c** is much larger (factor 20925) than the difference between primary alcohol **5a** and secondary alcohol **5b** (factor 20). Repeating the reaction in the presence of catalyst **3c** (30 mol%) under otherwise identical conditions leads to no acceleration of turnover, which again supports the Lewis basic solvent DMF- $d_7$  as the only catalytically active species under these conditions. This implies that the silyl chloride reagent (**1a**) used here is intrinsically not reactive enough to turn over tertiary substrates in a synthetically meaningful way. Even though catalyst **3c** is known to be much more nucleophilic than DMF, the amount of DMF molecules in comparison to catalyst **3c** makes it impossible to have any catalytic effect for the reaction with **5c**.

Based on these results, it can be stated that selectivity between primary and secondary alcohols can be achieved by a strong Lewis base catalyst and the right choice of solvent. For a tertiary alcohol only a very slow reaction could be observed even under rather harsh conditions (in DMF).

## 2.5 $^{29}\text{Si}$ NMR – Experiments and Theory

As shown in previous chapters, the mechanism of the silylation reaction in DMF (**3h**) actively involves the solvent as reaction partner. The experimental results are quite clear at the fact that DMF is not only a solvent, but is also acting as a Lewis base catalyst. However, an active intermediate has never been observed directly. In combination with  $^{29}\text{Si}$  NMR and computational shift predictions an effort has been made to prove the existence of possible transient intermediates formed between DMF (**3h**) and silyl chloride **1a**. The proposed mechanism by Hernandez starts with an attack of the Lewis base on the silyl chloride, generating a highly active intermediate.<sup>[4]</sup> The aim is to prove the existence of a reactive intermediate for the used catalyst (**3a** and **3c**) as well as for DMF (**3h**). All chemical shifts of  $^{29}\text{Si}$  NMR for reactants and products have first been determined in  $\text{CDCl}_3$  (non-reactive solvent) and then repeated in DMF- $\text{d}_7$  (reactive solvent). For the  $^{29}\text{Si}$  NMR measurements possible side products have also been synthesized and analyzed, for instance bissilylether **8** (Figure 2.12, Table 2.5).

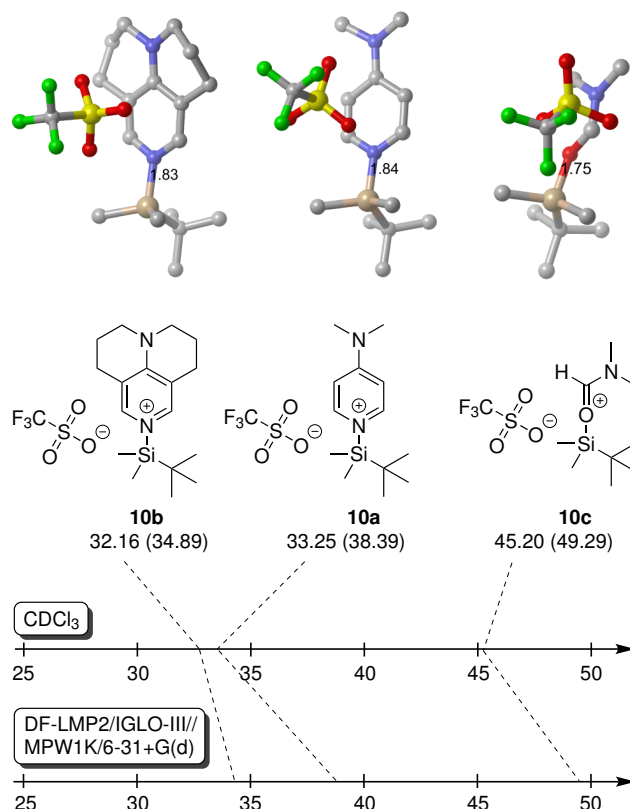


**Figure 2.12.**  $^{29}\text{Si}$  NMR spectra of reactants, products and selected intermediates measured in  $\text{CDCl}_3$ . a) TBSCl (**1a**) b) *tert*-butyldimethyl(1-(naphthalen-1-yl)ethoxy)silane (**7b**) c) Bissilylether (**8**) d) *tert*-butyldimethylsilanol (**9a**).

The starting material TBSCl (**1a**) appears at +36.1 ppm in  $\text{CDCl}_3$  and at +37.1 ppm in DMF- $\text{d}_7$ . This small downfield shift in DMF- $\text{d}_7$  can also be observed for most other species listed in Table 2.5. A second signal can be observed at +10.2 ppm when mixing silyl chloride **1a** with DMF- $\text{d}_7$  and is assigned to bissilylether **8**, most likely formed through reaction of **1a** with residual water in DMF. This species resonates in  $\text{CDCl}_3$  at +9.9 ppm. A second hydrolysis product



*tert*-butyl-dimethylsilanol (**9a**) can be detected at +20.4 ppm in  $\text{CDCl}_3$  (+14.0 ppm in  $\text{DMF-d}_7$ ), which can be crystallized in the form of the dimer hydrate (**9b**). The hydrate complex and *tert*-butyldimethylsilanol (**9a**) has been synthesized separately and lead to the same chemical shifts in both solvents. This implies that the hydrate complex is not stable in  $\text{CDCl}_3$  solution and that **9a** is shifted upfield by six ppm due to interaction with the solvent in  $\text{DMF-d}_7$ . This effect can also be observed in theoretical  $^{29}\text{Si}$  shift calculations where free silanol **9a** resonates at +18.6 ppm, while the corresponding DMF complex is shifted by 4.6 ppm to +14.0 ppm (Table 2.5). Addition of auxiliary base  $\text{Et}_3\text{N}$  to silyl chloride **1a** in either solvent did not lead to any new signals, while the addition of alcohol **5b** generates a new one at +18.4 ppm in  $\text{CDCl}_3$  and at +18.5 ppm in  $\text{DMF-d}_7$ . This signal belongs to the product silyl ether **7b** and remains unchanged through the presence of auxiliary or catalytic bases. Attempts to detect transient intermediates of the catalytic cycle in  $\text{CDCl}_3$  through adding an active catalyst like **3c** to the solution of  $\text{TBSOTf}$  (**1a**) does not lead to a new signal in the  $^{29}\text{Si}$  spectrum. Even an excess of catalyst only leads to more hydrolysis products, but not to new intermediate. However, signals at +32.2 ppm and +33.3 ppm have been observed when mixing catalysts **3a** or **3c** with  $\text{TBSOTf}$  (**1b**) in a 1 : 1 ratio in  $\text{CDCl}_3$  (Figure 2.13). With the aid of  $^1\text{H}$ ,  $^{13}\text{C}$  and NOESY spectroscopy these signals can be assigned to the silylated pyridines (**10a** for catalyst **3a**, **10b** for catalyst **3c**).



**Figure 2.13.** Adducts obtained in the reaction of  $\text{TBSOTf}$  (**1b**) with catalyst **3c** (left, **10b**), **3a** (middle, **10a**), and with DMF (right, **10c**) optimized at MPW1K/6-31+G(d) level of theory.

Bassindale and Stout measured a series of  $^{29}\text{Si}$  NMR with different Lewis bases in combination with trimethylsilyl triflate in  $\text{CD}_2\text{Cl}_2$ . They have obtained  $^{29}\text{Si}$  NMR shifts for trimethylsilyl triflate and DMF of +44.0 ppm and for DMAP (**3a**) of +31.7 ppm, which are similar to the obtained data in this study where TBSOTf (**1b**) has been used.<sup>[50,121]</sup>

In addition to the experimental measurements, an attempt has been made to calculate  $^{29}\text{Si}$  NMR shifts of the compounds of interest.<sup>1</sup> The biggest benefit of this quantum chemical approach is that it is possible to calculate intermediates and ion pairs, which might appear during the reaction. In order to achieve a chemical shift in ppm, the shielding numbers of the compound of interest and a chemical standard (tetramethylsilane, TMS) needed to be calculated first. The chemical shifts of  $^{29}\text{Si}$  containing species ( $\delta^{29}\text{Si}$ ) have been calculated using Equation 2.5. Shieldings have been calculated at DF-LMP2/IGLO-III//MPW1K/6-31+G(d) level, using the Gauge-Independent Atomic Orbital (GIAO) method as implemented in Gaussian 09 and MOLPRO. For conformationally flexible systems, the shifts correspond to Boltzmann-averaged values at 298 K based on free energies obtained at MPW1K/6-31+G(d) level of theory. The shielding of TMS used for the calculations is 380.55 ppm.<sup>[122]</sup>

$$\delta^{29}\text{Si} = \sigma(^{29}\text{Si}_{\text{TMS}}) - \sigma(^{29}\text{Si}) \quad (2.5)$$

The  $^{29}\text{Si}$  chemical shift of *tert*-butyldimethylsilyl triflate (**1b**) changes from +43.71 ppm in  $\text{CDCl}_3$  to +41.97 ppm in  $\text{DMF-d}_7$ . The latter value is also observed for mixtures of TBSCl (**1a**) with  $\text{AgSbF}_6$  in  $\text{CDCl}_3$ . Given the Lewis acidic character of **1b** and the Lewis base character of DMF, one may hypothesize, that the signal at +41.97 ppm corresponds to *O*-silylated DMF (**10a** in Figure 2.15)<sup>[50,121]</sup> with either the OTf or  $\text{SbF}_6$  counter ions.<sup>[123–125]</sup> Ion pairs such as intermediates **10a** and **10b** can be located in geometry optimizations at MPW1K/6-31+G(d) level of theory. The  $^{29}\text{Si}$  chemical shift predicted for these structures are, however, systematically shifted downfield by several ppm.

**Table 2.5.**  $^{29}\text{Si}$  NMR shifts in ppm in  $\text{CDCl}_3$  and  $\text{DMF-d}_7$  of several compounds in comparison with calculated  $^{29}\text{Si}$  shifts.

System	$\text{CDCl}_3$	$\text{DMF-d}_7$	DF-LMP2/IGLO-III// MPW1K/6-31+G(d)
TBSCl ( <b>1a</b> )	+36.1	+37.1, +10.2	+35.0
TBSCl ( <b>1a</b> ) + <b>2a</b>	+37.2, +10.1		
TBSCl ( <b>1a</b> ) + <b>3a</b>	+37.3, +18.5		
<b>1a</b> + $\text{AgSbF}_6$ (1 equiv)	+41.9, +10.2		
<b>1a</b> + $\text{AgSbF}_6$ (0.5 equiv)	+10.2		

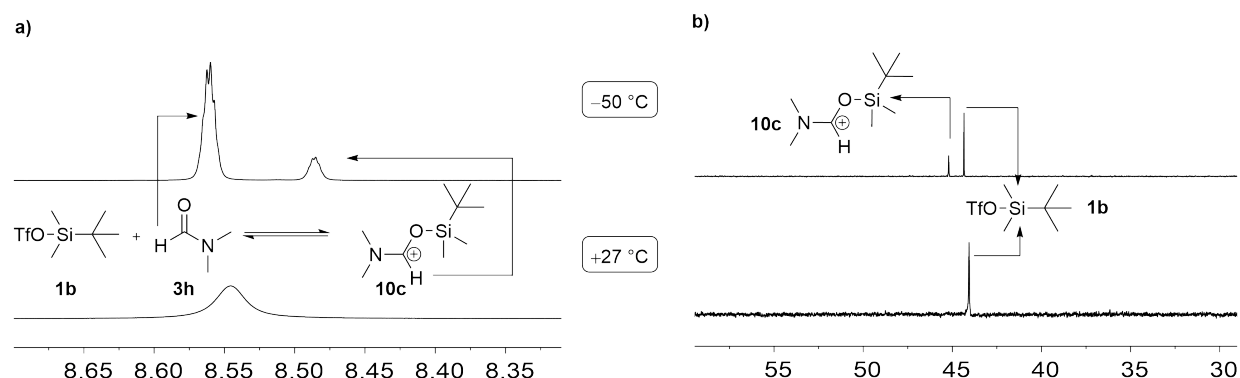
<sup>1</sup> Theoretical calculation of  $^{29}\text{Si}$  NMR shifts have been performed by Dr. Cong Zhang.

Table 2.5. Continuation.

System	$\text{CDCl}_3$	$\text{DMF-d}_7$	DF-LMP2/IGLO-III// MPW1K/6-31+G(d)
<b>7a</b>	+20.6	+20.3	+20.9
<b>7b</b>	+18.4	+18.5	+20.2
<b>7c</b>	+12.2	+12.0	+14.4
<b>8</b>	+9.91	+10.2	+11.3
<b>9a</b>	+20.4	+14.0	+18.6
<b>9b</b>	+20.4	+14.0, +10.3	+17.2
<b>9a</b> + DMF	+13.9		
TBSOTf ( <b>1b</b> )	+43.7, +9.9	+41.9, +10.4	+42.4
TBSOTf + <b>3a</b> ( <b>10a</b> )	+33.3, +9.9		+38.4
TBSOTf + <b>3c</b> ( <b>10b</b> )	+32.2, +9.8		+34.9
TBSOTf + DMF ( <b>10c</b> )	+45.2, +10.1		+49.3

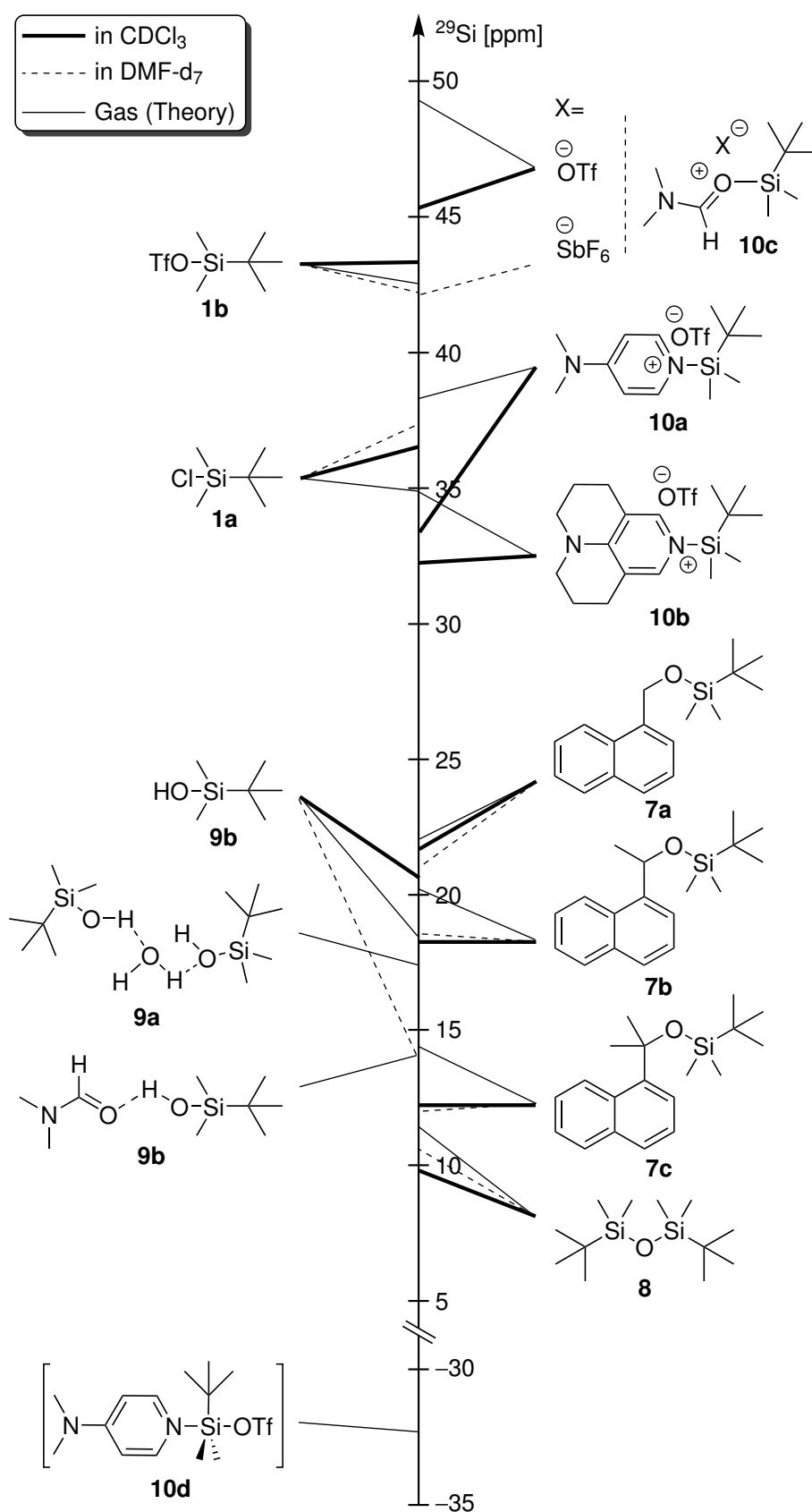
Even though all current NMR evidence points to tetracoordinated silicon intermediates, one should not dismiss the possibility of either pentacoordinated silicon species or true silyl cation intermediates.<sup>[123–125]</sup> A pentacoordinated isomer of ion pair **10a** (termed **10d**) can actually be identified as a local minimum on the MPW1K-D2/6-31+G(d) potential energy surface and is located 42.8 kJ mol<sup>−1</sup> higher than **10a**. The calculated  $^{29}\text{Si}$  chemical shift for **10d** amounts to −32.24 ppm, which is in line with the expectation for other pentacoordinated silicon species.<sup>[126–129]</sup> However, reoptimization of this structure at MPW1K/6-31+G(d) level leads back to ion pair intermediate **10a**.

In order to prove the existence of the DMF adduct (**10c**), temperature-dependent NMR measurements (−50 °C – +70 °C) have been performed for TBSOTf (**1b**) in  $\text{DMF-d}_7$  and show no new signals or alterations of the one observed in a 1 : 1 mixture at room temperature (+42.0 ppm). As for the other ion pair intermediates **10a** and **10b** before, the  $^{29}\text{Si}$  shift calculations predict a more downfield shifted signal for intermediate **10c** at +49.3 ppm. A second experiment in  $\text{CDCl}_3$  has been performed where TBSOTf (**1b**) and DMF have been mixed in 1.5 : 1 ratio and measured at +27 °C and −50 °C. A new signal can be observed at −50 °C in the  $^{29}\text{Si}$  NMR at +45.2 ppm, which is in an acceptable distance to the calculated value of +49.3 ppm. In addition to this new  $^{29}\text{Si}$  signal, two broad signals at 8.6 ppm and 3.5 ppm in the  $^1\text{H}$  spectra at room temperature split up into two sharp singlets at −50 °C. This indicates that equilibration between DMF (**3h**) and intermediate **10c** is sufficiently slow at this temperature as to allow individual observation of both participating species (Figure 2.14).



**Figure 2.14.** Mixture of DMF (**3h**, 1 equiv) and TBSOTf (**1b**, 1.5 equiv) in  $\text{CDCl}_3$  measured at  $+27^\circ\text{C}$  and  $-50^\circ\text{C}$  by a)  $^1\text{H}$  and b)  $^{29}\text{Si}$  NMR.

In this chapter it has been shown that the prediction of  $^{29}\text{Si}$  NMR shifts can be used to support experimental results. Especially with the calculated pentacoordinated silicon compound, it could be excluded that the reaction proceeds through these types of species, which strongly supports by the calculated and measured shifts of the active intermediates **10a–c**. Furthermore, the existence of an activated intermediate (**10c**) by DMF (**3h**) has been proven by NMR experiments and strongly supported by theoretical calculations. This intermediate (**10c**) can be seen as a highly reactive species which is able to transform primary and secondary alcohols faster than any other Lewis base tested in this study. A depiction of measured and calculated shifts is given as a summary of this chapter in Figure 2.15.



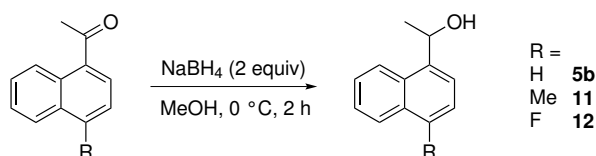
**Figure 2.15.** Comparison of  $^{29}\text{Si}$  NMR measurements in  $\text{CDCl}_3$  and  $\text{DMF-d}_7$  with gas phase calculations at DF-LMP2/IGLO-III//MPW1K/6-31+G(d) level of theory.

## 2.6 Influence of *para*-Substituted Alcohols

The Hammett equation is a broadly used mechanistic tool in physical organic chemistry.<sup>[130]</sup> It has been reported for triphenylsilyl chlorides that the *para*-position of the silyl reagent does have an influence on the rate of the silylation reaction with a secondary alcohol.<sup>[97]</sup> Since these results are promising, the influence of substituents in *para*-position on secondary alcohol **5b** for the silylation with TBSCl (**1a**) has been investigated. A broad range of electron donating and withdrawing groups have been synthesized and investigated in kinetic measurements.

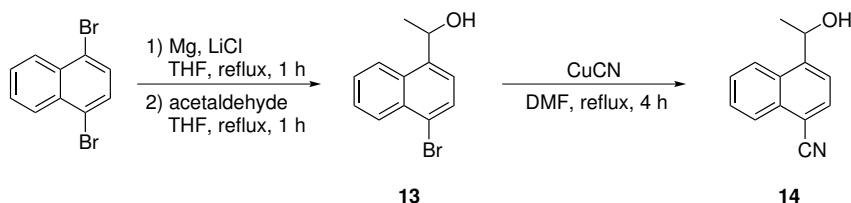
### 2.6.1 Synthesis of *para*-Substituted Secondary Alcohols

In order to avoid unnecessary steps, an approach following a direct reduction from possible *para*-substituted ketones with sodium borohydride have been performed for available compounds. The synthesis of 1-(4-methylnaphthalen-1-yl)ethan-1-ol (**11**) and 1-(4-fluoronaphthalen-1-yl)ethan-1-ol (**12**) following this approach and yielded in 94 % for **11**, 95 % for **12**, respectively. In addition to the high yields of these reactions, no additional workup is needed for these reactions (Scheme 2.4).<sup>[131]</sup>



**Scheme 2.4.** Reduction of *para*-substituted 1-(naphthalen-1-yl)ethan-1-one with NaBH<sub>4</sub> in MeOH.

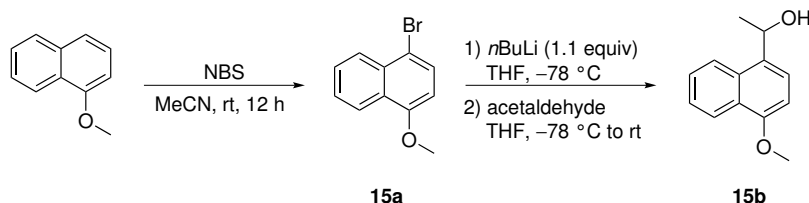
The synthesis of 1-(4-bromonaphthalen-1-yl)ethan-1-ol (**13**) has been performed by a modified Grignard approach, in which LiCl is used as an additive to increase the reaction effectiveness. The conversion of 1,4-dibromonaphthalene with acetaldehyde (1.0 equiv) in THF yielded 62 % of the desired product (**13**).<sup>[132]</sup> Further transformation of **13** with CuCN in DMF using the approach by Friedman and Shechter lead to **14** in 50 % yield (Scheme 2.5).<sup>[133]</sup>



**Scheme 2.5.** Synthesis of **13** obtained by a modified Grignard approach, followed by a bromo-cyano exchange to form **14**.

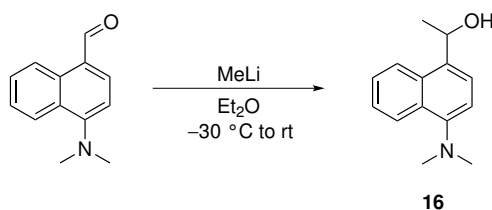
Starting from 2-methoxynaphthalene, a bromination with *N*-bromosuccinimide (NBS) has been performed in a shaded flask and yielded in 93 % of 2-bromo-4-methoxynaphthalene (**15a**). The

insertion of lithium at  $-78\text{ }^{\circ}\text{C}$  with *n*BuLi (1.1 equiv) and slow addition of acetaldehyde (0.8 equiv) lead to the desired product **15b** in 63 % yield as a pale solid.



**Scheme 2.6.** Two step synthesis of **15b**.

The compound with the strongest electron donating group ( $\text{NMe}_2$ , **16**) has been synthesized in a one-step reaction. 4-(Dimethylamino)-1-naphthaldehyde has been transformed with a nucleophilic methyl group by the addition of MeLi at  $-30\text{ }^{\circ}\text{C}$  in diethylether to form the desired product **16** in 93 % yield (Scheme 2.7).



**Scheme 2.7.** Synthesis of **16** by addition of MeLi in diethylether.

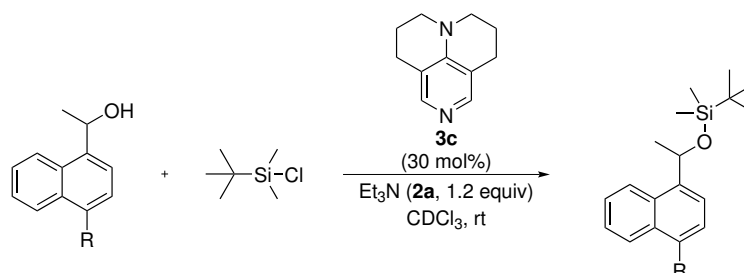
Based on the  $\sigma_p$ -parameters further alcohols might be of interest for synthesis which show either a moderate EDG, such as hydroxy ( $\sigma_p = -0.37$ ), or an EWG, such as trifluoromethyl ( $\sigma_p = +0.54$ ). Since for this study a strong donating group ( $\text{NMe}_2$ ,  $\sigma_p = -0.83$ ) as well as a deactivating, withdrawing group ( $\text{CN}$ ,  $\sigma_p = +0.66$ ) have been synthesized, a broad range of reactivity will be covered in terms of the *para*-substituent effect for the silylation reaction.

### 2.6.2 Kinetic Measurements of *para*-Substituted Secondary Alcohols

Aiming for further insight on the rate determining step of the silylation reaction this study might answer whether the attack of the oxygen on the silyl intermediate or the deprotonation of the hydroxy group is of bigger importance for the reaction rate. On one hand, it can be argued that electron donating groups (EDGs), such as dimethylamino ( $\sigma_p = -0.83$ ) or methoxy ( $\sigma_p = -0.27$ ), can increase the electron density close to the reaction center of the alcohol and therefore speed up the reaction rate. This would prefer the nucleophilic attack over the deprotonation. On the other hand, electron withdrawing groups (EWGs), like cyano ( $\sigma_p = +0.66$ ), can support the idea that the abstraction of the hydroxy proton is of higher importance for the rate.

## 2.6 Influence of *para*-Substituted Alcohols

Based on its high reactivity and good usability 9-azajulolidine (**3c**) has been chosen for this study as the Lewis base catalyst. The catalyst loading has been chosen at 30 mol% which is the upper limit for secondary alcohols, but is in a good range for taking precise measurements. For the reaction with non-modified secondary alcohol **5b** the reaction half-life of 159.9 min can be determined at 30 mol% catalyst loading (Scheme 2.8).



**Scheme 2.8.** Conditions for the kinetic measurements of *para*-substituted alcohols with TBSCl (**1a**), Et<sub>3</sub>N (**2a**) as auxiliary base, and 30 mol% **3c** as catalyst.

Slightly electron withdrawing groups, such as fluoro or bromo, lead to a small decrease in reaction rate, which is limited to a few minutes in the half-life time. For the reaction with the *para*-bromo (**13**) a reaction half-life of 164.4 min has been obtained and similar results can be observed for *para*-fluoro (**12**, 154.7 min). A mentionable decrease in rate can be observed for strong EDGs, such as cyano ( $\sigma_p = 0.66$ ), where a half-life time of (280.3 min) has been measured, which almost doubled the value obtained for secondary alcohol **5b**. The electron donating groups (EDGs) lead to an increase in rate for all studied compounds. Compounds with moderate EDG show already an noticeable increase in rate which, can be shown for *para*-methyl (**11**) with a reaction half-life of 117.3 min. As the strongest donor NMe<sub>2</sub> ( $\sigma_p = -0.83$ ) lead to a reaction half-life of 98.4 min, which is about one half of the one of secondary alcohol **5b**. All results are displayed in Table 2.6 in combination with the commonly used  $\sigma_p$ -parameters determined by Taft et al. in 1991.<sup>[130]</sup>

**Table 2.6.** Reaction half-lives of *para*-substituted secondary alcohols in combination with the  $\sigma_p$ -parameter. All data has been obtained by <sup>1</sup>H NMR measurements with catalyst **3c** in CDCl<sub>3</sub>.

R	No.	$\sigma_p$	$k_{\text{eff}}$ <b>5b</b> <sup>a</sup>	$t_{1/2}$ <sup>b</sup>
-NMe <sub>2</sub>	<b>16</b>	-0.83	$7.80 \cdot 10^{-03}$	$98.4 \pm 1.1$
-OMe	<b>15b</b>	-0.27	$6.71 \cdot 10^{-03}$	$114.4 \pm 1.0$
-Me	<b>11</b>	-0.17	$6.55 \cdot 10^{-03}$	$117.3 \pm 1.3$
-H	<b>5b</b>	0.00	$4.80 \cdot 10^{-03}$	$159.9 \pm 10.1$
-F	<b>12</b>	+0.06	$4.98 \cdot 10^{-03}$	$154.7 \pm 7.9$
-Br	<b>13</b>	+0.23	$4.67 \cdot 10^{-03}$	$164.4 \pm 2.8$

<sup>a</sup>  $k_{\text{eff}}$  in L mol<sup>-1</sup> s<sup>-1</sup>.

<sup>b</sup> Half-life time in min.



**Table 2.6.** Continuation.

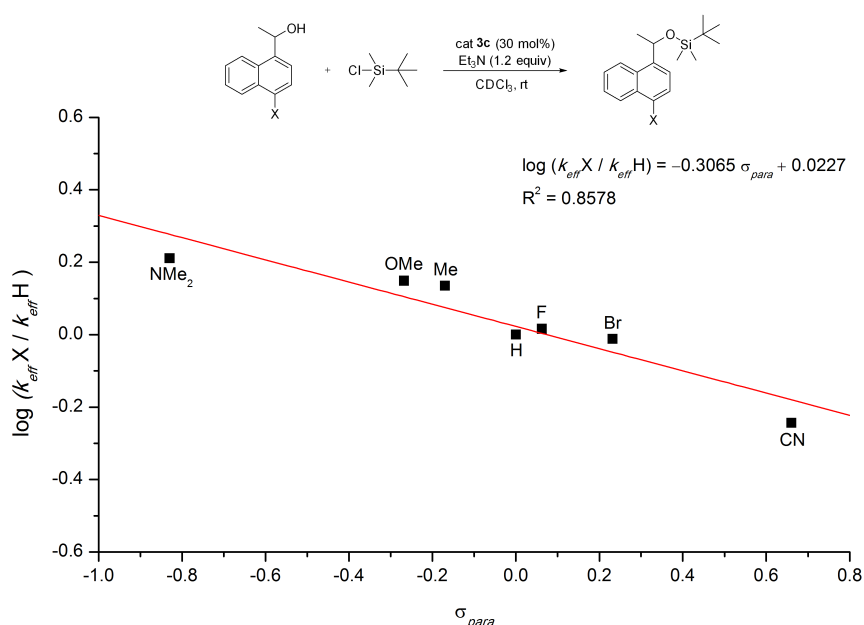
R	No.	$\sigma_p$	$k_{\text{eff}}$ <b>5b</b>	$t_{1/2}$
-CN	<b>14</b>	+0.66	$2.74 \cdot 10^{-03}$	$280.3 \pm 3.7$

<sup>a</sup>  $k_{\text{eff}}$  in L mol<sup>-1</sup> s<sup>-1</sup>.<sup>b</sup> Half-life time in min.

A formal analysis of the obtained rate data using the Hammett equation (2.6) leads to a linear correlation with a negative slope. The reaction constant  $\rho$  describes the susceptibility of the reaction to substituents, compared to the original ionization experiments of benzoic acid. A negative value for  $\rho$  of  $-0.3065$  implies that the reaction is accelerating when an EDG is attached in *para*-position of the substrate alcohol.

$$\log \left( \frac{k_{\text{eff}}X}{k_{\text{eff}}H} \right) = \rho \cdot \sigma \quad (2.6)$$

Even though the reaction center is not directly attached to the aromatic system, an influence on the reaction caused by the *para*-substituents and thus different electron densities is observed as can be seen Figure 2.16.



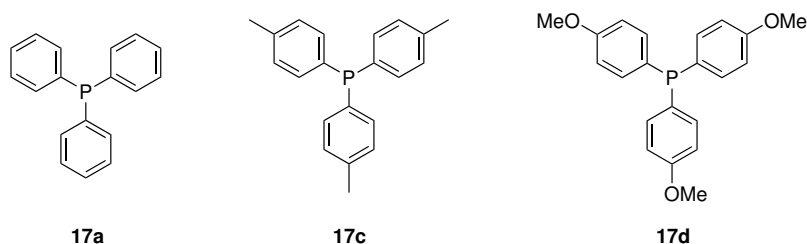
**Figure 2.16.** Hammett analysis for the silylation of various secondary alcohols with TBSCl (**1a**) with 30 mol% of **3c** in CDCl<sub>3</sub>.

The hypothesis that the attack of the alcohol to the silicon center is the rate determining step for

the silylation reaction can be supported by these results. Another study by Wiskur et al. strengthens this hypothesis, since EWGs attached to the *para*-position of triphenylsilyl chloride accelerate the silylation of secondary alcohols, while EDGs decrease the reaction rate.<sup>[97]</sup> Even though these results are contrary to the ones obtained in this study in terms of the influence of substituents, they support the same hypothesis. By removing electron density from the silicon center through EWGs the reaction rate is increased, which can be compared with increasing the electron density at the alcohol with EDGs, as shown before (Table 2.6). Both studies support the idea that the attack of the alcohol on the silicon center should be the rate determining step.

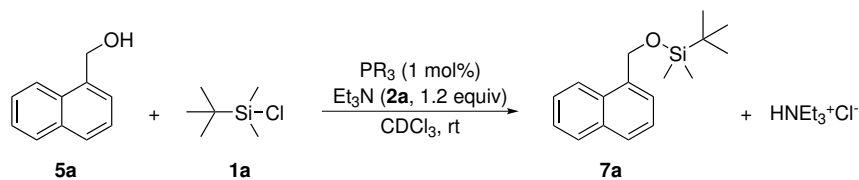
## 2.7 Alternative Lewis Base Catalysts for Silylation Reactions

It has been shown for several reactions, such as the *aza*-Morita-Baylis-Hillman reaction, that phosphanes can be effective Lewis base catalysts. Regarding the reaction rate, phosphanes can be similarly effective as the well established pyridine-based catalysts.<sup>[114,134]</sup> The question, whether phosphanes are suitable for silylation reactions, will be answered in this chapter.



**Figure 2.17.** Phosphane catalysts investigated for the silylation of primary alcohol **5a**.

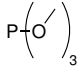
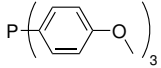
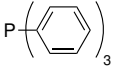
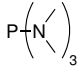
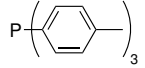
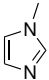
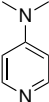
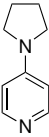
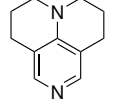
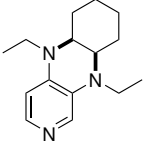
The reaction of alcohol **5a** has been investigated with well-known phosphane catalysts, such as triphenylphosphane (PPh<sub>3</sub>, **17a**), with a catalyst loading of 1 mol%. For PPh<sub>3</sub> (**17a**) a reaction half-life of 1700 min can be obtained, which is more than ten times slower as DMAP (**3a**, 124 min) under the same conditions (Scheme 2.9). The reaction with trimethyl phosphite (P(OMe)<sub>3</sub>, **17b**) as a catalyst lead to a slow half-life time of 3382 min. In order to increase the reaction rate, electron-enriched phosphanes, such as tri-*p*-tolylphosphane (P(*p*-Tol)<sub>3</sub>, **17c**) or tris(4-methoxyphenyl)phosphane (P(PhOMe)<sub>3</sub>, **17d**), have been used. By using P(*p*-Tol)<sub>3</sub> (**17c**) a gain in the reaction rate to a half-life time of 1201 min has been observed and can be increased further with P(PhOMe)<sub>3</sub> (**17d**) (577 min). An effort has been made to speed up the reaction by using strong nitrogen donors directly attached to the phosphorous atom with *N,N,N',N',N'',N''*-hexamethylphosphanetriamine (P(NMe<sub>2</sub>)<sub>3</sub>, **17e**). The increase in rate is good in comparison to **17d** with a half-life time of 225 min for **17e** (Table 2.7).



**Scheme 2.9.** Conditions for the kinetic measurements of primary alcohol (**5a**) with 1 mol% of various phosphanes as catalysts.

## 2.7 Alternative Lewis Base Catalysts for Silylation Reactions

**Table 2.7.** Reaction half-lives of **5a** with phosphorous- and nitrogen-based Lewis base catalysts obtained by  $^1\text{H}$  NMR data in  $\text{CDCl}_3$  at 1 mol% catalyst loading and silyl cation affinities (SCAs) relative to pyridine.

Catalyst	No.	SCA (gas) <sup>a</sup>	SCA (sol) <sup>b</sup>	$k_{\text{eff}}$ <sup>c</sup>	$t_{1/2}$ <sup>d</sup>
	<b>17b</b>	+36.9	+27.1	$2.27 \cdot 10^{-04}$	$3382.4 \pm 62.8$
	<b>17d</b>	−4.3	−14.4	$1.33 \cdot 10^{-03}$	$577.4 \pm 13.0$
	<b>17a</b>	−5.1	+2.1	$4.52 \cdot 10^{-04}$	$1700.7 \pm 81.7$
	<b>17e</b>	−5.7	−16.9	$3.41 \cdot 10^{-03}$	$225.2 \pm 4.6$
	<b>17c</b>	−21.0	−8.3	$6.39 \cdot 10^{-04}$	$1201.5 \pm 24.3$
<hr/>					
	<b>3e</b>	−36.4	−32.4	$2.71 \cdot 10^{-03}$	$283.9 \pm 2.6$
	<b>3a</b>	−57.0	−43.1	$6.30 \cdot 10^{-03}$	$123.9 \pm 0.0$
	<b>3b</b>	−64.8	−47.4	$8.46 \cdot 10^{-03}$	$90.8 \pm 0.7$
	<b>3c</b>	−75.6	−56.5	$1.76 \cdot 10^{-02}$	$43.6 \pm 1.3$
	<b>3g</b>	−93.2	−62.0	$1.68 \cdot 10^{-02}$	$45.7 \pm 0.2$

<sup>a</sup> SCA values (in  $\text{kJ mol}^{-1}$ ) have been calculated at MP2(FC)/G3MP2large//MPW1K/6-31+G(d) level.

<sup>b</sup> Solvation energies (in  $\text{kJ mol}^{-1}$ ) have been calculated at PCM/UAHF/MPW1K/6-31+G(d) level for  $\text{CHCl}_3$ .

<sup>c</sup>  $k_{\text{eff}}$  in  $\text{L mol}^{-1} \text{s}^{-1}$ .

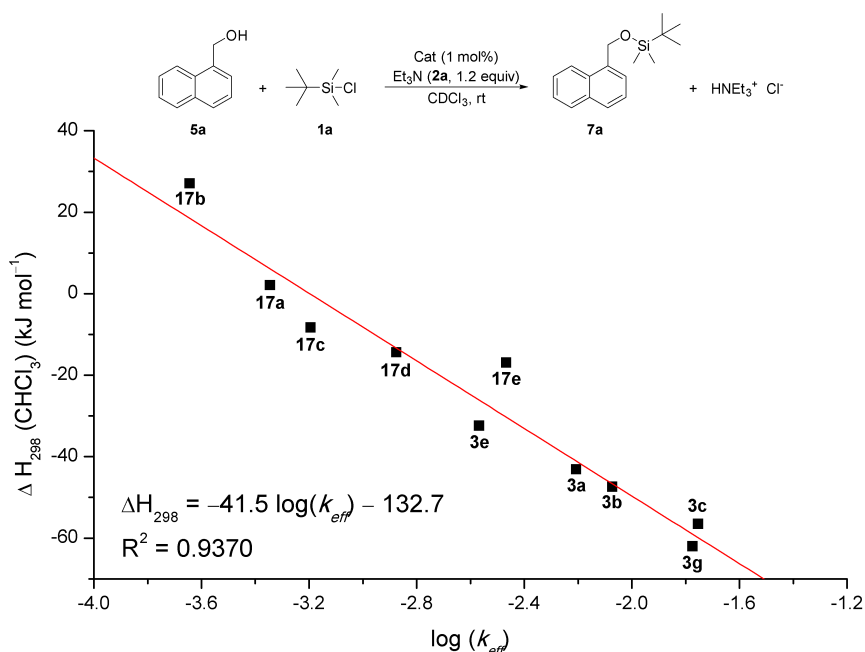
<sup>d</sup> Half-life time in min.

These results demonstrate that phosphanes can be used in silylation reactions in principle, but are not as effective as pyridines. To explain these results, one can easily argue with a less sterically favored intermediate formed with the catalyst and TBSCl (**1a**) during the catalytic cycle. All phosphanes are non-planar systems and therefore it is inevitable to create steric repulsion

between the *tert*-butyl group and one of the phosphane's substituents. This unfavorable steric demand of phosphanes is not that relevant for pyridine-based Lewis bases, because these are mostly planar systems. The fastest phosphane catalyst (**17e**, 225 min) is not only about two times slower than DMAP (**3a**, 124 min), but also highly toxic. Therefore, it cannot be advised to use phosphanes in silylation reactions.

### 2.7.1 SCA Values for Phosphane Catalysts

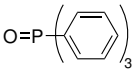
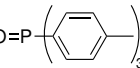
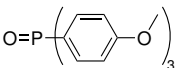
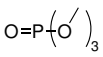

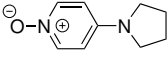
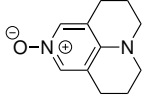
Even though, the reactivity of phosphanes have been moderate in comparison to pyridines, it is worth looking into the SCA values of this class of catalysts. As shown in Table 2.7 the affinity numbers of all phosphane catalysts are in general smaller ( $+30 \text{ kJ mol}^{-1} - -20 \text{ kJ mol}^{-1}$ ) than for the pyridines ( $-30 \text{ kJ mol}^{-1} - -70 \text{ kJ mol}^{-1}$ ), which is in accordance to the relative reaction rate. However, one needs to take into account that the rates have been obtained at 1 mol% catalyst loading and therefore they can only be compared to the pyridine at the same level of catalyst concentration (Table 2.7). Plotting the rates of all catalysts against the obtained SCA values leads to a linear correlation with  $R^2 = 0.9370$  (Figure 2.18). This result clearly shows that the SCA values are robust and can be used for different atoms at the reaction center. However, by taking a closer look at the plot, it becomes apparent that for the phosphanes alone (**17a–e**) an exponential fit might be possible as well. Similar SCA values for the catalysts **17d** ( $-14.4 \text{ kJ mol}^{-1}$ ) and **17e** ( $-16.9 \text{ kJ mol}^{-1}$ ) but different reaction rates lead to the conclusion that a saturation for phosphane might occur.



**Figure 2.18.** Correlation of thermodynamic data ( $\Delta H_{298}$ ) with kinetic data obtained for the reaction with **5a** at 1 mol% catalyst loading.

Moreover, it has been reported by Verkade et al. that phosphane-oxides can be used to catalyze silylation reactions.<sup>[135]</sup> Especially for electron-enriched phosphanes, which oxidize rather quickly, this might be an interesting perspective. In addition, two of the most commonly used pyridines, DMAP (3a) and PPY (3b), have been investigated in their oxidized form as catalysts.<sup>[136]</sup> In order to correlated the efficiency of these oxidized species with phosphanes and pyridines, SCA values have been calculated for selected compounds. In comparison to phosphanes (17a–e) phosphane oxides (18a–d) achieve higher stabilization energies of 50 kJ mol<sup>−1</sup> and therefore lower SCAs. This increase in stability can be explained by a different bonding situation or bonding partner, respectively. A bond between silicon and oxygen differs in several points from a Si–P-bond. First of all, the bond-length of 1.76 Å is much shorter than the average Si–P bond (2.35 Å), which is a sign of a different bonding situation. Secondly, the bond length of all pyridine oxides (19a–c) show the same values as for the phosphane oxides. However, the bond distance in Si–N-bonds is with 1.86 Å much shorter than in Si–P-bonds (Table 2.8).

**Table 2.8.** SCA values for oxydized phosphane and pyridine catalysts relative to pyridine.

Catalyst	No.	SCA (gas) <sup>a</sup>	SCA (sol) <sup>b</sup>	Bond Length (Si–O) <sup>c</sup>	Bond Length (Si–R) <sup>c</sup>
	<b>18a</b>	−80.5	−65.4	1.74	2.36
	<b>18b</b>	−94.5	−71.7	1.73	2.35
	<b>18c</b>	−106.7	−80.7	1.73	2.35
	<b>18d</b>	−13.3	−17.0	1.77	2.32
	<b>19a</b>	−87.2	−80.9	1.76	1.86
	<b>19b</b>	−95.6	−85.3	1.76	1.86
	<b>19c</b>	−102.8	−92.6	1.75	1.85

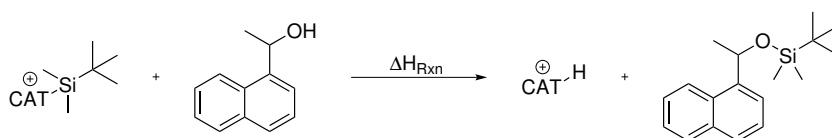
<sup>a</sup> SCA values (in kJ mol<sup>−1</sup>) have been calculated at MP2(FC)/G3MP2large//MPW1K/6-31+G(d) level.

<sup>b</sup> Solvation energies (in kJ mol<sup>−1</sup>) have been calculated at PCM/UAHF/MPW1K/6-31+G(d) level for CHCl<sub>3</sub>.

<sup>c</sup> Bond length in Å.

Besides the electronic situation, one might also consider steric repulsion as a reason for the increased stability of the oxides. For all phosphanes (17a–e) the reaction center is sterically demanding especially for a bulky group such as TBS. However, phosphane oxides contain an oxygen linker, which reduces the steric demand. Furthermore, it is well known that phospho-

rous is strongly oxophilic, as well as silicon, which explains the stability of these molecules.<sup>[137]</sup> Nonetheless, pyridine oxides obtain higher SCA values than pyridine catalysts, but the increase of  $20 \text{ kJ mol}^{-1}$  is smaller than for the phosphanes ( $40 \text{ kJ mol}^{-1}$ ). As well as for phosphanes, this increase can be explained by the oxophilicity of silicon. Even though the SCA values have been found to be good, it is not expected that these oxides perform very good in a kinetic measurements. Reasons for this hypothesis are based on the similarity between activated catalyst species and the final product. The benefit of breaking a Si–O-bond in order to form a new one seems to be rather small. In fact, calculations on MP2(FC)/GT3MP2large//MPW1K/6-31+G(d) level of theory in this matter show that the equilibrium for a transfer of the activated silyl group to the alcohol is focused on the starting material side (Scheme 2.10).

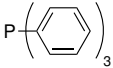
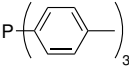
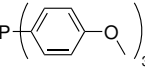
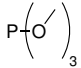
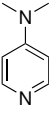
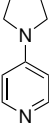
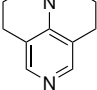


**Scheme 2.10.** Silyl group transfer reaction ( $\Delta H_{\text{Rxn}}$ ) from the activated catalyst species to the desired silyl ether.

For the pyridine compounds (**3a–c**) the enthalpies for this reaction in solution are found to be in the area of  $-40 \text{ kJ mol}^{-1}$ , while for the corresponding oxides values of  $+6 \text{ kJ mol}^{-1}$  have been obtained. The difference of more than  $40 \text{ kJ mol}^{-1}$  strengthens the doubt that a fast reaction with these compounds is possible. The differences between phosphanes (**17a–e**) and the corresponding oxides (**18a–d**) are in accordance to the trend observed for the pyridines. While for phosphanes the equilibrium is favored on the product side with enthalpies of around  $-50 \text{ kJ mol}^{-1}$ , the corresponding oxides have shown to be roughly  $100 \text{ kJ mol}^{-1}$  less stable and therefore not yielding into the desired product. In general, it can be stated that phosphanes and pyridines are equally up to the task with similar reaction enthalpies, while for phosphane oxides values of around  $+50 \text{ kJ mol}^{-1}$  lead to the conclusion that these systems are not able to form the final product. For pyridine oxides the values are found in an area around  $+6 \text{ kJ mol}^{-1}$ , where the reaction could still proceed with a possible influence of an auxiliary base.

## 2.7 Alternative Lewis Base Catalysts for Silylation Reactions

**Table 2.9.** Reaction enthalpies ( $\Delta H_{\text{Rxn}}$ ) for oxydized phosphane and oxydized pyridine catalysts relative to not oxidized species.

System	No.	Pyridines / Phosphanes		No.	Oxides	
		$\Delta H_{\text{Rxn}}$ (gas) <sup>a</sup>	$\Delta H_{\text{Rxn}}$ (sol) <sup>b</sup>		$\Delta H_{\text{Rxn}}$ (gas) <sup>a</sup>	$\Delta H_{\text{Rxn}}$ (sol) <sup>b</sup>
	<b>17a</b>	−43.0	−46.7	<b>18a</b>	+50.2	+2.1
	<b>17c</b>	−49.3	−50.7	<b>18b</b>	+45.6	+48.2
	<b>17d</b>	−49.9	−77.7	<b>18c</b>	+52.3	+13.6
	<b>17b</b>	−52.4	−51.7	<b>18d</b>	+43.3	+47.3
	<b>3a</b>	−15.5	−42.7	<b>19a</b>	+18.4	+6.6
	<b>3b</b>	−17.5	−40.3	<b>19b</b>	+16.5	+6.0
	<b>3c</b>	−17.9	−36.2	<b>19c</b>	+15.1	+6.4

<sup>a</sup> SCA values (in kJ mol<sup>−1</sup>) have been calculated at MP2(FC)/G3MP2large//MPW1K/6-31+G(d) level.

<sup>b</sup> Solvation energies (in kJ mol<sup>−1</sup>) have been calculated at PCM/UAHF/MPW1K/6-31+G(d) level for CHCl<sub>3</sub>.

Based on the data shown in this chapter, one can conclude that neither phosphanes nor phosphane oxides will be a good choice as catalysts for the silylation reaction. Even though the reactivity of P(NMe<sub>2</sub>)<sub>3</sub> (**17e**) has been reasonably fast for the silylation reaction, it can be excluded for general use because of its toxicity. Nonetheless, the results for the pyridine oxides might show a decrease in reactivity but might offer an opportunity in terms of selectivity. Since the reaction center has moved to an oxygen atom, which is slightly removed from the pyridine ring, one can think of modifying the 2-position. A decrease of reaction rate has been observed for in 2-position modified pyridine-based Lewis bases for the acylation of various alcohols in several studies.<sup>[20,138,139]</sup> However, for silylation reactions these catalyst systems (**19a–c**) might be used in kinetic resolution experiments when groups with specific stereo information are implemented in this position, as it has been demonstrated for acylation reactions.<sup>[19,83,140,141]</sup>







### 3 Leaving Group Effects on the Selectivity of the Silylation Reaction

It has been shown in the previous chapter that the silylation of alcohols can be strongly influenced in rate and selectivity by factors such as catalyst, auxiliary base, and choice of solvent. This chapter will focus on the most important part of the silylation reaction, which is the reagent transferring the silyl group. The often employed TBSCl (**1a**) combines a silyl group of intermediate size with a leaving group of moderate reactivity. The latter is compatible with a number of activation protocols, of which the 'Corey procedure' involving DMF as solvent and imidazole (**3d**) as base is the most common one. Other protocols of Lewis base-catalyzed activations in apolar, organic solvents with Et<sub>3</sub>N (**2a**) as auxiliary base have been developed and can be seen as an alternative to Corey's procedure. In organic synthesis, especially for sterically demanding targets, *tert*-butyldimethylsilyl triflate (**1b**) is often used as a reagent because of the high reactivity of the triflate leaving group.<sup>[49]</sup> The difference in reactivity between primary and secondary alcohols has already been discussed in detail for TBSCl in the previous chapter. This chapter will focus on the effect of the leaving groups present in *tert*-butyldimethylsilyl chloride (TBSCl, **1a**), *tert*-butyldimethylsilyl triflate (TBSOTf, **1b**), *tert*-butyldimethylsilyl cyanide (TBSCN, **1c**), *N*-*tert*-butyldimethylsilyl-*N*-methyltrifluoroacetamide (MTBSTFA, **1d**) and *tert*-butyldimethylsilyl imidazole (TBSImi, **1e**). All these reagents have been studied, at least in part, for their applicability towards protection group chemistry (Figure 3.1).<sup>[3,49,56,58,142,143]</sup>

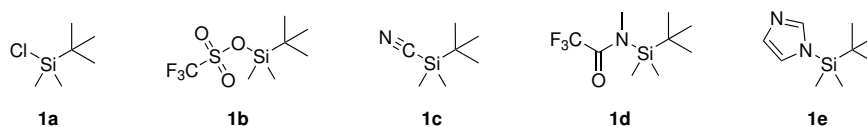


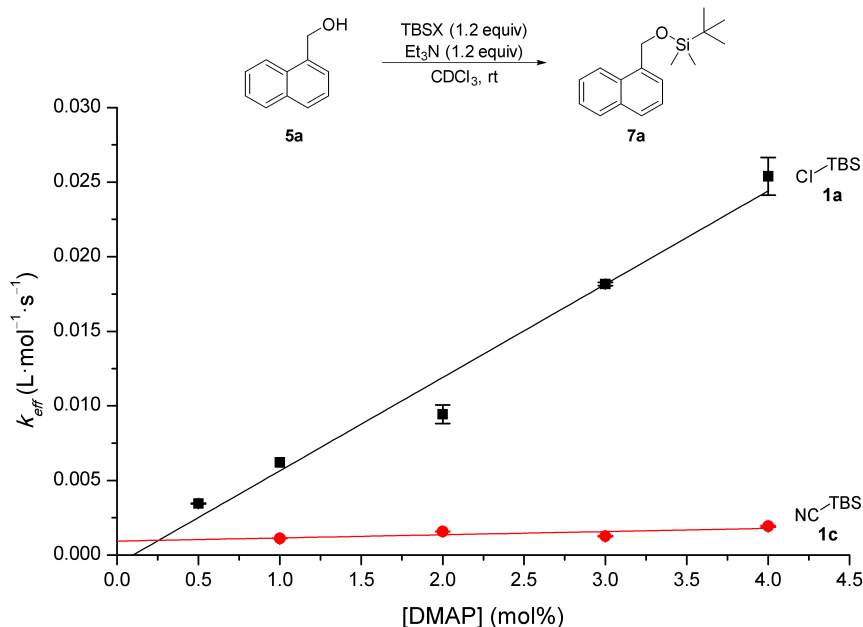
Figure 3.1. Selected *tert*-butyldimethyl silyl reagents with various leaving groups.

#### 3.1 Influence of the Leaving Group on the Reaction Rate

Initial experiments focus on the reaction of TBSCl (**1a**), TBSOTf (**1b**), and TBSCN (**1c**) with primary alcohol **5a** under the same reaction conditions as shown in Chapter 2. The use of various catalyst loadings of DMAP (**3a**) in CDCl<sub>3</sub> for TBSCl (**1a**) and TBSCN (**1c**) leads to a linear correlation for both reagents. The difference in reactivity can be illustrated through the reaction half-lives of 30.2 min for TBSCl (**1a**) and 392.8 min for TBSCN (**1c**), which is a decrease of about one order of magnitude by changing the silyl reagent (Figure 3.2). Due to the high reactivity of TBSOTf (**1b**) it has not been possible to determine absolute rates in a similar way as for TBSCl (**1a**) or TBSCN (**1c**). Reactions in DMF-d<sub>7</sub> with primary alcohol (**5a**) have been found to be too fast for accurate direct rate measurements for all reagents (**1a–1e**). It is worth noting that a de-

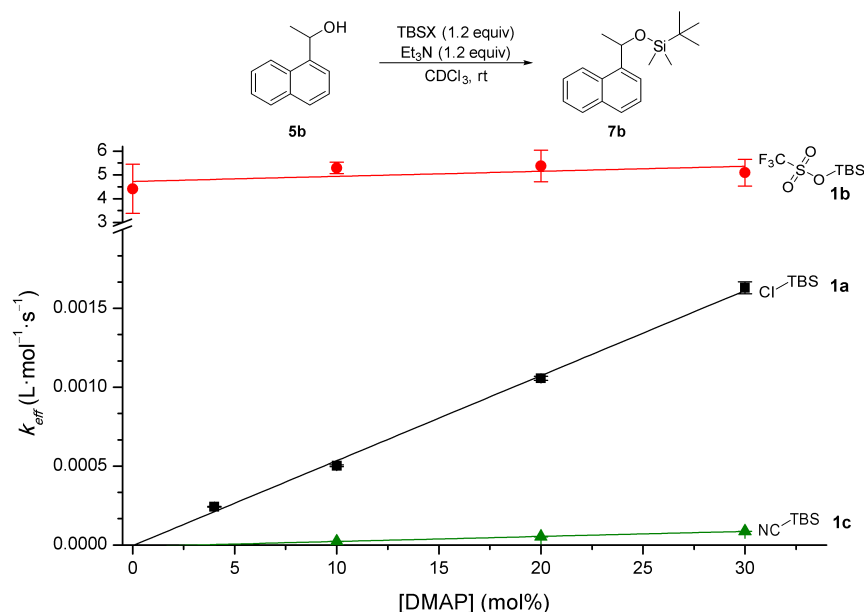
### 3.1 Influence of the Leaving Group on the Reaction Rate

crease in rate of one order of magnitude can also be observed when changing from a primary to a secondary alcohol for the reagents TBSCl (**1a**) and TBSCN (**1c**) in CDCl<sub>3</sub>.



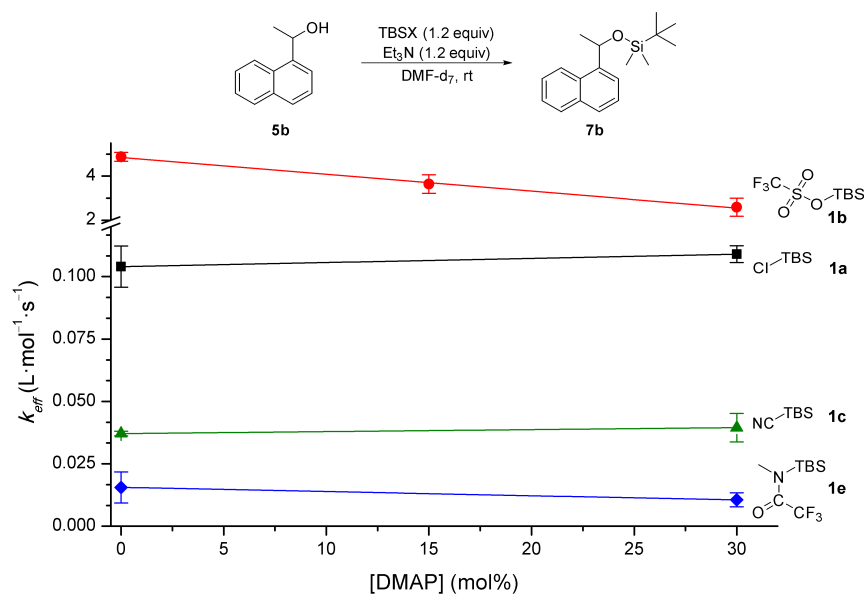
**Figure 3.2.** Influence of catalyst concentration (DMAP, **3a**) on the silylation of primary alcohol **5a** with TBSCl (**1a**) and TBSCN (**1c**) in CDCl<sub>3</sub>.

In order to make absolute rate measurements possible for fast reagents, the secondary alcohol **5b** has been used in CDCl<sub>3</sub> or DMF-d<sub>7</sub> with up to 30 mol% of DMAP (**3a**) as catalyst and Et<sub>3</sub>N (**2a**, 1.2 equiv) as auxiliary base. As well as for the primary alcohol **5a**, a decrease in the reaction rate of about one order of magnitude can be determined for TBSCl (**1a**) and TBSCN (**1c**). The reaction half-lives can be obtained as 471.1 min for TBSCl (**1a**) and 8832 min for TBSCN (**1c**). In comparison to TBSCl (**1a**) and TBSCN (**1c**), MTBSTFA (**1d**) performed poorly with a half-life time of over 10 d. Very little conversion can be observed under these conditions for silyl imidazole (TBSImi, **1e**), which has been estimated to react one order of magnitude slower than MTBSTFA (**1d**). TBSOTf (**1b**) reacts faster than any other reagent. The reaction with secondary alcohol **5b** is completed within minutes independent of the solvent, which has a big influence on the other reagents (Table 3.1). For the less reactive reagents **1a**, **1c**, and **1d** the rate in DMF-d<sub>7</sub> is increased by two orders of magnitude compared to that in CDCl<sub>3</sub>, while for TBSOTf (**1b**) the reaction rates are comparable in both solvents. Additional experiments in CDCl<sub>3</sub> demonstrate that the rate of reaction of TBSOTf (**1b**) is independent of the catalyst concentration, in significant contrast to the first-order dependence observed for the reagents TBSCl (**1a**) and TBSCN (**1c**). The reaction proceeds to full conversion even though no catalyst has been present, which implies that the strongly activated reagent TBSOTf (**1b**) undergoes a direct and therefore uncatalyzed reaction with the substrate alcohol **5b** (Figure 3.3).



**Figure 3.3.** Influence of catalyst concentration (DMAP, **3a**) on the silylation of secondary alcohol **5b** with various silylation reagents in  $\text{CDCl}_3$ .

An analogous set of measurements has been performed for alcohol **5b** in  $\text{DMF-d}_7$  as solvent and  $\text{Et}_3\text{N}$  (**2a**) as auxiliary base. This leads to the same absolute rates as in  $\text{CDCl}_3$  for TBSOTf (**1b**) that hardly depends on the DMAP (**3a**) concentration. One can even imagine that the reaction with TBSOTf (**1b**) is hindered by the presence of DMAP (**3a**) as Lewis base, which is indicated by a small decrease in rate at higher catalyst loadings (Figure 3.4).



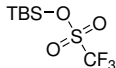
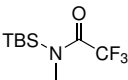
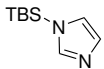
**Figure 3.4.** Influence of catalyst concentration (DMAP, **3a**) on the silylation of secondary alcohol **5b** with various silylation reagents in  $\text{DMF-d}_7$ .

### 3.2 Determination of Selectivity

In DMF-d<sub>7</sub> as a solvent, the Lewis base catalyst has no notable effect on TBSCl (**1a**), TBSCN (**1c**), and MTBSTFA (**1d**), since the respective reaction rates remain practically unchanged after addition of 30 mol% DMAP (**3a**) as a catalytic Lewis base (Figure 3.4). TBSImi (**1e**) shows almost no turnover under these conditions and the half-life time can only be estimated based on the conversion in comparison with MTBSTFA (**1d**) to be 833.8 min (Table 3.1).

To compare the reactivity between the investigated leaving groups, the data of the direct rate measurements with secondary alcohol **5b** are summarized in Table 3.1. These results already show that the choice of the silyl reagent can have an influence on the reaction rate. Furthermore, one needs to differentiate between the moderately active reagents, such as TBSCl (**1a**) and TBSCN (**1c**) and highly reactive reagents, like TBSOTf (**1b**). It has been shown that highly reactive reagents can neither be influenced by a Lewis base catalyst, nor by an interacting solvent, while for the less reactive reagents the difference is huge.

**Table 3.1.** Rate data for the silylation of **5b** with 30 mol% DMAP (**3a**) as catalyst for various leaving groups in CDCl<sub>3</sub> and DMF-d<sub>7</sub>.

Reagent	No.	$k_{\text{eff}}$ (CDCl <sub>3</sub> ) <sup>a</sup>	$t_{1/2}$ (CDCl <sub>3</sub> ) <sup>b</sup>	$k_{\text{eff}}$ (DMF-d <sub>7</sub> ) <sup>a</sup>	$t_{1/2}$ (DMF-d <sub>7</sub> ) <sup>b</sup>
	<b>1b</b>	5.1	0.15 ± 0.01	4.1	0.2 ± 0.1
TBS-Cl	<b>1a</b>	1.6 · 10 <sup>-03</sup>	471.1 ± 10	1.1 · 10 <sup>-01</sup>	7.2 ± 0.2
TBS-C≡N	<b>1c</b>	8.7 · 10 <sup>-05</sup>	8832 ± 23	4.9 · 10 <sup>-02</sup>	19.4 ± 2.9
	<b>1d</b>	4.9 · 10 <sup>-05</sup>	15682 ± 45	1.1 · 10 <sup>-02</sup>	72.6 ± 20.0
	<b>1e</b> <sup>c,d</sup>	4.1 · 10 <sup>-06</sup>	1.87 · 10 <sup>+06</sup>	1.1 · 10 <sup>-03</sup>	833.8

<sup>a</sup>  $k_{\text{eff}}$  in L mol<sup>-1</sup> s<sup>-1</sup>.

<sup>b</sup>  $t_{1/2}$  in min.

<sup>c</sup> Based on 4.4 % after 10 d in CDCl<sub>3</sub>.

<sup>d</sup> Based on 6.4 % after 120 min in DMF-d<sub>7</sub>.

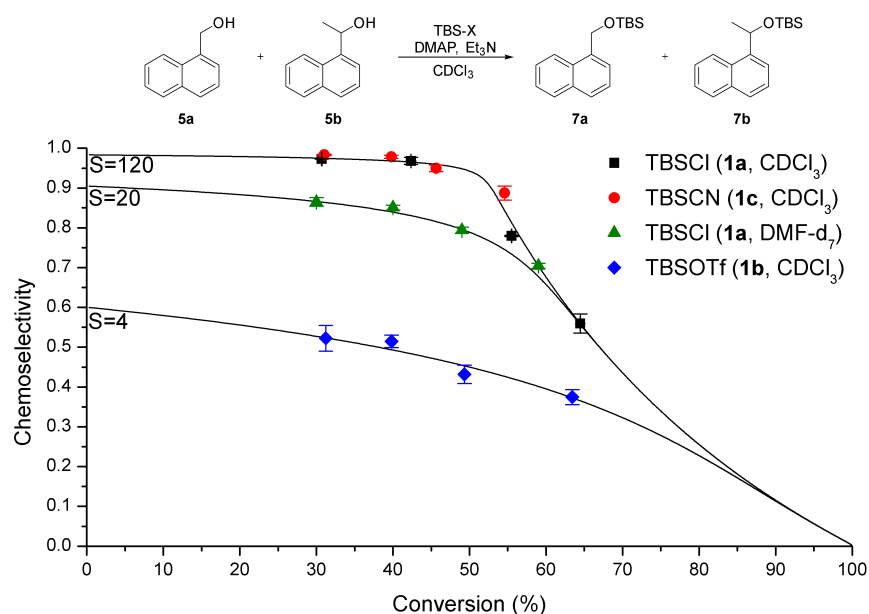
### 3.2 Determination of Selectivity

As mentioned before, direct rate measurements are not possible for primary alcohol **5a**, due to the high reaction rates and limitation in <sup>1</sup>H NMR spectroscopy. In order to determine the selectivity of the leaving groups, competition experiments have been performed. These experiments employ equimolar mixtures of both alcohols **5a** and **5b** and the underlying reaction kinetics are thus directly comparable to those of kinetic resolution experiments. It is known that the selectivity for this kind of experiment depends on the conversion and therefore on the amount

of silyl reagent.<sup>[87,144]</sup> Accordingly, the experiments have been performed with several different amounts of silyl reagents. The selectivity of the reagents has been measured in chemoselectivity (*C*) as a function of turnover of both substrate alcohols **5a** and **5b** and is expressed in Equation 3.1. The displayed data has been obtained by GC and <sup>1</sup>H NMR measurements (see Chapter 8 for more details).

$$C = \frac{[7a] - [7b]}{[7a] + [7b]} \quad (3.1)$$

For highly selective reactions the turnover curve is characterized by chemoselectivities *C* just below 1.0 for the first 50 % turnover and a subsequent systematic decline to *C* = 0.0 afterwards. With help of the program CoPaSi, simulations at various selectivities have been prepared to clarify the differences between the reagents.<sup>[145]</sup> It has been shown in Chapter 2.3.2 that good selectivity (primary over secondary alcohol) of around *S* = 120 can be achieved in Lewis base catalyzed silylation reactions in CDCl<sub>3</sub>. For the highly selective silylation using TBSCl (**1a**) with 4 mol% DMAP (**3a**) as catalyst and Et<sub>3</sub>N (**2a**, 1.2 equiv) as auxiliary base, it has been observed that primary alcohol **5a** turns over almost completely before secondary alcohol **5b** commences at a conversion >50 %. The selectivity *S*, which is the ratio of reaction rates for **5a** and **5b**, has been described earlier (Equation 2.4). The data points located in the critical region between 30 % and 70 % turnover can be fitted nicely with a selectivity value *S* = 120, simulated for various *S* values with CoPaSi. The obtained data is in good accordance to the results from previous direct kinetic measurements for alcohols **5a** and **5b**, thus confirming the validity of the relative rate measurements obtained here (Figure 3.5).



**Figure 3.5.** Competition experiments performed for **1a**, **1b**, and **1c** in CDCl<sub>3</sub> and DMF-d<sub>7</sub> with 4 mol% DMAP (**3a**).

### 3.2 Determination of Selectivity

Under these conditions the same high selectivity ( $S = 120$ ) can be obtained for TBSCN (**1c**), while the value obtained for TBSOTf (**1b**) is below  $S = 4$ . The difference in terms of selectivity between TBSCl (**1a**) and TBSOTf (**1b**) can be connected to the previous results concerning the reaction rate for the secondary alcohol (**5b**). While TBSOTf (**1b**) can transform a secondary alcohol (**5b**) rapidly without any catalyst, TBSCl (**1a**) is in need of a Lewis base catalyst to proceed with the reaction (Figure 3.3). Even though the reactivity-selectivity-principle was limited by the authors (Mayr and Ofial) to very fast reactions ( $k = >10^8 \text{ L mol}^{-1} \text{ s}^{-1}$ ), it is compelling to use that principle for this reaction.<sup>[146]</sup> While slow reagents, such as TBSCl (**1a**), lead to high selectivity ( $S = 120$ ), TBSOTf (**1b**) as a fast reagent ends at  $S = 4$ . However, one might argue that TBSOTf (**1b**) undergoes a direct reaction and needs no further activation of any kind which leads to the conclusion that the reaction pathway for TBSOTf (**1b**) is different from the one of TBSCl (**1a**). The experiment has been repeated in DMF- $d_7$  as a Lewis basic solvent with TBSCl (**1a**) which leads to a significantly lower selectivity of  $S = 20$ . As for the silylation before this number is in line with previous observations based on direct rate measurements (see Figure 2.10 on page 29). Whether the selectivity of the highly reactive TBSOTf (**1b**) can be increased through moving to lower reaction temperatures, has finally been addressed in competition experiments using 1 : 1 mixtures of the alcohols **5a** and **5b** in  $\text{CD}_2\text{Cl}_2$  at +20, 0, and  $-78^\circ\text{C}$ . A small increase in selectivity can be observed when reducing the reaction temperature from  $+20^\circ\text{C}$  ( $S = 4$ ) to  $0^\circ\text{C}$  ( $S = 6$ ). The selectivity is increased further to  $S = 15$  for a reaction at  $-78^\circ\text{C}$ , which is still less selective than the transformation in DMF with  $S = 20$  (Figure 3.6).

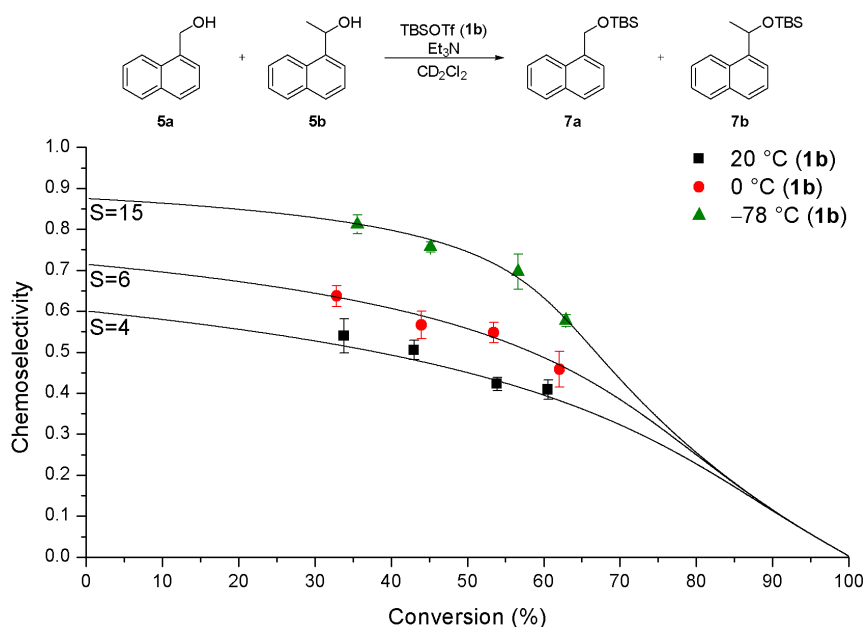
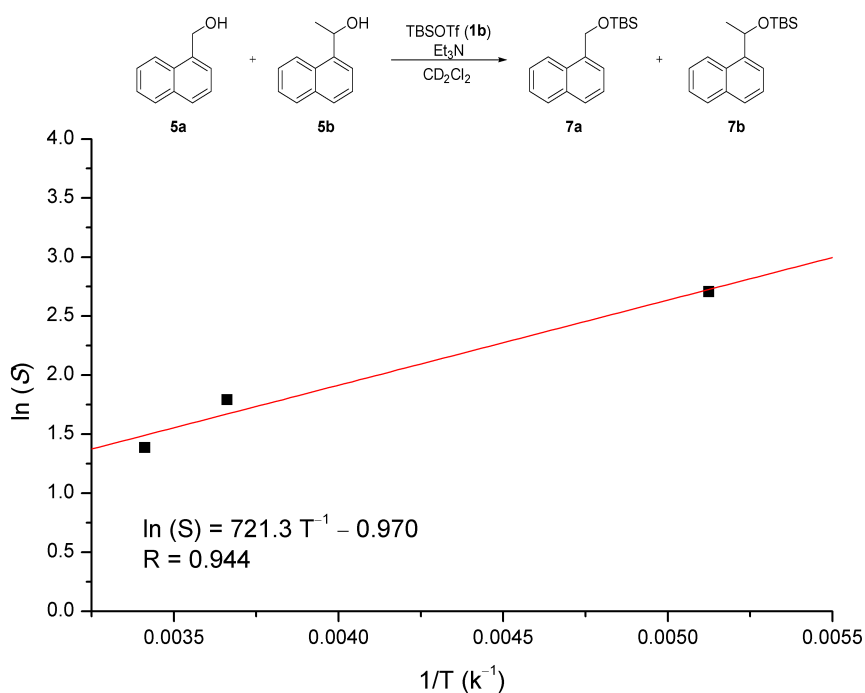


Figure 3.6. Temperature-dependent competition experiments with TBSOTf (**1b**) in  $\text{CD}_2\text{Cl}_2$ .



Using the obtained selectivities at different reaction temperatures an Eyring analysis can be performed, in which not the reaction rates but the selectivity ( $S = k_{\text{eff}}(\mathbf{5a})/k_{\text{eff}}(\mathbf{5b})$ ) can be used (see Chapter 8 for a full derivation). The analysis leads to a difference in activation enthalpy ( $\Delta\Delta H^\ddagger$ ) of  $+6.0 \text{ kJ mol}^{-1}$  and  $-8.1 \text{ J K}^{-1} \text{ s}^{-1}$  for the activation entropy ( $\Delta\Delta S^\ddagger$ ). These results are in accordance to the experimentally obtained reaction rates. Based on a smaller activation barrier of  $6.0 \text{ kJ mol}^{-1}$  it is plausible that the rates of primary alcohol **5a** are faster than for secondary alcohol **5b**. The activation entropy ( $\Delta S^\ddagger$ ) for the primary alcohol (**5a**) is about  $8.1 \text{ J K}^{-1} \text{ s}^{-1}$  smaller than for the secondary alcohol (**5b**), which should not influence the reaction very much. Even though the Eyring plot is only based on three measurements one can estimate a reaction temperature in order to achieve the selectivity of  $S = 120$ , which should be achieved at a temperature of  $-148^\circ\text{C}$ . However, this result is purely of academic interest and cannot be employed in organic synthesis based on no suitable solvent and possible solubility issues.

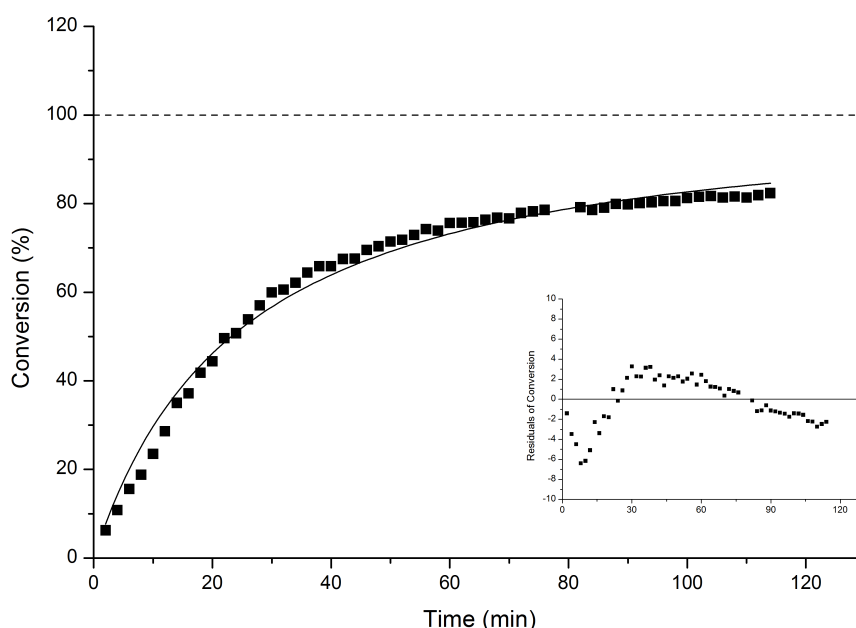


**Figure 3.7.** Eyring plot of the selectivity between  $k_{\text{eff}}(\mathbf{5a})$  and  $k_{\text{eff}}(\mathbf{5b})$ .

It can be concluded that the most reactive reagent (TBSOTf, **1b**) is the least selective ( $S = 4$ ) in differentiating between primary and secondary alcohol **5a** and **5b**. Comparatively low selectivities are also found when employing the (catalytically active) Lewis base solvent DMF-d<sub>7</sub> with a selectivity value of  $S = 20$ . Furthermore, it can be stated that selectivity cannot be achieved by highly reactive reagents even at low temperature, but only by using a moderately active reagent through a Lewis base activation mechanism in an apolar solvent.

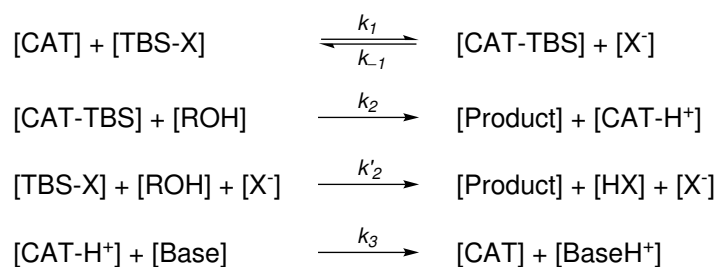
### 3.2.1 Possible Effects of Autocatalysis

In order to understand the strong deviations of some plots for the measurements in DMF-d<sub>7</sub>, for instance with TBSCN (**1c**) with no catalyst, an effort has been made to estimate the reaction rates by simulations using the program CoPaSi. In Figure 3.8 the standard fitting functions (Equation 2.1, page 15) is used and a deviation of the fit can be observed. The reaction proceeds to slow at the beginning and is not fast enough for the fitting function in the end, which can be observed in the residuals of this fit. A possible explanation is an autocatalytic pathway, where the reagents need more time to start the transformation. A typical S-shaped curve, as is common for autocatalytic reactions, could be observed in this reaction to some extent.



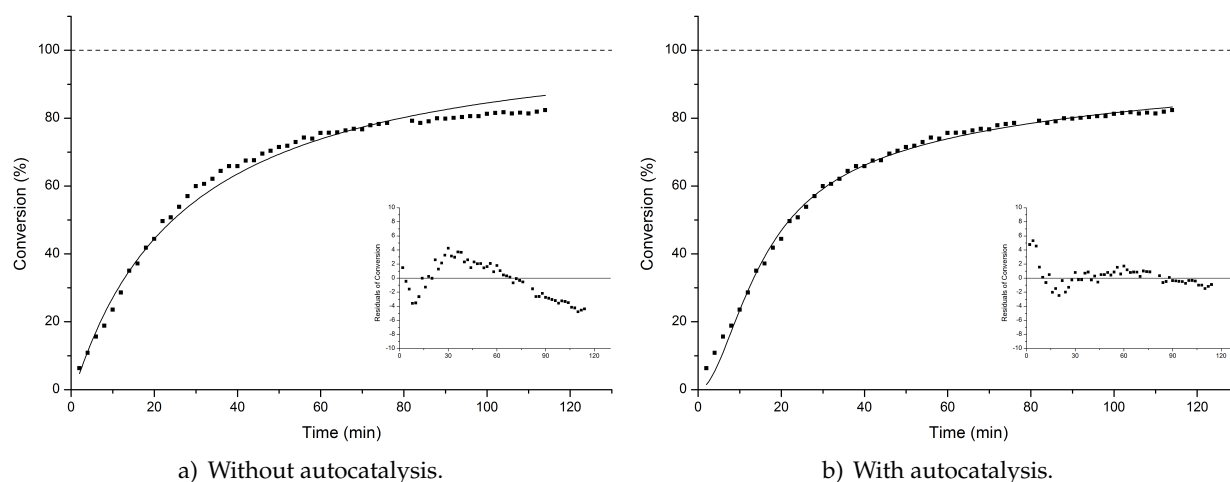
**Figure 3.8.** Time vs. conversion plot of secondary alcohol **5b** and TBSCN (**1c**) in DMF-d<sub>7</sub>.

Using CoPaSi as an analysis tool, all reactions of the mechanism have been included. For all simulations  $k_3$ , the reactivation of the catalyst, has been set as a fixed value ( $k_3 = 100$ ) and all starting values have been chosen randomly by the program for all remaining rates ( $k_1$ ,  $k_{-1}$ ,  $k_2$  and  $k'_2$ ). All settings and initial concentrations for CoPaSi are identical to the actual experimental setup. Furthermore, experimental data has been included in order to estimate the  $k$  values of each reaction with a higher accuracy. It is worth noting that the rates, obtained by CoPaSi, cannot be compared to the  $k_{eff}$  from the fitting functions, since  $k_{eff}$  can only be seen as a mixture of all rates for the whole mechanism.



**Scheme 3.1.** Mechanism used to describe the silylation reaction for a simulation with CoPaSi.

The estimated fit by CoPaSi for the obtained experimental data (Figure 3.9a) shows a similar deviation as for the fitting function (Figure 3.8). By adding the autocatalysis option ( $k'_2$ ), the fit can be significantly improved especially for later parts of the reaction (Figure 3.9b).

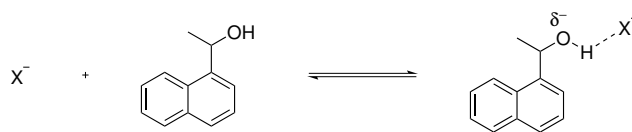


**Figure 3.9.** Simulation with CoPaSi for the experimentally obtained data of TBSCN (**1c**) in DMF- $d_7$ .

The plots shown in Figure 3.9 suggest that autocatalysis might be an alternative pathway for the silylation reaction under these conditions. To understand the autocatalysis pathway one can consider an equilibrium between the alcohol substrate and the basic anion, in which the anion is close to the hydroxy group and generates a negative partial charge at the oxygen center (Scheme 3.2). As mentioned earlier the attack of the alcohol is most likely the rate determining step and thus the anion would increase the reaction rate by slightly activating the substrate. It is beneficial for this pathway when the anion is strongly basic and is not influenced by the protonated auxiliary base which is formed during the reaction process. However, it should be noted that a Lewis base catalyst is still needed to attack the silyl reagent and form an intermediate and a counterion.

### 3.2 Determination of Selectivity

---



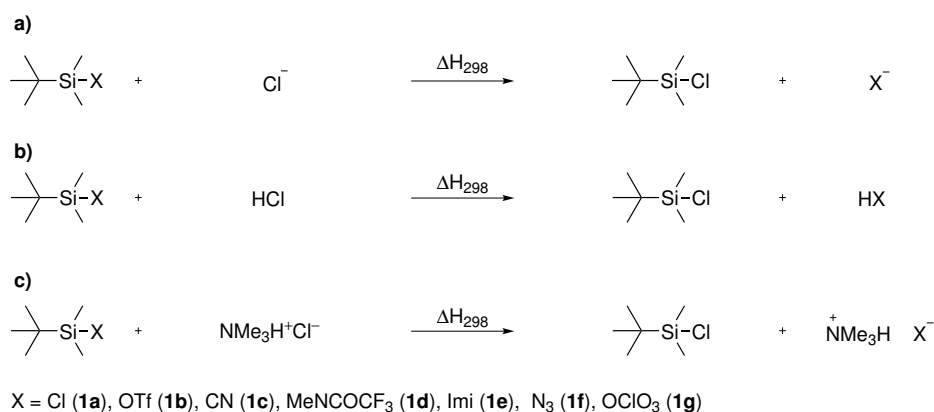
**Scheme 3.2.** Possible interaction between an basic anion and substrate alcohol **5b**.

The effect of the autocatalytic pathway is observed only for very slow reagents and can be determined as a small effect. The reaction half-life can be determined with the standard fitting functions for TBSCN (**1c**) in DMF- $d_7$  with no catalyst at 20.7 min. For the same data analyzed with CoPaSi without an autocatalysis option leads to 24.5 min, while with autocatalysis a half-life time of 22.1 min is obtained. All numbers are in a comparable range and thus it can be stated that the autocatalysis is only of minor importance concerning the reaction half-life. It is not possible to determine the exact rates for every reaction step, since the measured rates can only be seen as a mixture of all  $k$  values. It should be noted that using CoPaSi as a tool for analyzing the kinetic measurements is much more time-consuming than the approach with a fitting function. For slow leaving groups one has to consider a higher preference to the autocatalysis pathway and therefore a small change in the reaction rates.

### 3.3 Theoretical Studies on the Leaving Group Effect

In addition to the obtained experimental data, the effects of the leaving groups have been investigated with theoretical methods using MP2(FC)/G3MP2large//MPW1K/6-31+G(d) level of theory in combination with the SMD continuum solvation model in chloroform. These studies also include *tert*-butyldimethylsilyl azide (TBSN<sub>3</sub>, **1f**) and *tert*-butyldimethylsilyl perchlorate (TBSOCIO<sub>3</sub>, **1g**).<sup>[57,147]</sup> The aim of this study is a better understanding of the effect of leaving groups in terms of the basicity and in order to modify a silyl reagent for a specific purpose.

The first approach contains an anion exchange reaction for different TBS–X compounds with a chloride anion (Scheme 3.3). Since the exchange is made with a chloride anion, TBSCl (**1a**) is used as a reference here. One can observe a trend for the anion transfer reaction in which TBSOTf (**1b**) and TBSOCIO<sub>3</sub> (**1g**) show the highest anion stabilization with  $-136.26 \text{ kJ mol}^{-1}$  and  $-108.17 \text{ kJ mol}^{-1}$ , respectively. For TBSCN (**1c**), TBSImi (**1e**), and TBSN<sub>3</sub> (**1f**) the anion transfer reaction is destabilized up to  $+33.44 \text{ kJ mol}^{-1}$  for TBSImi (**1e**). These results seem to be reasonable that for the acidic anions with possible mesomeric stabilization (**1b** and **1g**) the highest numbers have been obtained, while basic reagents (**1c** and **1e**) show a smaller driving force. The addition of solvation corrections lead to similar results, in which triflate (**1b**) and perchlorate (**1g**) have the highest driving force. For nitrogen-based reagents such as MTBSTFA (**1d**) and TBSImi (**1e**) the strongest effect within the solvation model can be observed as a destabilization of about  $30 \text{ kJ mol}^{-1}$  for TBSImi (**1e**) and  $45 \text{ kJ mol}^{-1}$  for MTBSTFA (**1d**) (Table 3.2).



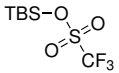
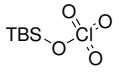
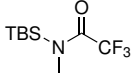
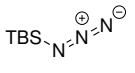
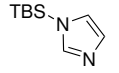
**Scheme 3.3.** Calculated reaction enthalpies for a) anion exchange reaction; b) protonated anion exchange; c) addition of auxiliary base for different leaving groups of *tert*-butyldimethylsilyl compounds.

It becomes apparent that the observed trend switches for the second reaction in which a proton is added to the equation. TBSOTf (**1b**) and TBSOCIO<sub>3</sub> (**1g**) are found to be the least stabilized compounds, while strong stabilization is observed for MTBSTFA (**1d**) with  $-60.61 \text{ kJ mol}^{-1}$  and TBSCN (**1c**) with  $-51.73 \text{ kJ mol}^{-1}$ . These results can be explained by the fact that triflate and perchlorate are strong acids and try to avoid the presence of a proton, while the basic

amide (MTBSTFA, **1d**) achieves a higher stabilization. Thus, the driving force for TBSOTf (**1b**) and TBSOClO<sub>3</sub> (**1h**) is rather small and leads to a reaction enthalpies of +29.93 kJ mol<sup>-1</sup> and +20.62 kJ mol<sup>-1</sup>, respectively. The solvent effects for this reaction are small which can be explained by the fact that no charged molecule is involved in this reaction. Small stabilization up to 5 kJ mol<sup>-1</sup> can be observed for all reagents (Table 3.2).

The addition of an auxiliary base (Me<sub>3</sub>N) to the reaction removes the proton as a driving force and leads to similar results as in the anion exchange reaction. All reagents, except TBSN<sub>3</sub> (**1f**), show a higher stabilization than TBSCl (**1a**), which changes after solvation corrections are added. Only for TBSOTf (**1b**, -28.33 kJ mol<sup>-1</sup>) and TBSOClO<sub>3</sub> (**1g**, -33.59 kJ mol<sup>-1</sup>) a higher stabilization can be observed, while all other reagents are found to be an area of +30 kJ mol<sup>-1</sup>. TBSN<sub>3</sub> (**1f**) is found at +62.23 kJ mol<sup>-1</sup> which is the highest destabilization found (Table 3.2).

**Table 3.2.** Reaction energies ( $\Delta H_{298}$ ) for silylation reagents in various transfer reactions (relative to TBSCl) (gas and solution phase data).

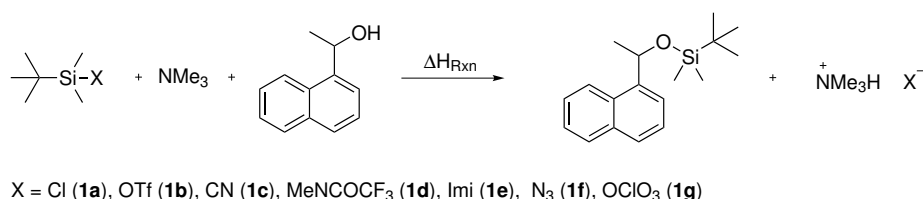
Reagent	No.	Anion Exchange		Protonated Anion		Auxiliary Base	
		$\Delta H_{298}^a$	$\Delta H_{298}^b$	$\Delta H_{298}^a$	$\Delta H_{298}^b$	$\Delta H_{298}^a$	$\Delta H_{298}^b$
	<b>1b</b>	-136.26	-72.56	+29.93	+26.70	-38.98	-28.33
	<b>1g</b>	-108.17	-58.89	+20.62	+17.37	-35.38	-33.59
	<b>1d</b>	-6.35	+41.20	-60.61	-66.20	-26.66	+27.76
TBS-Cl	<b>1a</b>	0.00	0.00	0.00	0.00	0.00	0.00
	<b>1f</b>	+5.47	+19.83	-7.62	-7.66	+10.90	+62.23
TBS-C≡N	<b>1c</b>	+28.75	+32.68	-51.73	-51.44	-21.87	+33.92
	<b>1e</b>	+33.44	+65.61	-30.83	-36.89	-9.18	+38.95

<sup>a</sup> Gas phase energies (in kJ mol<sup>-1</sup>) have been calculated at MP2(FC)/G3MP2large//MPW1K/6-31+G(d) level.

<sup>b</sup> Solvation energies (in kJ mol<sup>-1</sup>) have been calculated at SMD/MPW1K/6-31+G(d) level for CHCl<sub>3</sub>.

In addition to those reactions, reaction enthalpies with secondary alcohol **5b** have been calculated with and without trimethylamine as auxiliary base. The reaction enthalpy calculations without auxiliary base show that the reaction with TBSCl (**1a**) is only slightly exothermic in gas phase (-8.05 kJ mol<sup>-1</sup>) and almost thermoneutral with SMD correction (-0.25 kJ mol<sup>-1</sup>), which supports the fact that TBSCl (**1a**) is in need of a Lewis base catalyst to proceed in the reaction (Table 3.3). This reaction can be compared to the transfer of protonated leaving groups and a

similar order of the reagents can be observed. It can be stated that the product, which is the protonated counterion, is strongly manipulating the driving force for this reaction. As already mentioned, strong acids (TBSOTf or TBSOCIO<sub>3</sub>) seem to suffer under these conditions in terms of stabilization, while basic compounds such as TBSImi (**1e**,  $-37.14 \text{ kJ mol}^{-1}$ ) or MTBSTFA (**1d**,  $-66.45 \text{ kJ mol}^{-1}$ ) are more stable. For the compounds not studied experimentally, an endothermic reaction enthalpy has been found for TBSOCIO<sub>3</sub> (**1g**) with  $+17.12 \text{ kJ mol}^{-1}$ , while TBSN<sub>3</sub> (**1f**) yielded in  $-7.91 \text{ kJ mol}^{-1}$ , which is, compared to MTBSTFA (**1d**), just a small stabilization.



**Scheme 3.4.** Calculated reaction enthalpy for **5b** for different leaving groups of *tert*-butyldimethylsilyl compounds with trimethylamine as auxiliary base.

Furthermore, for the reaction with an auxiliary base, the obtained data is consistent for all silyl reagents in terms that faster reagents show a better stabilization than TBSCl (**1a**,  $-104.02 \text{ kJ mol}^{-1}$ ). For instance,  $-132.35 \text{ kJ mol}^{-1}$  can be obtained for TBSOTf (**1b**), while TBSCN (**1c**) is found at  $-70.10 \text{ kJ mol}^{-1}$  which is in accordance to the experimental data (Table 3.1). However, these calculations show a good reaction enthalpy of  $-37.14 \text{ kJ mol}^{-1}$  for TBSImi (**1e**), which shows a rather low reactivity in the experiments. Further experimental studies would be interesting for TBSOCIO<sub>3</sub> (**1g**,  $-137.62 \text{ kJ mol}^{-1}$ ) which might be as fast as TBSOTf (**1b**) based on the calculations.

**Table 3.3.** Reaction enthalpies ( $\Delta H_{\text{Rxn}}$ ) for silylation reagents for the silylation of secondary alcohol **5b** with and without auxiliary base (gas and solution phase data).

Reagent	No.	Without Me <sub>3</sub> N		With Me <sub>3</sub> N	
		$\Delta H_{\text{Rxn}}$ (gas) <sup>a</sup>	$\Delta H_{\text{Rxn}}$ (sol) <sup>b</sup>	$\Delta H_{\text{Rxn}}$ (gas) <sup>a</sup>	$\Delta H_{\text{Rxn}}$ (sol) <sup>b</sup>
	<b>1b</b>	+21.88	+26.45	-105.85	-132.35
	<b>1g</b>	+12.57	+17.12	-102.26	-137.62
	<b>1d</b>	-68.66	-66.45	-93.54	-76.26
TBS-Cl	<b>1a</b>	-8.05	-0.25	-66.88	-104.02

<sup>a</sup> Gas phase energies (in  $\text{kJ mol}^{-1}$ ) have been calculated at MP2(FC)/G3MP2large//MPW1K/6-31+G(d) level.

<sup>b</sup> Solvation energies (in  $\text{kJ mol}^{-1}$ ) have been calculated at SMD/MPW1K/6-31+G(d) level for CHCl<sub>3</sub>.

### 3.3 Theoretical Studies on the Leaving Group Effect

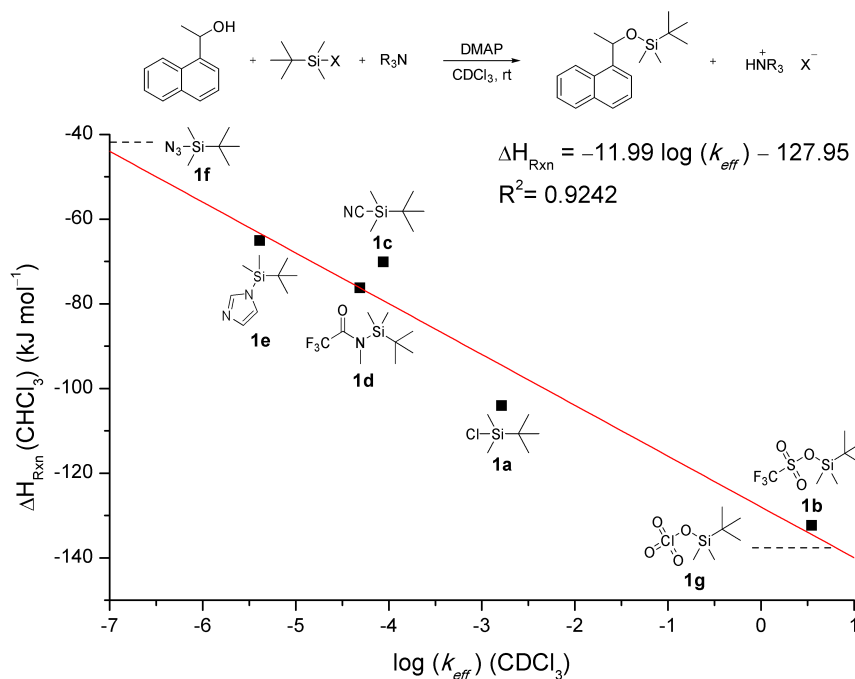
**Table 3.3.** Continuation.

Reagent	No.	Without Me <sub>3</sub> N		With Me <sub>3</sub> N	
		$\Delta H_{\text{Rxn}}$ (gas) <sup>a</sup>	$\Delta H_{\text{Rxn}}$ (sol) <sup>b</sup>	$\Delta H_{\text{Rxn}}$ (gas) <sup>a</sup>	$\Delta H_{\text{Rxn}}$ (sol) <sup>b</sup>
TBS-N <sup>⊖</sup> <sub>3</sub> N <sup>⊖</sup>	<b>1f</b>	-15.67	-7.91	-55.97	-41.79
TBS-C≡N	<b>1c</b>	-21.87	-59.78	-88.74	-70.10
TBS-N <sub>2</sub>	<b>1e</b>	-38.88	-37.14	-76.05	-65.07

<sup>a</sup> Gas phase energies (in kJ mol<sup>-1</sup>) have been calculated at MP2(FC)/G3MP2large//MPW1K/6-31+G(d) level.

<sup>b</sup> Solvation energies (in kJ mol<sup>-1</sup>) have been calculated at SMD/MPW1K/6-31+G(d) level for CHCl<sub>3</sub>.

The calculated data can be used to correlate the experimentally obtained data for the reagents **1a**, **1b**, **1c**, **1d**, and **1e** into a linear correlation ( $R^2 = 0.9242$ ) by plotting  $\Delta H_{\text{Rxn}}$  (sol) against the reaction rate determined in experiments in CDCl<sub>3</sub>. This linear correlation can be used to predict reaction rates for other reagents such as TBS perchlorate (**1g**) or azide (**1f**) and could be used prior to the synthesis of new compounds (Figure 3.10). The fact that the correlation is possible supports the idea that the properties of the leaving group are, at least in part, responsible for the rate of the silylation reaction.



**Figure 3.10.** Correlation of reaction enthalpy  $\Delta H_{\text{Rxn}}$  vs.  $\log(k_{\text{eff}})$  of the silylation secondary alcohol **5b** with various reagents, Et<sub>3</sub>N as auxiliary base, and DMAP (30 mol%) as catalyst in CDCl<sub>3</sub>.



Based on the experimental and theoretical results, one can conclude that the silylation of alcohols offers three different mechanistic scenarios, which emerge from the current results as a function of leaving groups, solvents, and Lewis bases. The fastest and least selective reactions are observed for TBSOTf (**1b**). These reactions show only small solvent effects and hardly respond to Lewis base catalysis. This can best be rationalized through direct, uncatalyzed reaction of alcohols with TBSOTf (**1b**), whose properties may approximately be depicted as those of a contact ion pair. Better selectivities at slower reaction rates are obtained in DMF as a Lewis basic solvent for the less reactive reagents TBSCl (**1a**), TBSCN (**1c**), and MTBSTFA (**1d**). These reactions are likely to involve silylated DMF as transient intermediate of the catalytic cycle. Best selectivities and slowest rates are obtained in apolar, organic solvents such as CDCl<sub>3</sub> and CD<sub>2</sub>Cl<sub>2</sub> for the Lewis base-catalyzed reaction of the reagents TBSCl (**1a**), TBSCN (**1c**), and MTBSTFA (**1d**). The reaction rates correlate systematically with selectivities which is likely due to steric demands of the respective transition states: while the uncatalyzed reaction of alcohols with TBSOTf (**1b**) proceeds through transition states composed only of two reactants, the Lewis base-catalyzed pathways have to accommodate the presence of either a small (such as DMF) or a larger (e.g. DMAP) Lewis base. This qualitative reasoning also implies that the development of sterically more encumbered Lewis bases may lead to still larger selectivities for the Lewis base-catalyzed processes.

A possible optimization in this matter might be the synthesis of new protection groups with different leaving groups, which are as fast as TBSOTf (**1b**) and similar in terms of selectivity as TBSCl (**1a**). Well known leaving groups such as tosylate or mesylates might have the ability to lower the activation barrier just to the point that Lewis base catalysis is needed, but to proceed at much faster rates.



## 4 Theoretical Evaluation of the Silyl Transfer Enthalpy

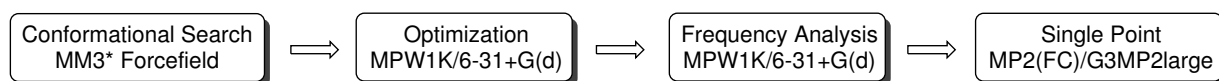
### 4.1 General Procedure for Calculations

Theoretical evaluations with quantum chemical methods have been used as important guidelines for the reactivity of Lewis and Brønsted bases as catalysts.<sup>[16,40,148]</sup> Proton affinity (PA) numbers, have been used to describe base-induced or base-catalyzed processes, either as gas phase data or as solution phase  $pK_a$  values. More appropriate methods arose recently, which focus on the affinity data towards carbon electrophiles rather than protons. One of these methods are methyl cation affinity (MCA) values, which can be used for various reactions where a Lewis base catalyst is involved. The MCA values grant a more specific prediction than the commonly used proton affinities.<sup>[31,114,149–152]</sup> Another benefit of this approach is that it can be modified to serve a specific reaction, when a carbon electrophile is involved. For instance, the acetyl cation affinities have been used to describe any kind of acetyl transfer reactions, such as the acylation of alcohols.<sup>[17,39,148,153]</sup> These numbers grant a better prediction than PA numbers or MCA values and have successfully been used to link a theoretical method to experimental data. Therefore, a specific descriptor for the silylation reaction can be used to predict the catalytic effect of several catalysts. The silyl cation affinity (SCA) can be used to describe the Lewis basicity of the investigated compounds. All values have been determined relative to pyridine as the reference base using an isodesmic silyl group transfer reaction (Scheme 4.1).



**Scheme 4.1.** Definition of silyl cation affinities (SCA) via an isodesmic silyl group transfer reaction.

In order to calculate SCA values the following steps have to be performed. Starting with a search of the conformational space using a MM3\* forcefield conformational search in MacroModel 9.7.<sup>[154]</sup> The detected conformers have been optimized using the hybridfunctional MPW1K<sup>[155]</sup> with the 6-31+G(d) basis set on Gaussian03.<sup>[156]</sup> In combination with the optimization one can calculate thermal corrections by performing a frequency analysis on the same level of theory. As a final step the single point calculation will be done on MP2(FC)/G3MP2large. This procedure can be summarized as MP2(FC)/G3MP2large//MPW1K/6-31+G(d) and is shown in Scheme 4.2.

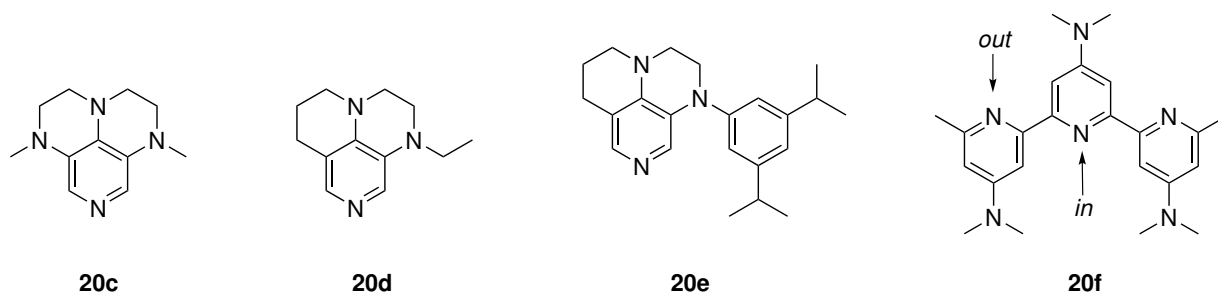


**Scheme 4.2.** Depiction of the procedure to calculate the silyl cation affinity (SCA) values.

In order to optimize the calculated values for the actual experiments, solvent effects in  $\text{CHCl}_3$  have been calculated at PCM/UAHF/MPW1K/6-31+G(d) level of theory.<sup>[157]</sup> In addition to the SCA values, the MCA data has been calculated on the same level of theory and will be used to compare silicon- and carbon-based electrophiles in Chapter 4.4. For all further discussions the SCA values which have been calculated with PCM corrections in chloroform will be used.

## 4.2 SCA Values for Various Pyridine Systems

All catalysts used in the kinetic measurements (see Chapter 2) are nitrogen-based nucleophiles and either pyridine- or imidazole-systems. To take advantage of this data, further catalysts have been investigated. This study includes catalytically less effective systems such as 4-methylpyridine (**20a**) or 1,1,3,3-tetramethyl-2-(pyridin-4-yl)guanidine (**20b**) and also stronger catalysts with increased nucleophilicity based on strong donors or an annelation of the ring system, shown in Scheme 4.3. Most of these catalysts have already been tested for their reactivity in various reactions, for instance 1,6-dimethyl-2,3,5,6-tetrahydro-1*H*,4*H*-1,3a,6,8-tetraaza-phenalene (**20c**), 1-ethyl-1,2,3,5,6,7-hexahydropyrazino[3,2,1-*ij*][1,6]naphthyridine (**20d**), 1-(3,5-diisopropylphenyl)-2,3,6,7-tetrahydro-1*H*,5*H*-pyrazino[3,2,1-*ij*][1,6]naphthyridine (**20e**), and 4,4',4''-tris(dimethylamino)terpyridine (**20f**).<sup>[16,39,152]</sup> Since synthesizing all compounds is time consuming and rather complex, especially for **20f**, the SCA values with PCM correction in  $\text{CDCl}_3$  have been calculated in order to estimate their Lewis basicity towards silyl cations and will be compared to the data of **3a–g** in the following.



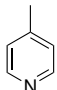
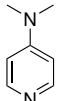
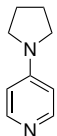
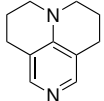
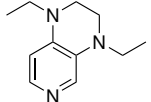
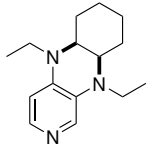
**Scheme 4.3.** Lewis base catalysts based on the aminopyridine substructure.

It is not surprising that 4-methylpyridine (**20a**) shows a low SCA value ( $-26.4 \text{ kJ mol}^{-1}$ ) since a strong electron donating group is missing. However, this number is only slightly higher than the one for imidazole (**3d**,  $-24.7 \text{ kJ mol}^{-1}$ ), which suggests that **20a** might perform similar to imidazole (**3d**). By increasing the EDG to *N*-dimethylamino group (DMAP, **3a**) the SCA value increases to  $-43.1 \text{ kJ mol}^{-1}$  and can be increased further by adding a guanidine (**20b**), which leads to a SCA value of  $-63.6 \text{ kJ mol}^{-1}$ . One of the best catalysts investigated by experiment **3c** is characterized by a SCA value of  $-56.5 \text{ kJ mol}^{-1}$ , which indicates that 1,1,3,3-tetramethyl-2-

(pyridin-4-yl)guanidine (**20b**) might also be a suitable catalyst for silylation reactions based on its Lewis basicity.

For tricyclic aminopyridines the range of the SCA values is rather small and is neither influenced by the amount of nitrogen atoms in the ring system (**20c**, **20d**), nor by a sterically demanding group attached to it (**20e**). All catalysts of this kind (**20c–e**) yield very high SCA values below  $-80 \text{ kJ mol}^{-1}$  (Table 4.1). Not only do these catalysts have one or two nitrogen atoms attached to the pyridine ring system, but they also profit from a ring annelation as an extra boost in electron density. Taking into account that good catalysts with two donating nitrogen substituents such as **3f** and **3g** achieve SCA values around  $-60 \text{ kJ mol}^{-1}$ , the ring annelation can be considered an important factor to increase the Lewis basicity by about  $20 \text{ kJ mol}^{-1}$  further. This is a well-known phenomenon which has also been observed for acylation reactions in combination with Lewis base catalysts.<sup>[18,39,43]</sup>

**Table 4.1.** Calculated SCA and MCA values for pyridine-based Lewis base catalysts.

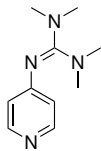
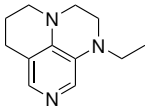
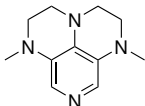
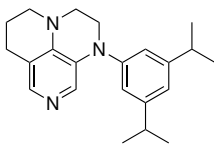
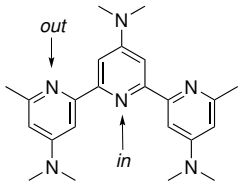
Catalyst	No.	SCA (gas) <sup>a</sup>	SCA (sol) <sup>b</sup>	MCA (gas) <sup>a</sup>	MCA (sol) <sup>b</sup>
	<b>20a</b>	-15.5	-26.4	-15.0	-9.2
	<b>3a</b>	-57.0	-43.1	-63.9	-41.9
	<b>3b</b>	-64.8	-47.4	-74.5	-45.4
	<b>3c</b>	-75.6	-56.5	-87.2	-52.6
	<b>3f</b>	-83.4	-58.5	-92.0	-59.2
	<b>3g</b>	-93.2	-62.0	-102.2	-67.7

<sup>a</sup> Gas phase energies (in  $\text{kJ mol}^{-1}$ ) have been calculated at MP2(FC)/G3MP2large//MPW1K/6-31+G(d) level.

<sup>b</sup> Solvation energies (in  $\text{kJ mol}^{-1}$ ) have been calculated at PCM/UAHF/MPW1K/6-31+G(d) level for  $\text{CHCl}_3$ .

## 4.2 SCA Values for Various Pyridine Systems

**Table 4.1.** Continuation.

Catalyst	No.	SCA (gas) <sup>a</sup>	SCA (sol) <sup>b</sup>	MCA (gas) <sup>a</sup>	MCA (sol) <sup>b</sup>
	<b>20b</b>	−72.3	−63.6	−82.4	−47.9
	<b>20d</b>	−87.8	−82.5	−96.3	−65.1
	<b>20c</b>	−94.0	−86.7	−102.9	−70.1
	<b>20e</b>	−100.5	−88.8	−104.7	−63.9
	<b>20f-in</b>	−58.3	−35.3	−87.7	−28.2
	<b>20f-out</b>	−59.8	−39.7	−87.1	−35.6

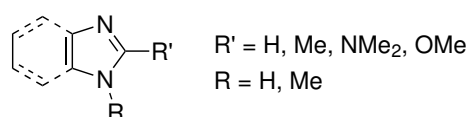
<sup>a</sup> Gas phase energies (in kJ mol<sup>−1</sup>) have been calculated at MP2(FC)/G3MP2large//MPW1K/6-31+G(d) level.

<sup>b</sup> Solvation energies (in kJ mol<sup>−1</sup>) have been calculated at PCM/UAHF/MPW1K/6-31+G(d) level for CHCl<sub>3</sub>.

The complex structure of **20f** containing several dimethylamino substituents can react with electrophiles on the central or outer pyridine ring. This complex structure makes **20f** probably the most electron rich catalyst. However, the Lewis basicity of **20f** is rather poor with −35.3 kJ mol<sup>−1</sup> for the center part and −39.7 kJ mol<sup>−1</sup> for the outer part of the system, respectively. With these affinity numbers **20f** is less basic than the commercially available DMAP (**3a**, −43.1 kJ mol<sup>−1</sup>). Taking a closer look at the structure, it becomes apparent that the nucleophilic center part of **20f** is strongly sterically hindered and unsuitable for a big electrophiles, such as the TBS group. The molecules need to distort in order to avoid the steric repulsion, which can never be achieved completely and ends up with a high SCA value. Nevertheless, the unique structure with three possible catalytic sites makes this molecule an interesting target for further experimental investigation.

### 4.3 SCA Values for Various Imidazole Systems

Used as Lewis base by Corey and Venkateswarlu in the early days of protection group chemistry imidazole and its derivatives are still interesting for this type of reaction.<sup>[3]</sup> The SCA values have been calculated for several molecules from the family of imidazoles and compared to similarly substituted pyridines. This chapter focuses on imidazole (**21a**), *N*-methylimidazole (**22a**), benzimidazole (**23a**), *N*-methylbenzimidazole (**24a**), which will be modified in the 2-position with various EDGs in order to optimize the catalytic efficiency (Figure 4.1).



**Figure 4.1.** General structure of imidazole compounds.

Before we take a closer look on the effect of the substituents on the 2-position, it should be noted that from the starting compounds *N*-methylbenzimidazole (**24a**) has by far the highest Lewis basicity based on a SCA value of  $-44.0 \text{ kJ mol}^{-1}$ . Furthermore, a negligibly small difference of  $0.3 \text{ kJ mol}^{-1}$  can be observed for imidazole (**21a**,  $-24.7 \text{ kJ mol}^{-1}$ ) and benzimidazole (**23a**,  $-25.0 \text{ kJ mol}^{-1}$ ), while the SCA value for *N*-methylimidazole (**22a**) can be found in between at  $-32.4 \text{ kJ mol}^{-1}$ . This small data set already shows that secondary amines (**21a**, **23a**) are not very useful as Lewis bases (Table 4.2). These systems will be discussed separately in the following.

**Table 4.2.** Calculated SCA and MCA values for imidazoles and benzimidazoles.

Catalyst	No.	SCA (gas) <sup>a</sup>	SCA (sol) <sup>b</sup>	MCA (gas) <sup>a</sup>	MCA (sol) <sup>b</sup>
	<b>21a</b>	-20.0	-24.7	-13.9	-16.8
	<b>23a</b>	-24.3	-25.0	-21.9	-14.6
	<b>22a</b>	-36.4	-32.4	-31.8	-24.6
	<b>24a</b>	-38.8	-44.0	-37.2	-20.4

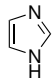
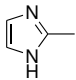
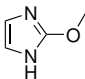
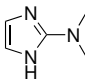
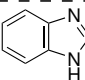
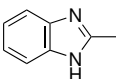
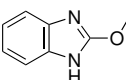
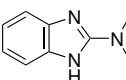
<sup>a</sup> Gas phase energies (in  $\text{kJ mol}^{-1}$ ) have been calculated at MP2(FC)/G3MP2large//MPW1K/6-31+G(d) level.

<sup>b</sup> Solvation energies (in  $\text{kJ mol}^{-1}$ ) have been calculated at PCM/UAHF/MPW1K/6-31+G(d) level for  $\text{CHCl}_3$ .

### 4.3 SCA Values for Various Imidazole Systems

The systems with a secondary amine (**21a** and **23a**) have been modified in 2-position and analyzed further. Adding a methyl group leads to an increase of 5 kJ mol<sup>-1</sup> for 2-methylimidazole (**21b**, -30.4 kJ mol<sup>-1</sup>), and 10 kJ mol<sup>-1</sup> for 2-methylbenzimidazole (**23b**, -34.7 kJ mol<sup>-1</sup>). Stronger donors such as a methoxy or a dimethylamino group are also increasing the steric demand for the silylated system. Since the benzimidazole systems are already conformationally more constrained, the effect of these groups should be bigger than for the imidazole compounds. The results support this hypothesis with much lower SCA values for 2-methoxybenzimidazole (**23c**, -3.3 kJ mol<sup>-1</sup>) and only a small increase for 2-(*N,N*-dimethylamino)benzimidazole (**23d**, -28.2 kJ mol<sup>-1</sup>) compared to the unsubstituted compound (**23a**). For the corresponding imidazole systems such an effect cannot be observed and the electron donating groups increase the SCA values stepwise from -33.4 kJ mol<sup>-1</sup> for 2-methoxyimidazole (**21c**) to -42.5 kJ mol<sup>-1</sup> for 2-(*N,N*-dimethylamino)imidazole (**21d**). The latter value is of interest since **21d** is almost as basic as DMAP (**3a**, -43.1 kJ mol<sup>-1</sup>). Even though compound **21d** is in the same area as **3a**, it is doubtful that it performs as well as DMAP (**3a**) in a silylation reaction, based on possible steric repulsion of the activated species.

**Table 4.3.** Calculated SCA and MCA values for imidazoles (**21a–d**) and benzimidazoles (**23a–d**).

Catalyst	No.	SCA (gas) <sup>a</sup>	SCA (sol) <sup>b</sup>	MCA (gas) <sup>a</sup>	MCA (sol) <sup>b</sup>
	<b>21a</b>	-20.0	-24.7	-13.9	-16.8
	<b>21b</b>	-30.3	-30.4	-32.1	-28.8
	<b>21c</b>	-16.2	-33.4	-11.8	-7.0
	<b>21d</b>	-32.6	-42.5	-39.8	-27.3
<hr/>					
	<b>23a</b>	-24.3	-25.0	-21.9	-14.6
	<b>23b</b>	-25.9	-34.7	-36.5	-18.7
	<b>23c</b>	+7.1	-3.3	-15.8	-1.8
	<b>23d</b>	-23.4	-28.2	-41.5	-20.4

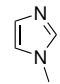
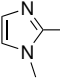
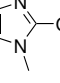
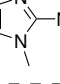
<sup>a</sup> Gas phase energies (in kJ mol<sup>-1</sup>) have been calculated at MP2(FC)/G3MP2large//MPW1K/6-31+G(d) level.

<sup>b</sup> Solvation energies (in kJ mol<sup>-1</sup>) have been calculated at PCM/UAHF/MPW1K/6-31+G(d) level for CHCl<sub>3</sub>.



A strong steric influence can also be observed for the *N*-methylbenzimidazole compounds. The calculated SCA values show a decrease of basicity with each EDG attached to the 2-position of the molecule (Table 4.4). The best value is obtained for the unsubstituted *N*-methylbenzimidazole (**24a**) with  $-44.0 \text{ kJ mol}^{-1}$ , which is as strong as DMAP (**3a**). An addition of a methyl group (**24b**) leads to a small drop to  $-38.1 \text{ kJ mol}^{-1}$ , while for 2-methoxy-*N*-methyl-benzimidazole (**24c**) a big decrease of roughly  $20 \text{ kJ mol}^{-1}$  can be observed. By adding the strongest donor to the system (**24d**) a moderate SCA value of  $-29.8 \text{ kJ mol}^{-1}$  has been obtained, which is close to imidazole. For both investigated benzimidazoles it becomes apparent that a methoxy has a strong decreasing effect on the Lewis basicity based on the calculated SCA values. This observation cannot be explained by steric effect alone and thus it might be of interest for further investigations. For the *N*-methylimidazole compounds the results reveal another possible class of catalysts for the silylation reaction. While *N*-methylbenzimidazole (**24a**) can be seen as the strongest base in its group, *N*-methylimidazole (**22a**) is the weakest in the group of *N*-methylimidazole compounds. The good SCA value of  $-32.4 \text{ kJ mol}^{-1}$  for **22a** can be increased through addition of a methyl group (**22b**) to  $-52.0 \text{ kJ mol}^{-1}$ . However, the steric repulsion can also be observed for compounds **22c** and **22d** as shown through smaller SCA values of  $-34.4 \text{ kJ mol}^{-1}$  (**22c**) and  $-46.7 \text{ kJ mol}^{-1}$  (**22d**), respectively. Even though the size of the EDG is bigger in **22d**, the effect of the electron donation seems to be of higher importance in these systems as it has been observed by comparing imidazoles (**21a–d**) with benzimidazoles (**23a–d**) earlier. A reason might be the blocked positions 4 and 5 by a phenylring for all benzimidazoles. In conclusion all imidazole- and *N*-methylimidazole-systems have, sterically speaking, more degrees of freedom to distort the TBS group into a good position.

**Table 4.4.** Calculated SCA and MCA values for *N*-methylimidazoles (**22a–d**) and *N*-methylbenzimidazoles (**24a–d**).

Catalyst	No.	SCA (gas) <sup>a</sup>	SCA (sol) <sup>b</sup>	MCA (gas) <sup>a</sup>	MCA (sol) <sup>b</sup>
	<b>22a</b>	$-36.4$	$-32.4$	$-31.8$	$-24.6$
	<b>22b</b>	$-43.2$	$-52.0$	$-49.5$	$-37.9$
	<b>22c</b>	$-22.8$	$-34.4$	$-19.0$	$-17.4$
	<b>22d</b>	$-37.7$	$-46.7$	$-42.4$	$-26.3$

<sup>a</sup> Gas phase energies (in  $\text{kJ mol}^{-1}$ ) have been calculated at MP2(FC)/G3MP2large//MPW1K/6-31+G(d) level.

<sup>b</sup> Solvation energies (in  $\text{kJ mol}^{-1}$ ) have been calculated at PCM/UAHF/MPW1K/6-31+G(d) level for  $\text{CHCl}_3$ .

### 4.3 SCA Values for Various Imidazole Systems

**Table 4.4.** Continuation.

Catalyst	No.	SCA (gas) <sup>a</sup>	SCA (sol) <sup>b</sup>	MCA (gas) <sup>a</sup>	MCA (sol) <sup>b</sup>
	<b>24a</b>	−38.8	−44.0	−37.1	−21.4
	<b>24b</b>	−34.8	−38.1	−46.2	−25.4
	<b>24c</b>	−12.6	−17.9	−16.1	+4.6
	<b>24d</b>	−27.5	−29.8	−44.8	−21.4

<sup>a</sup> Gas phase energies (in kJ mol<sup>−1</sup>) have been calculated at MP2(FC)/G3MP2large//MPW1K/6-31+G(d) level.

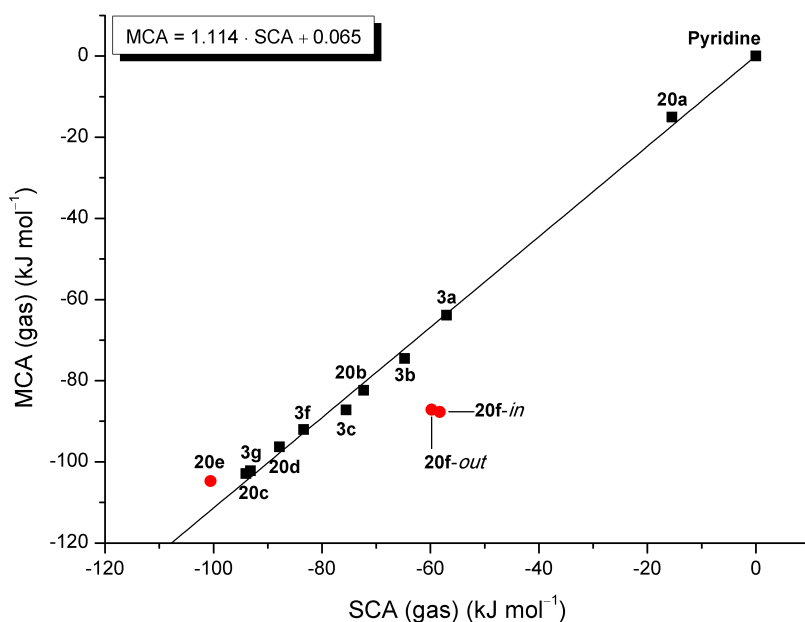
<sup>b</sup> Solvation energies (in kJ mol<sup>−1</sup>) have been calculated at PCM/UAHF/MPW1K/6-31+G(d) level for CHCl<sub>3</sub>.

It can be summarized that for imidazole and benzimidazole systems, in contrast to pyridines, steric effects have a higher influence on the SCA values. While this effect is rather small for imidazoles (**21a–d**) and *N*-methylimidazoles (**22a–d**), it can decrease the SCA values up to 20 kJ mol<sup>−1</sup> for benzimidazoles (**23a–d**) and *N*-methylbenzimidazoles (**22a–d**). This is mainly based on the antiperiplanar positioning of the substituents and their proximity to the reaction center. Therefore, a steric repulsion especially with the TBS groups cannot be excluded. However, the calculated SCA values must always be considered as a combination of steric and electronic effects. This hypothesis is supported by the fact that all imidazole compounds seem to have higher SCA values than benzimidazoles, which is in accordance with a less sterically restricted system.

## 4.4 Silyl Cation Affinity vs. Methyl Cation Affinity

As mentioned earlier the MCA value is a well accepted descriptor for reactions with a carbon-based electrophiles. This chapter will focus on the difference in Lewis basicity concerning the data calculated with a carbon- and a silicon-based electrophile and will compare their benefits. In this chapter the gas phase data will be taken as basis for all discussed compounds, which have been displayed in the Tables 4.1 – 4.4.

Plotting MCA against SCA values shows a good correlation between those two methods, which is shown in Figure 4.2 for all pyridine systems. One can easily correlate this data in a linear fashion ( $R^2 = 0.9935$ ) with only a few exceptions depicted in red. These systems are highly flexible and sterically demanding, which can be explained by the simple difference in size of the systems. A methyl cation demands less space than a silyl cation with a bulky *tert*-butyl group (Figure 4.2).

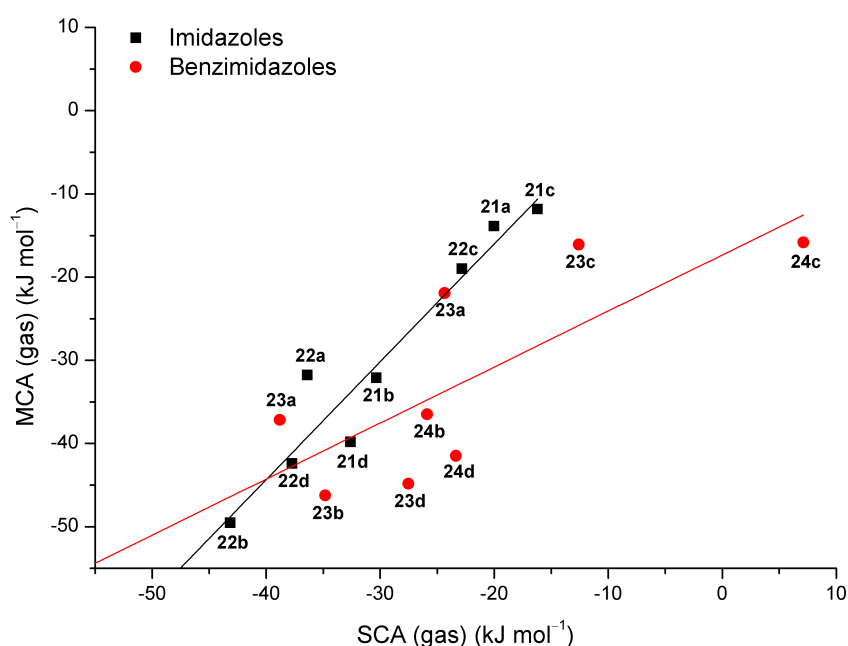


**Figure 4.2.** Correlation between methyl and silyl cation affinities for pyridines.

The biggest deviation of the correlation line are terpyridine **20f** and compound **20e**, which in both cases is most likely based on steric repulsion and a complex molecular structure. Nevertheless, except for these two systems the correlation is good and one can consider using the MCA values instead of the SCAs for the prediction of Lewis basicities. To calculate more precise results it is highly advisable to use a designed isodesmic reaction, like it has been done with the silyl cation affinity values for the silylation reaction.

As discussed earlier for all imidazole systems, the reaction center is much closer to the modified position and therefore the modifications have a higher influence on the system contrast to

pyridine systems. Therefore, a correlation between two groups (imidazole and benzimidazole), which differ in size and have been modified close to the reaction center cannot be expected to be very good. In fact, it is not possible to correlate the data of the benzimidazole compounds (**23a–d** and **24a–d**) in a reasonable linear plot ( $R^2 = 0.511$ ). It becomes clear that for these systems donating groups are counterproductive since they generate a bigger steric repulsion, which decreases the overall SCA value. Again, it can be observed, that methoxy substituents (**23c**, **24c**) lead to a decrease for Lewis basicity based of SCAs, while *N,N*-dimethylamino substituent (**23d**, **24d**) increase the stability of the systems (Figure 4.3). Yet, for imidazole systems it is possible to correlate MCA and SCA data in a linear plot with a  $R^2$  value of 0.912.



**Figure 4.3.** Correlation between of methyl and silyl cation affinities for imidazoles and benzimidazoles.

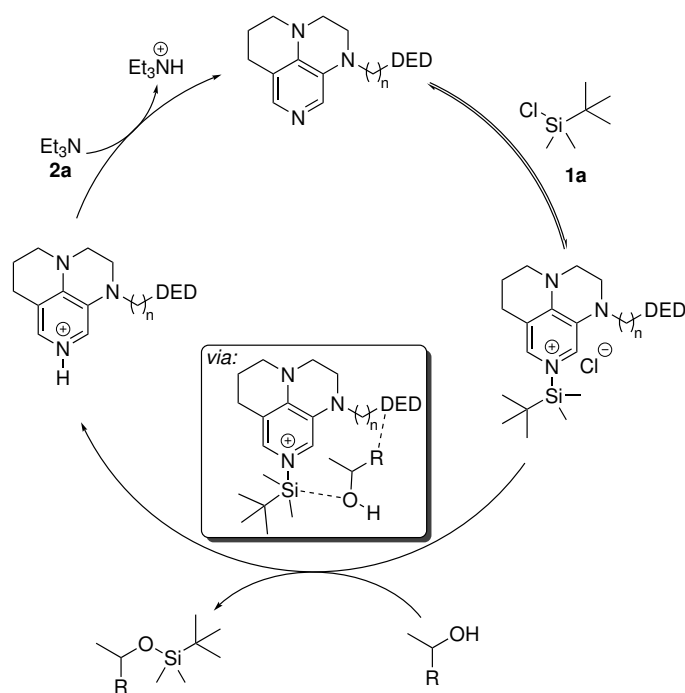
As a conclusion it can be stated, that the structure of the investigated molecules are very important, for the Lewis basicities towards carbon- and silicon-based electrophiles. Complex structures (**20f**) and sterically demanding molecules can have a negative impact on the results and lead to uncertainties in predictions of reactions. Furthermore, it is not advisable to use catalysts, where the reaction center is rather close to the area of modification. This might not only lead to an increase of electron density at the reaction center, but also to more steric hinderance for the system.





## 5 Chemoselectivity Through London Dispersion Forces

Another approach to achieve a selective silylation from a mixture of substrates will be discussed in the following chapter. The idea is based on attractive London dispersion forces (LDFs) between a catalyst intermediate and a substrate alcohol (Figure 5.1). LDFs are intermolecular interactions between atoms and/or molecules, which are weaker than hydrogen bondings, but often play a large role in supermolecular chemistry.<sup>[158,159]</sup> The dispersive interaction between molecules results from Coulomb-correlated fluctuations of electrons and for large intermolecular distances it can be related to the molecular polarizabilities.<sup>[160]</sup> Stronger dispersion forces can be created by a higher polarizability or bigger contact areas of two interacting molecules. To observe dispersive interactions, it might be possible to design an experimental setup based on large contact areas, such as in  $\pi$ - $\pi$ -stacking of aryl systems. The mechanism of the silylation reaction passes through a transition state in which the activated silyl reagent is attacked by the substrate alcohol. It seems to be legit that in this trimolecular transition state the selectivity between different substrates is decided either through attractive or repulsive interactions. By modifying the Lewis base catalyst with a dispersion energy donor (DED) group the possible interaction areas can be increased and thus stronger attractive or repulsive interactions can occur in the suggested transition state (Figure 5.1). In addition to the Lewis base catalyst, the reagents as well as the substrate alcohol might be of importance for the selectivity of this reaction. A high selective transformation in which one substrate is exclusively converted while the others remain untouched is the major goal of this project.



**Figure 5.1.** Mechanism of the Lewis base-catalyzed silylation with a possible transition state.

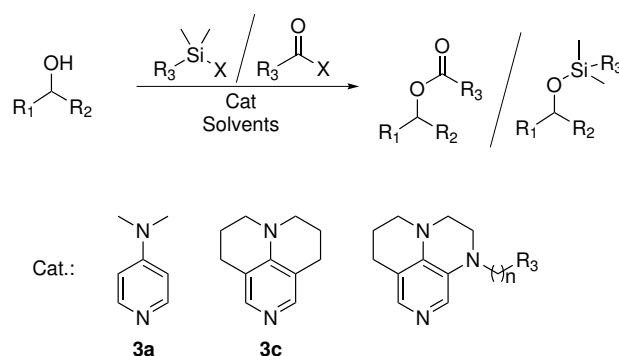
---

It is known from recent research that in the field of describing noncovalent interactions such as LDF quantum chemical computing is used and is constantly evolving during the last few years.<sup>[161–164]</sup> Nowadays, it is possible to calculate intermolecular interactions with the widely used density functional theory (DFT) in combination with additional d3-corrections.<sup>[165–167]</sup> Nonetheless, this chapter mostly presents the results of competition experiments with various substrates and the effects of using DED-catalysts for the silylation as well as for the acylation. In addition various silyl reagents have been studied based on their group size using theoretical calculations.



## 5.1 Effects of Dispersion Catalysts on the Selectivity

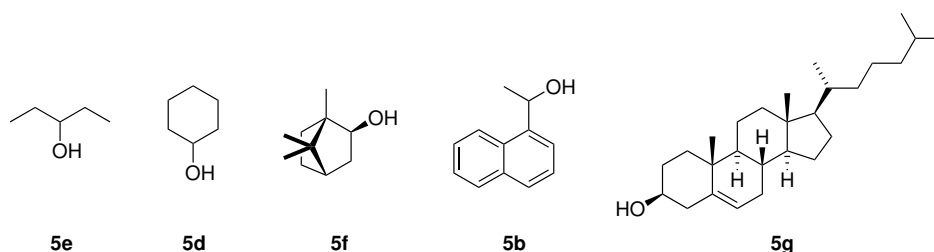
For this study two similar reactions, silylation and acylation, have been chosen based on a good understanding of the reaction mechanisms and the availability of several, different reagents (Figure 5.2). These reactions are both catalyzed by a Lewis base and it has been shown for the silylation that the reaction rate can be manipulated by the choice of catalyst (Chapter 2). Furthermore, the response to changes in reagents and catalysts in acylation reactions has been studied for the alcohols cyclohexanol (**5d**) and 1-(naphthalen-1-yl)ethan-1-ol (**5b**) in detail before.<sup>[83,113]</sup>



**Figure 5.2.** The Lewis base-catalyzed silylation or acylation of secondary alcohols.

Reliable kinetic data have been obtained in these prior studies using NMR- and GC-measurements, the latter choice offering the benefit of running the benchmark reactions in practically any solvent. Best results concerning the reaction rate for acylation as well as for silylation reactions of secondary alcohols have been obtained with catalysts of annelated pyridine derivatives such as **3c**.<sup>[16,39,114]</sup> Depending on the chosen substrates and reagents, these catalysts are five to ten times more efficient than DMAP (**3a**), as shown in Chapter 2 for the silylation reaction.

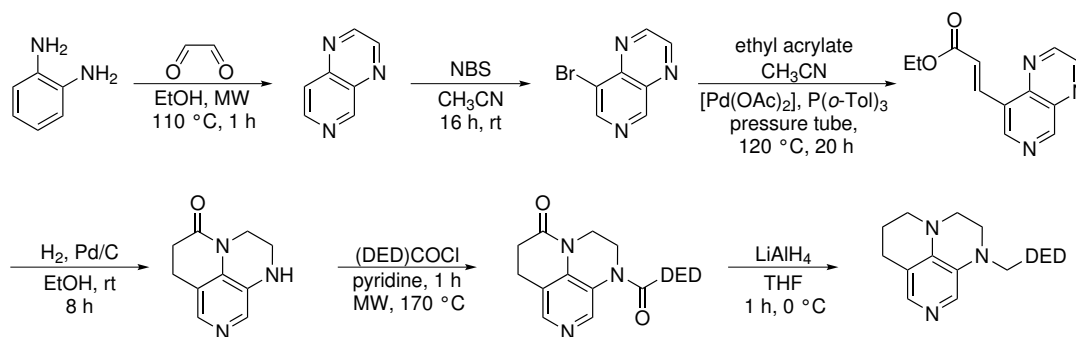
The secondary alcohols chosen as substrates differ in size, steric demand, and surface area for Lewis base-catalyzed reactions. Preliminary experiments have shown that the detection of product ratios by GC will also be effective for mixtures containing equal amounts of the five alcohols, which are pentan-3-ol (**5e**), cyclohexanol (**5d**), isoborneol (**5f**), 1-(naphthalen-1-yl)ethan-1-ol (**5b**), and cholesterol (**5g**) (Figure 5.3).



**Figure 5.3.** Secondary alcohols for the dispersion experiments.

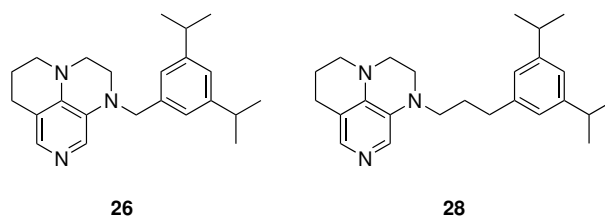
## 5.1.1 Synthesis of Dispersion Catalysts

The catalysts used for this study have been synthesized following literature known procedures for annelated pyridines.<sup>[16,39]</sup> In order to increase dispersive interaction at the reaction center it is necessary to modify the catalyst with a dispersion energy donor (DED). As a first generation of DED-catalysts, 3,5-diisopropylbenzyl-groups have been attached to the catalyst motif using acid chloride and following the synthesis as shown in Scheme 5.1. The 3,5-diisopropylbenzyl-group has been chosen based on its surface area and good solubility in organic solvents. Furthermore, it is possible to systematically increase the size of the DED groups by coupling the 3,5-diisopropylbenzyl group using cross coupling reactions with either a 1,4-dibromobenzene or a 1,3,5-tribromobenzene.



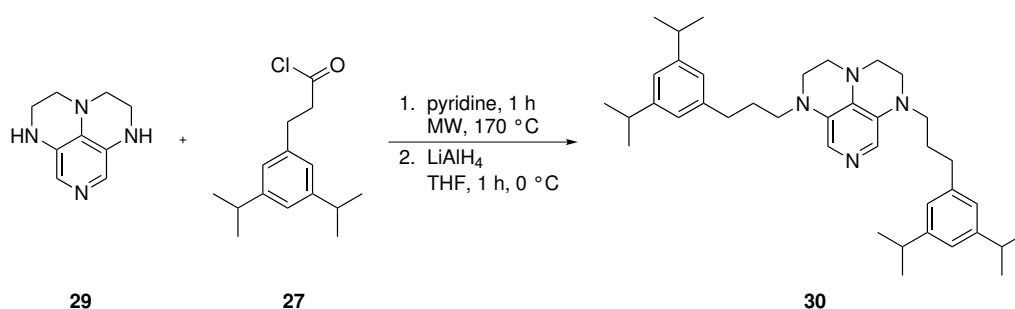
**Scheme 5.1.** Synthetic approach for dispersion active catalysts.

Following the synthesis above for a C1-linker, 3,5-diisopropylbenzoyl chloride (**25**) has been reacted with the catalyst core and reduced afterwards with  $\text{LiAlH}_4$ , leading to catalyst **26**. In addition, a C3-linker has been synthesized by using 3-(3,5-diisopropylphenyl)propanoyl chloride (**27**) instead of **25**, leading to catalyst **28** (Scheme 5.2). A difference between a C1- and a C3-linker might occur during the reaction since a C1-linker is less flexible and might not be able to reach the reaction center. Therefore, a better selectivity based on dispersive interactions might be observable for catalyst **28** with a C3-linker.



**Scheme 5.2.** Synthesized DED-catalyst **26** and **28** with a various linker lengths.

The DED substituents in catalysts **26** and **28** can possibly avoid direct interaction with the reaction center by conformational reorientation. A third catalyst has therefore been synthesized with two DED substituents. Catalyst synthesis starts from the annelated ring system **29**, which can react with two equivalents of 3-(3,5-diisopropylphenyl)propanoyl chloride (**27**) to generate catalyst **30** over two steps (Scheme 5.3).<sup>1</sup>



**Scheme 5.3.** Synthesized DED-catalyst **30** with two attached substituents.

These three DED-catalysts (**26**, **28**, and **30**) will be used to investigate the influence of dispersive forces on acylation and silylation reactions. Therefore, an equimolar mixture of all alcohols (**5b,d–g**) have been mixed with 0.2 equivalents of reagent ( $\text{Ac}_2\text{O}$ , **31a** and TBSCl, **1a**),  $\text{Et}_3\text{N}$  (**2a**, 0.2 equiv), 1 mol% catalyst loading for acylation and 10 mol% for silylation, respectively. All reactions have been performed at room temperature under constant stirring and analyzed by GC. For all products the area factors have been obtained by a calibration curve with tetracosane as reference (see Chapter 8 for further information).

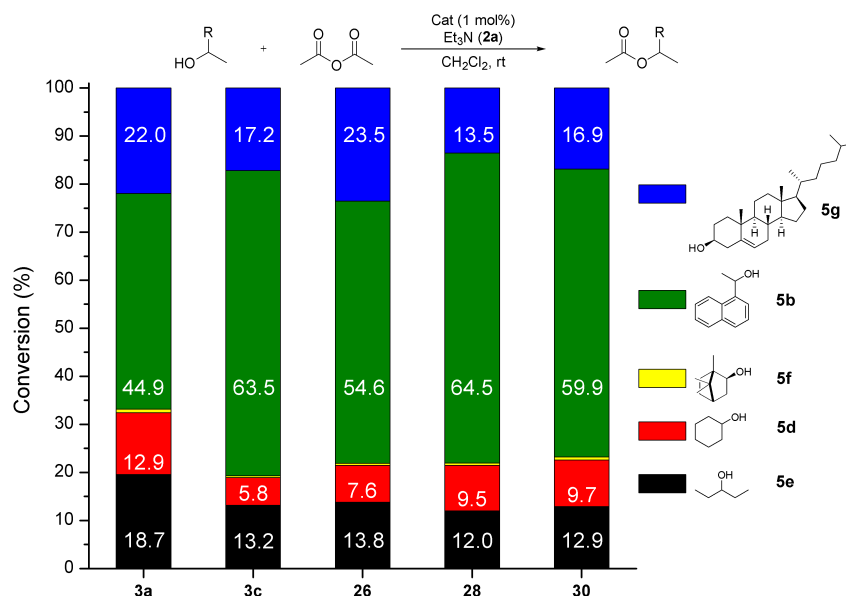
### 5.1.2 Selectivity in Acylation and Silylation

Reaction of the secondary alcohols (**5b**, **5d–g**) with acetic anhydride (**31a**) as reagent has been studied first. Starting with well known catalysts such as DMAP (**3a**) and 9-azajulolidine (**3c**), the acylation reaction has been investigated at a catalyst loading of 1 mol%. In addition the DED-catalysts **26**, **28**, and **30** have been studied under identical conditions. The results for the reaction with DMAP (**3a**) document a clear preference of 1-(naphthalen-1-yl)ethan-1-ol (**5b**) (44.9 %) over the other alcohols. For pentan-3-ol (**5e**) 18.7 % of the resulting product has been obtained, while compounds cyclohexanol (**5d**) and cholesterol (**5g**) led to 12.9 % and 22.0 %, respectively. Even though all alcohols are of secondary nature, the difference in reactivity is tremendous. For instance, for isoborneol (**5f**) almost no conversion can be observed for all catalysts with acetic anhydride (**31a**). A change of catalyst to a more nucleophilic compound (**3c**) leads to an increase of selectivity towards **5b**, where the acylated product can be found in 63.5 %, while all other alcohols show lower conversion. Nonetheless, this difference in product ratio is most likely caused

<sup>1</sup> **29** has been provided by Dr. R. Tandon

## 5.1 Effects of Dispersion Catalysts on the Selectivity

by a general increase in reaction rate rather than dispersive interaction.<sup>[153]</sup> Because of the similar structure of **3c** and the DED-catalysts (**26**, **28**, and **30**) a comparable reactivity for the acylation reaction has been expected.



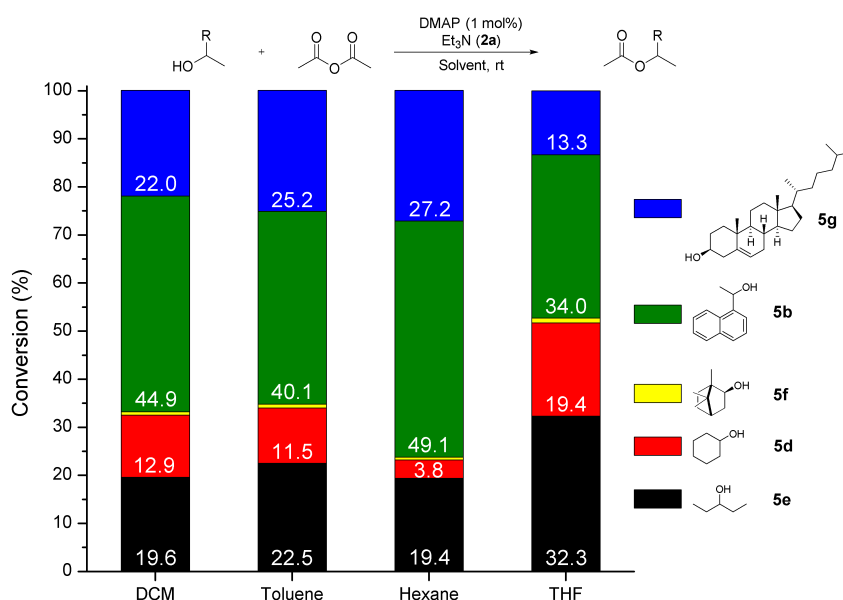
**Figure 5.4.** Normed product ratios for the competition experiments of **5b**, **5d–g** with acetic anhydride (**31a**) and 1 mol% of various catalysts in methylene chloride.

All DED-catalysts (**26**, **28**, and **30**) show similar product ratios as **3c**. The naphthyl alcohol **5b** is strongly preferred with over 50 % for all catalysts, while the ratios of all other alcohols are found to be in the same area as observed for **3c**. These results show no effect of any dispersive interaction of the DED-catalysts in the rate determining step of the reaction. The favored compound **5b** contains, in contrast to all other systems, a planar, aromatic  $\pi$ -system, which can support the idea of  $\pi$ - $\pi$ -interaction in the transition state and therefore the preference of this substrate. However, the results are almost similar for all catalyst even though not all of them contain a DED substituent. One might also consider an increased electron density based on the aromatic system as a reason for the preference in reactivity. It can be stated that for the acylation reaction the catalyst influence is rather small and selectivity is mostly driven by the properties of the substrate alcohols.

Repeating the acylation experiments initially performed in methylene chloride (DCM) in two organic solvents of lower polarity (toluene and isohexane) with DMAP (**3a**) as catalyst leads only to a small change in the selectivities (Figure 5.5). The preferred naphthyl alcohol (**5b**) is found in over 40 % in both solvents. It should be noted though that the reaction rate in hexane is much slower compared to DCM and toluene. This might cause only a slightly higher selectivity, when only the fastest alcohols can be converted.<sup>[146]</sup> In addition, tetrahydrofuran (THF) has been inves-

tigated as a solvent of higher polarity in this matter. As for the other solvents naphthyl alcohol (**5b**) is the fastest and isoborneol (**5f**) the slowest reacting substrate in THF. However, the selectivity profile in THF is somewhat different than before. Substrate **5b** (34.0 %) is closely followed by pentan-3-ol (**5e**, 32.3 %), while isoborneol (**5f**) is almost not transformed at all (Figure 5.5).

Furthermore, the priority between cyclohexanol (**5d**) and cholesterol (**5g**) switched in THF towards cyclohexanol (**5d**), which is less favored than cholesterol (**5g**) in all other solvents. One may argue that a polar solvent such as THF has a big influence on the reactivity for all alcohols leading to systematically smaller selectivities. Since the change is decreasing the selectivity, polar solvents should not be used in this matter. As for the example of DMF in the silylation reaction, it has been shown that strongly polar solvents can have an influence on the reaction rates. However, fluorinated solvents might be of interest, because of their low polarity, which might be able to optimize the selectivity much further. One might need to modify the catalyst loadings and should also be aware of solubility issues.

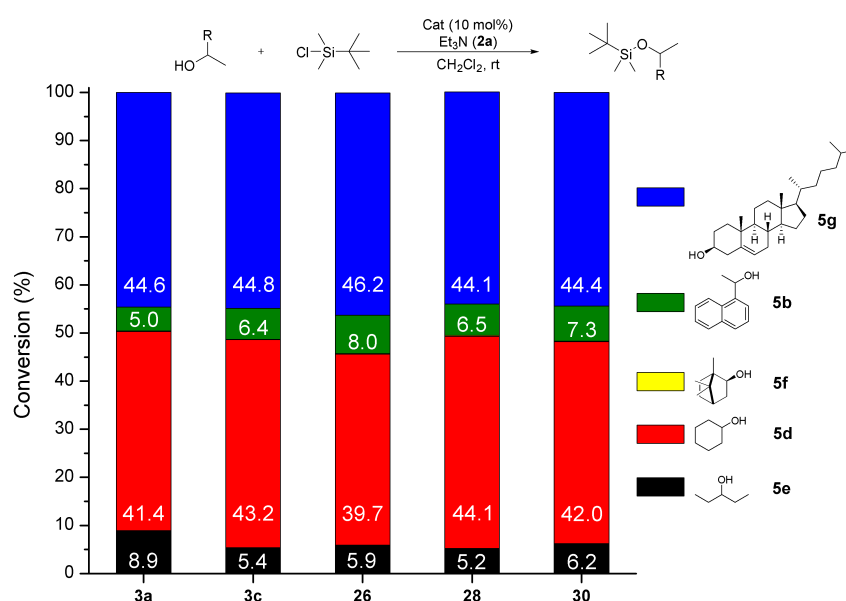


**Figure 5.5.** Normed product ratios for the competition experiments of **5b**, **5d–g** with acetic anhydride (**31a**) and 1 mol% DMAP (**3a**) in various solvents.

In a second series of experiments, the silylation reaction of the five substrates with TBSCl (**1a**) is investigated under similar reaction conditions. The silylation of secondary alcohols is known to be much slower in comparison to the acylation reaction and therefore a higher catalyst loading of 10 mol% and longer reaction times are employed. DED-catalysts **26**, **28**, and **32**, as well as for the acylation, barely show any influence on the selectivity profiles of the reaction in comparison with **3a** and **3c**. More importantly, the selectivity profiles for the silylation differ very much from the acylation. While naphthyl alcohol (**5b**) is clearly preferred for the reaction with acetic anhy-

## 5.1 Effects of Dispersion Catalysts on the Selectivity

drider (31a), it shows less than 10 % conversion in the silylation reaction. Pentan-3-ol 5e shows similar results as 5b for the reaction with TBSCl, while isoborneol (5f) is almost not reacting at all (<0.2 %). The substrates cyclohexanol (5d) and cholesterol (5g) lead to conversions higher than 40 % for all reactions with the investigated catalysts and are thus the fastest alcohols in the silylation reactions (Figure 5.6). These results clearly show that the electronic properties at the reaction center are of minor importance for the silylation as for the acylation reaction. The substrate with an electron-rich aryl system (5b) is reacting at a similar rate as pentan-3-ol (5e). The fastest systems, however, share a similar reaction center, which might be more influential for silylation than for acylation.

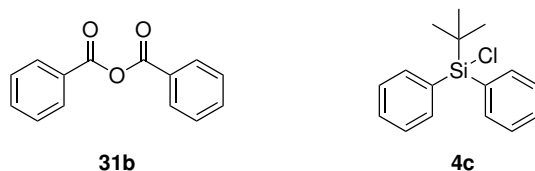


**Figure 5.6.** Normed product ratios for the competition experiments of 5b, 5d–g with TBSCl (1a) and 10 mol% of various catalysts in methylene chloride.

Nonetheless, both reactions follow a similar reaction pathway, where the reagent is attacked by a Lewis base catalyst to form an active intermediate. This intermediate will then be attacked by the substrate, which causes the difference in the selectivity profiles here. For the silylation an oxophilic silicon atom will be in focus of the attack, while at the acylation a carbon is targeted. One might also consider steric demand as a reason for the low conversion of the naphthyl alcohol (5b) in the reaction with TBSCl (1a) since a TBS group is larger than an acetyl group. The combination of a bulky alcohol and a sterically demanding reagent can lead to steric repulsion in the rate determining step and can thus slow down the reaction of this specific alcohol.

### 5.1.3 Increase of Selectivity by Enlarged Reagents

As described in the previous section, a strong influence of DED-catalysts (**26**, **28**, and **30**) on the selectivity cannot be observed easily. Instead of focusing on the catalyst, one can also change the reagents to enlarge the surface area of acylation and silylation reagents, which might increase the interaction with the catalysts and/or the substrate. Both reactions show a clear preference for a particular substrates. While for the acylation the naphthyl alcohol (**5b**) is preferred, in the silylation similar reactivity could be observed for cyclohexanol (**5d**) and cholesterol (**5g**). A logical next step involves enlarging the reagents with aromatic ring systems, which for the acylation leads to benzoic anhydride (**31b**) and for the silylation to *tert*-butyldiphenylsilyl chloride (TBDPSCl, **4c**). Throughout the experiments the reaction conditions remained otherwise unchanged.



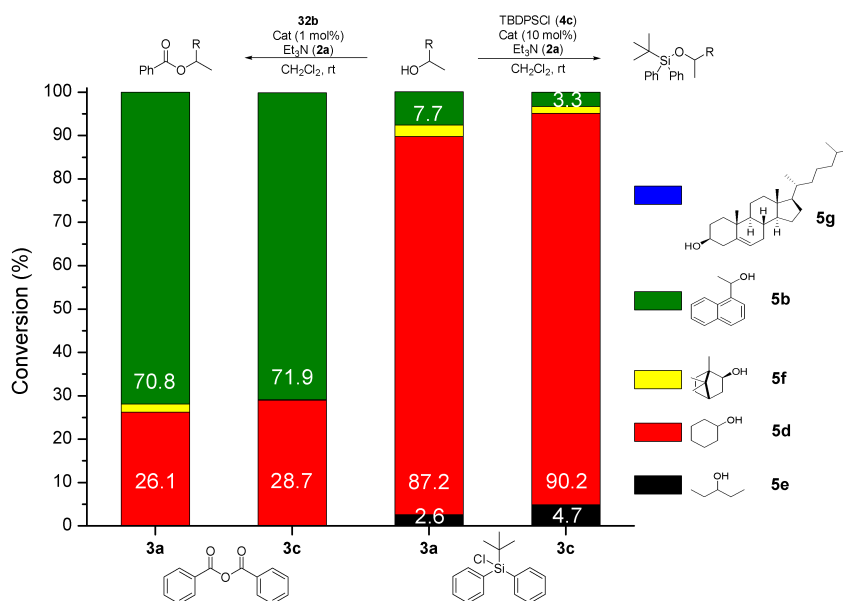
**Scheme 5.4.** Enlarged reagents benzoic anhydride (**31b**) and *tert*-butyldiphenylsilyl chloride (TBDPSCl, **4c**) used in competition experiments.

As a consequence of the enlarged molecules, analytical problems occurred concerning the largest systems cholesteryl benzoate and silylated cholesterol. No usable analytical data could be obtained by gas chromatography analysis, where the signals appear as very broad and in an irregular fashion. A change in the heating program of the GC to create longer measurements did not lead to better results. As a conclusion one can consider that the cholesterol products cannot be evaporated completely and that they only partially show signals in the spectra. Therefore, cholesterol (**5g**) will be excluded from further discussion, even though the alcohol has been present during the experiments. Only the products of alcohols **5b**, **d**, **e**, and **f** can be fully observed and will be discussed.

For both reactions the overall yield is smaller with values below 50 %, which might in part be due to the non-detectable cholesterol products and also to longer reaction times. Furthermore, the selectivity is increased for both reactions. While naphthyl alcohol (**5b**) is preferred for the benzylation with 70 %, cyclohexanol (**5d**) is highly favored with a conversion of around 90 % in the reaction with TBDPSCl (**4c**). As observed for the reactions before, isoborneol (**5f**) shows almost no conversion in both reactions. In addition, pentan-3-ol (**5e**) shows almost no conversion for the benzylation (>0.2 %) and less than 5 % conversion for the silylation. For the silylation with TBSCl (**1a**), cyclohexanol (**5d**) and cholesterol (**5g**) have already been strongly favored and the selectivity can be increased by a larger protection group. However, these results are clearly preliminary, since cholesterol (**5g**) could not be analyzed and the selectivity might be inaccurate. The high selectivity of cyclohexanol (**5d**) might also be based on the fact that the product of

## 5.1 Effects of Dispersion Catalysts on the Selectivity

cholesterol (**5g**) could not be detected (Figure 5.7).



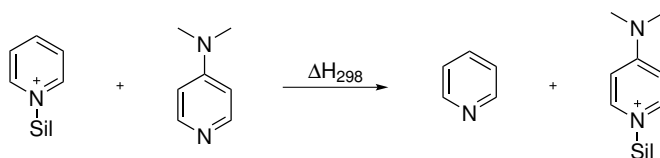
**Figure 5.7.** Normed product ratios for the competition experiments of **5b**, **5d–g** with benzoic anhydride (**31b**) and TBDPSCI (**4c**) with **3a** and **3c** as catalysts in methylene chloride.

It can be concluded that an effect of the DED-catalysts used under the described conditions, is not observable. Reasons for this might be the catalyst structure, the linker length or the attached DED group. Further investigations in this field can possibly lead to higher selectivities in the competition experiments. Furthermore, a difference can be observed comparing two different reactions (acylation and silylation). While 1-(naphthalen-1-yl)ethan-1-ol (**5b**) has been preferred for the acylation, cylcohexanol (**5d**) and cholesterol (**5g**) are strongly favored using TBSCl (**1a**) as a reagent. Larger reagents lead to a promising increase in selectivity, but also entail analytical difficulties. For further research one should consider taking a closer look at the influence of solvents which might lead to more promising results as shown earlier. Moreover, various group sizes for both reactions could be studied in more detail.



## 5.2 Does the Size of the Silyl Group Matter?

In the following chapter, differently sized silyl groups will be investigated by quantum chemical methods. For all reactions it has been observed that a change in size of the reagent can also influence the product ratios. In the following, the effect of size on the Lewis basicity (SCA values) and on the protection of an alcohol will be discussed ( $\Delta H_{\text{Rxn}}$ , Scheme 5.6). In the absence of sufficiently detailed experimental data, the silyl cation affinities (SCAs) have been calculated in combination with DMAP (**3a**). In addition, gas phase reaction enthalpies at 298.15 K for various silyl groups have been obtained at the MP2(FC)/G3MP2large//MPW1K/6-31+G(d) level of theory in combination with the SMD solvation model in  $\text{CHCl}_3$ .<sup>[168]</sup> The used methods are known for underestimating dispersive interaction, however, it is not the goal of this study to define dispersive forces between the catalyst and the reagents, but to achieve a rough estimate of how much the reaction is influenced by the size of the reagent.<sup>[161,169]</sup> The size of each silyl group has been determined by the cavity volumes ( $\text{Vol}_{\text{rel}}$ ) obtained from the calculated Lewis base adducts for each compound in  $\text{CHCl}_3$  (relative to the TBS adduct). Since the solvation data is closer to the actual experiment, these values will be compared here. Shown in Table 5.1 are activated silyl species attached to DMAP (**3a**) in a small selection including TMSCl (**4a**), TBDPSCl (**4c**), and tris(trimethylsilyl)silyl chloride (TTMSSCl, **4d**) in comparison to TBSCl (**1a**). The difference, especially in size, is clearly observable for the larger compounds and should make an attack at the silicon center more difficult than for a smaller group such as TMSCl (**4a**).



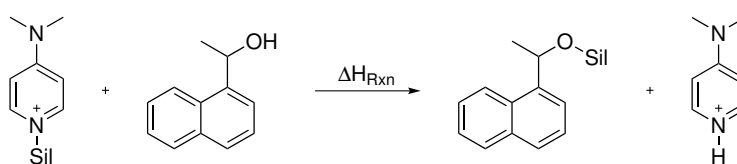
**Scheme 5.5.** Silyl cation affinities (SCAs) for different silyl compounds with DMAP (**3a**).

The SCA values obtained for all silyl compounds show that size does not influence the formation of an active intermediate as shown on Table 5.1 (Scheme 5.5). The variation for these values is rather small and in an area of  $5 \text{ kJ mol}^{-1}$ . The smallest compound TMSCl (**4a**) achieved a value of  $-34.2 \text{ kJ mol}^{-1}$ , which is close to the reference compound TBSCl (**1a**) with  $-36.2 \text{ kJ mol}^{-1}$ . Systems of almost identical volume, TESCl (**4e**), lead to  $-35.2 \text{ kJ mol}^{-1}$ , while larger systems, such as TBDPSCl (**4c**) or TTMSSCl (**4d**), provided values of  $-38.5 \text{ kJ mol}^{-1}$  and  $-33.0 \text{ kJ mol}^{-1}$ , respectively. Compounds of similar size, for instance TIPSCl (**4b**) and dimethyl(naphthalen-1-yl)silyl chloride (DMNSCl, **4f**), led to similar SCA values of  $-35.7 \text{ kJ mol}^{-1}$  and  $-37.3 \text{ kJ mol}^{-1}$ . Multiple phenyl groups attached to the silicon center as in TPSCl (**4g**) lead to the most stable product with an SCA value of  $-39.4 \text{ kJ mol}^{-1}$  (Table 5.1). One can conclude that the SCA values for all silyl compounds seem not to be of help for a better understanding of the influence of size in the silylation reaction. These results can be explained by the planar structure of the Lewis base

## 5.2 Does the Size of the Silyl Group Matter?

catalyst which is not influenced by the size of the reagent. Therefore, it can be stated that there is no thermochemical control in terms of reagent size for the pre-equilibrium.

Nonetheless, the rate-determining step of the silylation reaction, which is most likely the attack of the alcohol on the activated silyl-species, should be more sensitive to the size of the reagent. Therefore, the reaction enthalpies ( $\Delta H_{\text{Rxn}}$ ) for the attack of secondary alcohol (**5b**) on the activated species have been calculated for all silyl reagents (Scheme 5.6). All compounds show a strong preference to form the product silyl ether in solution in a range of  $30 \text{ kJ mol}^{-1}$ , which is a much broader range than for the SCA values before.



**Scheme 5.6.** Reaction enthalpies ( $\Delta H_{\text{Rxn}}$ ) for different silyl compounds with **5b**.

For TBSCl (**1a**)  $\Delta H_{\text{Rxn}}$  is determined as  $-36.4 \text{ kJ mol}^{-1}$ , which is about  $3 \text{ kJ mol}^{-1}$  less stable than for the smallest group TMSCl (**4a**,  $-39.7 \text{ kJ mol}^{-1}$ ). It is worth noting that groups with three identical substituents perform similar to TBS in the reaction enthalpy independent of the size. TESCl (**4e**), which is of almost identical size ( $\text{Vol}_{\text{rel}} = 1.01$ ), leads to  $-35.0 \text{ kJ mol}^{-1}$ , while the larger TIPSCl (**4b**,  $\text{Vol}_{\text{rel}} = 1.19$ ) shows a similar reaction enthalpy ( $-34.6 \text{ kJ mol}^{-1}$ ), too. The largest molecule TTMSSCl (**4d**) achieves a rather small stabilization with  $-26.7 \text{ kJ mol}^{-1}$ , which can be rationalized with the higher electron density of the silicon center of this molecule. However, TPSCl (**4g**), which is similar in size to TTMSSCl (**4d**), yields a good reaction enthalpie of ( $-46.6 \text{ kJ mol}^{-1}$ ). Systems with various substitutes, such as TBDPSCl (**4c**) and DMNSCl (**4f**), show better results for the attack of alcohol **5b**. The reaction enthalpy of these compounds is found to be in the area of  $-50 \text{ kJ mol}^{-1}$ , in which TBDPSCl (**4c**) performs best with  $-53.2 \text{ kJ mol}^{-1}$ . In all cases where bulky substituents are attached to the catalyst system the reduction of steric repulsion might also be a driving force for this reaction (**4c,f,g**). Even though the size of DMNSCl (**4f**) and TIPSCl (**4b**) is similar (1.25 and 1.29), they differ by  $10 \text{ kJ mol}^{-1}$  in the reaction enthalpies. One might argue that the overall bulkiness is bigger for TIPSCl (**4b**) and therefore the reaction enthalpy decreases from  $-44.7 \text{ kJ mol}^{-1}$  for DMNSCl (**4f**) to  $-34.6 \text{ kJ mol}^{-1}$  for TIPS (**4b**), while for [1,1'-biphenyl]-4-yl dimethylsilyl chloride (BPDMSCl, **4h**) the smallest reaction enthalpy has been achieved ( $-14.1 \text{ kJ mol}^{-1}$ ). It can be stated that dispersive effects might be involved especially for DMNSCl (**4f**) and BPDMSCl (**4h**) since two big  $\pi$ -areas can overlap and increase the stability of the final product (Table 5.1).

**Table 5.1.** Comparison of SCA values and reaction enthalpies (in  $\text{kJ mol}^{-1}$ ) of various silyl chlorides in combination with DMAP (**3a**) and alcohol **5b** (gas and solution phase data) and relative volumes ( $V_{\text{rel}}$ ).

System	No.	SCA Values		Reaction Enthalpy		$V_{\text{rel}}$
		$\Delta H_{298}(\text{gas})^a$	$\Delta H_{298}(\text{sol})^b$	$\Delta H_{\text{Rxn}}(\text{gas})^a$	$\Delta H_{\text{Rxn}}(\text{sol})^b$	
	<b>4d</b>	−49.4	−33.0	+5.5	−26.7	1.49
	<b>4c</b>	−53.4	−38.5	−16.7	−53.2	1.35
	<b>4g</b>	−53.4	−39.4	−4.9	−46.6	1.48
	<b>4h</b>	−53.7	−35.8	+15.8	−14.1	1.24
	<b>4f</b>	−54.6	−37.3	−15.9	−44.7	1.13
	<b>4b</b>	−55.4	−35.7	−11.0	−34.6	1.19
	<b>4e</b>	−55.4	−35.2	−13.8	−35.0	1.01
	<b>4a</b>	−56.3	−34.2	−20.7	−39.7	0.83
	<b>1a</b>	−56.6	−36.2	−15.3	−36.4	1.00

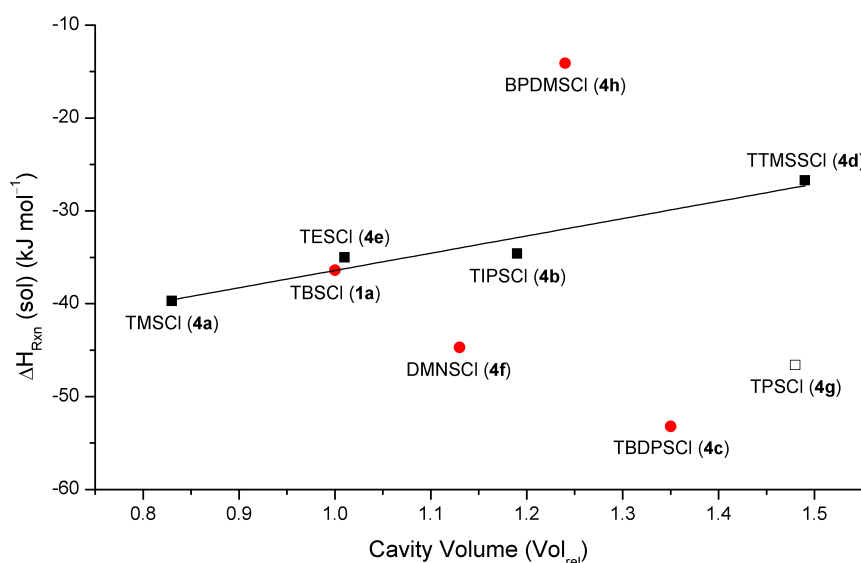
<sup>a</sup> Gas phase energies (in  $\text{kJ mol}^{-1}$ ) have been calculated at MP2(FC)/G3MP2large//MPW1K/6-31+G(d) level.<sup>b</sup> Solvation energies (in  $\text{kJ mol}^{-1}$ ) have been calculated at SMD/MPW1K/6-31+G(d) level for  $\text{CHCl}_3$ .

However, the used method MPW1K is known to underestimate dispersive forces and therefore these can be excluded as a reason for the increased stability.<sup>[161]</sup> In order to describe a dispersive effect one should consider transition state calculations for the attack of the alcohol. Furthermore, steric effects should also be taken into account as a factor, especially for TIPSCl (**4b**), TTMSS (**4d**), and TPSCl (**4g**) with three bulky groups interacting with DMAP (**3a**) as catalyst and the naphthyl ring of the silylated product. Nonetheless, a comparison between reaction enthalpy ( $\Delta H_{\text{Rxn}}$ ) and the relative volume ( $V_{\text{rel}}$ ) leads to further insights for this reaction. Almost all reagents with three identical substituents (**4a,b,d,e**), besides TPSCl (**4g**), can be correlated in a linear fashion.

## 5.2 Does the Size of the Silyl Group Matter?

In case of TPSCI (**4g**) the intermediate is less favored based on strong steric repulsions and a larger deviation from the linear correlation can be observed (Figure 5.8). The reagents with various substituents (**4c,f,h**) show no correlation concerning  $\Delta H_{\text{Rxn}}$  when compared to their size. Nonetheless, it becomes apparent that for reagents with bulky substituents such as DMNSCI (**4f**) and TBDPSCI (**4c**) the stabilization of the products is higher than for the reagent.

With an increased size by a factor of 1.35 *tert*-butyldiphenylsilyl chloride (TBDPSCI, **4c**) shows the highest reaction energy of all compounds with  $-53.2 \text{ kJ mol}^{-1}$ . Even though this group has a higher steric demand, the influence of the reaction enthalpy seems to be rather small. In contrast, the largest system tris(trimethylsilyl)silyl chloride (TTMSSCI, **4d**) with a relative volume of 1.49 compared to TBSCl (**1a**) performs badly concerning the reaction enthalpy for this reaction. However, as mentioned earlier for TTMSSCI (**4d**), the reaction enthalpy ( $\Delta H_{\text{Rxn}}$ ) might not only be influenced by its size, but also by the electronic structure with three trimethylsilyl groups directly attached to the silicon center. For TTMSSCI (**4d**) the small reaction enthalpy of  $-26.7 \text{ kJ mol}^{-1}$  might thus be a combination of steric and electronic effects (Table 5.1).



**Figure 5.8.** Reaction enthalpies ( $\Delta H_{\text{Rxn}}$ ) vs. relative volumes ( $\text{Vol}_{\text{rel}}$ ) for various silyl reagents. Squares represent reagents with three identical substituents, while circles have different ones.

The discussed calculations clearly show that the choice of the silyl reagent can influence the reaction, within a range of roughly  $30 \text{ kJ mol}^{-1}$ . Steric and electronic effects should be taken into account when it comes to silylation reagents. Furthermore, it should be noted that reagents with three identical groups generally perform worse than silyl chlorides with different groups (**4c,f**, and **1a**). However, TPSCI (**4g**) is the exception in this matter, but is most likely driven by a disfavored reagent than a strongly stabilized product. A correlation between size and reaction enthalpies based on all reagents is not possible over all investigated reagents. It is in parts possi-

ble to correlated reagents with identical substituents in a linear fashion. This theoretical estimate differs from the corresponding reaction under experimental conditions in one important aspect. An auxiliary base, such as  $\text{Et}_3\text{N}$ , will be used in the experiments and is needed to deprotonate the catalyst for reactivation for the catalytic cycle. This can also have an influence on the reaction rate for the shown compounds. Nevertheless, these results can give a rough validation for various silyl reagents and could be optimized by using different computational methods, which focus on specific aspects, for instance dispersive interaction, more accurately.

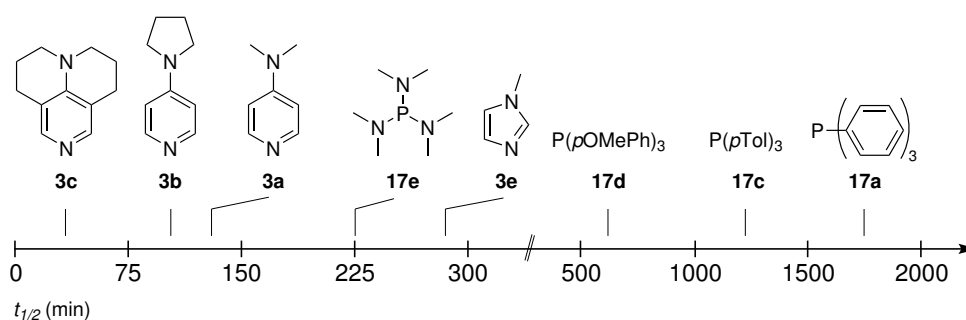


## 6 Summary

In this thesis the silylation of alcohols has been investigated in terms of the influence of auxiliary bases, Lewis base catalysts, solvents, temperature, and the effect of reagents. A better understanding of this broadly used reaction could be achieved in several aspects. Furthermore, with use of quantum chemical approaches the effectiveness of various catalysts have been predicted and, in part, experimentally validated. In addition, effects of large  $\pi$ -systems on a Lewis base catalysts have been studied in terms of dispersive interaction with substrate molecules.

### 6.1 General Summary

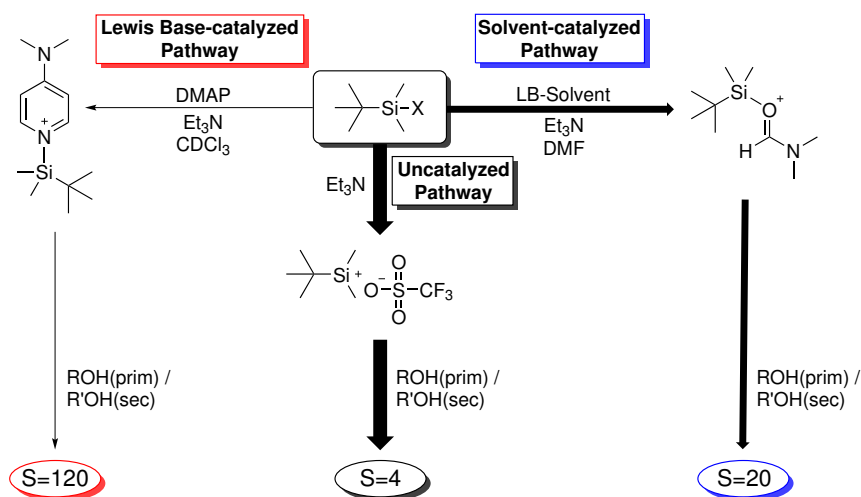
One of the most important findings concerning the silylation reaction, is the fact that DMF (**3h**) cannot be seen as an 'innocent' solvent in the 'Corey procedure', but is also interacting with the silyl reagent to form an active intermediate, which has been observed by NMR spectroscopy. The fast reaction rates in DMF can therefore be seen as a reaction performed in a weak Lewis base catalyst. The influence of auxiliary bases has been found to be rather small on the reaction rate. As long as the amount of auxiliary base equals the silyl reagent the reaction proceeds to full conversion. The reaction stops when not enough auxiliary base is present due to the fact that the catalyst is not regenerated anymore. In DMF as solvent a lack of auxiliary base leads to only 80 % conversion, due to too much hydrogen chloride in the reaction mixture. When a strong Lewis base is used as catalyst, one can reduce the reaction half-life from 163.9 min for imidazole (**3d**) to 9.0 min for 9-azajulolidine (**3c**) for the reaction with primary alcohol **5a**. In addition to pyridine-based Lewis base catalysts, phosphanes have been studied and showed a lower reactivity in general (Figure 6.1). The effect of temperature can be seen as mostly beneficial to solubility issues, but increases the reaction rate only moderately.



**Figure 6.1.** Reaction half-lives for the silylation of primary alcohol **5a** with TBSCl (**1a**, 1.2 equiv) catalyzed by various catalysts (1 mol%) in the presence of  $Et_3N$  (**2a**, 1.2 equiv) in  $CDCl_3$ .

Moreover, it has been shown that donor-substituted, secondary alcohols lead to an increased reaction rate, thus supporting the idea that the attack of the alcohol is the rate determining step for the silylation reaction. While a reaction half-life of 159.9 min has been determined for sec-

ondary alcohol **5b** in  $\text{CDCl}_3$  with 30 mol% of **3c** as catalyst, it could be decreased with an EDG such as  $\text{NMe}_2$  in *para*-position to 98.4 min under otherwise unchanged conditions. In addition to the variation of the substrate alcohol, the silyl reagent has been changed concerning the use of various leaving groups, which has been found to have an impressive effect on the reaction rate. While for the silylation of secondary alcohol **5b** with TBSCl (**1a**) and 30 mol% DMAP (**3a**) a half-life of 471.1 min has been obtained, TBSOTf (**1b**) achieved full conversion within a few minutes. This tremendous difference can only be explained by a change in the reaction mechanism, in which the silyl reagent (TBSOTf, **1b**) exists as an ion pair and can directly be attacked by the alcohol. The usual Lewis base activation of the silyl reagents is not needed for these specific reagents, such as TBSOTf (**1b**). Instead of the accommodation of three molecules in a transition state for the Lewis base-catalyzed pathway, only two reactants need to proceed through a less complex transition state for TBSOTf (**1b**), which explains the faster reaction rates. The silylation reaction can undergo three possible pathways, depending on the given conditions, which are depicted in Figure 6.2.



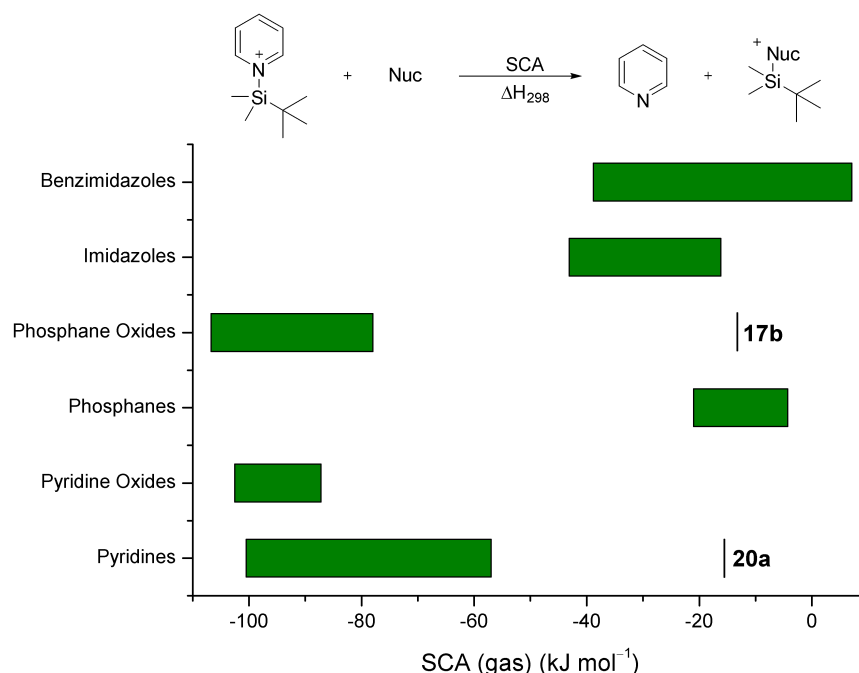
**Figure 6.2.** Overview of various pathways for the silylation reaction depending on the choice of solvent and leaving group of the reagent.

Using direct rate measurements by  $^1\text{H}$  NMR spectroscopy, the selectivity between primary, secondary, and tertiary alcohol can be determined as  $4.2 \times 10^6$ :  $2.0 \times 10^5$ : 1, which leads to the conclusion that a secondary or a tertiary alcohol are most likely not to be silylated when a primary alcohol is present. Through kinetic measurements (direct rate approach) and competition experiments (indirect rate approach) the selectivity between primary and secondary for different reaction pathways has been determined. As a result it can be stated that the Lewis base-catalyzed reaction is able to generate the highest selectivity ( $S = 120$ ) when performed in an apolar solvent ( $\text{CDCl}_3$ ). The overall reaction rate increases by changing the solvent to DMF, which also decreases the selectivity to  $S = 20$ . For the fast reagent TBSOTf (**1b**) a low selectivity of  $S = 4$  has



been observed, which leads to the conclusion that for a selective protection, when two different hydroxy groups are present, the Lewis base approach in an apolar solvent should be used.

Quantum chemical calculations have been performed to quantify the Lewis basicity of the catalysts towards silyl cations. It has been shown that for the used catalysts (**3a–g**) the calculated silyl cation affinity (SCA) values are in good agreement with the obtained rate data (Chapter 2.2.2). This method can be used to predict the effectiveness of different classes of catalysts, including pyridines, phosphanes, and imidazoles, with good accuracy. It can be concluded that a Lewis basicity vs. reaction rate correlation can be helpful when the compared catalyst can be sorted in groups. For planar systems, such as pyridines, methyl cation affinities (MCAs) lead to similar results and can be correlated with the SCAs. The SCAs and MCAs could be correlated for different modifications on the 2-position of imidazole, while a closely related system benzimidazole no correlation can be found. Therefore it should be noted that these approaches have limitations and different angles, such as steric repulsion, have to be considered as a reason for bigger variations even in related systems. The strongest stabilizations and therefore the lowest SCA values have been obtained for pyridine systems, which can be found in an area of  $-100 \text{ kJ mol}^{-1}$ – $-60 \text{ kJ mol}^{-1}$  (Figure 6.3).

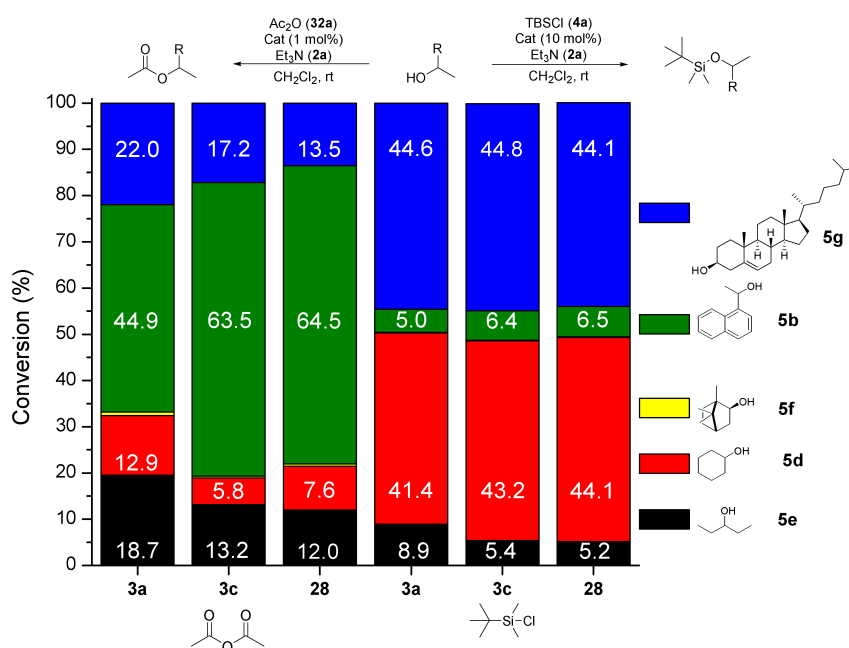


**Figure 6.3.** Silyl cation affinities (SCAs) of respective catalysts from different classes, including pyridines, phosphanes, and imidazoles.

For pyridine oxides, as well as for phosphane oxides, the SCA values have been found in a similar area as the pyridines, however there is reasonable doubt that these systems perform as fast

as pyridine-based catalyst. A reason might be that the Si–O bond, which will be formed during the catalytic cycle, is similar to the bond in the product silyl ester and therefore the driving force should be smaller for these reactions. The performance of phosphane compounds is not convincing for usage as Lewis base catalyst in the silylation reaction, which is supported by the low SCA values of  $-20 \text{ kJ mol}^{-1}$ — $-5 \text{ kJ mol}^{-1}$  and by the experimentally determined reaction half-lives. In contrast to phosphanes, imidazoles and benzimidazoles show slightly higher SCAs and could be used as catalysts for the silylation with possible higher reaction half-lives than pyridine catalysts.

The selective transformation of five different substrates has been discussed with the focus on dispersive interactions for the acylation and for the silylation reaction (Chapter 5). The use of modified pyridine-based catalysts should create a dispersive interaction within the transition states and thus prefer one substrate over the other four. An effort has been made by synthesizing various catalyst with possible dispersive energy donors (DED) and comparing these with established catalysts, such as DMAP (**3a**) and 9-azajulolidine (**3c**). The difference in the obtained product ratio, shown in Figure 6.4, has been found to be rather small regarding the influence of a Lewis base catalyst. However, it is worth noting that a mentionable difference in terms of substrate selectivity can be observed by comparing the reaction with acetic anhydride (**31a**) to the silylation with TBSCl (**1a**).



**Figure 6.4.** Normed product ratios for the competition experiments of **5b**, **5d–g** with acetic anhydride (**31a**) and TBSCl (**1a**) with various catalyst (**3a**, **3c**, and **28**) in methylene chloride.

While for the acylation mostly 1-(naphthalen-1-yl)ethanol (**5b**) is transformed with a selectivity up to 64 %, this alcohol is of minor importance in the silylation (<7 %). Cyclohexanol (**5d**) and cholesterol (**5g**) are clearly preferred for the transformation with TBSCl (**1a**) and yielded in ratios over 40 %. For the silylation, as well as for the acetylation, isoborneol (**5f**) showed almost no reactivity which is most likely caused by its sterically demanding structure. Since both reactions follow a similar reaction pathway, in which the reagent is activated by a Lewis base, it becomes apparent that the selectivity is decided within the transition state of the reaction. The reagents differ in size which might be a reason for the preference of alcohol **5b** in the acylation reaction, since the activated species is smaller compared to the TBS adduct.

Further investigations with different reagents lead to analytical problems, however the limited data obtained from this reaction shows promising results. The quantum chemical calculations for the silylation reaction showed that silyl reagents with three identical substituents lead to less stabilized systems when substrate **5b** is used. In order to increase the selectivity further, one should consider using larger systems attached to a Lewis base catalyst.

## 6.2 Outlook

Having obtained a better general knowledge of the silylation reaction the next goal in future research could be an in-depth study of regio- or enantioselective protection chemistry. The development of a fast silylation reagent which selectively transforms one substrate in the presence of another might be a challenge for the next years. Modifications on the leaving group of the different silyl reagents might be a possible angle as well as using modified Lewis base catalysts. The aim should always be a broad applicability of these methods in order to modify the synthetic, organic chemistry further. The idea of using silyl reagents in kinetic resolution experiments has just arrived in nowadays research and will be developing during the next years. A combination of modified silyl reagents with kinetic resolution experiments are a promising starting point for further research.

In the field of selective transformations driven by dispersive interactions, many modifications are possible to increase the outcome. A good starting point would be further modifications of the catalyst motif and of the reagent itself in order to increase the dispersive interaction. For this project to succeed it is necessary that theoretical calculations are used either to determine the relevant transition state, where the selectivity is decided, or to predict the catalyst efficiency.



## 7 Experimental Part

### 7.1 General Information

All air and water sensitive manipulations were carried out under a nitrogen atmosphere using standard Schlenk techniques. Calibrated flasks for kinetic measurements were dried in the oven at 120 °C for at least 12 hours prior to use and then assembled quickly while still hot, cooled under a nitrogen stream and sealed with a rubber septum. All commercial chemicals were of reagent grade and were used as received unless noted otherwise. CDCl<sub>3</sub> was refluxed for at least one hour over CaH<sub>2</sub> and subsequently distilled. <sup>1</sup>H and <sup>13</sup>C NMR spectra were recorded on Varian 300 or Varian INOVA 400 machines at room temperature (27 °C). All <sup>1</sup>H chemical shifts are reported in ppm ( $\delta$ ) relative to CDCl<sub>3</sub> (7.26); <sup>13</sup>C chemical shifts are reported in ppm ( $\delta$ ) relative to CDCl<sub>3</sub> (77.16). <sup>1</sup>H NMR kinetic data were measured on a Varian Mercury 200 MHz spectrometer at (23 °C). HRMS spectra (ESI-MS) were carried out using a Thermo Finnigan LTQ FT instrument. IR spectra were measured on a Perkin-Elmer FT-IR BX spectrometer mounting ATR technology. All kinetic measurements with reaction times longer than 24 hours were mechanically shaken; for each reaction the rotation speed was set at 480 turns/minute. Analytical TLCs were carried out using aluminium sheets silica gel Si60 F254

### 7.2 NMR Kinetics

In order to achieve consistent data stock solutions of various compounds have been prepared. CDCl<sub>3</sub> and TEA were freshly distilled under N<sub>2</sub> from CaH<sub>2</sub> before use for the stock solutions. In case of DMF-d<sub>7</sub> as solvent all stock solutions have been prepared under glove box atmosphere. The NMR tube is dried under vacuum and flushed with N<sub>2</sub> three times to eliminate water. 200  $\mu$ L of each stock solution was transferred to a NMR tube using a Hamilton syringe or a 200  $\mu$ L Eppendorf pipette, which is closed with a cap and sealed with parafilm. In case of a very long reaction time ( $t_{1/2} > 400$  min) the tube is flame-sealed.

**Table 7.1.** Overview of stock solutions for kinetic measurements of alcohol **5a** with DMAP (**3a**, 4 mol%). The concentration of the catalyst can be changed if necessary.

	substance	n [mmol]	m [g]	Volume [mL]	c [M]	equiv.
Stock A	TBSCl ( <b>1a</b> )	3.6	0.542		0.72	1.2
	Dioxane	1.0	0.088	0.086	0.20	0.33
Stock B	TEA ( <b>2a</b> )	3.6	0.364	0.498	0.72	1.2
	Alcohol ( <b>5a</b> )	3.0	0.475		0.60	1.0
Stock C	Catalyst	0.12	0.015		0.024	0.04

#### 7.2.1 General Procedure for NMR Kinetics

In following the general procedures for the performed NMR measurements will be listed. Small deviation appear based on the catalyst loadings and size of the stock solutions.

**General procedure (I)** for reactions of **5a** with 2, 3, and 4 mol% catalyst:

0.2 mL from 5 mL of stock solution A (TBSCl (542 mg, 3.6 mmol), dioxane (0.088 g, 0.086 mL)), 0.2 mL from 5 mL of stock solution B **5a** (475 mg, 3.0 mmol), triethylamine (**2a**, (364 mg, 3.0 mmol) and 0.2 mL of 5 mL stock solution C (0.06 / 0.09 / 0.12 mmol of catalyst) were mixed in a NMR tube and sealed.

**General procedure (II)** for reactions of **5a** with 0.25, 0.5, and 1 mol% catalyst:

0.2 mL from 5 mL of stock solution A (TBSCl (542 mg, 3.6 mmol), dioxane (0.088 g, 0.086 mL)), 0.2 mL from 5 mL of stock solution B (**5a** (475 mg, 3.0 mmol), triethylamine (**2a**, (364 mg, 3.0 mmol)) and 0.2 mL from 10 mL stock solution C (0.012 / 0.015 / 0.03 mmol of catalyst) were mixed in a NMR tube and flame sealed.

**General procedure (III)** for reactions of **5b** with 4, 10, 20, and 30 mol%:

0.2 mL from 5 mL of stock solution A (TBSCl (542 mg, 3.6 mmol), dioxane (0.088 g, 0.086 mL)), 0.2 mL from 5 mL of stock solution B (**5b** (517 mg, 3.0 mmol), triethylamine (**2a**, (364 mg, 3.0 mmol)) and 0.2 mL from 2 mL stock solution C (0.048 / 0.12 / 0.24 / 0.36 mmol of catalyst) were mixed in a NMR tube and flame sealed.

**General procedure (IV)** for temperature-dependent reactions of **5b** with 30 mol% of catalyst **3g**:

0.2 mL from 5 mL of stock solution A (TBSCl (542 mg, 3.6 mmol), dioxane (0.088 g, 0.086 mL)), 0.2 mL from 5 mL of stock solution B (**5b** (517 mg, 3.0 mmol), triethylamine (**2a**, 364 mg, 3.0 mmol)) and 0.2 mL from 2 mL stock solution C (0.36 mmol of catalyst **3g**) were mixed in a NMR tube and flame sealed. During the NMR measurement the temperature was set to the temperatures of choice.

### 7.3 Procedure for the Competition Experiments

In the following the competition experiments of chapter 3 and 5 will be explained and described further. The biggest difference between both experiment is the for the effects of the leaving groups indirect comparison was performed, while for the dispersion experiments all reagents were compared directly with each other.

### 7.3.1 Selectivity of Leaving Groups

In order to achieve the needed accuracy three stock solutions have been prepared. This is necessary to guarantee the experiment reproducibility, however one should always try to minimize the number of stock solutions. The alcohols **5a** and **5b** were mixed in a separate stock solutions (0.66 M), while the silyl reagent was in a third stock solution (2.2 M). Since no catalyst is needed for this reaction in DMF, no further stock solution was prepared. Dry DMF is stored in a glovebox over molecular sieves as well as freshly distilled Et<sub>3</sub>N (**2a**). All stock solutions have been prepared in a glovebox atmosphere in order to avoid water or other impurities in the reaction mixture for the reactions in DMF. Moreover, both alcohols have been dried by washing with dry toluene and removing the solvent afterwards for several times. For the reaction in CDCl<sub>3</sub> the stock solution have been prepared under bench conditions. 3 mL of each alcohol were mixed in a 25 mL dried flask with a magnetic stir bar and sealed with a septa. Freshly distilled Et<sub>3</sub>N was added in equimolar amounts as compared to the silyl reagent. Under steady mixing with a magnetic stirrer and temperature control with a water bath various amounts of silyl reagent were added using a syringe pump within 15 min. In contrast to the prior method for the reaction in chloroform a catalyst (DMAP, **3a**) was added in various amounts based on the concentration of silyl reagent. A sample of 0.05 mL was taken and diluted with 1 mL methylene chloride and analyzed by GC, 55(0)–5–150(0)–20–280(20). The determination of conversion will be explained in chapter 8.1.2.

### 7.3.2 Selectivity of Five Alcohols

For all products the retention times were determined and a calibration curve was measured using tetracosane (**33**) as an internal standard. Stock solution (2 M) were prepared for the alcohols **5b**, **5d**, **5e**, and **5f**, while cholesterol (**5g**) was directly added to the reaction flask. In addition, stock solutions for the catalyst with Et<sub>3</sub>N (various concentration depending on the catalyst loading), tetracosane (0.12 M), and reagent (2 M) have been prepared. All alcohols were mixed in a one to one ratio and 1 mL of catalyst and 1 mL of reagents stock solution were added to the mixture. 4 mL of freshly distilled solvent were added and the reaction proceeded at rt. 0.2 mL of the reaction mixture were mixed with 0.2 mL of tetracosane stock solution and diluted with 1 mL solvent. Samples were taken at different times of reaction process and measure by GC. The GC measurements have been performed using the following heating program 45(2)–5–150(0)–20–280(20) for acetylation and bezoylation, while for silylation reactions 55(0)–5–150(0)–20–280(30) was used. The calibration curves for the five converted alcohols can be found in chapter 8.1.2.

## 7.4 Synthesis of Starting Materials and Catalysts

### 7.4.1 General Procedures

In the following the most frequently used steps will be explained in detail for the silylation as well as for the acylation reactions.

#### General procedure (*Sil1*) for Silylation

One equivalent of alcohol and 1.2 equivalents of silyl reagent were dissolved in 20 mL DCM and 1.2 equivalents triethylamine (**2a**) was added. After adding up to 30 mol% of a catalyst, such as DMAP (**3a**), the reaction mixture was stirred at rt up to 7 d. The reaction mixture was washed with sat. aq.  $\text{NH}_4\text{Cl}$  solution, extracted three times with DCM (10 mL) and the combined organic phases dried over  $\text{MgSO}_4$ . The solvent was removed under reduced pressure and column chromatography on silica was used to purify the product.

#### General procedure (*Sil2*) for Silylation

One equivalent of alcohol and 10 equivalents of imidazole were dissolved in 20 mL DMF and 5 equivalents of silyl reagent were added. The reaction mixture was stirred at rt or at 70 °C up to 7 d depending on the steric demand of the alcohol. The reaction mixture was washed with sat. aq.  $\text{NH}_4\text{Cl}$  solution, extracted three times with DCM (20 mL), washed once with brine (10 mL) and the combined organic phases dried over  $\text{MgSO}_4$ . The solvent was removed under reduced pressure and column chromatography on silica was used to purify the product.

#### General procedure (*Sil3*) for Silylation

One equivalent of alcohol and 9 equivalents of imidazole were mixed with 0.9 equivalents of silyl chloride without any solvent. The reaction mixture stirred at 110 °C under microwave radiation for 10 min. The reaction mixture was washed with 2 M HCl solution, extracted three times with DCM (10 mL), washed once with brine (10 mL) and the combined organic phases dried over  $\text{MgSO}_4$ . The solvent was removed under reduced pressure and column chromatography on silica was used to purify the product.

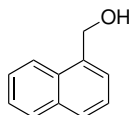
#### General procedure (*Ac1*) for Acylation

One equivalent of alcohol and 2 equivalents of anhydride were dissolved in 20 mL DCM and 2.5 equivalents triethylamine was added. After adding up to 10 mmol% of a catalyst, such as DMAP (**3a**), the reaction mixture was stirred at rt up to 7 d. The reaction mixture was washed with sat. aq.  $\text{NH}_4\text{Cl}$  solution, extracted three times with DCM (10 mL) and the combined organic phases dried over  $\text{MgSO}_4$ . The solvent was removed under reduced pressure and column chromatography on silica was used to purify the product.



### 7.4.2 Starting Materials and Products of Silylation Reactions

#### (1-Naphthyl)methanol (5a)



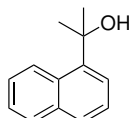
15 mmol (0.567 g, 0.5 equiv) of  $\text{NaBH}_4$  are solved in 100 mL THF and cooled down to  $-10^\circ\text{C}$ . 30 mmol (4.68 g, 4.07 mL, 1.0 equiv) of 1-naphthaldehyde were dissolved in 50 mL THF and added dropwise to the solution. The reaction was allowed to stir for 30 min at rt. The reaction process was monitored by TLC. The reaction was quenched by adding 2 M HCl until no  $\text{H}_2$  appeared anymore. The reaction mixture was extracted three times with DCM (20 mL) and washed with brine (20 mL). The combined organic phases were dried over  $\text{MgSO}_4$  and the solvent was removed under reduced pressure. A column chromatography on silica (i-hexane:EtOAc; 4:1) led to a white solid product **5a** in 95 % yield (4.50 g, 14.25 mmol).

$R_f = 0.20$  (i-hexane:EtOAc, 4:1).  $^1\text{H NMR}$  (300 MHz,  $\text{CDCl}_3$ ):  $\delta = 2.67$  (bs, 1H, OH), 5.05 (s, 2H), 7.40 – 7.61 (m, 4H), 7.81 – 7.87 (m, 1H), 7.88 – 7.96 (m, 1H), 8.03 – 8.14 (m, 1H).  $^{13}\text{C NMR}$  (75 MHz,  $\text{CDCl}_3$ ):  $\delta = 63.37, 123.69, 125.27, 125.88, 126.32, 128.48, 128.69, 131.25, 133.80, 136.33$ .

**HRMS** (EI)  $\text{C}_{11}\text{H}_{10}\text{O}$  requires  $158.0732 \text{ g mol}^{-1}$ , found  $158.0726 \text{ g mol}^{-1}$ .

In accordance with literature.<sup>[170]</sup>

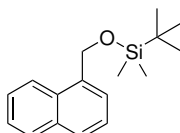
#### 2-(Naphthalen-1-yl)propan-2-ol (5c)



15 mmol (2.38 g) magnesium and 50 mmol (2.08 g) LiCl were dissolved in 150 mL THF and a little bit of iodine was added. The reaction mixture was allowed to stir for 15 min. 40 mmol (8.22 g) of 1-bromo-naphthalene was added slowly, stirred for 30 min and refluxed for 1 h. The reaction mixture was cooled down to rt and 80 mmol (4.64 g) of acetone were added slowly. After 1 h of stirring at rt the mixture was refluxed for 3 h. The reaction was quenched by adding saturated  $\text{NH}_4\text{Cl}$  under ice cooling. The reaction mixture was extracted three times with DCM (50 mL) and washed with brine (20 mL). The combined organic phases were dried over  $\text{MgSO}_4$  and the solvent removed under reduced pressure. Recrystallization from i-hexane led to a white solid product **5c** in 82 % yield (6.10 g, 12.3 mmol).

**<sup>1</sup>H NMR** (300 MHz, CDCl<sub>3</sub>):  $\delta$  = 1.89 (s, 6H), 7.36 – 7.74 (m, 4H), 7.80 (d, <sup>3</sup>*J* = 8.1 Hz, 1H), 7.85 – 7.98 (m, 1H), 8.76 – 9.01 (m, 1H). **<sup>13</sup>C NMR** (75 MHz, CDCl<sub>3</sub>):  $\delta$  = 31.64, 74.12, 122.70, 124.82, 125.19, 125.30, 127.35, 128.62, 129.08, 130.97, 134.93, 143.43. **HRMS (GC/EI)** C<sub>13</sub>H<sub>14</sub>O requires 186.1045 g mol<sup>-1</sup>, found 186.1036 g mol<sup>-1</sup>.

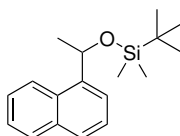
***tert*-Butyldimethyl(naphthalen-1-yl-methoxy)silane (7a)**



The reaction was performed using general procedure *Sil1*. The crude product was purified by flash-chromatography on SiO<sub>2</sub> (i-hexane:DCM; 4:1) to obtain 82 % of product **7a** as a colorless oil.

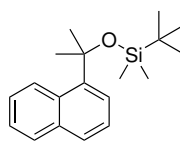
**<sup>1</sup>H NMR** (300 MHz, CDCl<sub>3</sub>):  $\delta$  = 0.14 (s, 6H, Si(CH<sub>2</sub>)<sub>2</sub>), 0.97 (s, 9H), 5.22 (s, 2H), 7.47 – 7.59 (m, 3H), 7.59 – 7.61 (m, 1H), 7.79 (d, <sup>3</sup>*J* = 8.1 Hz, 1H), 7.86 – 7.93 (m, 1H), 8.00 – 8.05 (m, 1H). **<sup>13</sup>C NMR** (75 MHz, CDCl<sub>3</sub>):  $\delta$  = -5.22, 18.46, 25.98, 29.17, 63.39, 123.27, 123.77, 125.45, 125.51, 125.79, 127.54, 128.57. **<sup>29</sup>Si NMR** (80 MHz, CDCl<sub>3</sub>):  $\delta$  = 20.58. **HRMS (EI)** C<sub>17</sub>H<sub>24</sub>OSi requires 271.1596 g mol<sup>-1</sup>, found 271.1590 g mol<sup>-1</sup>.

***tert*-Butyldimethyl(1-(naphthalen-1-yl)ethoxy)silane (7b)**



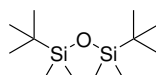
The reaction was performed using general procedure *Sil1*. The crude product was purified by flash-chromatography on SiO<sub>2</sub> (i-hexane:DCM; 4:1) to obtain 76 % of product **7b** as a yellowish oil.

**<sup>1</sup>H NMR** (300 MHz, CDCl<sub>3</sub>):  $\delta$  = -0.01 (s, 3H, SiCH<sub>3</sub>-*t*Bu), 0.10 (s, 3H, SiCH<sub>3</sub>-*t*Bu), 0.95 (s, 9H), 1.60 (d, <sup>3</sup>*J* = 6.4 Hz, 3H), 5.61 (q, <sup>3</sup>*J* = 6.6 Hz, 1H), 7.44 – 7.55 (m, 3H), 7.67 – 7.78 (m, 2H), 7.85 – 7.91 (m, 1H), 8.11 (d, <sup>3</sup>*J* = 7.3 Hz, 1H). **<sup>13</sup>C NMR** (75 MHz, CDCl<sub>3</sub>):  $\delta$  = -4.92, -4.83, 18.30, 25.89, 26.62, 68.48, 122.67, 123.34, 125.15, 125.53, 125.57, 127.17, 128.82, 129.88. **<sup>29</sup>Si NMR** (80 MHz, CDCl<sub>3</sub>):  $\delta$  = 18.4. **HRMS (EI)** C<sub>18</sub>H<sub>26</sub>OSi requires 286.1753 g mol<sup>-1</sup>, found 286.1744 g mol<sup>-1</sup>.

**tert-Butyldimethyl((2-(naphthalen-1-yl)propan-2-yl)oxy)silane (7c)**

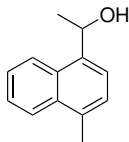
The reaction was performed using general procedure *Sil2*. The crude product was purified by flash-chromatography on SiO<sub>2</sub> (*i*hexane) to obtain 50 % of product **7c** as a colorless oil.

**<sup>1</sup>H NMR** (300 MHz, CDCl<sub>3</sub>):  $\delta$  = −0.14 (s, 6H), 0.91 (s, 9H), 1.89 (s, 6H), 7.36 – 7.53 (m, 3H), 7.55 (dd, <sup>3,3</sup>*J* = 7.3, 1.2 Hz, 1H), 7.74 – 7.77 (m, 1H), 7.84 – 7.87 (m, 1H), 8.82 – 8.85 (m, 1H). **<sup>13</sup>C NMR** (75 MHz, CDCl<sub>3</sub>):  $\delta$  = −2.15, 18.57, 26.31, 32.70, 76.38, 122.46, 124.75, 124.85, 125.14, 128.37, 128.75, 128.88, 131.34, 134.91, 144.21. **<sup>29</sup>Si NMR** (80 MHz, CDCl<sub>3</sub>):  $\delta$  = 12.18. **HRMS (EI)** C<sub>18</sub>H<sub>26</sub>OSi requires 285.1675 g mol<sup>−1</sup> (**7c**−CH<sub>3</sub>), found 285.1662 g mol<sup>−1</sup>.

**1,3-Di-tert-Butyl-1,1,3,3-tetramethyldisiloxane (9b)**

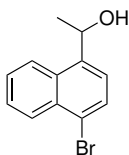
13.4 mmol (2.0 g) TBSCl (**1a**) was dissolved in 5 mL acetonitrile and 1 mL of H<sub>2</sub>O. After the addition of 15 mmol (2.49 g) of KI the reaction mixture stirred at rt for 12 h. The upper layer was pipetted off and distilled (80 °C, 15 mbar; oilbath: 100 °C) to lead to a colorless liquid **9b** in 29 % (0.95 g, 3.85 mmol) yield.

**<sup>1</sup>H NMR** (300 MHz, CDCl<sub>3</sub>):  $\delta$  = 0.00 (s, 12H), 0.85 (s, 18H). **<sup>13</sup>C NMR** (75 MHz, CDCl<sub>3</sub>):  $\delta$  = −2.99, 18.08, 25.66. **<sup>29</sup>Si NMR** (80 MHz, CDCl<sub>3</sub>):  $\delta$  = 9.91. **MS (EI)** *m/z* (%) = 246.02 (0.02, [M<sup>+</sup>]), 189.11 (2.8, [M−*t*Bu]), 147.05 (100), 73.04 (1.9, [M−*t*Bu(CH<sub>3</sub>)<sub>3</sub>Si]). **HRMS (EI)** C<sub>18</sub>H<sub>26</sub>OSi requires 246.1835 g mol<sup>−1</sup>, found 246.1828 g mol<sup>−1</sup>.

7.4.3 *para*-Substituted Alcohols and Silylated Products1-(4-Methylnaphthalen-1-yl)ethan-1-ol (**11**)

10 mmol (1.84 g) 1-(4-methylnaphthalen-1-yl)ethan-1-one was dissolved in 20 mL MeOH and cooled to 0 °C. 20 mmol (0.76 g) of sodium borohydride was added slowly and stirred for 2 h. The reaction mixture was extracted three times with DCM (10 mL) and washed with brine (20 mL). The combined organic phases were dried over MgSO<sub>4</sub> and the solvent was removed under reduced pressure which led to a white solid product **11** in 94 % yield (1.75 g, 9.4 mmol).

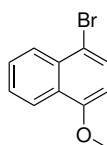
**<sup>1</sup>H NMR** (400 MHz, CDCl<sub>3</sub>):  $\delta$  = 1.65 (d,  $^3J$  = 6.4 Hz, 3H), 1.81 (s, 1H), 3.99 (s, 3H), 5.58 (q,  $^3J$  = 6.4 Hz, 1H), 6.79 (d,  $^3J$  = 8.0 Hz, 1H), 7.44 – 7.56 (m, 3H), 8.09 (d,  $^3J$  = 8.4 Hz, 1H), 8.30 (d,  $^3J$  = 8.2 Hz, 1H). **<sup>13</sup>C NMR** (100 MHz, CDCl<sub>3</sub>):  $\delta$  = 24.49, 55.90, 67.38, 103.49, 122.64, 123.08, 123.42, 125.34, 126.21, 126.99, 131.74, 133.53, 155.44. **HRMS (EI)** C<sub>13</sub>H<sub>14</sub>O requires 186.1045 g mol<sup>-1</sup>, found 186.1040 g mol<sup>-1</sup>.

1-(4-Bromonaphthalen-1-yl)ethan-1-ol (**13**)

15 mmol (0.36 g) magnesium and 7.5 mmol (0.32 g) LiCl were dissolved in 60 mL THF and one bead of iodine was added. The reaction mixture was allowed to stir for 15 min. 10 mmol (2.86 g) of 1,4-dibromo-naphthalene was added slowly, stirred for 30 min and refluxed for 30 min. The reaction mixture was cooled down to rt and 15 mmol (0.66 g) of acetaldehyde was added slowly. After 1 h of stirring at rt the reaction was quenched by adding saturated NH<sub>4</sub>Cl under ice cooling. The reaction mixture was extracted three times with DCM (20 mL) and washed with brine (20 mL). The combined organic phases were dried over MgSO<sub>4</sub> and the solvent was removed under reduced pressure. Column chromatography on silica (i-hexane:EtOAc; 4:1) yielded in 39 % (0.97 g, 5.85 mmol) of **13** as a pale solid.

**$^1\text{H}$  NMR** (300 MHz,  $\text{CDCl}_3$ ):  $\delta$  = 1.65 (d,  $^3J$  = 6.5 Hz, 3H), 1.97 (s, 1H), 5.64 (q,  $^3J$  = 6.4 Hz, 1H), 7.53 (dd,  $^3J$  = 7.8, 0.7 Hz, 1H), 7.56 – 7.65 (m, 2H), 7.79 (d,  $^3J$  = 7.8 Hz, 1H), 8.05 – 8.37 (m, 2H).  **$^{13}\text{C}$  NMR** (75 MHz,  $\text{CDCl}_3$ ):  $\delta$  = 24.99, 67.37, 123.01, 123.12, 124.02, 127.33, 127.47, 128.60, 130.18, 132.03, 132.51, 141.99. **HRMS (EI)**  $\text{C}_{12}\text{H}_{11}\text{OBr}$  requires 249.9993  $\text{g mol}^{-1}$ , found 249.9971  $\text{g mol}^{-1}$ .

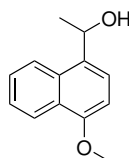
### 1-Bromo-4-methoxynaphthalene (15a)



In a shaded flask 10 mmol (1.58 g) 1-methoxynaphthalene was dissolved in 30 mL acetonitrile and 10 mmol (1.78 g) *N*-bromosuccinimide was added. One drop of bromine was added to kick-start the reaction, which was allowed to stir over night at rt. The solvent was removed under reduced pressure and the crude product purified by column chromatography (*i*hexane), which yielded in 93 % (2.19 g, 9.30 mmol) of **15a** as a yellowish oil.

**$^1\text{H}$  NMR** (300 MHz,  $\text{CDCl}_3$ ):  $\delta$  = 3.99 (s, 3H), 6.68 (d,  $^3J$  = 8.3 Hz, 1H), 7.53 (ddd,  $^{3,3,3}J$  = 8.2, 6.9, 1.3 Hz, 1H), 7.62 (ddd,  $^{3,3,3}J$  = 8.4, 6.9, 1.4 Hz, 1H), 7.67 (d,  $^3J$  = 8.2 Hz, 1H), 8.18 (dd,  $^{3,3}J$  = 8.4, 1.3 Hz, 1H), 8.29 (dd,  $^{3,3}J$  = 8.3, 1.4 Hz, 1H).  **$^{13}\text{C}$  NMR** (75 MHz,  $\text{CDCl}_3$ ):  $\delta$  = 56.16, 104.99, 113.72, 122.89, 126.41, 127.28, 127.33, 128.22, 129.93, 132.90, 155.72. **HRMS (EI)**  $\text{C}_{11}\text{H}_9\text{OBr}$  requires 235.9837  $\text{g mol}^{-1}$ , found 235.9849  $\text{g mol}^{-1}$ .

### 1-(4-Methoxynaphthalen-1-yl)ethan-1-ol (15b)

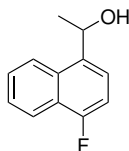


5 mmol (1.19 g) of **15a** was dissolved in 30 mL THF and cooled to  $-78^\circ\text{C}$ . After 10 min 6 mmol (1.6 M, 3.75 mL) *n*BuLi was added slowly and stirred for another 10 min. 3.7 mmol (0.21 mL) acetaldehyde was added slowly and stirred for 1 h at  $-78^\circ\text{C}$ . The temperature was allowed to raise to rt, stirred for 30 min and the reaction was quenched by adding saturated  $\text{NH}_4\text{Cl}$ . After removing the solvent under reduced pressure the crude product was solved in EtOAc and washed with 2 M HCl (10 mL), saturated  $\text{NaHCO}_3$  (10 mL), and with brine ( $2 \times 20$  mL). The combined organic

phases were dried over  $\text{MgSO}_4$  and the solvent was removed under reduced pressure. Column chromatography (i-hexane:EtOAc; 4:1) yielded in 63 % (0.63 g, 3.15 mmol) of **15b** as a grey solid.

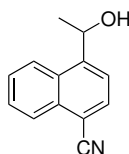
**$^1\text{H}$  NMR** (400 MHz,  $\text{CDCl}_3$ ):  $\delta$  = 1.65 (d,  $^3J$  = 6.4 Hz, 4H), 1.81 (s, 1H), 3.99 (s, 3H), 5.58 (q,  $^3J$  = 6.4 Hz, 1H), 6.79 (d,  $^3J$  = 8.0 Hz, 1H), 7.44 – 7.56 (m, 3H), 8.09 (d,  $^3J$  = 8.4 Hz, 1H), 8.30 (d,  $^3J$  = 8.2 Hz, 1H).  **$^{13}\text{C}$  NMR** (100 MHz,  $\text{CDCl}_3$ ):  $\delta$  = 24.25, 55.67, 67.14, 103.25, 122.41, 122.84, 123.18, 125.10, 125.97, 126.75, 131.50, 133.29, 155.20. **HRMS (EI)**  $\text{C}_{13}\text{H}_{14}\text{O}_2$  requires 202.0994  $\text{g mol}^{-1}$ , found 202.0988  $\text{g mol}^{-1}$ .

#### 1-(4-Fluoronaphthalen-1-yl)ethan-1-ol (**12**)



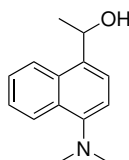
5 mmol (0.94 g) 1-(4-fluoronaphthalen-1-yl)ethan-1-one was dissolved in 10 mL MeOH and cooled to 0 °C. 10 mmol (0.38 g) of sodium borohydride was added slowly and stirred for 2 h. The reaction mixture was extracted with DCM (3 × 10 mL) and washed with brine (20 mL). The combined organic phases were dried over  $\text{MgSO}_4$ , the solvent was removed under reduced pressure, and led to a yellow oil of **12** in 95 % yield (1.75 g, 4.75 mmol).

**$^1\text{H}$  NMR** (300 MHz,  $\text{CDCl}_3$ ):  $\delta$  = 1.65 (d,  $^3J$  = 6.4 Hz, 1H), 2.06 (s, 1H), 5.59 (q,  $^3J$  = 6.5 Hz, 1H), 7.12 (dd,  $^3,^3J$  = 10.2, 8.0 Hz, 1H), 7.51 – 7.63 (m, 2H), 8.07 – 8.21 (m, 1H).  **$^{13}\text{C}$  NMR** (75 MHz,  $\text{CDCl}_3$ ):  $\delta$  = 24.52 (d,  $^5J$  = 0.8 Hz), 67.03, 108.92 (d,  $^2J$  = 19.8 Hz), 121.42 (d,  $^3J$  = 6.0 Hz), 122.17 (d,  $^3J$  = 8.6 Hz), 123.35 (d,  $^3J$  = 2.8 Hz), 124.03 (d,  $^2J$  = 16.1 Hz), 125.99 (d,  $^4J$  = 2.0 Hz), 127.08 (d,  $^5J$  = 0.8 Hz), 131.74 (d,  $^3J$  = 4.4 Hz), 137.26 (d,  $^3J$  = 4.4 Hz), 158.42 (d,  $^1J$  = 251.3 Hz).  **$^{19}\text{F}$  NMR** (282 MHz,  $\text{CDCl}_3$ ):  $\delta$  = –124.03. **HRMS (EI)**  $\text{C}_{12}\text{H}_{11}\text{FO}$  requires 190.0794  $\text{g mol}^{-1}$ , found 190.0774  $\text{g mol}^{-1}$ .

**1-(4-(Cyano)naphthalen-1-yl)ethan-1-ol (14)**

3 mmol (0.75 g) **13** and 3.45 mmol (0.31 g) CuCN were dissolved in 5 mL DMF and refluxed for 5 h. The reaction mixture was transferred into a solution of 10 g FeCl<sub>3</sub> and 15 mL HCl in 20 mL H<sub>2</sub>O and stirred for 20 min at rt. The mixture was extracted with toluene (2×50 mL), washed with 2 M HCl (20 mL) and 10 % NaOH (20 mL), filtered, and the solvent was removed under reduced pressure. The crude product was purified by column chromatography (i-hexane:EtOAc; 1:1) and led to a yellowish solid **14** in 50 % yield (0.30 g, 1.5 mmol).

**<sup>1</sup>H NMR (400 MHz, CDCl<sub>3</sub>):**  $\delta$  = 1.65 (d, <sup>3</sup>J = 6.3 Hz, 3H), 2.28 (s, 1H), 5.70 (q, <sup>3</sup>J = 6.5 Hz, 1H), 7.55 – 7.72 (m, 2H), 7.78 (d, <sup>3</sup>J = 7.4 Hz, 1H), 7.88 (d, <sup>3</sup>J = 7.4 Hz, 1H), 8.12 (d, <sup>3</sup>J = 8.2 Hz, 1H), 8.24 (d, <sup>3</sup>J = 8.4 Hz, 1H). **<sup>13</sup>C NMR (100 MHz, CDCl<sub>3</sub>):**  $\delta$  = 24.91, 66.88, 109.66, 118.14, 121.34, 123.83, 126.18, 127.69, 128.25, 129.82, 132.60, 132.71, 147.88. **HRMS (EI)** C<sub>13</sub>H<sub>11</sub>NO requires 197.0841 g mol<sup>-1</sup>, found 197.0833 g mol<sup>-1</sup>.

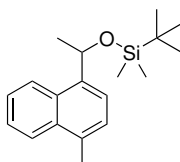
**1-(4-(Dimethylamino)naphthalen-1-yl)ethan-1-ol (16)**

10 mmol (1.84 g) 4-(dimethylamino)-1-naphthaldehyde was dissolved in 40 mL Et<sub>2</sub>O and cooled to –30 °C. 20 mmol (0.76 g) of methyl lithium was added slowly and stirred for 1 h and the mixture was allowed to warm up to rt. The reaction mixture was extracted three times with DCM (3×20 mL) and washed with brine (20 mL). The combined organic phases were dried over MgSO<sub>4</sub> and the solvent was removed under reduced pressure. The crude mixture was purified by column chromatography (i-hexane:EtOAc; 4:1) and led to a yellow oil **16** in 93 % yield (2.00 g, 9.30 mmol).

**<sup>1</sup>H NMR (400 MHz, CDCl<sub>3</sub>):**  $\delta$  = 1.67 (d, <sup>3</sup>J = 6.4 Hz, 3H), 1.94 (s, 1H), 2.89 (s, 6H), 5.61 (q, <sup>3</sup>J = 6.5 Hz, 1H), 7.07 (d, <sup>3</sup>J = 7.8 Hz, 1H), 7.46 – 7.56 (m, 2H), 7.57 (dd, <sup>3,4</sup>J = 7.8, 0.7 Hz, 1H), 8.08

– 8.18 (m, 1H), 8.25 – 8.39 (m, 1H).  $^{13}\text{C}$  NMR (100 MHz,  $\text{CDCl}_3$ ):  $\delta$  = 24.23, 45.41, 67.12, 113.63, 122.25, 123.73, 124.99, 125.05, 126.06, 129.15, 131.77, 135.82, 150.78. HRMS (EI)  $\text{C}_{14}\text{H}_{17}\text{NO}$  requires 215.1310  $\text{g mol}^{-1}$ , found 215.1312  $\text{g mol}^{-1}$ .

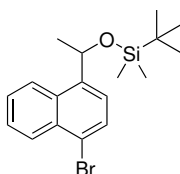
***tert*-Butyldimethyl(1-(4-methylnaphthalen-1-yl)ethoxy)silane (34)**



The reaction was performed using general procedure *Sil1*. The crude product was purified by flash-chromatography on  $\text{SiO}_2$  (i-hexane:DCM; 4:1) to obtain 90 % of product **34** as a colorless oil.

$^1\text{H}$  NMR (300 MHz,  $\text{CDCl}_3$ ):  $\delta$  = 0.01 (s, 3H), 0.11 (s, 3H), 0.97 (s, 9H), 1.61 (d,  $^3J$  = 6.3 Hz, 3H), 2.72 (s, 3H), 5.61 (q,  $^3J$  = 6.3, 1H), 7.35 (d,  $^3J$  = 7.3 Hz, 1H), 7.50 – 7.57 (m, 2H), 7.62 (d,  $^3J$  = 7.3 Hz, 1H), 8.04 – 8.10 (m, 1H), 8.12 – 8.18 (m, 1H).  $^{13}\text{C}$  NMR (75 MHz,  $\text{CDCl}_3$ ):  $\delta$  = –4.38, –4.27, 18.83, 20.07, 26.43, 27.26, 69.02, 122.91, 124.36, 125.40, 125.54, 125.70, 126.93, 130.47, 133.27, 133.56, 141.24.  $^{29}\text{Si}$  NMR (80 MHz,  $\text{CDCl}_3$ ):  $\delta$  = 17.97. HRMS (EI)  $\text{C}_{19}\text{H}_{28}\text{OSi}$  requires 300.1909  $\text{g mol}^{-1}$ , found 300.1908  $\text{g mol}^{-1}$ .

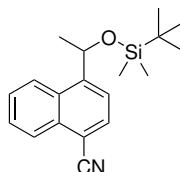
***tert*-Butyldimethyl(1-(4-bromonaphthalen-1-yl)ethoxy)silane (35)**



The reaction was performed using general procedure *Sil1*. The crude product was purified by flash-chromatography on  $\text{SiO}_2$  (i-hexane:DCM; 4:1) to obtain 93 % of product **35** as a colorless oil.

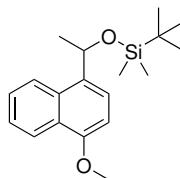
$^1\text{H}$  NMR (300 MHz,  $\text{CDCl}_3$ ):  $\delta$  = –0.02 (s, 3H), 0.09 (s, 3H), 0.94 (s, 9H), 1.57 (d,  $^3J$  = 6.4 Hz, 3H), 5.56 (q,  $^3J$  = 6.3 Hz, 1H), 7.51 – 7.63 (m, 3H), 7.79 (d,  $^3J$  = 7.8 Hz, 1H), 8.07 – 8.12 (m, 1H), 8.29 – 8.34 (m, 1H).  $^{13}\text{C}$  NMR (75 MHz,  $\text{CDCl}_3$ ):  $\delta$  = –4.37, –4.30, 18.81, 26.40, 27.14, 68.68, 122.25, 123.86, 124.13, 126.93, 127.17, 128.56, 130.30, 131.63, 132.39, 143.31.  $^{29}\text{Si}$  NMR (80 MHz,  $\text{CDCl}_3$ ):  $\delta$  = 18.86. HRMS (EI)  $\text{C}_{18}\text{H}_{25}\text{BrOSi}$  requires 364.0858  $\text{g mol}^{-1}$ , found 364.0845  $\text{g mol}^{-1}$ .



**4-(1-((*tert*-Butyldimethylsilyl)oxy)ethyl)-1-naphthonitrile (36)**

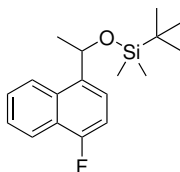
The reaction was performed using general procedure *Sil1*. The crude product was purified by flash-chromatography on SiO<sub>2</sub> (*i*hexane:DCM, 4:1) to obtain 91 % of product **36** as a colorless oil.

**<sup>1</sup>H NMR** (300 MHz, CDCl<sub>3</sub>):  $\delta$  = −0.02 (s, 3H), 0.10 (s, 3H), 0.93 (s, 9H), 1.57 (d, <sup>3</sup>*J* = 6.4 Hz, 3H), 5.62 (q, *J* = 6.4 Hz, 1H), 7.60 – 7.72 (m, 2H), 7.79 (dd, <sup>3,4</sup>*J* = 7.6, 0.6 Hz 1H), 7.93 (d, <sup>3</sup>*J* = 7.5 Hz, 1H), 8.14 (dd, <sup>3,4</sup>*J* = 7.7, 1.7 Hz, 1H), 8.27 – 8.32 (m, 1H). **<sup>13</sup>C NMR** (75 MHz, CDCl<sub>3</sub>):  $\delta$  = −4.75, −4.72, 18.38, 25.96, 26.68, 68.13, 109.34, 118.28, 122.04, 123.96, 126.28, 127.40, 128.03, 129.57, 132.74, 132.78, 149.07. **<sup>29</sup>Si NMR** (80 MHz, CDCl<sub>3</sub>):  $\delta$  = 19.66. **HRMS (EI)** C<sub>19</sub>H<sub>25</sub>ONSi requires 311.1705 g mol<sup>−1</sup>, found 311.1694 g mol<sup>−1</sup>.

***tert*-Butyl(1-(4-methoxynaphthalen-1-yl)ethoxy)dimethylsilane (37)**

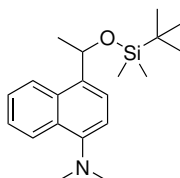
The reaction was performed using general procedure *Sil1*. The crude product was purified by flash-chromatography on SiO<sub>2</sub> (*i*hexane:DCM; 4:1) to obtain 92 % of product **37** as a colorless oil.

**<sup>1</sup>H NMR** (300 MHz, CDCl<sub>3</sub>):  $\delta$  = −0.02 (s, 3H), 0.08 (s, 3H), 0.94 (s, 9H), 1.58 (d, <sup>3</sup>*J* = 6.3 Hz, 3H), 4.01 (s, 3H), 5.52 (q, <sup>3</sup>*J* = 6.3 Hz, 1H), 6.82 (d, <sup>3</sup>*J* = 8.0 Hz, 1H), 7.50 (ddt, <sup>3,3</sup>*J* = 9.6, 8.2, 3.3 Hz, 2H), 7.58 (dd, <sup>3,4</sup>*J* = 8.0, 0.6 Hz, 1H), 8.05 – 8.10 (m, 1H), 8.31–8.36 (m, 1H). **<sup>13</sup>C NMR** (75 MHz, CDCl<sub>3</sub>):  $\delta$  = −4.38, −4.25, 18.84, 26.44, 27.19, 55.93, 69.09, 103.83, 123.15, 123.24, 123.73, 125.06, 126.20, 126.58, 131.33, 135.00, 154.98. **<sup>29</sup>Si NMR** (80 MHz, CDCl<sub>3</sub>):  $\delta$  = 17.97. [M−C<sub>6</sub>H<sub>15</sub>OSi]. **HRMS (EI)** C<sub>19</sub>H<sub>28</sub>O<sub>2</sub>Si requires 316.1859 g mol<sup>−1</sup>, found 316.1860 g mol<sup>−1</sup>.

***tert*-Butyl(1-(4-methoxynaphthalen-1-yl)ethoxy)dimethylsilane (38)**

The reaction was performed using general procedure *Sil1*. The crude product was purified by flash-chromatography on SiO<sub>2</sub> (i-hexane:DCM; 4:1) to obtain 92 % of product **38** as a colorless oil.

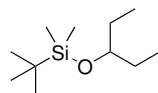
**<sup>1</sup>H NMR** (300 MHz, CDCl<sub>3</sub>):  $\delta$  = −0.03 (s, 3H), 0.09 (s, 3H), 0.94 (s, 9H), 1.57 (d, <sup>3</sup>*J* = 6.3 Hz, 3H), 5.54 (q, <sup>3</sup>*J* = 6.3 Hz, 1H), 7.13 (dd, <sup>3,3</sup>*J* = 10.4, 8.0 Hz, 1H), 7.49 – 7.67 (m, 2H), 8.05 – 8.22 (m, 3H). **<sup>13</sup>C NMR** (75 MHz, CDCl<sub>3</sub>):  $\delta$  = −4.75, −4.68, 18.44, 26.03, 26.86, 68.50, 109.01 (d, <sup>2</sup>*J* = 19.6 Hz), 121.40 (d, <sup>3</sup>*J* = 6.0 Hz), 122.70 (d, <sup>3</sup>*J* = 8.4 Hz), 123.89 (d, <sup>2</sup>*J* = 16.0 Hz), 126.65 (d, <sup>5</sup>*J* = 0.8 Hz), 131.16 (d, <sup>3</sup>*J* = 4.2 Hz), 138.52 (d, <sup>3</sup>*J* = 4.4 Hz), 158.04 (d, <sup>1</sup>*J* = 250.1 Hz). **<sup>19</sup>F NMR** (282 MHz, CDCl<sub>3</sub>):  $\delta$  = −125.27. **<sup>29</sup>Si NMR** (80 MHz, CDCl<sub>3</sub>):  $\delta$  = 18.61. **HRMS (EI)** C<sub>18</sub>H<sub>25</sub>FOSi requires 304.1659 g mol<sup>−1</sup>, found 304.1645 g mol<sup>−1</sup>.

**4-(1-((*tert*-Butyldimethylsilyl)oxy)ethyl)-*N,N*-dimethylnaphthalen-1-amine (39)**

The reaction was performed using general procedure *Sil1*. The crude product was purified by flash-chromatography on SiO<sub>2</sub> (i-hexane:EtOAc; 20:1) to obtain 86 % of product **39** as a colorless oil.

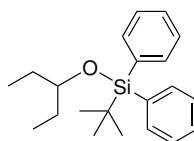
**<sup>1</sup>H NMR** (300 MHz, CDCl<sub>3</sub>):  $\delta$  = −0.02 (s, 3H), 0.08 (s, 3H), 0.94 (s, 9H), 1.57 (d, <sup>3</sup>*J* = 6.3 Hz, 3H), 2.89 (s, 6H), 5.53 (q, <sup>3</sup>*J* = 6.3 Hz, 1H), 7.08 (d, <sup>3</sup>*J* = 7.8 Hz, 1H), 7.44 – 7.51 (m, 2H), 7.59 (dd, <sup>3,3</sup>*J* = 7.8, 0.9 Hz, 1H), 8.04 – 8.11 (m, 1H), 8.26 – 8.36 (m, 1H). **<sup>13</sup>C NMR** (75 MHz, CDCl<sub>3</sub>):  $\delta$  = −4.71, −4.60, 18.47, 26.09, 26.81, 45.50, 68.63, 113.88, 122.78, 123.88, 124.59, 124.98, 125.50, 129.09, 131.23, 137.18, 150.03. **<sup>29</sup>Si NMR** (80 MHz, CDCl<sub>3</sub>):  $\delta$  = 18.09. **HRMS (EI)** C<sub>20</sub>H<sub>31</sub>NOSi requires 329.2175 g mol<sup>−1</sup>, found 329.2162 g mol<sup>−1</sup>.

## 7.4.4 Synthesis of the Products of Silylation and Acylation

*tert*-Butyldimethyl(pentan-3-yloxy)silane (**40a**)

The reaction was performed using general procedure *Sil1*. The crude product was purified by flash-chromatography on SiO<sub>2</sub> (*i*hexane) to obtain 86 % of product **40a** as a colorless oil.

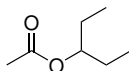
**<sup>1</sup>H NMR** (300 MHz, CDCl<sub>3</sub>):  $\delta$  = 0.04 (s, 6H), 0.83 – 0.90 (m, 15H), 1.39 – 1.53 (m, 4H), 3.51 (q, <sup>3</sup>*J* = 5.8 Hz). **<sup>13</sup>C NMR** (75 MHz, CDCl<sub>3</sub>):  $\delta$  = –4.31, 9.80, 18.35, 26.09, 29.36, 74.72. **<sup>29</sup>Si NMR** (80 MHz, CDCl<sub>3</sub>):  $\delta$  = 15.54 **HRMS (EI)** C<sub>18</sub>H<sub>26</sub>OSi requires 202.1753 g mol<sup>–1</sup>, found 202.1747 g mol<sup>–1</sup>.

*tert*-Butyl(pentan-3-yloxy)diphenylsilane (**40b**)

The reaction was performed using general procedure *Sil1*. The crude product was purified by flash-chromatography on SiO<sub>2</sub> (*i*hexane) to obtain 80 % of product **40b** as a colorless oil.

**<sup>1</sup>H NMR** (300 MHz, CDCl<sub>3</sub>):  $\delta$  = 0.80 (t, <sup>3</sup>*J* = 7.5 Hz, 6H), 1.07 (s, 9H), 1.36 – 1.58 (m, 4H), 3.65 (q, <sup>3</sup>*J* = 5.6 Hz, 1H), 7.33 – 7.47 (m, 6H), 7.65 – 7.75 (m, 4H). **<sup>13</sup>C NMR** (75 MHz, CDCl<sub>3</sub>):  $\delta$  = 9.33, 19.61, 27.25, 28.42, 75.57, 127.51, 129.49, 135.96, 136.08. **<sup>29</sup>Si NMR** (80 MHz, CDCl<sub>3</sub>):  $\delta$  = –7.23. **HRMS (EI)** C<sub>18</sub>H<sub>26</sub>OSi requires 326.2066 g mol<sup>–1</sup>, found 326.2006 g mol<sup>–1</sup>.

### Pentan-3-yl acetate (40c)

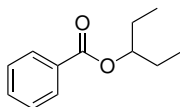


The reaction was performed using general procedure *Ac1*. The crude product was purified by flash-chromatography on SiO<sub>2</sub> (i-hexane:EtOAc; 10:1) to obtain 76 % of product **40c** as a colorless oil.

**<sup>1</sup>H NMR** (300 MHz, CDCl<sub>3</sub>):  $\delta$  = 0.85 (t, <sup>3</sup>*J* = 7.5 Hz, 6H), 1.47 – 1.59 (m, 4H), 2.02 (s, 3H), 4.72 (quint, 1H). **<sup>13</sup>C NMR** (75 MHz, CDCl<sub>3</sub>):  $\delta$  = 9.48, 21.11, 26.35, 76.57, 176.56. **HRMS (EI)** C<sub>7</sub>H<sub>14</sub>O requires 130.0994 g mol<sup>-1</sup>, found 130.0985 g mol<sup>-1</sup>.

In accordance with literature.<sup>[171]</sup>

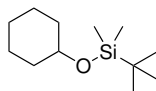
### Pentan-3-yl benzoate (40d)



The reaction was performed using general procedure *Ac1*. The crude product was purified by flash-chromatography on SiO<sub>2</sub> (i-hexane:EtOAc; 9:1) to obtain 86 % of product **40d** as a colorless oil.

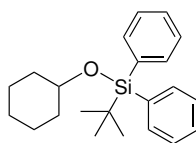
**<sup>1</sup>H NMR** (300 MHz, CDCl<sub>3</sub>):  $\delta$  = 0.95 (t, <sup>3</sup>*J* = 7.4 Hz, 6H), 1.71 (m, 4H), 5.02 (quint, <sup>3</sup>*J* = 6.2 Hz, 1H), 7.44 (t, <sup>3</sup>*J* = 7.8 Hz, 2H), 7.55 (t, <sup>3</sup>*J* = 7.6 Hz, 1H), 8.06 (t, <sup>3</sup>*J* = 7.0 Hz, 2H). **<sup>13</sup>C NMR** (75 MHz, CDCl<sub>3</sub>):  $\delta$  = 9.62, 26.54, 76.58, 128.25, 129.49, 130.86, 132.63, 166.41. **HRMS (EI)** C<sub>12</sub>H<sub>16</sub>O<sub>2</sub> requires 192.1150 g mol<sup>-1</sup>, found 192.1159 g mol<sup>-1</sup>.

In accordance with literature.<sup>[172]</sup>

***tert*-Butyl(cyclohexyloxy)dimethylsilane (41a)**

The reaction was performed using general procedure *Sil1*. The crude product was purified by flash-chromatography on SiO<sub>2</sub> (*i*hexane) to obtain 76 % of product **41a** as a colorless oil.

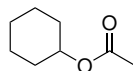
**<sup>1</sup>H NMR** (300 MHz, CDCl<sub>3</sub>):  $\delta$  = 0.04 (s, 6H), 0.98 (s, 9H), 1.36 – 1.43 (m, 5H), 1.43 – 1.52 (m, 1H), 1.67 – 1.78 (m, 4H), 3.56 – 3.64 (m, 1H). **<sup>13</sup>C NMR** (75 MHz, CDCl<sub>3</sub>):  $\delta$  = –4.47, 18.39, 24.25, 25.84, 26.08, 36.06, 70.94. **<sup>29</sup>Si NMR** (80 MHz, CDCl<sub>3</sub>):  $\delta$  = 15.80. **HRMS (EI)** C<sub>18</sub>H<sub>26</sub>OSi requires 214.1753 g mol<sup>–1</sup>, found 214.1751 g mol<sup>–1</sup>.

***tert*-Butyl(cyclohexyloxy)dimphenylsilane (41b)**

The reaction was performed using general procedure *Sil1*. The crude product was purified by flash-chromatography on SiO<sub>2</sub> (*i*hexane:EtOAc; 50:1) to obtain 90 % of product **41b** as a colorless oil.

**<sup>1</sup>H NMR** (300 MHz, CDCl<sub>3</sub>):  $\delta$  = 1.07 (s, 9H), 1.17 (dt, <sup>3,3</sup>*J* = 13.0 9.9 Hz 4H), 1.32 – 1.49 (m, 2H), 1.61 – 1.77 (m, 4H), 3.70 (tt, <sup>3,3</sup>*J* = 8.7, 3.4 Hz 1H), 7.32 – 7.46 (m, 6H), 7.66 – 7.72 (m, 4H). **<sup>13</sup>C NMR** (75 MHz, CDCl<sub>3</sub>):  $\delta$  = 19.38, 23.88, 25.87, 35.62, 71.43, 127.56, 129.52, 135.09, 135.94. **HRMS (EI)** C<sub>22</sub>H<sub>30</sub>OSi requires 338.2066 g mol<sup>–1</sup>, found 338.2069 g mol<sup>–1</sup>.

### Cyclohexyl acetate (**41c**)

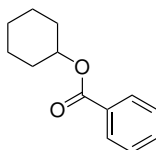


The reaction was performed using general procedure *Ac1*. The crude product was purified by flash-chromatography on SiO<sub>2</sub> (*i*hexane:EtOAc; 10:1) to obtain 88 % of product **41c** as a colorless oil.

**<sup>1</sup>H NMR** (300 MHz, CDCl<sub>3</sub>):  $\delta$  = 1.15 – 1.57 (m, 8H), 1.64 – 1.87 (m, 2H), 2.00 (s, 3H), 4.67 – 4.76 (m, 1H). **<sup>13</sup>C NMR** (75 MHz, CDCl<sub>3</sub>):  $\delta$  = 21.38, 23.76, 25.33, 31.61, 72.66, 170.60. **HRMS (EI)** C<sub>8</sub>H<sub>15</sub>O<sub>2</sub> requires 143.1027 g mol<sup>-1</sup>, found 143.1078 g mol<sup>-1</sup>.

In accordance with literature.<sup>[173]</sup>

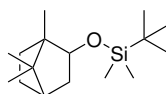
### Cyclohexyl benzoate (**41d**)



The reaction was performed using general procedure *Ac1*. The crude product was purified by flash-chromatography on SiO<sub>2</sub> (*i*hexane:EtOAc; 9:1) to obtain 80 % of product **41d** as a colorless oil.

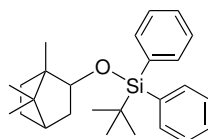
**<sup>1</sup>H NMR** (300 MHz, CDCl<sub>3</sub>):  $\delta$  = 1.51 (m, 6H), 1.71 (m, 2H), 1.88 – 2.01 (m, 2H), 7.43 (t, <sup>3</sup>*J* = 7.4 Hz, 2H), 7.49 – 7.60 (m, 1H), 8.05 (d, <sup>3</sup>*J* = 7.0 Hz, 2H). **<sup>13</sup>C NMR** (75 MHz, CDCl<sub>3</sub>):  $\delta$  = 23.64, 25.47, 31.62, 72.99, 128.22, 129.49, 131.02, 132.62, 165.95. **HRMS (EI)** C<sub>13</sub>H<sub>16</sub>O<sub>2</sub> requires 204.1150 g mol<sup>-1</sup>, found 204.1156 g mol<sup>-1</sup>.

In accordance with literature.<sup>[172]</sup>

***tert*-Butyldimethyl((1,7,7-trimethylbicyclo[2.2.1]heptan-2-yl)oxy)silane (**42a**)**

The reaction was performed using general procedure *Sil3*. The crude product was purified by flash-chromatography on SiO<sub>2</sub> (*i*hexane) to obtain 40 % of product **42a** as a colorless oil.

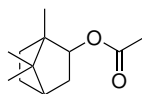
**<sup>1</sup>H NMR** (300 MHz, CDCl<sub>3</sub>):  $\delta$  = 0.00 (s, 6H), 0.79, (s, 3H), 0.81 (s, 3H), 0.87 (s, 9H), 0.90 – 0.98 (m, 2H), 1.00 (s, 3H) 1.42 – 1.74 (m, 5H), 3.51 (dd, <sup>3,3</sup>*J* = 7.4 3.3 Hz, 1H). **<sup>13</sup>C NMR** (75 MHz, CDCl<sub>3</sub>):  $\delta$  = –4.92, –4.45, 12.13, 18.10, 20.28, 20.72, 25.96, 27.51, 34.04, 42.28, 45.42, 46.65, 49.25, 79.84. **<sup>29</sup>Si NMR** (80 MHz, CDCl<sub>3</sub>):  $\delta$  = 15.72. **HRMS (EI)** C<sub>16</sub>H<sub>32</sub>OSi requires 268.2222 g mol<sup>–1</sup>, found 268.2222 g mol<sup>–1</sup>.

***tert*-Butyldiphenyl((1,7,7-trimethylbicyclo[2.2.1]heptan-2-yl)oxy)silane (**42b**)**

The reaction was performed using general procedure *Sil3*. The crude product was purified by flash-chromatography on SiO<sub>2</sub> (*i*hexane:EtOAc; 50:1) to obtain 42 % of product **42b** as a colorless oil.

**<sup>1</sup>H NMR** (300 MHz, CDCl<sub>3</sub>):  $\delta$  = 0.65 – 0.75 (m, 1H), 0.79 (s, 6H), 0.83 – 0.94 (m, 1H), 1.09 (s, 9H), 1.16 (s, 3H), 1.22 – 1.34 (m, 1H), 1.34 – 1.48 (m, 2H), 1.50 – 1.66 (m, 2H), 1.69 – 1.83 (m, 1H), 3.71 (dd, <sup>3,3</sup>*J* = 7.7, 3.4 Hz, 1H), 7.32 – 7.47 (m, 6H), 7.66 (dd, <sup>3,3</sup>*J* = 7.9, 1.6 Hz, 4H). **<sup>13</sup>C NMR** (75 MHz, CDCl<sub>3</sub>):  $\delta$  = 12.46, 19.33, 20.56, 20.65, 27.27, 33.95, 42.41, 45.34, 46.80, 49.68, 80.56, 127.50, 127.51, 129.51, 129.55, 134.76, 135.03, 136.28, 136.30. **<sup>29</sup>Si NMR** (80 MHz, CDCl<sub>3</sub>):  $\delta$  = –5.85. **HRMS (EI)** C<sub>16</sub>H<sub>32</sub>OSi requires 392.2535 g mol<sup>–1</sup>, found 392.2512 g mol<sup>–1</sup>.

### Isobornyl acetate (42c)

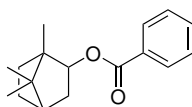


The reaction was performed using general procedure *Ac1*. The crude product was purified by flash-chromatography on SiO<sub>2</sub> (i-hexane:EtOAc; 10:1) to obtain 92 % of product **42c** as a colorless oil.

**<sup>1</sup>H NMR** (300 MHz, CDCl<sub>3</sub>):  $\delta$  = 0.82 (s, 3H), 0.83 (s, 3H), 0.96 (s, 3H), 1.02 – 1.18 (m, 2H), 1.55 – 1.70 (m, 3H), 1.75 – 1.77 (m, 2H), 2.01 (s, 3H), 4.66 (q, <sup>3</sup>*J* = 3.3 Hz, 1H). **<sup>13</sup>C NMR** (75 MHz, CDCl<sub>3</sub>):  $\delta$  = 11.33, 19.82, 20.08, 21.27, 33.71, 38.73, 45.01, 46.89, 48.57, 80.93, 170.64. **HRMS (EI)** C<sub>12</sub>H<sub>20</sub>O<sub>2</sub> requires 196.1463 g mol<sup>-1</sup>, found 196.1455 g mol<sup>-1</sup>.

In accordance with literature.<sup>[174]</sup>

### Isobornyl benzoate (42d)

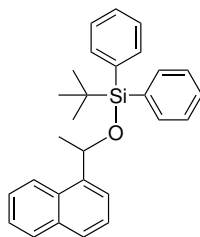


The reaction was performed using general procedure *Ac1*. The crude product was purified by flash-chromatography on SiO<sub>2</sub> (i-hexane:EtOAc; 9:1) to obtain 77 % of product **42d** as a colorless oil.

**<sup>1</sup>H NMR** (300 MHz, CDCl<sub>3</sub>):  $\delta$  = 0.89 (s, 3H), 0.94 (s, 3H), 1.13 (s, 3H), 1.15 – 1.23 (m, 2H), 1.54 – 1.88 (m, 2H), 1.92 (d, <sup>3</sup>*J* = 6.9 Hz, 2H), 4.92 (dd, <sup>3,3</sup>*J* = 6.8, 4.7 Hz, 1H), 7.43 (t, <sup>3</sup>*J* = 7.5 Hz, 2H), 7.50 – 7.60 (m, 1H), 8.01 (t, <sup>3</sup>*J* = 7.0 Hz, 2H). **<sup>13</sup>C NMR** (75 MHz, CDCl<sub>3</sub>):  $\delta$  = 11.58, 20.07, 20.13, 27.07, 33.76, 38.92, 45.12, 47.02, 49.01, 81.55, 128.31, 129.44, 130.89, 132.66, 166.02. **HRMS (EI)** C<sub>17</sub>H<sub>22</sub>O<sub>2</sub> requires 258.1620 g mol<sup>-1</sup>, found 258.1616 g mol<sup>-1</sup>.

In accordance with literature.<sup>[175]</sup>

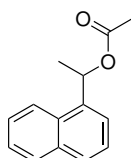


***tert*-Butyl(1-(naphthalen-1-yl)ethoxy)diphenylsilane (43a)**

The reaction was performed using general procedure *Sil1*. The crude product was purified by flash-chromatography on SiO<sub>2</sub> (i-hexane:EtOAc; 30:1) to obtain 95 % of product **43a** as a colorless oil.

**<sup>1</sup>H NMR (300 MHz, CDCl<sub>3</sub>):**  $\delta$  = 1.08 (s, 9H) 1.50 (d, <sup>3</sup>*J* = 6.3 Hz, 3H), 5.58 (q, <sup>3</sup>*J* = 6.4 Hz, 1H), 7.14 – 7.24 (m, 2H), 7.27 – 7.55 (m, 9H), 7.65 – 7.96 (m, 6H). **<sup>13</sup>C NMR (75 MHz, CDCl<sub>3</sub>):**  $\delta$  = 19.51, 26.57, 27.15, 69.71, 123.19, 123.64, 125.27, 125.58, 125.69, 127.39, 127.53, 127.72, 128.85, 129.57, 129.95, 133.71, 133.86, 134.64, 135.70, 135.94, 136.03, 142.31. **<sup>29</sup>Si NMR (80 MHz, CDCl<sub>3</sub>):**  $\delta$  = –3.74. **HRMS (EI)** C<sub>21</sub>H<sub>31</sub>OSi requires 410.2066 g mol<sup>–1</sup>, found 410.2027 g mol<sup>–1</sup>.

#### 1-(Naphthalen-1-yl)ethyl acetate (**43b**)

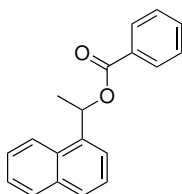


The reaction was performed using general procedure *Ac1*. The crude product was purified by flash-chromatography on SiO<sub>2</sub> (i-hexane:EtOAc; 10:1) to obtain 93 % of product **43b** as a colorless oil.

**<sup>1</sup>H NMR** (300 MHz, CDCl<sub>3</sub>):  $\delta$  = 1.71 (d, <sup>3</sup>*J* = 6.6 Hz, 3H), 2.12 (s, 3H), 6.66 (q, <sup>3</sup>*J* = 6.5 Hz, 1H), 7.46 – 7.51 (m, 2H), 7.51 – 7.56 (m, 1H), 7.61 (d, <sup>3</sup>*J* = 7.2 Hz, 1H), 7.80 (d, <sup>3</sup>*J* = 8.1 Hz, 1H), 7.88 (d, <sup>3</sup>*J* = 7.4 Hz, 1H), 8.09 (d, <sup>3</sup>*J* = 8.1 Hz, 1H). **<sup>13</sup>C NMR** (75 MHz, CDCl<sub>3</sub>):  $\delta$  = 21.68, 69.43, 123.13, 123.17, 125.32, 125.63, 126.27, 128.41, 128.88, 130.24, 134.00, 137.40, 170.31. **HRMS (EI)** C<sub>14</sub>H<sub>14</sub>O<sub>2</sub> requires 240.0994 g mol<sup>-1</sup>, found 240.0993 g mol<sup>-1</sup>.

In accordance with literature.<sup>[176]</sup>

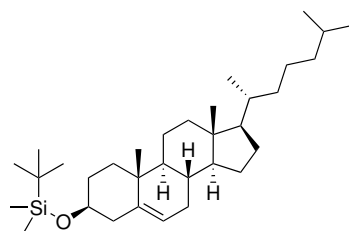
#### 1-(Naphthalen-1-yl)ethyl benzoate (**43c**)



The reaction was performed using general procedure *Ac1*. The crude product was purified by flash-chromatography on SiO<sub>2</sub> (i-hexane:EtOAc; 9:1) to obtain 79 % of product **43c** as a colorless oil.

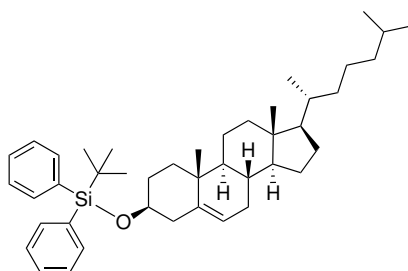
**<sup>1</sup>H NMR** (300 MHz, CDCl<sub>3</sub>):  $\delta$  = 1.85 (d, <sup>3</sup>*J* = 6.6 Hz, 3H), 6.90 (q, <sup>3</sup>*J* = 6.6 Hz, 1H), 7.39 – 7.65 (m, 6H), 7.71 (d, <sup>3</sup>*J* = 7.1 Hz, 1H), 7.82 (d, <sup>3</sup>*J* = 8.2 Hz, 1H), 7.89 (d, <sup>3</sup>*J* = 7.9 Hz, 1H), 8.12 (d, <sup>3</sup>*J* = 7.0 Hz, 1H), 8.20 (d, <sup>3</sup>*J* = 8.7 Hz, 1H). **<sup>13</sup>C NMR** (75 MHz, CDCl<sub>3</sub>):  $\delta$  = 21.91, 70.26, 123.22, 125.37, 125.66, 126.33, 128.35, 128.46, 129.68, 130.28, 130.48, 132.93, 133.85, 137.54, 165.83. **HRMS (EI)** C<sub>19</sub>H<sub>16</sub>O<sub>2</sub> requires 276.1150 g mol<sup>-1</sup>, found 276.1147 g/mol.

In accordance with literature data.<sup>[177]</sup>

***tert*-Butyl(cholesteryl)dimehtylsilane (44a)**

The reaction was performed using general procedure *Sil2*. The crude product was purified by flash-chromatography on SiO<sub>2</sub> (*i*hexane:EtOAc; 30:1) to obtain 84 % of product **44a** as a colorless oil.

**<sup>1</sup>H NMR** (600 MHz, CDCl<sub>3</sub>):  $\delta$  = 0.06 (s, 6 H), 0.67 (s, 3 H), 0.86 – 1.19 (m, 31H), 1.22 – 1.60 (m, 11H), 1.69 – 1.74 (m, 1H), 1.79 – 1.86 (m, 2H), 1.94 – 2.02 (m, 2H), 2.16 (ddd, <sup>3,3,3</sup>*J* = 13.4, 4.9, 2.3 Hz, 1H), 2.24 – 2.29 (m, 1H), 3.48 (tt, <sup>3,3</sup>*J* = 11.0, 4.7 Hz, 1H), 5.31 – 5.32 (m, 1H). **<sup>13</sup>C NMR** (100 MHz, CDCl<sub>3</sub>):  $\delta$  = –4.42, 12.01, 18.43, 18.88, 19.60, 21.23, 22.73, 22.99, 23.97, 24.46, 26.11, 28.18, 28.40, 32.07, 32.11, 32.25, 35.94, 36.35, 37.55, 39.68, 39.97, 42.48, 42.98, 50.37, 56.30, 56.96, 72.80, 121.32, 141.73. **<sup>29</sup>Si NMR** (80 MHz, CDCl<sub>3</sub>):  $\delta$  = 16.67. **HRMS (EI)** C<sub>29</sub>H<sub>51</sub>OSi (*M*–*t*Bu) requires 443.3704 g mol<sup>–1</sup>, found 443.3725 g mol<sup>–1</sup>.

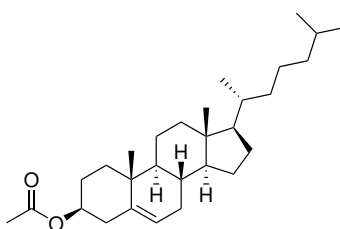
***tert*-Butyl(cholesteryl)diphenylsilane (44b)**

The reaction was performed using general procedure *Sil2*. The crude product was purified by flash-chromatography on SiO<sub>2</sub> (*i*hexane:EtOAc; 50:1) to obtain 78 % of product **44b** as a white solid.

**<sup>1</sup>H NMR** (600 MHz, CDCl<sub>3</sub>):  $\delta$  = 0.66 (s, 3H), 0.78 – 0.84 (m, 1H), 0.87 (dd, <sup>3,3</sup>*J* = 6.72.8 Hz, 7H), 0.90 (d, <sup>3</sup>*J* = 6.5 Hz, 3H), 0.99 (s, 3H), 1.02 – 1.19 (m, 13H), 1.19 – 1.29 (m, 1H), 1.29 – 1.48 (m, 6H), 1.48 – 1.65 (m, 3H), 1.65 – 1.74 (m, 2H), 1.81 (dtd, <sup>3,3,3</sup>*J* = 13.4, 9.4, 6.2 Hz, 1H), 1.90 (ddd, <sup>3,3,3</sup>*J*

= 12.8, 5.5, 3.0 Hz, 1H), 1.98 (dt,  $^3J = 12.8, 3.6$  Hz, 1H), 2.14 (ddd,  $^3J = 13.3, 5.0, 2.1$  Hz, 1H), 2.34 (ddd,  $^3J = 13.9, 11.2, 2.8$  Hz, 1H), 3.54 (hept, 1H), 5.13 (d,  $^3J = 4.8$  Hz, 1H), 1H), 7.33 – 7.39 (m, 4H), 7.39 – 7.44 (m, 2H), 7.66 – 7.71 (m, 4H).  $^{13}\text{C}$  NMR (150 MHz,  $\text{CDCl}_3$ ):  $\delta = 11.82, 19.12, 19.40, 21.01, 22.54, 22.80, 23.79, 24.25, 26.99, 27.99, 28.20, 31.86, 35.75, 36.16, 36.47, 37.19, 39.50, 39.75, 42.28, 42.47, 50.03, 56.09, 56.74, 73.24, 121.11, 127.40, 127.42, 129.39, 134.79, 134.82, 135.74, 141.27$ .  $^{29}\text{Si}$  NMR (80 MHz,  $\text{CDCl}_3$ ):  $\delta = -6.50$ . HRMS (EI)  $\text{C}_{43}\text{H}_{64}\text{OSi}$  (M–2Ph–*t*Bu) requires 413.3240 g mol $^{-1}$ , found 413.3204 g mol $^{-1}$ .

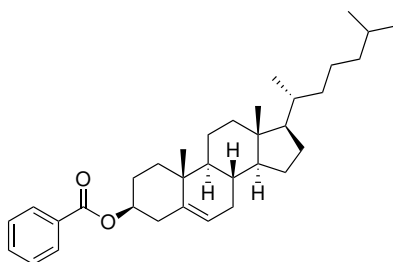
#### Cholesteryl acetate (45a)



The reaction was performed using general procedure *Ac1*. The crude product was purified by flash-chromatography on  $\text{SiO}_2$  (i-hexane:EtOAc; 10:1) to obtain 98 % of product **45a** as a white solid.

$^1\text{H}$  NMR (300 MHz,  $\text{CDCl}_3$ ):  $\delta = 0.69$  (s, 3H), 0.87 (d,  $^3J = 4.4$  Hz, 6H), 0.91 (d,  $^3J = 4.6$  Hz, 3H), 1.02 (s, 3H), 1.21 – 1.81 (m, 26H), 2.03 (s, 3H), 2.30 (d,  $^3J = 5.1$  Hz, 2H), 4.60 (m, 1H), 5.38 (m, 1H).  $^{13}\text{C}$  NMR (75 MHz,  $\text{CDCl}_3$ ):  $\delta = 11.83, 18.69, 19.29, 21.01, 21.41, 22.53, 22.79, 23.81, 24.26, 27.76, 27.99, 28.20, 31.85, 31.88, 35.77, 36.17, 36.98, 38.11, 39.50, 39.72, 42.30, 50.02, 56.12, 56.67, 73.96, 122.61, 139.64, 170.49$ .

In accordance with literature data.<sup>[178]</sup>

**Cholesteryl benzoate (45b)**

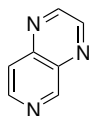
The reaction was performed using general procedure *Ac1*. The crude product was purified by flash-chromatography on SiO<sub>2</sub> (i-hexane:EtOAc; 9:1) to obtain 56 % of product **45b** as a white solid.

**<sup>1</sup>H NMR** (600 MHz, CDCl<sub>3</sub>):  $\delta$  = 0.69 (s, 3H), 0.87 (dd,  $^3J$  = 6.6, 2.7 Hz, 6H), 0.92 (d,  $^3J$  = 6.6 Hz, 3H), 0.92 – 1.96 (m, 26H), 2.01 (dt,  $^3J$  = 17.8, 8.8 Hz, 3H), 2.47 (d,  $^3J$  = 7.6 Hz, 2H), 4.81 – 4.91 (m, 1H), 5.42 (d,  $^3J$  = 3.6 Hz, 1H), 7.43 (t,  $^3J$  = 7.8 Hz, 2H), 7.54 (t,  $^3J$  = 7.4 Hz, 2H), 8.04 (dd,  $^3J$  = 8.4, 1.3 Hz, 2H). **<sup>13</sup>C NMR** (151 MHz, CDCl<sub>3</sub>):  $\delta$  = 11.86, 18.71, 19.37, 21.05, 22.55, 22.81, 23.82, 24.29, 27.88, 28.01, 28.22, 31.88, 31.93, 35.79, 36.18, 36.65, 37.03, 38.21, 39.51, 39.73, 42.32, 50.04, 56.13, 56.69, 74.56, 122.76, 128.23, 129.51, 130.83, 139.65, 165.98.

In accordance with literature data.<sup>[179]</sup>

### 7.4.5 Synthesis of Catalysts

#### Pyrido[3,4-*b*]pyrazin (46)

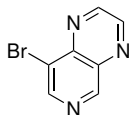


22.9 mmol (2.50 g) of 3,4-diaminopyridine was dissolved in 30 mL ethanol under a nitrogen atmosphere. After adding 22.9 mmol (2.50 g) of glyoxal (40 wt.% in water) the reaction mixture was started in a microwave reactor for 1 h at 110 °C (70 W). The solvent was removed under reduced pressure and a yellow solid (**46**) was obtained in quantitative yield (3.01 g, 22.9 mmol).

**<sup>1</sup>H NMR** (300 MHz, CDCl<sub>3</sub>):  $\delta$  = 7.91 (d,  $^4J$  = 0.8 Hz), 8.92 (d,  $^3J$  = 1.8 Hz 1H), 8.99 (d,  $^3J$  = 1.8 Hz), 9.53 (d,  $^4J$  = 0.8 Hz, 1H).

In accordance with literature data.<sup>[39]</sup>

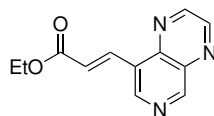
#### 8-Bromopyrido[3,4-*b*]pyrazine (47)



54.9 mmol (7.20 g) **46** was dissolved in 280 mL MeCN and stirred in the dark. 60.1 mmol (10.7 g) *N*-bromosuccinimide was added in portions to the solution under a nitrogen atmosphere. After stirring the reaction mixture at rt over night the solvent was removed under reduced pressure. The crude product was purified by column chromatography on silica gel (EtOAc:hexane:Et<sub>3</sub>N:Et<sub>2</sub>O; 20:15:1:1.5) yielded in 48 % (5.53 g, 26.4 mmol) of **47** as pale solid.

**<sup>1</sup>H NMR** (300 MHz, CDCl<sub>3</sub>):  $\delta$  = 9.02 (d,  $^4J$  = 1.8 Hz, 1H), 9.08 (s, 1H), 9.15 (d,  $^4J$  = 1.8 Hz), 9.50 (s, 1H).

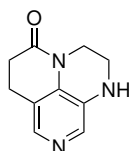
In accordance with literature data.<sup>[39]</sup>

**(E)-Ethyl-3-(pyrido[3,4-*b*]pyrazin-8-yl)acrylate (48)**

A flame dried pressure tube was filled with 0.29 mmol (64.2 mg, 2.6 mol%) Pd(OAc)<sub>2</sub>, 0.72 mmol (217.6 mg) P(*o*-tol)<sub>3</sub>, 7.4 mmol (0.749 g, 1.04 mL) Et<sub>3</sub>N, 11 mmol (2.3 g) of **47**, 18.7 mmol (1.87 g, 2.02 mL) ethylacrylate, and was dissolved in 15 mL dry MeCN. The reaction mixture was heated for 20 h at 120 °C. After cooling to rt the solvent was removed at reduced pressure and the crude product was purified by column chromatography on silica (gradient of *n*hexane:EtOAc; 1:1 to 1:9). The product **48** was obtained in 50 % yield (1.26 g, 5.5 mmol) as a yellow solid.

<sup>1</sup>H NMR (300 MHz, CDCl<sub>3</sub>): δ = 1.38 (t, <sup>3</sup>J = 7.1 Hz, 3H), 4.33 (q, <sup>3</sup>J = 7.1 Hz, 2H), 7.13 (d, <sup>3</sup>J = 16.3 Hz, 1H), 8.49 (dd, <sup>3,4</sup>J = 16.3, 0.6 Hz, 1H), 9.01 (d, <sup>3</sup>J = 1.7 Hz, 1H), 9.05 (s, 1H), 9.09 (d, <sup>3</sup>J = 1.7 Hz, 1H), 9.54 (s, 1H).

In accordance with literature data.<sup>[39]</sup>

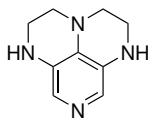
**2,3,6,7-Tetrahydropyrazino[3,2-*i*][1,6]naphthyridine-5(1H)-on (49)**

5 mmol (1.15 g) of **48** was dissolved in 250 mL ethanol and 0.38 g of palladium on charcoal (10%) was added. The flask was purged three times with hydrogen and the reaction mixture was allowed to stir under hydrogen atmosphere for 8 h at rt. The reaction mixture was filtered through Celite and washed with ethanol and DCM. A column chromatography on neutral aluminum oxide (CH<sub>3</sub>Cl:MeOH; 40:1) led to a brown solid as product **49** in 84 % yield (0.79 g, 4.20 mmol).

<sup>1</sup>H NMR (300 MHz, CDCl<sub>3</sub>): δ = 2.64 – 2.80 (m, 2H), 2.90 (t, <sup>3</sup>J = 7.5 Hz, 2H), 3.32 – 3.46 (m, 2H), 3.93 – 4.00 (m, 2H), 4.03 (bs, 1H, NH), 7.79 (s, 1H), 7.88 (s, 1H).

In accordance with literature data.<sup>[39]</sup>

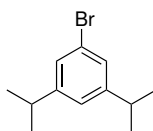
**2,3,5,6-tetrahydro-1*H*,4*H*-1,3*a*,6,8-tetraazaphenalene (29)**



Compound **29** was synthesized following the literature known procedure and provided by Dr. R. Tandon.

**<sup>1</sup>H NMR (200 MHz, CDCl<sub>3</sub>):**  $\delta$  = 3.22 (t, <sup>3</sup>*J* = 4.9 Hz, 4H), 3.40 (t, <sup>3</sup>*J* = 4.1 Hz, 4H), 7.14 (s, 2H).  
In accordance with literature data.<sup>[16]</sup>

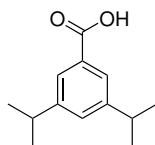
**1-Bromo-3,5-diisopropylbenzene (50)**



26.5 mmol (2.80 g) of *n*Bu<sub>4</sub>NBr<sub>3</sub> was dissolved in 250 mL DCM and added to 26.5 mmol (4.69 g, 5.0 mL) 2,6-diisopropylaniline dissolved in 250 mL DCM. The mixture stirred for 30 min at rt and the solvent was removed at reduced pressure. The mixture was extracted with diethylether (3×200 mL), washed with 0.5 M NaOH solution (200 mL) and water (150 mL). The combined organic phases were dried over MgSO<sub>4</sub> and the solvent was removed under reduced pressure. The achieved colorless oil was directly converted further. After addition of 70 mL 2 M HCl the mixture was cooled down to −5 °C and 64.5 mmol (4.30 g) of sodium nitrite was added slowly. The mixture was stirred at −5 °C for 10 min, 30 mL of H<sub>3</sub>PO<sub>2</sub> (50 %) was added and the reaction stirred for 24 h at 0 °C and 24 h at rt. The reaction mixture was extracted with diethylether (3×100 mL) and the combined organic phases dried over MgSO<sub>4</sub>. A column chromatography on silica (*i*hexane:EtOAc; 30:1) led to an orange liquid product **50** in 87 % yield (4.95 g, 20.5 mmol).

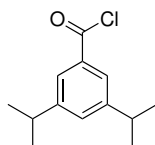
**<sup>1</sup>H NMR (200 MHz, CDCl<sub>3</sub>):**  $\delta$  = 1.21 (d, <sup>3</sup>*J* = 6.9 Hz, 12H), 2.81 (hept, 2H), 6.96 (t, <sup>4</sup>*J* = 1.6 Hz, 1H), 7.16 (d, <sup>4</sup>*J* = 1.6 Hz, 2H).  
In accordance with literature data.<sup>[180]</sup>



**3,5-Diisopropylbenzoic acid (51)**

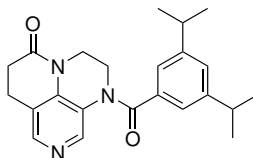
1.24 mmol (0.30 g) of **50** was dissolved in 10 mL THF and cooled to  $-78^{\circ}\text{C}$ . 0.85 mL (1.36 mmol) of *n*BuLi in hexane was added slowly over 20 min. The mixture stirred for 30 min at  $-78^{\circ}\text{C}$  and  $\text{CO}_2$  was added to the reaction mixture and stirred for 2 h. The reaction mixture was quenched with 3 mL  $\text{NaHCO}_3$ , extracted with diethylether ( $3 \times 10$  mL) and washed with 0.5 M HCl solution (20 mL). The combined organic phases were extracted with DCM (20 mL) and dried over  $\text{MgSO}_4$ . The solvent was removed under reduced pressure and yielded in a white solid product **51** in 98 % yield (0.25 g, 1.22 mmol).

$^1\text{H}$  NMR (200 MHz,  $\text{CDCl}_3$ ):  $\delta$  = 1.29 (d,  $^3J$  = 6.9 Hz, 12H), 2.97 (hept, 2H), 7.33 (t,  $^4J$  = 1.8 Hz, 1H), 7.82 (d,  $^4J$  = 1.8 Hz, 2H).

**3,5-Diisopropylbenzoyl chloride (25)**

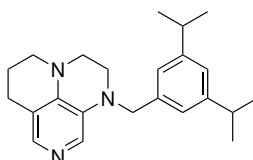
8.25 mmol (1.7 g) of **51** was dissolved in benzene (5 mL) and cooled to  $0^{\circ}\text{C}$ . Two drops of DMF and 50 mmol (6.2 g) of thionyl chloride were added slowly. The mixture was refluxed for 4 h. The solvent was removed under reduced pressure and product **25** was obtained in 81 % (1.50 g, 6.7 mmol) yield as a white solid.

$^1\text{H}$  NMR (200 MHz,  $\text{CDCl}_3$ ):  $\delta$  = 1.29 (d,  $^3J$  = 6.9 Hz, 12H), 2.96 (hept, 2H), 7.37 (s, 1H), 7.81 (d,  $^4J$  = 1.7 Hz, 2H).

**1-(3,5-Diisopropylbenzoyl)-2,3,6,7-tetrahydro-1*H*,5*H*-pyrazino[3,2-*ij*][1,6]naphthyridin-5-one (52)**

2.11 mmol (0.4 g) of **49** and 6.34 mmol (1.42 g) of **25** were mixed in a microwave vial and dissolved in 2.5 mL of pyridine. The mixture was allowed to stir for 10 min at rt and was heated via microwave radiation to 170 °C for 1 h and was allowed to stir over night. The solvent was removed under reduced pressure and the crude product was purified by column chromatography on silica (EtOAc:Et<sub>3</sub>N:MeOH; 10:1:1). The product **52** was achieved in 92 % (0.73 g, 1.94 mmol) yield as white foam.

**<sup>1</sup>H NMR (200 MHz, CDCl<sub>3</sub>):**  $\delta$  = 1.18 (d, <sup>3</sup>*J* = 6.9 Hz, 12H), 2.68 – 3.13 (m, 6H), 3.94 – 4.06 (m, 4H), 7.11 (d, <sup>4</sup>*J* = 1.7 Hz, 2H), 7.15 (d, <sup>4</sup>*J* = 1.7 Hz, 1H), 8.06 (d, <sup>4</sup>*J* = 0.9 Hz, 2H).

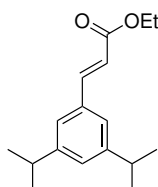
**1-(3,5-Diisopropylbenzyl)-2,3,6,7-tetrahydro-1*H*,5*H*-pyrazino[3,2-*ij*][1,6]naphthyridine (53)**

4.2 mmol (0.29 g) of LiAlH<sub>4</sub> was dissolved in 15 mL THF and 2.60 mmol (0.65 g) AlCl<sub>3</sub> was added slowly. The reaction mixture was allowed to stir for 30 min at rt, while 1.88 mmol (0.71 g) of **52** was dissolved in 10 mL THF and slowly added to the reaction flask. After 1 h reaction time at room temperature, 2 mL of water and 1 mL of NaOH were added at 0 °C. The crude mixture was filtered over Celite, washed with DCM:EtOAc (1:1) and dried over MgSO<sub>4</sub>. The solvent was removed under reduced pressure and the crude product was purified by column chromatography on silica (EtOAc:Et<sub>3</sub>N:MeOH; 10:1:1). The product **28** was obtained in 81 % (0.53 g, 1.52 mmol) yield as a yellow oil.

**<sup>1</sup>H NMR (400 MHz, CDCl<sub>3</sub>):**  $\delta$  = 1.23 (d, <sup>3</sup>*J* = 6.9 Hz, 12H), 1.95–2.09 (m, 2H), 2.71 (t, <sup>3</sup>*J* = 6.4 Hz, 2H), 2.86 (hept, 2H), 3.15–3.37 (m, 6H), 4.22–4.42 (m, 2H), 6.97 (s, 3H), 7.59 (s, 1H), 7.65 (s, 1H). **<sup>13</sup>C NMR (100 MHz, CDCl<sub>3</sub>):**  $\delta$  = 21.33, 24.07, 24.25, 34.27, 45.97, 48.03, 49.40, 55.47, 114.90, 123.27,

123.60, 130.63, 137.84, 138.23, 140.54, 149.39. **HRMS (EI)**:  $C_{23}H_{31}N_3$  requires  $349.2518 \text{ g mol}^{-1}$ , found  $349.2523 \text{ g mol}^{-1}$ .

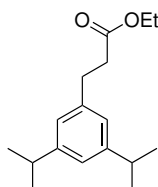
**(E)-Ethyl-3-(3,5-diisopropylphenyl)acrylate (54)**



0.12 mmol (28 mg)  $Pd(OAc)_2$ , 0.22 mmol (67 mg)  $P(o\text{-tol})_3$ , 10 mmol (1.01 g)  $Et_3N$  were added to a microwave vial and dissolved in 15 mL MeCN. The mixture was stirred for 10 min at rt, 10 mmol (2.44 g) of **50**, 10 mmol (1.00 g) ethylacrylate were added and the reaction mixture heated for 1 h at  $180^\circ C$  by microwave (200 W). The crude product was extracted with EtOAc ( $3 \times 20 \text{ mL}$ ), washed with water (15 mL) and the combined organic phases were dried over  $MgSO_4$ . A column chromatography on silica (i-hexane:EtOAc; 30:1) led to a colorless oil as compound **54** in 73 % (1.89 g, 7.20 mmol) yield.

$R_f = 0.37$  (i-hexane:EtOAc; 30:1).  $^1H$  NMR (300 MHz,  $CDCl_3$ ):  $\delta = 1.24$  (d,  $^3J = 6.8 \text{ Hz}$ , 12H), 2.88 (hept, 2H), 4.25 (q,  $^3J = 7.1 \text{ Hz}$ , 2H), 6.41 (d,  $^3J = 16.0 \text{ Hz}$ , 1H), 7.08 (s, 1H), 7.19 (d,  $^4J = 1.6 \text{ Hz}$ , 2H), 7.66 (d,  $^4J = 1.6 \text{ Hz}$ , 1H).  $^{13}C$  NMR (75 MHz,  $CDCl_3$ ):  $\delta = 14.32, 23.92, 33.93, 60.42, 117.57, 123.54, 127.14, 134.39, 145.22, 149.46, 167.14$ . **HRMS (EI)**:  $C_{17}H_{24}O_2$  requires  $260.1776 \text{ g mol}^{-1}$ , found  $260.1780 \text{ g mol}^{-1}$ .

**Ethyl-3-(3,5-diisopropylphenyl)propanoate (55)**

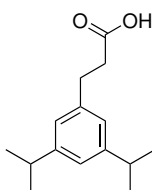


7.7 mmol (2.0 g) of **54** and 1.92 mmol (0.2 g)  $Pd/C$  were dissolved in 30 mL ethanol. The flask was purged with hydrogen for three times and the reaction was allowed to stir under  $H_2$  for 18 h. The crude product was filtered over celite and washed several times with ethanol ( $3 \times 30 \text{ mL}$ ). The

solvent was removed under reduced pressure and yielded into 95 % (1.03 g, 7.30 mmol) of a colorless oil **55**.

**$^1\text{H}$  NMR** (300 MHz,  $\text{CDCl}_3$ ):  $\delta$  = 1.22 (d,  $^3J$  = 6.9 Hz, 12H), 1.25 (m, 3H), 2.60 (m, 4H), 2.85 (hept, 2H), 4.12 (q,  $^3J$  = 7.1 Hz, 2H), 6.87 (s, 2H), 6.91 (s, 1H).  **$^{13}\text{C}$  NMR** (75 MHz,  $\text{CDCl}_3$ ):  $\delta$  = 14.21, 24.04, 31.18, 60.33, 122.74, 123.77, 140.39, 149.07, 173.06. **HRMS (EI)**:  $\text{C}_{17}\text{H}_{26}\text{O}_2$  requires 262.1933 g/mol, found 262.1928 g/mol.

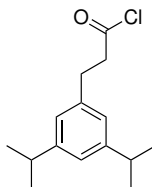
### 3-(3,5-Diisopropylphenyl)propanoic acid (**56**)



7.2 mmol (1.9 g) of **55** was dissolved in 70 mL methanol, 25 mL water and 12 mmol (0.68 g) KOH was added. The reaction mixture was allowed to stir for 24 h and the pH-value was adjusted with 2 M HCl to 2. The mixture was extracted with EtOAc (3×30 mL), washed with 2 M NaOH and the combined organic phases were dried over  $\text{MgSO}_4$ . The solvent was removed under reduced pressure and product **56** was achieved in 98 % (1.66 g, 7.1 mmol) yield as a yellow oil.

**$^1\text{H}$  NMR** (300 MHz,  $\text{CDCl}_3$ ):  $\delta$  = 1.23 (d,  $^3J$  = 6.8 Hz, 12H), 2.68 (m, 2H), 2.85 (hept, 2H), 2.93 (m, 2H), 6.89 (d,  $^4J$  = 1.6 Hz, 2H), 6.93 (d,  $^4J$  = 1.5 Hz, 1H).  **$^{13}\text{C}$  NMR** (75 MHz,  $\text{CDCl}_3$ ):  $\delta$  = 24.04, 30.82, 34.12, 35.71, 122.82, 123.77, 139.96, 149.13, 179.12. **HRMS (EI)**:  $\text{C}_{15}\text{H}_{22}\text{O}_2$  requires 231.1620 g mol<sup>-1</sup>, found 231.1620 g mol<sup>-1</sup>.

### 3-(3,5-Diisopropylphenyl)propanoyl chloride (**27**)

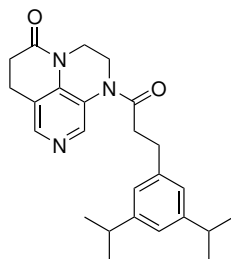


3.0 mmol (0.70 g) of **56** was dissolved in freshly distilled DCM (5 mL) and cooled to 0 °C. Two drops of DMF and 3.9 mmol (0.46 g) of thionyl chloride were added slowly. The mixture was

allowed to stir over night at rt. The solvent was removed under reduced pressure and product **27** was obtained in 99 % (0.75 g, 3.0 mmol) yield as a colorless oil.

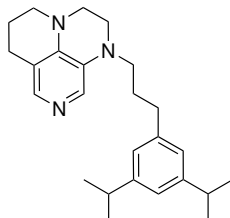
**<sup>1</sup>H NMR** (300 MHz, CDCl<sub>3</sub>):  $\delta$  = 1.23 (d,  $^3J$  = 6.9 Hz, 12H), 2.86 (hept, 2H), 2.97 (t,  $^3J$  = 7.6 Hz, 2H), 3.19 (t,  $^3J$  = 7.7 Hz, 2H), 6.85 (s, 2H), 6.94 (s, 1H). **<sup>13</sup>C NMR** (75 MHz, CDCl<sub>3</sub>):  $\delta$  = 23.69, 30.98, 34.18, 48.76, 123.14, 123.72, 138.38, 149.17, 173.01. **HRMS (EI)**: C<sub>15</sub>H<sub>21</sub>O<sub>1</sub>Cl requires 251.1281 g mol<sup>-1</sup>, found 251.1252 g mol<sup>-1</sup>.

**1-(3-(3,5-Diisopropylphenyl)propanoyl)-2,3,6,7-tetrahydro-1*H*,5*H*-pyrazino[3,2-*ij*][1,6]naphthyridin-5-one (57)**



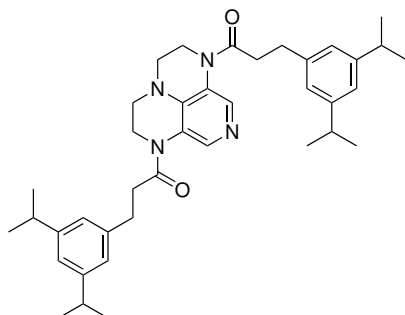
1.62 mmol (0.31 g) of **49** and 1.62 mmol (0.41 g) of **27** were mixed in a microwave vial and dissolved in 2.5 mL pyridine. 0.16 mmol (0.03 g, 10 mol%) of **3c** was added and the mixture was allowed to stir for 10 min at rt. The reaction mixture was heated via microwave radiation to 170 °C for 1 h and was allowed to stir at rt over night. The solvent was removed under reduced pressure and the crude product was purified by column chromatography on silica (EtOAc:Et<sub>3</sub>N:MeOH; 10:1:1). The product **57** was achieved in 53 % (0.35 g, 0.87 mmol) yield as a brown solid.

$R_f$  = 0.73 (EtOAc:Et<sub>3</sub>N:MeOH; 10:1:1). **<sup>1</sup>H NMR** (300 MHz, CDCl<sub>3</sub>):  $\delta$  = 1.21 (s, 12H), 2.05 (t,  $^3J$  = 4.0 Hz, 2H), 2.48 (t,  $^3J$  = 3.5 Hz, 2H), 2.68 – 3.00 (m, 6H), 3.22 (m, 2H), 3.67 – 3.75 (m, 4H), 6.79 – 6.95 (m, 3H), 8.46 (d,  $^3J$  = 4.4 Hz, 2H). **<sup>13</sup>C NMR** (75 MHz, CDCl<sub>3</sub>):  $\delta$  = 24.02, 30.59, 31.89, 34.04, 35.80, 36.81, 42.44, 119.25, 122.74, 122.98, 123.89, 131.711, 140.13, 140.48, 148.18, 149.14, 168.42, 170.95. **HRMS (EI)**: C<sub>25</sub>H<sub>32</sub>O<sub>2</sub>N<sub>3</sub> requires 406.2450 g mol<sup>-1</sup>, found 406.2487 g mol<sup>-1</sup>.

**1-(3-(3,5-diisopropylphenyl)propyl)-1,2,3,5,6,7-hexahydropyrazino-[3,2,1-ij][1,6]naphthyridine (28)**

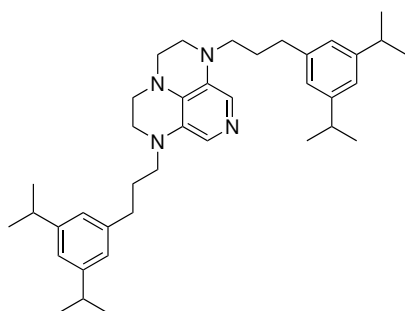
2.41 mmol (0.09 g) of  $\text{LiAlH}_4$  was dissolved in 12 mL THF and 1.50 mmol (0.03 g)  $\text{AlCl}_3$  was added slowly. The reaction mixture was allowed to stir for 30 min at rt, while 0.57 mmol (0.23 g) of **57** was dissolved in 10 mL THF and slowly added to the reaction flask. After 1 h reaction time at room temperature, 2 mL of water and 1 mL of NaOH were added under cooling at 0 °C. The crude mixture was filtered over Celite, washed with DCM:EtOAc (1:1) and dried over  $\text{MgSO}_4$ . The solvent was removed under reduced pressure and the crude product was purified by column chromatography on basic Alox (EtOAc:Et<sub>3</sub>N:MeOH; 10:1:1). The product **28** was obtained in 80 % (0.17 g, 0.46 mmol) yield as a yellow oil.

$R_f$  = 0.4 (basic Alox, EtOAc:Et<sub>3</sub>N:MeOH; 10:1:1). **<sup>1</sup>H NMR** (300 MHz,  $\text{CDCl}_3$ ):  $\delta$  = 1.23 (d,  $^3J$  = 7.1 Hz, 12H), 1.90 – 1.96 (m, 2H), 1.98 – 2.04 (m, 2H), 2.24 (t,  $^3J$  = 6.8 Hz, 2H), 2.27 (t,  $^3J$  = 1.3 Hz, 2H), 2.61 – 2.70 (m, 2H), 2.90 (t,  $^3J$  = 6.9 Hz, 2H), 3.15 – 3.29 (m, 4H), 3.71 (t,  $^3J$  = 6.4 Hz, 2H), 6.87 – 6.91 (m, 3H), 7.55 (t,  $^4J$  = 2.1 Hz, 2H). **<sup>13</sup>C NMR** (75 MHz,  $\text{CDCl}_3$ ):  $\delta$  = 21.15, 24.08, 27.21, 30.31, 33.57, 34.12, 46.14, 47.68, 49.26, 50.86, 114.49, 122.31, 123.82, 128.65, 129.76, 138.05, 139.68, 141.39, 148.91. **HRMS (EI)**:  $\text{C}_{25}\text{H}_{35}\text{N}_3$  requires 378.2865 g mol<sup>-1</sup>, found 378.2901 g mol<sup>-1</sup>.

**1,1'-(2,3,4,5-Tetrahydro-1*H*,6*H*-1,3*a*,6,8-tetraazaphenalene-1,6-diyl)bis(3-(3,5-diisopropylphenyl)propan-1-one) (58)**

1.00 mmol (0.17 g) of **59** and 3.00 mmol (0.75 g) of **27** were mixed in a microwave vial and dissolved in 3.0 mL pyridine. 0.10 mmol (17.4 mg, 10 mol%) of **3c** was added and the reaction mixture was heated via microwave radiation to 180 °C for 1 h and was allowed to stir at rt over night. The solvent was removed under reduced pressure and the crude product was purified by column chromatography on silica (EtOAc:Et<sub>3</sub>N:MeOH; 10:1:1). The product **58** was obtained in 48 % (0.29 g, 0.48 mmol) yield as a brown oil.

$R_f$  = 0.76 (EtOAc:Et<sub>3</sub>N:MeOH, 10:1:1). <sup>1</sup>H NMR (300 MHz, CDCl<sub>3</sub>):  $\delta$  = 1.18 (d, <sup>3</sup>*J* = 6.9 Hz, 24H), 2.86 (m, 12H), 3.23 (t, <sup>3</sup>*J* = 8.2 Hz, 4H), 3.85 (s, 4H), 6.80 (s, 4H), 6.88 (s, 2H), 7.90 (s, 2H). <sup>13</sup>C NMR (75 MHz, CDCl<sub>3</sub>):  $\delta$  = 24.09, 31.85, 34.03, 48.72, 122.53, 123.97, 140.38, 149.04, 170.88. HRMS (EI): C<sub>39</sub>H<sub>52</sub>O<sub>2</sub>N<sub>4</sub> [M+H]<sup>+</sup> requires 609.4163 g mol<sup>-1</sup>, found 609.4157 g mol<sup>-1</sup>.

**1,6-bis(3-(3,5-Diisopropylphenyl)propyl)-2,3,5,6-tetrahydro-1*H*,4*H*-1,3*a*,6,8-tetraazaphenalene (30)**

1.9 mmol (72.0 mg) of LiAlH<sub>4</sub> was dissolved in 10 mL THF and 1.20 mmol (16.0 mg) AlCl<sub>3</sub> was added slowly. The reaction mixture was allowed to stir for 30 min at rt, while 0.46 mmol (28.0 mg)

of **58** was dissolved in 15 mL THF and slowly added to the reaction flask. After 1 h reaction time at rt, 0.5 mL water was added under cooling at 0 °C. The crude mixture was filtered over Celite, washed with DCM:EtOAc (1:1) and dried over MgSO<sub>4</sub>. The solvent was removed under reduced pressure and the crude product was purified by column chromatography on basic Alox (EtOAc:Et<sub>3</sub>N:MeOH; 10:1:1). The product **30** was obtained in 72 % (0.19 g, 0.32 mmol) yield as a yellow oil.

$R_f$  = 0.67 (basic Alox, EtOAc:Et<sub>3</sub>N:MeOH, 10:1:1). **<sup>1</sup>H NMR** (300 MHz, CDCl<sub>3</sub>):  $\delta$  = 1.22 (d, <sup>3</sup> $J$  = 6.9 Hz, 24H), 1.91 (dt, <sup>3</sup> $J$  = 15.3 Hz, 4H), 2.60 (m, 8H), 2.82 (m, 4H), 3.23 (t, <sup>3</sup> $J$  = 7.3 Hz, 4H), 3.29 (s, 4H), 6.84 (s, 4H), 6.89 (s, 2H), 7.30 (s, 2H). **<sup>13</sup>C NMR** (75 MHz, CDCl<sub>3</sub>):  $\delta$  = 24.09, 27.38, 30.31, 33.44, 34.16, 47.61, 51.03, 122.19, 123.72, 128.81, 129.21, 140.50, 141.43, 149.17. **HRMS (EI)**: C<sub>39</sub>H<sub>56</sub>N<sub>4</sub> requires 580.4505 g mol<sup>-1</sup>, found 580.4506 g mol<sup>-1</sup>.







## 8 Appendix

### 8.1 Methodological Approach

#### 8.1.1 NMR-Kinetics

In the following chapter it will be explained how to work with a set of data after the measurement has been performed. First of all one compares the integrals of the reactant and the product in all measured NMR spectra. Furthermore, the reaction time at the point of measuring this specific NMR is recorded. For analyzing the NMR spectra the program *MestReNova 5.2.5* was used. All spectra were imported in MestReNova and the subsequent steps have been carried out: Apodization, exponential 0.1; Baseline Correction, Bernstein polynomial fit; Phase correction, Auto (Global Method). In order to calculate the conversion from the integrals equation 8.1 was used. One has to multiply with 120 % in case of the TBS signals (Equation 8.1).

$$Conversion = \left[ \frac{I_{\text{Produkt TBSCl}}}{\sum I_{\text{Produkt TBSCl}} + I_{\text{TBSCl}}} \right] \cdot 120\% \quad (8.1)$$

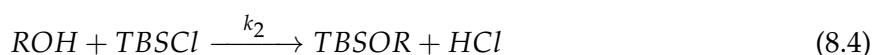
Using programs like *OriginPro 8* for preparing a plot of conversion  $y$  versus reaction time one can easily fit different integrated rate laws. Before fitting the data one has to choose, which kinetic rate law is most suitable for this type of reaction. On the following pages several rate laws will be shown and the best one will be used for fitting. The plots of conversion versus time were fitted with Equation 8.2.

$$y = y_0 \cdot \left( 1 - \frac{0.2}{1.2 e^{k_{\text{eff}} \cdot (0.2) \cdot (t-t_0)} - 1} \right) \quad (8.2)$$

A half-life time can be calculated with Equation 8.3:

$$t_{1/2} = \frac{\ln(1.166)}{0.2 \cdot k_{\text{eff}}} \quad (8.3)$$

Previous equation are based on a modified second order rate law. For the silylation of an alcohol one needs an alcohol **5a** as well as a silylating reagent (TBSCl, **1a**) as reactants. By assuming that during the reaction the concentration of the catalyst is constant and that triethylamine (**2a**) does not participate at all in the rate determining step, the following equation for the second-order reaction can be written:



The rate law for a second-order reaction is shown in Equation 8.5.

$$-\frac{d[ROH]}{dt} = k_2 \cdot [ROH] \cdot [TBSCl] \quad (8.5)$$

Since there is no one to one ratio in this reaction one has to take the actual ratio of reactants into account. The ratio at the beginning of the reaction between both reactants is important for the further proceeding and is expressed in Equation 8.6.

$$\frac{[TBSCl]_0}{[ROH]_0} = n \quad (n > 1) \quad (8.6)$$

Furthermore, the concentrations of the alcohol can be expressed from the conversion and the initial concentration  $[ROH]_0$ . If the ratio of the initial concentrations of alcohol and TBSCl is assumed to be  $n$  (Equation 8.6), then the concentration of TBSCl can be expressed by Equation 8.8.

$$[ROH] = [ROH]_0 \cdot (1 - y) \quad (8.7)$$

$$[TBSCl] = [ROH]_0 \cdot (n - y) \quad (8.8)$$

By taking Equation 8.7 and 8.8 into account the effective rate law can be written as:

$$-[ROH]_0 \frac{d(1 - y)}{dt} = k_2 \cdot [ROH]_0^2 \cdot (1 - y)(n - y) \quad (8.9)$$

Rearranging the variables under the condition that  $k_{eff} = k_2 \cdot [ROH]_0$  leads to Equation 8.10.

$$\frac{d(1 - y)}{(1 - y)(n - y)} = -k_{eff} \cdot dt \quad (8.10)$$

Integration and several transformations of Equation 8.10 leads to Equation 8.16.

$$\int_0^y \frac{d(1 - y)}{(1 - y)(n - y)} = - \int_{t_0}^t k_{eff} \cdot dt \quad (8.11)$$

$$\frac{1}{(1 - y)(n - y)} = \left( \frac{1}{1 - y} - \frac{1}{n - y} \right) / (n - 1) \quad (8.12)$$

$$\ln \left( \frac{1 - y}{1} \right) - \ln \left( \frac{n - y}{n} \right) = -(n - 1) \cdot k_{eff} \cdot (t - t_0) \quad (8.13)$$

$$\ln \left( \frac{n - y}{n \cdot (1 - y)} \right) = -(n - 1) \cdot k_{eff} \cdot (t - t_0) \quad (8.14)$$

$$\frac{n - y}{n \cdot (1 - y)} = e^{k_{\text{eff}} \cdot (n-1) \cdot (t-t_0)} \quad (8.15)$$

$$y = 1 - \frac{n - 1}{ne^{k_{\text{eff}} \cdot (n-1) \cdot (t-t_0)} - 1} \quad (8.16)$$

Equation 8.16 expresses the conversion for the ideal second-order reaction, but only works for  $n > 1$ . For a kinetic measurement it is necessary to take errors of preparing and mixing the samples into account. This can be achieved by adding another variable  $y_0$ , which acts as conversion axis rescaling parameter. The final equation is given below by Equation 8.17:

$$y = y_0 \cdot \left( 1 - \frac{n - 1}{ne^{k_{\text{eff}} \cdot (n-1) \cdot (t-t_0)} - 1} \right) \quad (8.17)$$

For the silylation of an alcohol the silylation reagent (TBSCl, **1a**) is used in 1.2 equivalents which leads to Equation 8.2. Since the ratio between ROH and TBSCl is known to be 1.2, one can change this equation to Equation 8.2 for the reaction rate and Equation 8.3 for the reaction half-life.

For all experiments performed in this study with variable catalysts concentrations, it is found that the rate of reaction (and thus  $k_{\text{eff}}$ ) depends on the catalyst concentration to first order. This implies that the effective rate constant  $k_{\text{eff}}$  can be expressed as the product of the catalyst concentration and a modified rate constant  $k'_{\text{eff}}$ :

$$k_{\text{eff}} = k'_{\text{eff}} \cdot [\text{cat}] + b \quad (8.18)$$

## 8.1.2 GC Measurements

## Determining Conversion for Leaving Group Effects

The determination of the selectivity was performed by GC and  $^1\text{H}$  NMR, if possible. This area-factor between both alcohols was taken into account by measuring a calibration curve of **5a** and **5b** in different concentrations. These area-factors will be used to calculate the exact ratio between both products (Figure 8.1).

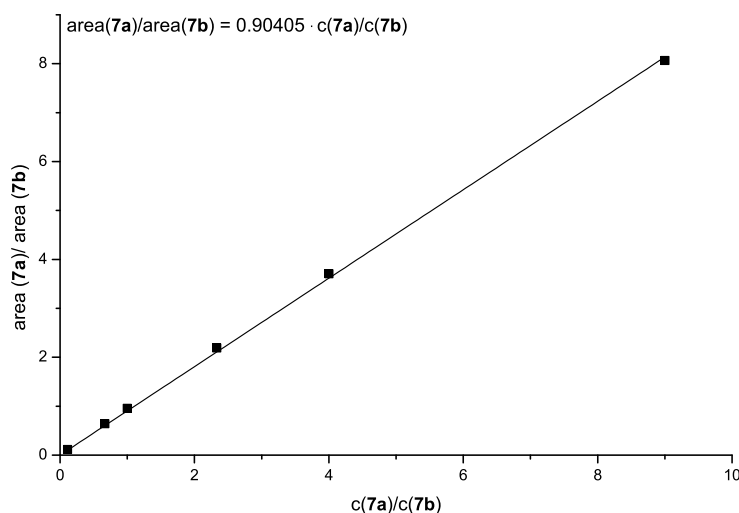


Figure 8.1. Calibration curve for GC analysis **7a** and **7b** measured in methylene chloride.

The calibration curve provides Equation 8.19, which can be easily transformed in Equation 8.20. Using this Equation 8.20 one can achieve the ratio from the GC areas between **7a** and **7b**.

$$\frac{\text{area}(\mathbf{7a})}{\text{area}(\mathbf{7b})} = 0.90405 \cdot \frac{[\mathbf{7a}]}{[\mathbf{7b}]}$$
 (8.19)

$$\frac{\text{area}(\mathbf{7a})}{\text{area}(\mathbf{7b})} \cdot \frac{1}{0.90405} = \frac{[\mathbf{7a}]}{[\mathbf{7b}]}$$
 (8.20)

The chemoselectivity (C) will be achieved using equation 8.21 by GC peak areas. For NMR measurements the concentration can be directly obtained by the integrals divided by amount of protons 8.22.<sup>[87]</sup>

$$C = \frac{[\mathbf{7a}] - [\mathbf{7b}]}{[\mathbf{7a}] + [\mathbf{7b}]}$$
 (8.21)

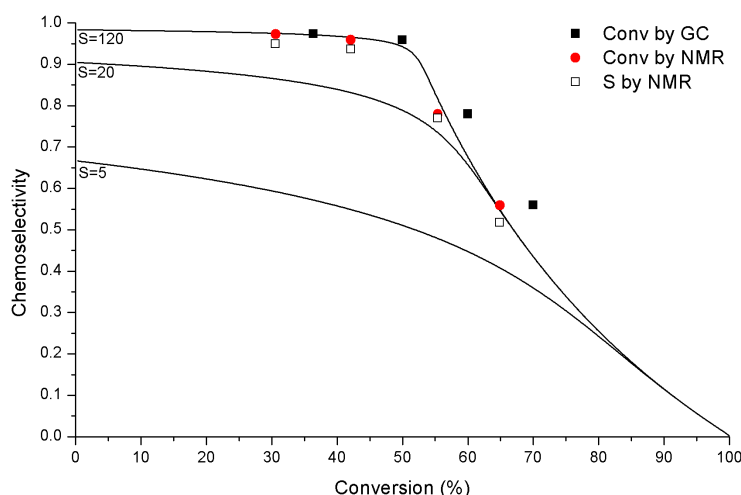
$$C_{\text{NMR}} = \frac{\text{Int}_{\mathbf{7a}/2} - \text{Int}_{\mathbf{7b}/3}}{\text{Int}_{\mathbf{7a}/2} + \text{Int}_{\mathbf{7b}/3}}$$
 (8.22)

Conversion can't be obtained by GC measurements since **5a** and **5b** appear at almost the same

retention time. Therefore, the most accurate conversion can be obtained by NMR measurements using the signals **5a**, **5b**, **7a**, and **7b** with Equation 8.23.

$$\text{Conversion} = \frac{\text{Int}_{7a}/2 - \text{Int}_{7b}/3}{\text{Int}_{7a}/2 + \text{Int}_{7b}/3 + \text{Int}_{5a}/2 + \text{Int}_{5b}/3} \quad (8.23)$$

Since the conversion by experimental design is inaccurate, we tried to modify this number by NMR measurements of the reaction mixtures. Therefore it was not the purpose to detect the chemoselectivity with NMR but to obtain an exact conversion. Figure 8.2 displays the importance of this step and the influence on the analysis of the data. We measured the relative rate of TBSCl (**1a**) with DMAP (**3a**) in our last publication separately ( $S = 120$ ), we take this as a value for the quality of the fit. Since, it is known that the accuracy of NMR measurements when it comes to ratios of 1 : 100 lacks behind GC accuracy. A combination of NMR conversions and GC selectivities provides the best values for this purpose.



**Figure 8.2.** Chemoselectivity vs. conversion using various methods for data processing for the reaction of alcohols **5a** and **5b** with TBSCl (**1a**) in  $\text{CDCl}_3$ .

### Derivation of the Eyring Equation

Starting from the Eyring equation for the primary alcohol **5a** (Equation 8.24) and for the secondary alcohol **5b** (Equation 8.25), leads to the ratio which is shown in Equation 8.26.

$$k_{eff}(\text{prim}) = \frac{k_B \cdot T}{h} \exp \frac{\Delta S_{prim}^\ddagger}{R} \exp \frac{\Delta H_{prim}^\ddagger}{RT} \quad (8.24)$$

$$k_{eff}(\text{sec}) = \frac{k_B \cdot T}{h} \exp \frac{\Delta S_{sec}^\ddagger}{R} \exp \frac{\Delta H_{sec}^\ddagger}{RT} \quad (8.25)$$

$$\frac{k_{eff}(prim)}{k_{eff}(sec)} = \frac{\frac{k_B \cdot T}{h} \exp \frac{\Delta S_{prim}^\ddagger}{R} \exp \frac{\Delta H_{prim}^\ddagger}{RT}}{\frac{k_B \cdot T}{h} \exp \frac{\Delta S_{sec}^\ddagger}{R} \exp \frac{\Delta H_{sec}^\ddagger}{RT}} \quad (8.26)$$

Modification and rearrangements lead to a more clear Equation 8.27.

$$\frac{k_{eff}(prim)}{k_{eff}(sec)} = \exp \frac{\Delta S_{prim}^\ddagger - \Delta S_{sec}^\ddagger}{R} \cdot \exp \frac{\Delta H_{sec}^\ddagger - \Delta H_{prim}^\ddagger}{RT} \quad (8.27)$$

Taking the logarithm of Equation 8.27 and further rearrangements lead to Equation 8.29.

$$\ln \left( \frac{k_{eff}(prim)}{k_{eff}(sec)} \right) = \frac{\Delta S_{prim}^\ddagger - \Delta S_{sec}^\ddagger}{R} \cdot \frac{\Delta H_{sec}^\ddagger - \Delta H_{prim}^\ddagger}{RT} \quad (8.28)$$

$$\ln \left( \frac{k_{eff}(prim)}{k_{eff}(sec)} \right) = \frac{\Delta H_{sec}^\ddagger - \Delta H_{prim}^\ddagger}{R} \cdot \frac{1}{T} - \frac{\Delta S_{prim}^\ddagger - \Delta S_{sec}^\ddagger}{R} \quad (8.29)$$

The slope of Equation 8.29 is given by the difference of  $\Delta H^\ddagger$  and the intercept by  $\Delta S^\ddagger$ .

### Determining Conversion for Five Alcohol Experiment

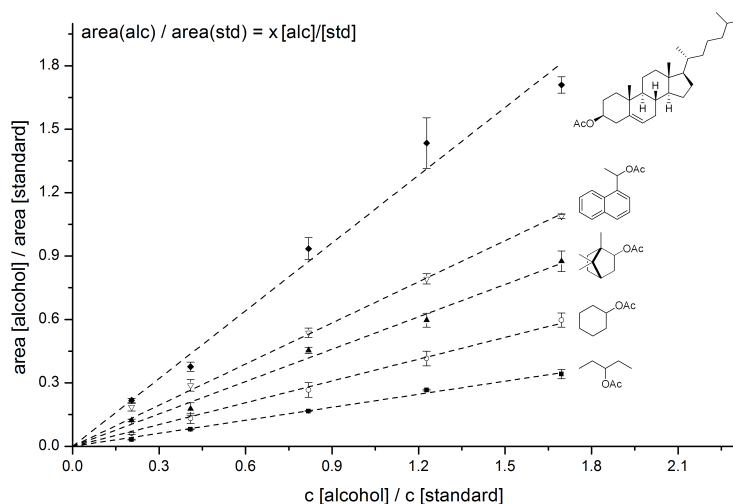
Since the amount of internal standard in each sample is known, one can use the calibration curves, depicted below, to determine area factors against tetracosane and can be used to calculate the conversion of all five alcohols in a single measurement. For all calibration curves a linear plot was possible and therefore equation 8.30 can be used. However, the calibration curves were fitted in a way that they cross the y axes at 0.

$$\frac{area(alcohol)}{area(tetracosane)} = x \cdot \frac{[alcohol]}{[tetracosane]} \quad (8.30)$$

The area factor  $x$  derived for equation 8.30 and was determined for each transformed alcohol. With the knowledge of the concentration of tetracosane and the area factors for each alcohol, one can calculate the conversion using equation 8.31. The measured integral will be correct by the area factor followed by the calculation of the concentration in the sample. Based on the used concentrations and the internal standard (0.0171 M), full conversion will be achieved at 0.029 M.

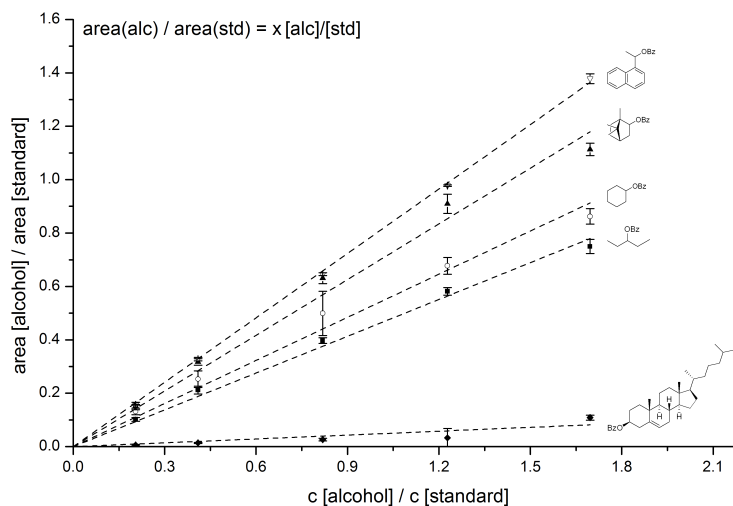
$$\frac{x}{0.029 \text{ M}} \cdot 0.0171 \text{ M} \cdot 100 = yield \quad (8.31)$$





**Figure 8.3.** Calibration lines for the acylation of various alcohols and tetracosane as internal standard.

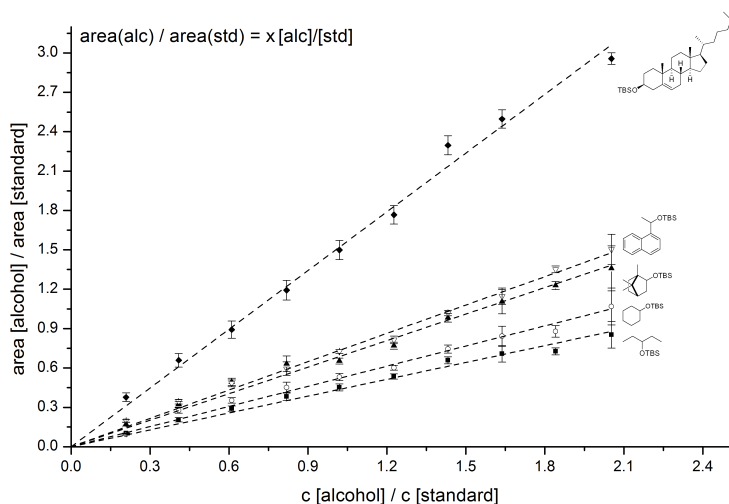
Cholesteryl acetate ( <b>45a</b> )	$R^2 = 0.9932$	$x = 1.0685$
1-(Naphthalen-1-yl)ethyl acetate ( <b>43b</b> )	$R^2 = 0.9980$	$x = 0.6483$
Isobornyl acetate ( <b>42c</b> )	$R^2 = 0.9967$	$x = 0.5104$
Cyclohexyl acetate ( <b>41c</b> )	$R^2 = 0.9987$	$x = 0.3435$
Pentan-3-yl acetate ( <b>40c</b> )	$R^2 = 0.9979$	$x = 0.2054$



**Figure 8.4.** Calibration lines for the benzylation of various alcohols and tetracosane as internal standard.

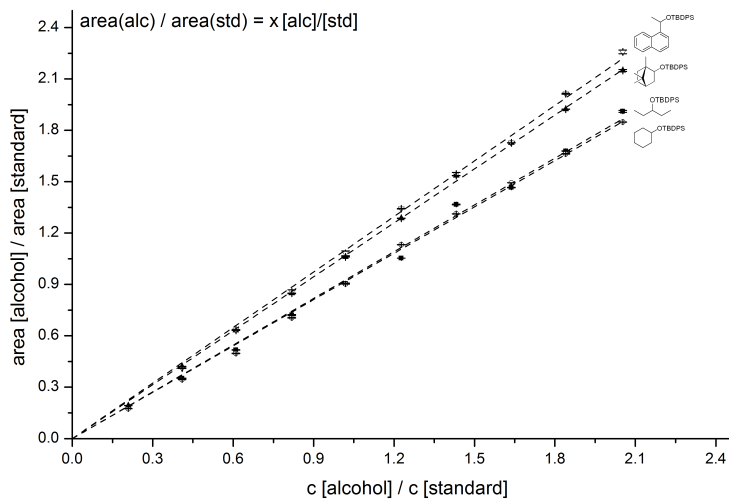
Cholesteryl benzoate ( <b>45b</b> )	$R^2 = 0.8535$	$x = 0.0483$
1-(Naphthalen-1-yl)ethyl benzoate ( <b>43c</b> )	$R^2 = 0.9998$	$x = 0.8041$
Isobornyl benzoate ( <b>42d</b> )	$R^2 = 0.9930$	$x = 0.6953$
Cyclohexyl benzoate ( <b>41d</b> )	$R^2 = 0.9937$	$x = 0.5382$
Pentan-3-yl benzoate ( <b>40d</b> )	$R^2 = 0.9975$	$x = 0.4594$

## 8.1 Methodological Approach



**Figure 8.5.** Calibration lines for the silylation with TBSCl of various alcohols and tetracosane as internal standard.

<i>tert</i> -butyl(cholesteryl)dimehtylsilane ( <b>44a</b> )	$R^2 = 0.9979$	$x = 1.4918$
<i>tert</i> -butyl(1-(naphthalen-1-yl)ethoxy)dimethylsilane ( <b>5b</b> )	$R^2 = 0.9982$	$x = 0.7198$
<i>tert</i> -butyldimethyl-isobornyl-silane ( <b>42a</b> )	$R^2 = 0.9967$	$x = 0.6737$
<i>tert</i> -butyl(cyclohexyloxy)dimethylsilane ( <b>41a</b> )	$R^2 = 0.9967$	$x = 0.5115$
<i>tert</i> -butyldimethyl(pentan-3-yloxy)silane ( <b>40a</b> )	$R^2 = 0.9963$	$x = 0.4281$



**Figure 8.6.** Calibration lines for the silylation with TBDPSCl of various alcohols and tetracosane as internal standard.

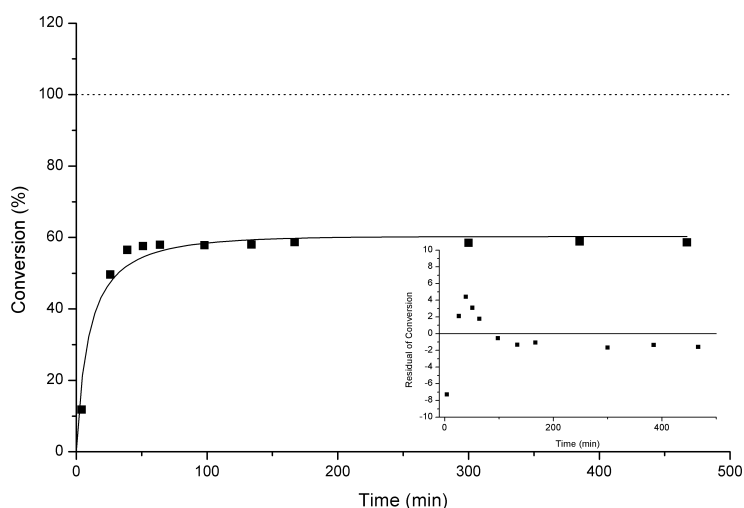
<i>tert</i> -butyl(cholesteryl)diphenylsilane ( <b>44b</b> )	$R^2 = \text{n.d.}$	$x = \text{n.d.}$
<i>tert</i> -butyl(1-(naphthalen-1-yl)ethoxy)diphenylsilane ( <b>43a</b> )	$R^2 = 0.996$	$x = 1.0801$
<i>tert</i> -butyldiphenyl-isobornyl-silane ( <b>42b</b> )	$R^2 = 0.9998$	$x = 1.0497$
<i>tert</i> -butyl(cyclohexyloxy)diphenylsilane ( <b>41b</b> )	$R^2 = 0.9995$	$x = 0.9017$
<i>tert</i> -butyl(pentan-3-yloxy)diphenylsilane ( <b>40b</b> )	$R^2 = 0.9988$	$x = 0.9096$

## 8.2 Data of Direct Rate Measurements

The time conversion plot of all kinetic measurements are plotted on the following pages. These measurement have been taken at room temperature with changing reaction conditions like catalyst, catalyst loading, auxiliary base and solvent. Even though these measurements had been for at least two times only one time conversion plot for each measurement will be displayed. In addition to the figure  $k_{\text{eff}}$ ,  $t_{1/2}$ , and  $R^2$  will be shown for every measurement. The resulting reaction half life time is depicted in minutes if not stated otherwise. The plot have been normed based on the conversion at infinite time, which does not influence the slope of the plot.

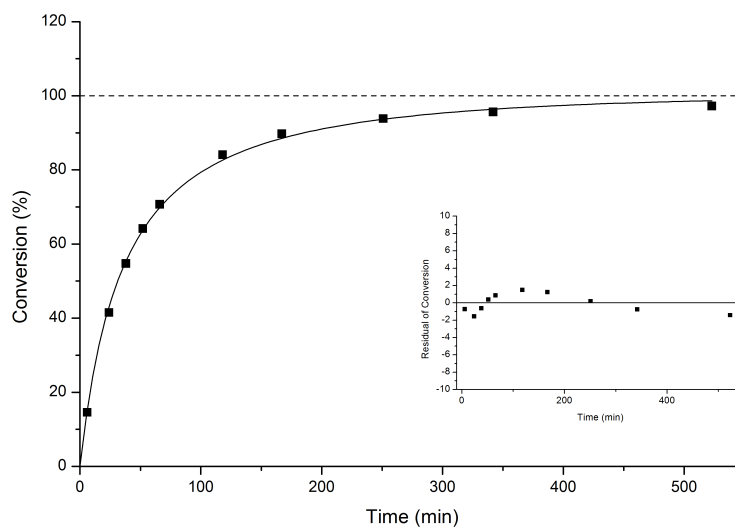
### 8.2.1 Variation of Auxiliary Base Concentration

This data and plots are used for the results shown and discussed in Chapter 2.2.1.



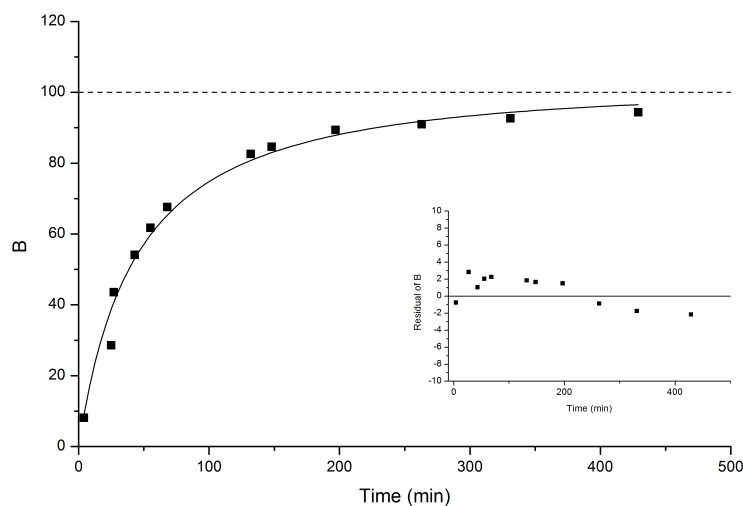
**Figure 8.7.** Time vs. conversion plot of **5a** with 0.7 equiv  $\text{Et}_3\text{N}$  (**2a**) and DMAP (**3a**) with 4 mol% catalyst loading.

M1:	$R^2 = 0.9973$	$k_{\text{eff}} = 9.31 \cdot 10^{-2} \text{ L mol}^{-1} \text{ s}^{-1}$	$t_{1/2} = 8.25 \text{ min}$
M2:	$R^2 = 0.9973$	$k_{\text{eff}} = 9.34 \cdot 10^{-2} \text{ L mol}^{-1} \text{ s}^{-1}$	$t_{1/2} = 8.23 \text{ min}$
Avg.:		$9.32 \cdot 10^{-2} \text{ L mol}^{-1} \text{ s}^{-1}$	$8.24 \pm 0.1 \text{ min}$



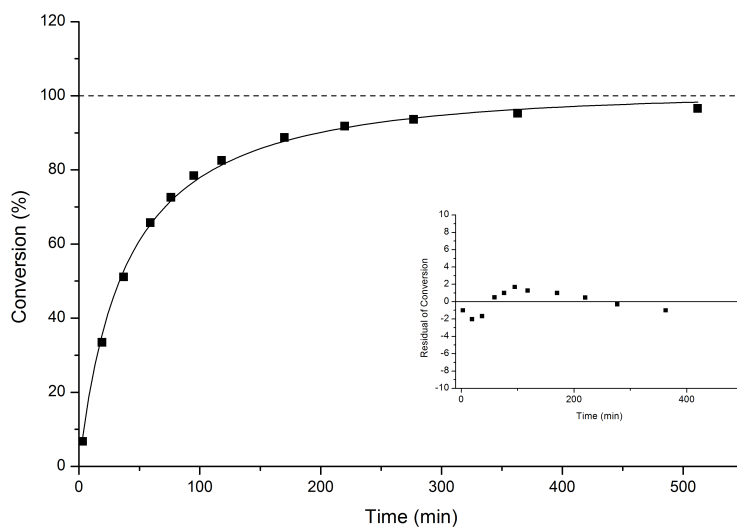
**Figure 8.8.** Time vs. conversion plot of **5a** with 1.2 equiv Et<sub>3</sub>N (**2a**) and DMAP (**3a**) with 4 mol% catalyst loading.

M1:	$R^2 = 0.9975$	$k_{eff} = 2.45 \cdot 10^{-2} \text{ L mol}^{-1} \text{ s}^{-1}$	$t_{1/2} = 31.3 \text{ min}$
M2:	$R^2 = 0.9961$	$k_{eff} = 2.76 \cdot 10^{-2} \text{ L mol}^{-1} \text{ s}^{-1}$	$t_{1/2} = 27.9 \text{ min}$
M3:	$R^2 = 0.9942$	$k_{eff} = 2.47 \cdot 10^{-2} \text{ L mol}^{-1} \text{ s}^{-1}$	$t_{1/2} = 31.1 \text{ min}$
M4:	$R^2 = 0.9982$	$k_{eff} = 2.47 \cdot 10^{-2} \text{ L mol}^{-1} \text{ s}^{-1}$	$t_{1/2} = 31.0 \text{ min}$
Avg.:		$2.54 \cdot 10^{-2} \text{ L mol}^{-1} \text{ s}^{-1}$	$30.2 \pm 1.4 \text{ min}$



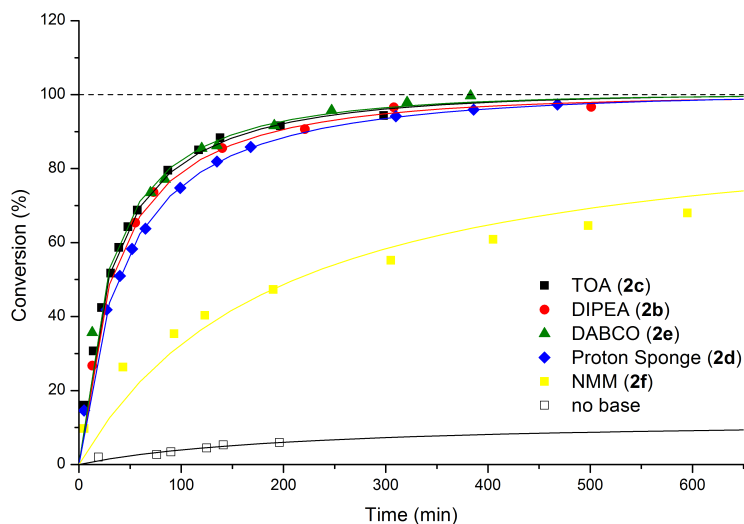
**Figure 8.9.** Time vs. conversion plot of **5a** with 1.7 equiv Et<sub>3</sub>N (**2a**) and DMAP (**3a**) with 4 mol% catalyst loading.

M1:	$R^2 = 0.9823$	$k_{eff} = 2.01 \cdot 10^{-2} \text{ L mol}^{-1} \text{ s}^{-1}$	$t_{1/2} = 38.2 \text{ min}$
M2:	$R^2 = 0.9975$	$k_{eff} = 2.21 \cdot 10^{-2} \text{ L mol}^{-1} \text{ s}^{-1}$	$t_{1/2} = 34.7 \text{ min}$
Avg.:		$2.11 \cdot 10^{-2} \text{ L mol}^{-1} \text{ s}^{-1}$	$36.4 \pm 1.8 \text{ min}$



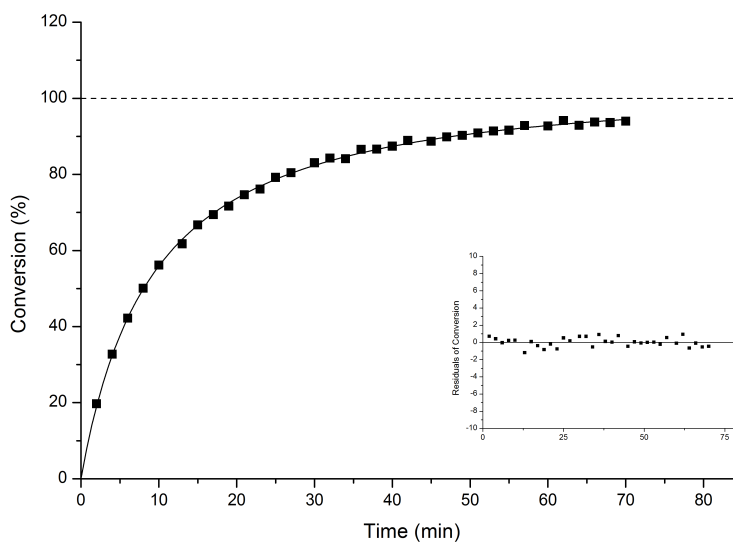
**Figure 8.10.** Time vs. conversion plot of **5a** with 2.2 equiv **Et<sub>3</sub>N (2a)** and **DMAP (3a)** with 4 mol% catalyst loading.

M1:	$R^2 = 0.9976$	$k_{eff} = 2.31 \cdot 10^{-2} \text{ L mol}^{-1} \text{ s}^{-1}$	$t_{1/2} = 33.2 \text{ min}$
M2:	$R^2 = 0.9971$	$k_{eff} = 2.12 \cdot 10^{-2} \text{ L mol}^{-1} \text{ s}^{-1}$	$t_{1/2} = 36.2 \text{ min}$
Avg.:		$2.22 \cdot 10^{-2} \text{ L mol}^{-1} \text{ s}^{-1}$	$34.7 \pm 1.5 \text{ min}$



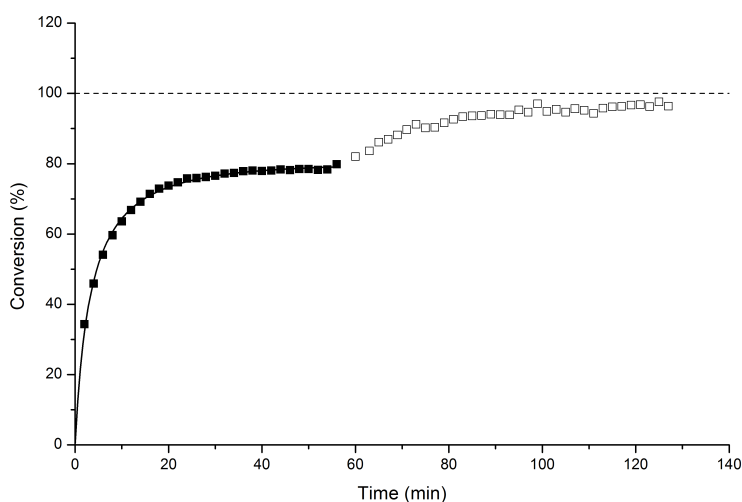
**Figure 8.11.** Time vs. conversion plot of **5a** with 1.2 equiv of different auxiliary base and **DMAP (3a)** with 4 mol% catalyst loading.

TOA ( <b>2c</b> ):	$R^2 = 0.9979$	$k_{eff} = 2.72 \cdot 10^{-2} \text{ L mol}^{-1} \text{ s}^{-1}$	$t_{1/2} = 30.5 \text{ min}$
DIPEA ( <b>2b</b> ):	$R^2 = 0.9965$	$k_{eff} = 2.79 \cdot 10^{-2} \text{ L mol}^{-1} \text{ s}^{-1}$	$t_{1/2} = 30.7 \text{ min}$
DABCO ( <b>2e</b> ):	$R^2 = 0.9903$	$k_{eff} = 2.90 \cdot 10^{-2} \text{ L mol}^{-1} \text{ s}^{-1}$	$t_{1/2} = 26.5 \text{ min}$
Proton Sponge ( <b>2d</b> ):	$R^2 = 0.9976$	$k_{eff} = 2.05 \cdot 10^{-2} \text{ L mol}^{-1} \text{ s}^{-1}$	$t_{1/2} = 37.5 \text{ min}$
NMM ( <b>2f</b> ):	$R^2 = 0.9592$	$k_{eff} = 6.01 \cdot 10^{-3} \text{ L mol}^{-1} \text{ s}^{-1}$	$t_{1/2} = 127.7 \text{ min}$
no base:	$R^2 = 0.8429$	$k_{eff} = 4.10 \cdot 10^{-3} \text{ L mol}^{-1} \text{ s}^{-1}$	$t_{1/2} = 187.3 \text{ min}$



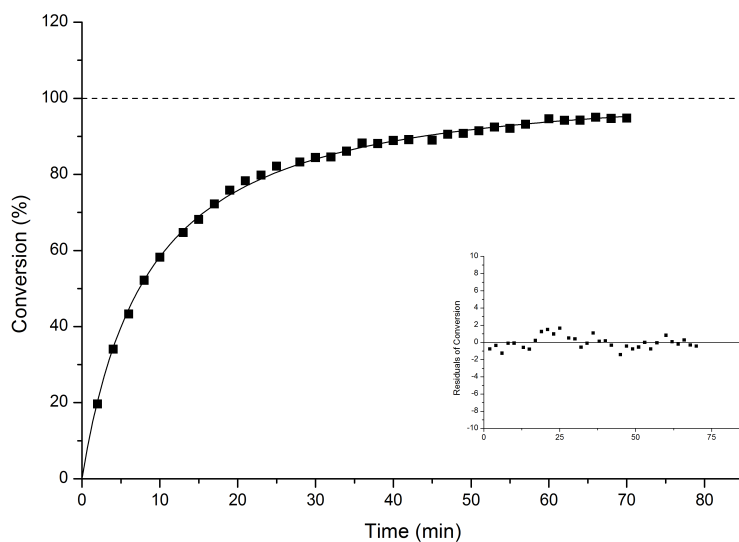
**Figure 8.12.** Time vs. conversion plot of **5b** and 1.2 equiv TBSCl (**1a**) with 1.2 equiv Et<sub>3</sub>N (**2a**) in DMF-d<sub>7</sub>.

M1:	$R^2 = 0.9723$	$k_{eff} = 1.15 \cdot 10^{-1} \text{ L mol}^{-1} \text{ s}^{-1}$	$t_{1/2} = 6.7 \text{ min}$
M2:	$R^2 = 0.9986$	$k_{eff} = 9.97 \cdot 10^{-2} \text{ L mol}^{-1} \text{ s}^{-1}$	$t_{1/2} = 7.7 \text{ min}$
M3:	$R^2 = 0.9991$	$k_{eff} = 9.59 \cdot 10^{-2} \text{ L mol}^{-1} \text{ s}^{-1}$	$t_{1/2} = 8.0 \text{ min}$
Avg.:		$1.04 \cdot 10^{-1} \text{ L mol}^{-1} \text{ s}^{-1}$	$7.4 \pm 0.6 \text{ min}$



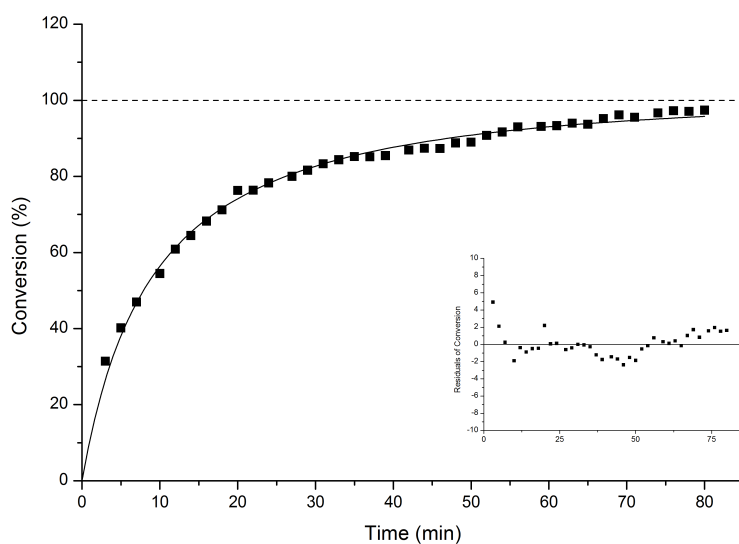
**Figure 8.13.** Time vs. conversion plot of **5b** with 1.2 equiv TBSCl (**1a**) in DMF-d<sub>7</sub> (Black) and the addition of 1.2 equiv of Et<sub>3</sub>N (**2a**) (Hollow).

M1:	$R^2 = 0.9958$	$k_{eff} = 2.64 \cdot 10^{-1} \text{ L mol}^{-1} \text{ s}^{-1}$	$t_{1/2} = 2.9 \text{ min}$
-----	----------------	--	-----------------------------



**Figure 8.14.** Time vs. conversion plot of **5b** and 1.2 equiv TBSCl (**1a**) with 1.2 equiv imidazole as auxiliary base (**2a**) in DMF- $d_7$ .

M1:	$R^2 = 0.9984$	$k_{eff} = 1.05 \cdot 10^{-1} \text{ L mol}^{-1} \text{ s}^{-1}$	$t_{1/2} = 7.3 \text{ min}$
M2:	$R^2 = 0.9955$	$k_{eff} = 9.87 \cdot 10^{-2} \text{ L mol}^{-1} \text{ s}^{-1}$	$t_{1/2} = 7.8 \text{ min}$
Avg.:		$1.02 \cdot 10^{-1} \text{ L mol}^{-1} \text{ s}^{-1}$	$7.6 \pm 0.2 \text{ min}$

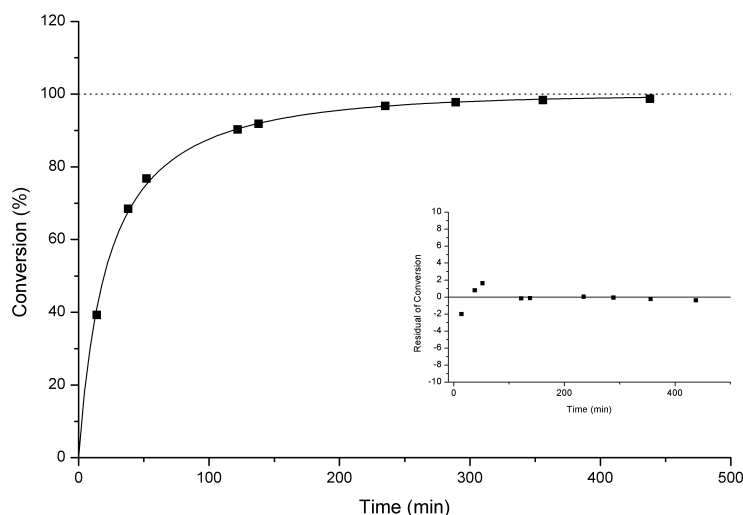


**Figure 8.15.** Time vs. conversion plot of **5b** and 1.2 equiv TBSCl (**1a**) with 1.8 equiv imidazole as auxiliary base (**2a**) in DMF- $d_7$ .

M1:	$R^2 = 0.9920$	$k_{eff} = 9.8 \cdot 10^{-2} \text{ L mol}^{-1} \text{ s}^{-1}$	$t_{1/2} = 7.8 \text{ min}$
M2:	$R^2 = 0.9810$	$k_{eff} = 1.1 \cdot 10^{-1} \text{ L mol}^{-1} \text{ s}^{-1}$	$t_{1/2} = 7.0 \text{ min}$
Avg.:		$1.04 \cdot 10^{-1} \text{ L mol}^{-1} \text{ s}^{-1}$	$7.4 \pm 0.4 \text{ min}$

### 8.2.2 Variation of Lewis Base Catalysts at 4 mol% Catalyst Loading

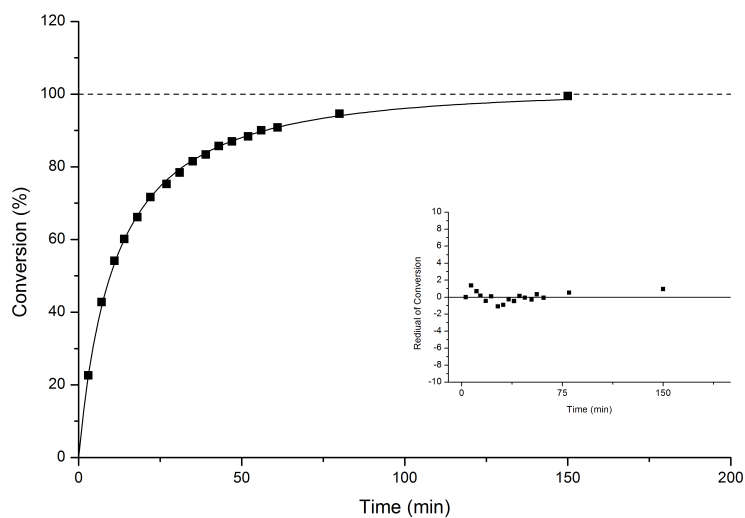
This data and plots are used for the results shown and discussed in Chapter 2.2.2. The first plots are with different catalyst **3b–3g** at catalyst loading of 4 %. The time-conversion plots of DMAP (**3a**) had already been shown in Figure 8.8. Later in this chapter variation of catalyst concentration will be shown for **3a**, **3b**, **3c**, **3e**, and **3g**.



**Figure 8.16.** Time vs. conversion plot of **5a** with 1.2 equiv  $\text{Et}_3\text{N}$  (**2a**) and PPY (**3b**) with 4 mol% catalyst loading.

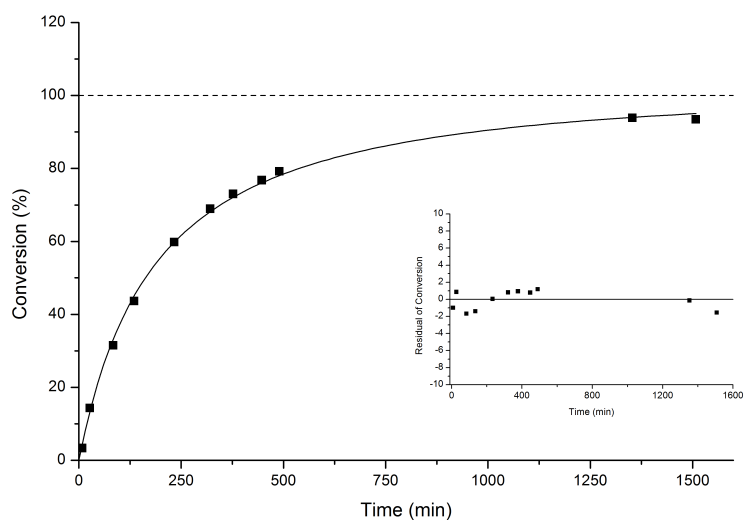
M1:	$R^2 = 0.9993$	$k_{\text{eff}} = 3.82 \cdot 10^{-2} \text{ L mol}^{-1} \text{ s}^{-1}$	$t_{1/2} = 20.1 \text{ min}$
M2:	$R^2 = 0.9973$	$k_{\text{eff}} = 3.98 \cdot 10^{-2} \text{ L mol}^{-1} \text{ s}^{-1}$	$t_{1/2} = 19.3 \text{ min}$
Avg.:		$3.90 \cdot 10^{-2} \text{ L mol}^{-1} \text{ s}^{-1}$	$19.7 \pm 0.4 \text{ min}$





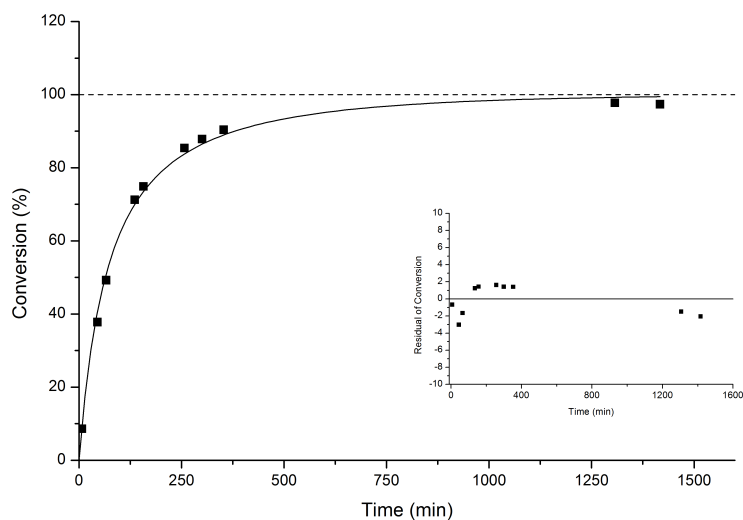
**Figure 8.17.** Time vs. conversion plot of **5a** with 1.2 equiv  $\text{Et}_3\text{N}$  (**2a**) and catalyst **3c** with 4 mol% catalyst loading.

M1:	$R^2 = 0.9970$	$k_{\text{eff}} = 8.93 \cdot 10^{-2} \text{ L mol}^{-1} \text{ s}^{-1}$	$t_{1/2} = 8.6 \text{ min}$
M2:	$R^2 = 0.9990$	$k_{\text{eff}} = 7.93 \cdot 10^{-2} \text{ L mol}^{-1} \text{ s}^{-1}$	$t_{1/2} = 9.7 \text{ min}$
M3:	$R^2 = 0.9972$	$k_{\text{eff}} = 8.62 \cdot 10^{-2} \text{ L mol}^{-1} \text{ s}^{-1}$	$t_{1/2} = 8.9 \text{ min}$
Avg.:		$8.49 \cdot 10^{-2} \text{ L mol}^{-1} \text{ s}^{-1}$	$9.0 \pm 0.5 \text{ min}$



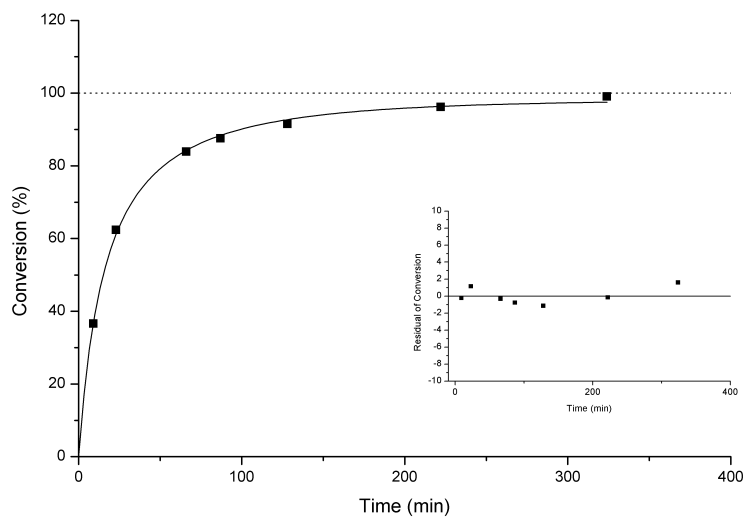
**Figure 8.18.** Time vs. conversion plot of **5a** with 1.2 equiv  $\text{Et}_3\text{N}$  (**2a**) and imidazole (**3d**) with 4 mol% catalyst loading.

M1:	$R^2 = 0.9985$	$k_{\text{eff}} = 4.75 \cdot 10^{-2} \text{ L mol}^{-1} \text{ s}^{-1}$	$t_{1/2} = 161.7 \text{ min}$
M2:	$R^2 = 0.9983$	$k_{\text{eff}} = 4.62 \cdot 10^{-2} \text{ L mol}^{-1} \text{ s}^{-1}$	$t_{1/2} = 166.2 \text{ min}$
Avg.:		$4.69 \cdot 10^{-2} \text{ L mol}^{-1} \text{ s}^{-1}$	$163.9 \pm 2.3 \text{ min}$



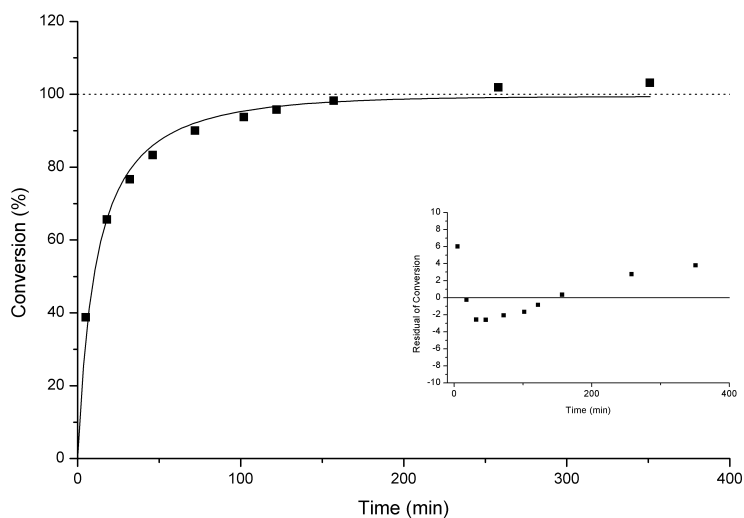
**Figure 8.19.** Time vs. conversion plot of **5a** with 1.2 equiv **Et<sub>3</sub>N** (**2a**) and *N*-methylimidazole (**3e**) with 4 mol% catalyst loading.

M1:	$R^2 = 0.9958$	$k_{eff} = 1.21 \cdot 10^{-2} \text{ L mol}^{-1} \text{ s}^{-1}$	$t_{1/2} = 63.6 \text{ min}$
M2:	$R^2 = 0.9929$	$k_{eff} = 1.20 \cdot 10^{-2} \text{ L mol}^{-1} \text{ s}^{-1}$	$t_{1/2} = 63.9 \text{ min}$
M3:	$R^2 = 0.9933$	$k_{eff} = 1.09 \cdot 10^{-2} \text{ L mol}^{-1} \text{ s}^{-1}$	$t_{1/2} = 70.7 \text{ min}$
Avg.:		$1.17 \cdot 10^{-2} \text{ L mol}^{-1} \text{ s}^{-1}$	$65.9 \pm 3.3 \text{ min}$



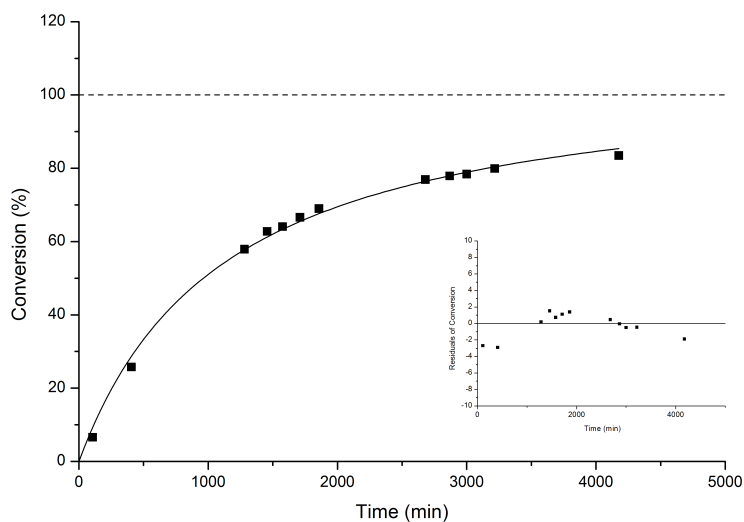
**Figure 8.20.** Time vs. conversion plot of **5a** with 1.2 equiv **Et<sub>3</sub>N** (**2a**) and catalyst **3f** with 4 mol% catalyst loading.

M1:	$R^2 = 0.9950$	$k_{eff} = 5.41 \cdot 10^{-2} \text{ L mol}^{-1} \text{ s}^{-1}$	$t_{1/2} = 14.2 \text{ min}$
M2:	$R^2 = 0.9976$	$k_{eff} = 5.32 \cdot 10^{-2} \text{ L mol}^{-1} \text{ s}^{-1}$	$t_{1/2} = 14.4 \text{ min}$
M3:	$R^2 = 0.9901$	$k_{eff} = 5.18 \cdot 10^{-2} \text{ L mol}^{-1} \text{ s}^{-1}$	$t_{1/2} = 14.8 \text{ min}$
Avg.:		$1.17 \cdot 10^{-2} \text{ L mol}^{-1} \text{ s}^{-1}$	$14.5 \pm 0.3 \text{ min}$



**Figure 8.21.** Time vs. conversion plot of **5a** with 1.2 equiv Et<sub>3</sub>N (**2a**) and catalyst **3g** with 4 mol% catalyst loading.

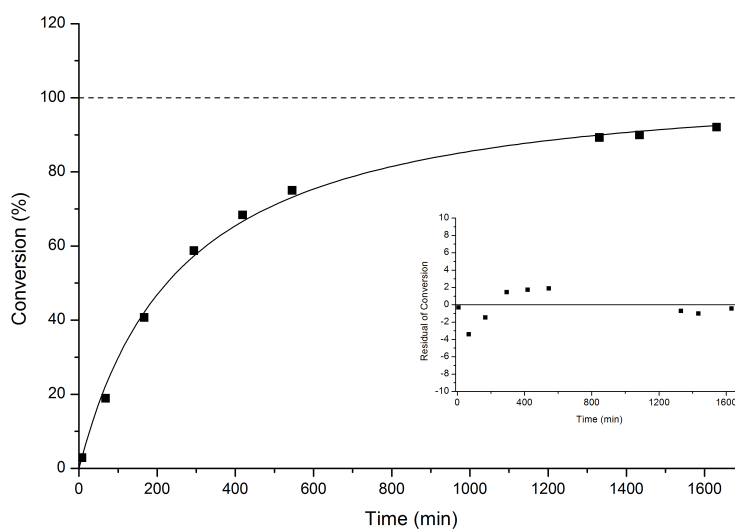
M1:	$R^2 = 0.9756$	$k_{eff} = 7.87 \cdot 10^{-2} \text{ L mol}^{-1} \text{ s}^{-1}$	$t_{1/2} = 9.8 \text{ min}$
M2:	$R^2 = 0.9597$	$k_{eff} = 8.91 \cdot 10^{-2} \text{ L mol}^{-1} \text{ s}^{-1}$	$t_{1/2} = 8.6 \text{ min}$
M3:	$R^2 = 0.9830$	$k_{eff} = 7.77 \cdot 10^{-2} \text{ L mol}^{-1} \text{ s}^{-1}$	$t_{1/2} = 9.9 \text{ min}$
Avg.:		$8.18 \cdot 10^{-2} \text{ L mol}^{-1} \text{ s}^{-1}$	$9.4 \pm 0.6 \text{ min}$



**Figure 8.22.** Time vs. conversion plot of **5a** with 1.2 equiv Et<sub>3</sub>N (**2a**), and DMF as catalyst with 4 mol% catalyst loading in CDCl<sub>3</sub>.

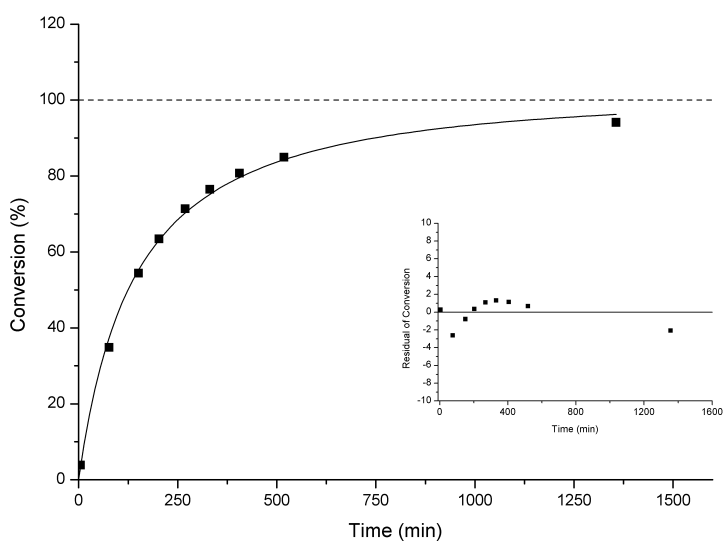
M1:	$R^2 = 0.9934$	$k_{eff} = 8.15 \cdot 10^{-4} \text{ L mol}^{-1} \text{ s}^{-1}$	$t_{1/2} = 942.8 \text{ min}$
M2:	$R^2 = 0.9997$	$k_{eff} = 7.94 \cdot 10^{-4} \text{ L mol}^{-1} \text{ s}^{-1}$	$t_{1/2} = 967.7 \text{ min}$
Avg.:		$8.04 \cdot 10^{-4} \text{ L mol}^{-1} \text{ s}^{-1}$	$955.1 \pm 12.4 \text{ min}$

## Variation of Catalyst Loadings for Different Catalyst



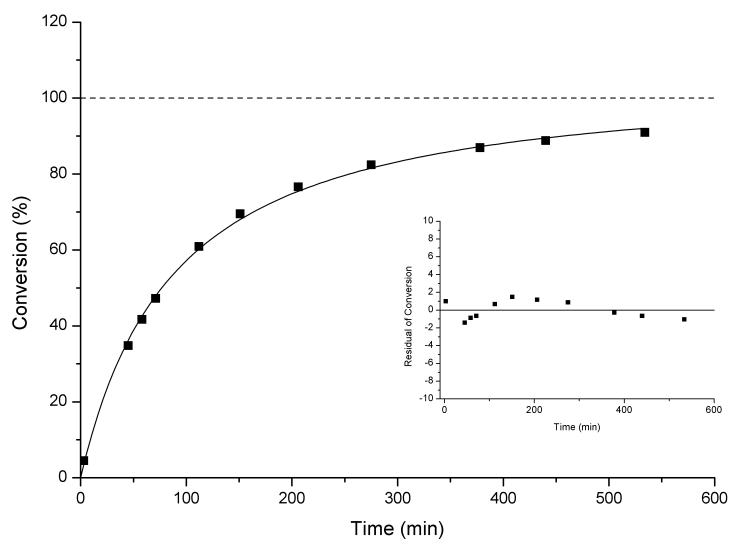
**Figure 8.23.** Time vs. conversion plot of **5a** with 1.2 equiv **Et<sub>3</sub>N (2a)** and **DMAP (3a)** with 0.5 mol% catalyst loading.

M1:	$R^2 = 0.9967$	$k_{eff} = 3.43 \cdot 10^{-3} \text{ L mol}^{-1} \text{ s}^{-1}$	$t_{1/2} = 223.9 \text{ min}$
M2:	$R^2 = 0.9974$	$k_{eff} = 3.47 \cdot 10^{-3} \text{ L mol}^{-1} \text{ s}^{-1}$	$t_{1/2} = 221.3 \text{ min}$
Avg.:		$8.49 \cdot 10^{-3} \text{ L mol}^{-1} \text{ s}^{-1}$	$222.6 \pm 1.3 \text{ min}$



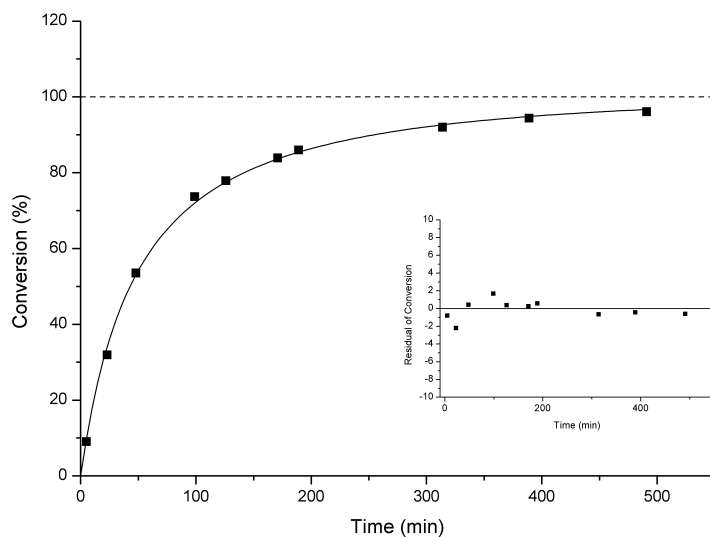
**Figure 8.24.** Time vs. conversion plot of **5a** with 1.2 equiv **Et<sub>3</sub>N (2a)** and **DMAP (3a)** with 1 mol% catalyst loading.

M1:	$R^2 = 0.9970$	$k_{eff} = 6.20 \cdot 10^{-3} \text{ L mol}^{-1} \text{ s}^{-1}$	$t_{1/2} = 123.9 \text{ min}$
M2:	$R^2 = 0.9965$	$k_{eff} = 6.20 \cdot 10^{-3} \text{ L mol}^{-1} \text{ s}^{-1}$	$t_{1/2} = 123.9 \text{ min}$
Avg.:		$6.20 \cdot 10^{-3} \text{ L mol}^{-1} \text{ s}^{-1}$	$123.9 \pm 0.0 \text{ min}$



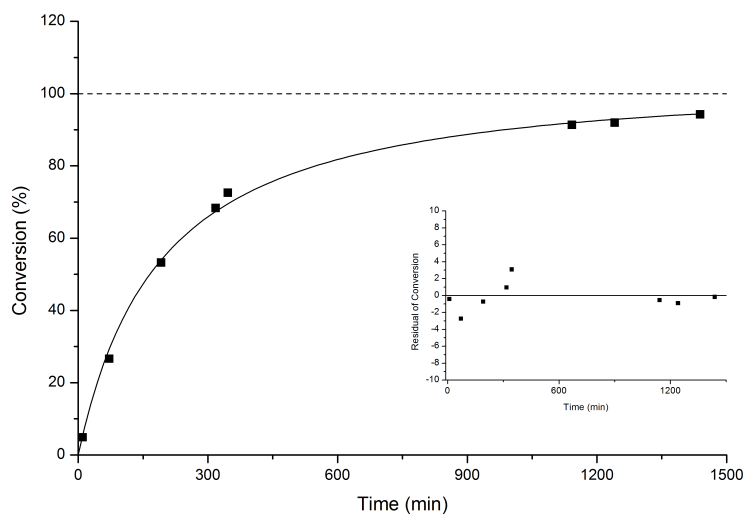
**Figure 8.25.** Time vs. conversion plot of **5a** with 1.2 equiv **Et<sub>3</sub>N (2a)** and **DMAP (3a)** with 2 mol% catalyst loading.

M1:	$R^2 = 0.9984$	$k_{eff} = 1.01 \cdot 10^{-2} \text{ L mol}^{-1} \text{ s}^{-1}$	$t_{1/2} = 76.4 \text{ min}$
M2:	$R^2 = 0.9988$	$k_{eff} = 9.67 \cdot 10^{-3} \text{ L mol}^{-1} \text{ s}^{-1}$	$t_{1/2} = 79.4 \text{ min}$
M3:	$R^2 = 0.9951$	$k_{eff} = 8.58 \cdot 10^{-3} \text{ L mol}^{-1} \text{ s}^{-1}$	$t_{1/2} = 89.5 \text{ min}$
Avg.:		$9.43 \cdot 10^{-3} \text{ L mol}^{-1} \text{ s}^{-1}$	$81.4 \pm 5.6 \text{ min}$



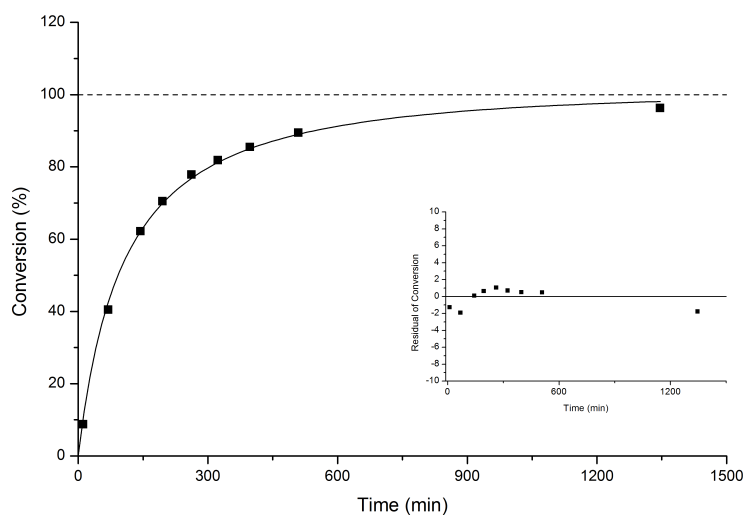
**Figure 8.26.** Time vs. conversion plot of **5a** with 1.2 equiv **Et<sub>3</sub>N (2a)** and **DMAP (3a)** with 3 mol% catalyst loading.

M1:	$R^2 = 0.9966$	$k_{eff} = 1.83 \cdot 10^{-2} \text{ L mol}^{-1} \text{ s}^{-1}$	$t_{1/2} = 42.0 \text{ min}$
M2:	$R^2 = 0.9986$	$k_{eff} = 1.80 \cdot 10^{-2} \text{ L mol}^{-1} \text{ s}^{-1}$	$t_{1/2} = 42.6 \text{ min}$
M3:	$R^2 = 0.9989$	$k_{eff} = 1.82 \cdot 10^{-2} \text{ L mol}^{-1} \text{ s}^{-1}$	$t_{1/2} = 42.2 \text{ min}$
Avg.:		$1.82 \cdot 10^{-2} \text{ L mol}^{-1} \text{ s}^{-1}$	$42.3 \pm 0.3 \text{ min}$



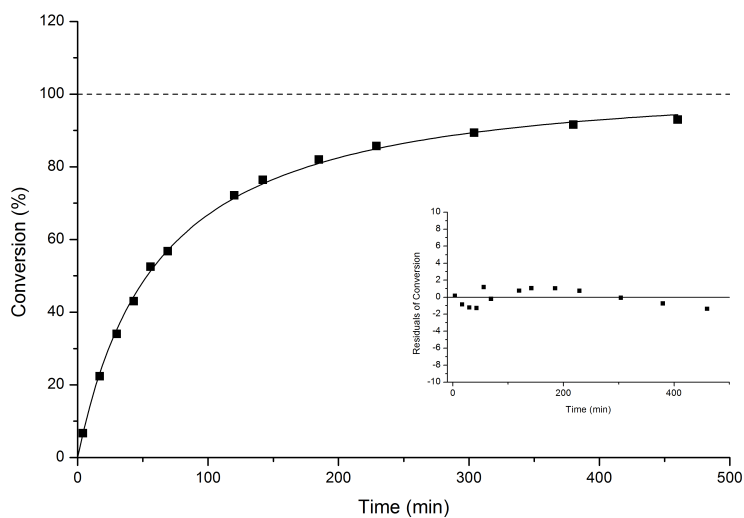
**Figure 8.27.** Time vs. conversion plot of **5a** with 1.2 equiv **Et<sub>3</sub>N (2a)** and **PPY (3b)** with 0.5 mol% catalyst loading.

M1:	$R^2 = 0.9969$	$k_{eff} = 4.65 \cdot 10^{-3} \text{ L mol}^{-1} \text{ s}^{-1}$	$t_{1/2} = 165.1 \text{ min}$
M2:	$R^2 = 0.9963$	$k_{eff} = 4.75 \cdot 10^{-3} \text{ L mol}^{-1} \text{ s}^{-1}$	$t_{1/2} = 161.7 \text{ min}$
Avg.:		$4.70 \cdot 10^{-3} \text{ L mol}^{-1} \text{ s}^{-1}$	$163.4 \pm 1.7 \text{ min}$



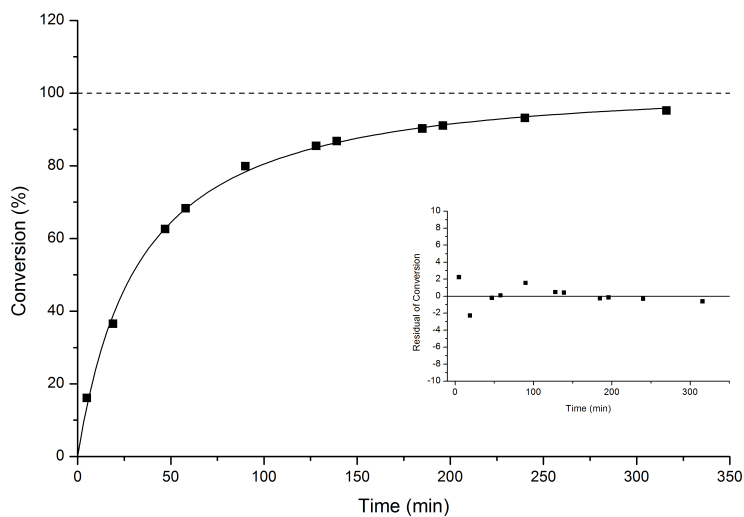
**Figure 8.28.** Time vs. conversion plot of **5a** with 1.2 equiv **Et<sub>3</sub>N (2a)** and **PPY (3b)** with 1 mol% catalyst loading.

M1:	$R^2 = 0.9967$	$k_{eff} = 8.52 \cdot 10^{-3} \text{ L mol}^{-1} \text{ s}^{-1}$	$t_{1/2} = 90.1 \text{ min}$
M2:	$R^2 = 0.9980$	$k_{eff} = 8.39 \cdot 10^{-3} \text{ L mol}^{-1} \text{ s}^{-1}$	$t_{1/2} = 91.5 \text{ min}$
Avg.:		$8.46 \cdot 10^{-3} \text{ L mol}^{-1} \text{ s}^{-1}$	$90.8 \pm 0.7 \text{ min}$



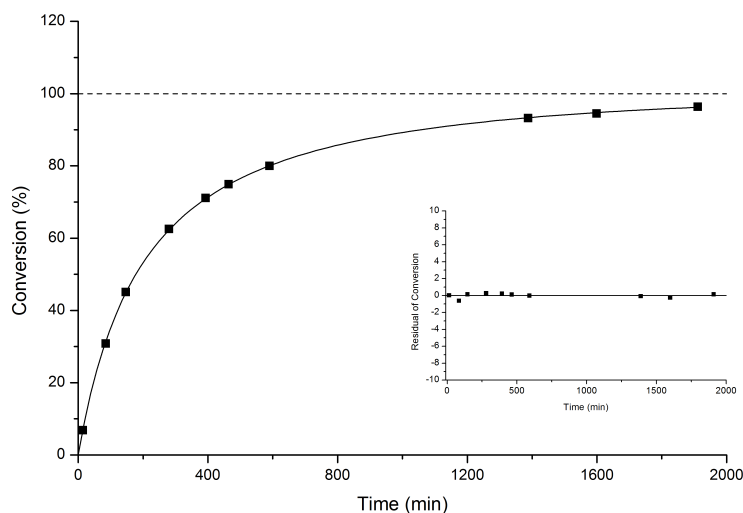
**Figure 8.29.** Time vs. conversion plot of **5a** with 1.2 equiv **Et<sub>3</sub>N (2a)** and **PPY (3b)** with 2 mol% catalyst loading.

M1:	$R^2 = 0.9975$	$k_{eff} = 1.45 \cdot 10^{-2} \text{ L mol}^{-1} \text{ s}^{-1}$	$t_{1/2} = 52.9 \text{ min}$
M2:	$R^2 = 0.9933$	$k_{eff} = 1.51 \cdot 10^{-2} \text{ L mol}^{-1} \text{ s}^{-1}$	$t_{1/2} = 50.8 \text{ min}$
M3:	$R^2 = 0.9988$	$k_{eff} = 1.45 \cdot 10^{-2} \text{ L mol}^{-1} \text{ s}^{-1}$	$t_{1/2} = 53.0 \text{ min}$
Avg.:		$8.46 \cdot 10^{-2} \text{ L mol}^{-1} \text{ s}^{-1}$	$52.2 \pm 1.0 \text{ min}$



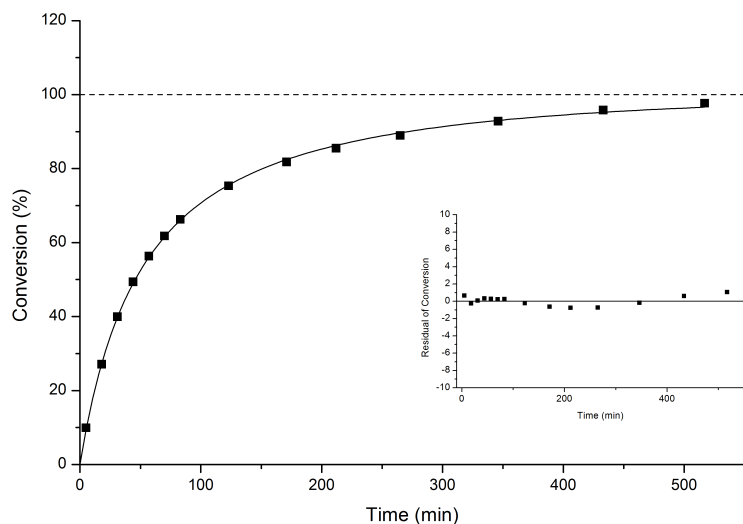
**Figure 8.30.** Time vs. conversion plot of **5a** with 1.2 equiv **Et<sub>3</sub>N (2a)** and **PPY (3b)** with 3 mol% catalyst loading.

M1:	$R^2 = 0.9977$	$k_{eff} = 2.67 \cdot 10^{-2} \text{ L mol}^{-1} \text{ s}^{-1}$	$t_{1/2} = 28.7 \text{ min}$
M2:	$R^2 = 0.9982$	$k_{eff} = 2.47 \cdot 10^{-2} \text{ L mol}^{-1} \text{ s}^{-1}$	$t_{1/2} = 31.1 \text{ min}$
M3:	$R^2 = 0.9978$	$k_{eff} = 2.43 \cdot 10^{-2} \text{ L mol}^{-1} \text{ s}^{-1}$	$t_{1/2} = 31.6 \text{ min}$
Avg.:		$2.45 \cdot 10^{-2} \text{ L mol}^{-1} \text{ s}^{-1}$	$31.3 \pm 1.2 \text{ min}$



**Figure 8.31.** Time vs. conversion plot of **5a** with 1.2 equiv  $\text{Et}_3\text{N}$  (**2a**) and catalyst **3c** with 0.25 mol% catalyst loading.

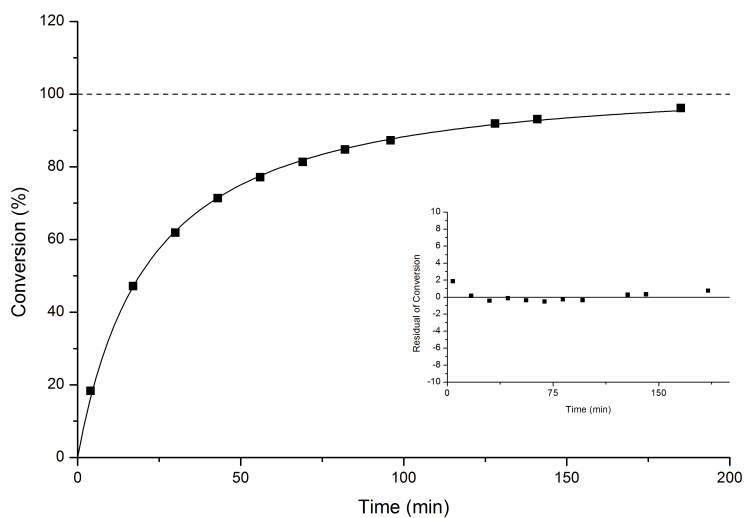
M1:	$R^2 = 0.9999$	$k_{\text{eff}} = 4.34 \cdot 10^{-3} \text{ L mol}^{-1} \text{ s}^{-1}$	$t_{1/2} = 176.9 \text{ min}$
M2:	$R^2 = 0.9998$	$k_{\text{eff}} = 3.96 \cdot 10^{-3} \text{ L mol}^{-1} \text{ s}^{-1}$	$t_{1/2} = 193.9 \text{ min}$
M3:	$R^2 = 0.9997$	$k_{\text{eff}} = 4.10 \cdot 10^{-3} \text{ L mol}^{-1} \text{ s}^{-1}$	$t_{1/2} = 187.3 \text{ min}$
Avg.:		$4.13 \cdot 10^{-3} \text{ L mol}^{-1} \text{ s}^{-1}$	$185.8 \pm 7.0 \text{ min}$



**Figure 8.32.** Time vs. conversion plot of **5a** with 1.2 equiv  $\text{Et}_3\text{N}$  (**2a**) and catalyst **3c** with 1 mol% catalyst loading.

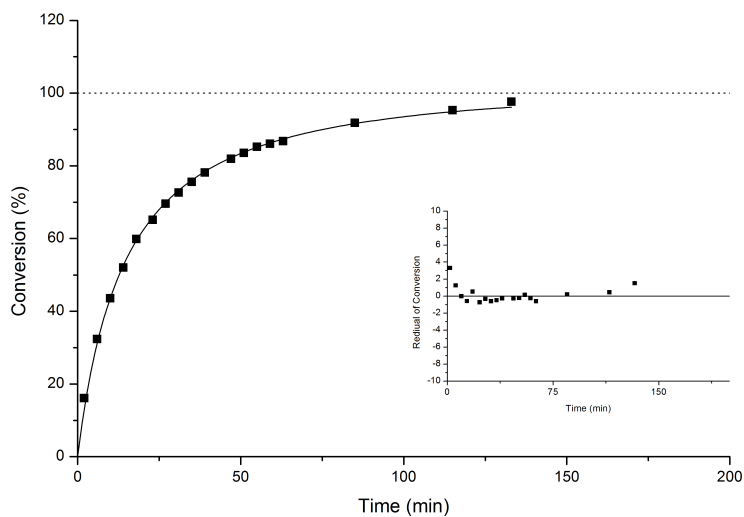
M1:	$R^2 = 0.9996$	$k_{\text{eff}} = 1.69 \cdot 10^{-2} \text{ L mol}^{-1} \text{ s}^{-1}$	$t_{1/2} = 45.4 \text{ min}$
M2:	$R^2 = 0.9990$	$k_{\text{eff}} = 1.82 \cdot 10^{-2} \text{ L mol}^{-1} \text{ s}^{-1}$	$t_{1/2} = 42.2 \text{ min}$
M3:	$R^2 = 0.9974$	$k_{\text{eff}} = 1.78 \cdot 10^{-2} \text{ L mol}^{-1} \text{ s}^{-1}$	$t_{1/2} = 43.2 \text{ min}$
Avg.:		$1.76 \cdot 10^{-2} \text{ L mol}^{-1} \text{ s}^{-1}$	$43.6 \pm 1.3 \text{ min}$





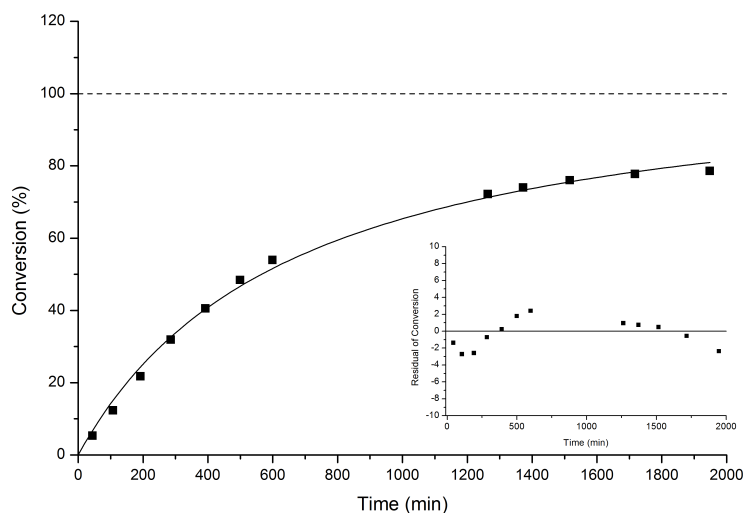
**Figure 8.33.** Time vs. conversion plot of **5a** with 1.2 equiv  $\text{Et}_3\text{N}$  (**2a**) and catalyst **3c** with 2 mol% catalyst loading.

M1:	$R^2 = 0.9984$	$k_{\text{eff}} = 4.22 \cdot 10^{-2} \text{ L mol}^{-1} \text{ s}^{-1}$	$t_{1/2} = 18.2 \text{ min}$
M2:	$R^2 = 0.9999$	$k_{\text{eff}} = 3.53 \cdot 10^{-2} \text{ L mol}^{-1} \text{ s}^{-1}$	$t_{1/2} = 21.8 \text{ min}$
M3:	$R^2 = 0.9990$	$k_{\text{eff}} = 4.06 \cdot 10^{-2} \text{ L mol}^{-1} \text{ s}^{-1}$	$t_{1/2} = 18.9 \text{ min}$
Avg.:		$3.94 \cdot 10^{-2} \text{ L mol}^{-1} \text{ s}^{-1}$	$19.5 \pm 1.5 \text{ min}$



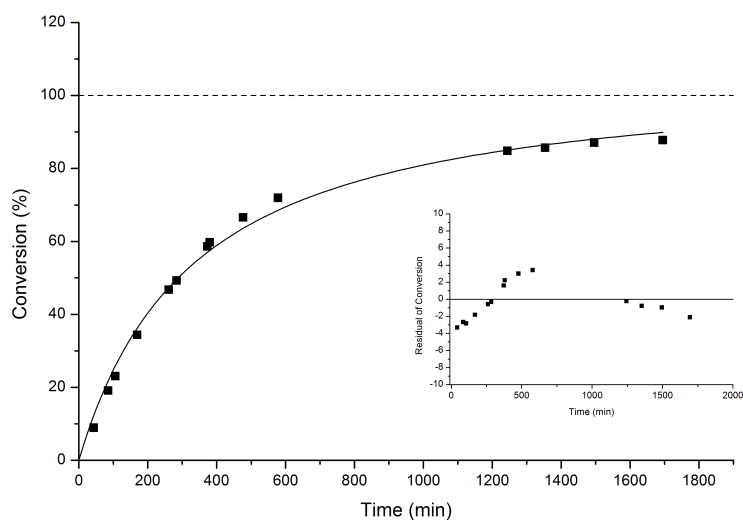
**Figure 8.34.** Time vs. conversion plot of **5a** with 1.2 equiv  $\text{Et}_3\text{N}$  (**2a**) and catalyst **3c** with 3 mol% catalyst loading.

M1:	$R^2 = 0.9965$	$k_{\text{eff}} = 5.39 \cdot 10^{-2} \text{ L mol}^{-1} \text{ s}^{-1}$	$t_{1/2} = 14.2 \text{ min}$
M2:	$R^2 = 0.9999$	$k_{\text{eff}} = 5.50 \cdot 10^{-2} \text{ L mol}^{-1} \text{ s}^{-1}$	$t_{1/2} = 14.0 \text{ min}$
M3:	$R^2 = 0.9978$	$k_{\text{eff}} = 6.05 \cdot 10^{-2} \text{ L mol}^{-1} \text{ s}^{-1}$	$t_{1/2} = 12.7 \text{ min}$
Avg.:		$5.64 \cdot 10^{-2} \text{ L mol}^{-1} \text{ s}^{-1}$	$13.6 \pm 0.7 \text{ min}$



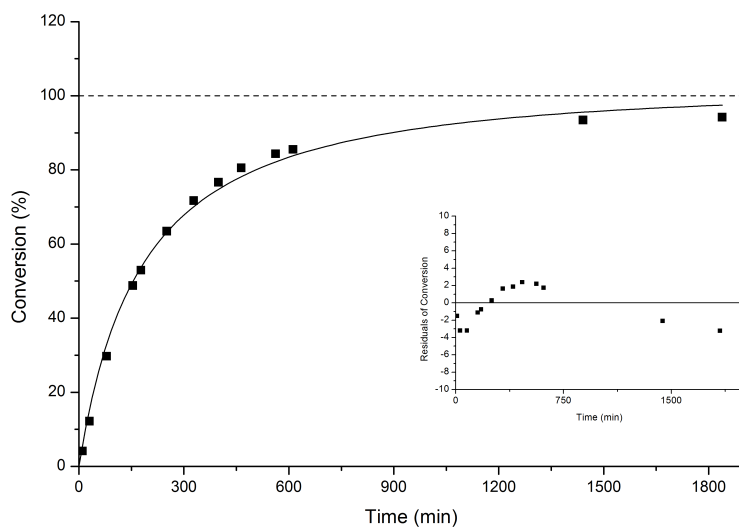
**Figure 8.35.** Time vs. conversion plot of **5a** with 1.2 equiv **Et<sub>3</sub>N (2a)** and *N*-methylimidazole (**3e**) with 0.5 mol% catalyst loading.

M1:	$R^2 = 0.9946$	$k_{eff} = 1.40 \cdot 10^{-3} \text{ L mol}^{-1} \text{ s}^{-1}$	$t_{1/2} = 548.5 \text{ min}$
M2:	$R^2 = 0.9954$	$k_{eff} = 1.35 \cdot 10^{-3} \text{ L mol}^{-1} \text{ s}^{-1}$	$t_{1/2} = 568.8 \text{ min}$
Avg.:		$1.38 \cdot 10^{-3} \text{ L mol}^{-1} \text{ s}^{-1}$	$558.5 \pm 10.2 \text{ min}$



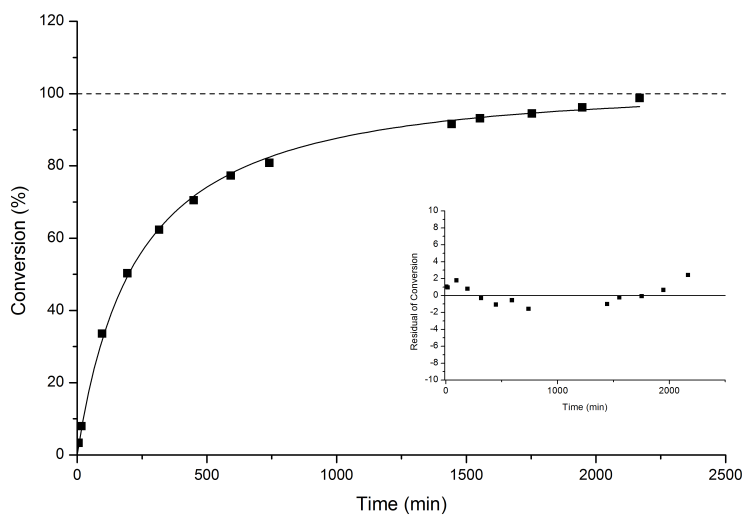
**Figure 8.36.** Time vs. conversion plot of **5a** with 1.2 equiv **Et<sub>3</sub>N (2a)** and *N*-methylimidazole (**3e**) with 1 mol% catalyst loading.

M1:	$R^2 = 0.9925$	$k_{eff} = 2.68 \cdot 10^{-3} \text{ L mol}^{-1} \text{ s}^{-1}$	$t_{1/2} = 286.5 \text{ min}$
M2:	$R^2 = 0.9923$	$k_{eff} = 2.73 \cdot 10^{-3} \text{ L mol}^{-1} \text{ s}^{-1}$	$t_{1/2} = 281.3 \text{ min}$
Avg.:		$2.71 \cdot 10^{-3} \text{ L mol}^{-1} \text{ s}^{-1}$	$283.9 \pm 2.6 \text{ min}$



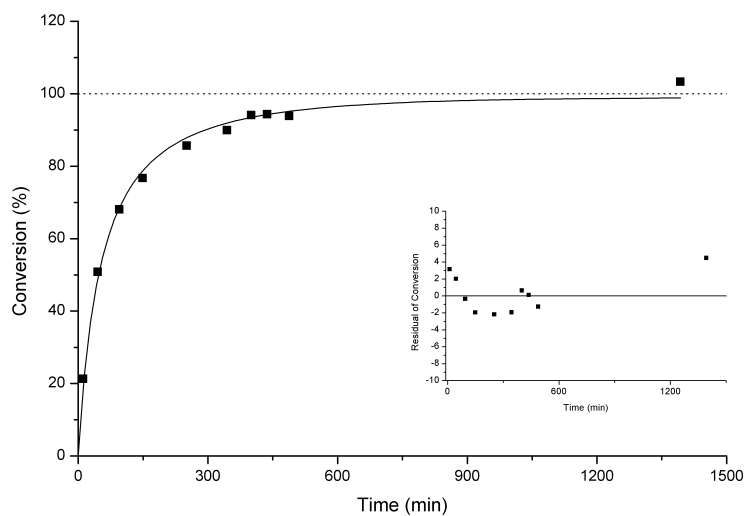
**Figure 8.37.** Time vs. conversion plot of **5a** with 1.2 equiv **Et<sub>3</sub>N** (**2a**) and *N*-methylimidazole (**3e**) with 2 mol% catalyst loading.

M1:	$R^2 = 0.9944$	$k_{eff} = 4.77 \cdot 10^{-3} \text{ L mol}^{-1} \text{ s}^{-1}$	$t_{1/2} = 161.0 \text{ min}$
M2:	$R^2 = 0.9941$	$k_{eff} = 4.95 \cdot 10^{-3} \text{ L mol}^{-1} \text{ s}^{-1}$	$t_{1/2} = 155.4 \text{ min}$
Avg.:		$4.86 \cdot 10^{-3} \text{ L mol}^{-1} \text{ s}^{-1}$	$158.2 \pm 2.8 \text{ min}$



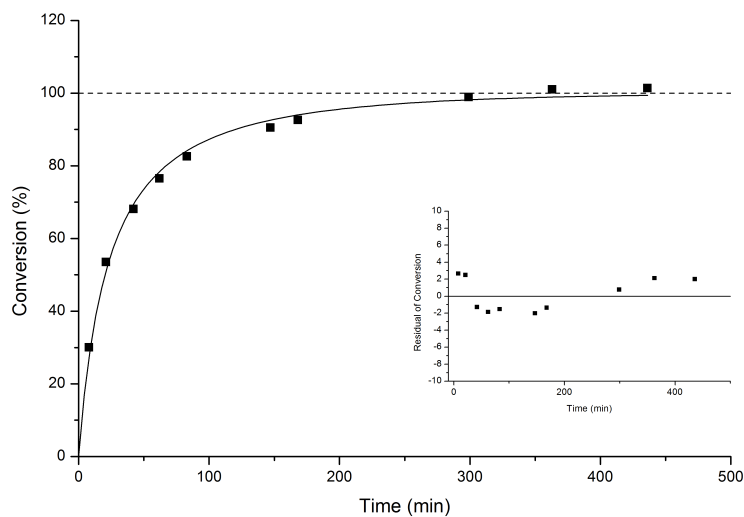
**Figure 8.38.** Time vs. conversion plot of **5a** with 1.2 equiv **Et<sub>3</sub>N** (**2a**) and catalyst **3g** with 0.25 mol% catalyst loading.

M1:	$R^2 = 0.9986$	$k_{eff} = 3.90 \cdot 10^{-3} \text{ L mol}^{-1} \text{ s}^{-1}$	$t_{1/2} = 196.9 \text{ min}$
M2:	$R^2 = 0.9992$	$k_{eff} = 3.69 \cdot 10^{-3} \text{ L mol}^{-1} \text{ s}^{-1}$	$t_{1/2} = 208.1 \text{ min}$
M3:	$R^2 = 0.9980$	$k_{eff} = 3.85 \cdot 10^{-3} \text{ L mol}^{-1} \text{ s}^{-1}$	$t_{1/2} = 199.5 \text{ min}$
Avg.:		$3.81 \cdot 10^{-3} \text{ L mol}^{-1} \text{ s}^{-1}$	$201.4 \pm 4.8 \text{ min}$



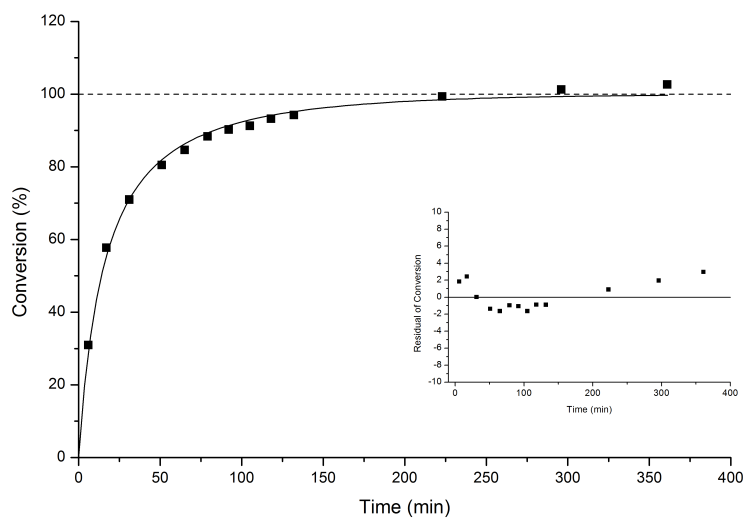
**Figure 8.39.** Time vs. conversion plot of **5a** with 1.2 equiv Et<sub>3</sub>N (**2a**) and catalyst **3g** with 1 mol% catalyst loading.

M1:	$R^2 = 0.9904$	$k_{eff} = 1.67 \cdot 10^{-2} \text{ L mol}^{-1} \text{ s}^{-1}$	$t_{1/2} = 46.0 \text{ min}$
M2:	$R^2 = 0.9937$	$k_{eff} = 1.68 \cdot 10^{-2} \text{ L mol}^{-1} \text{ s}^{-1}$	$t_{1/2} = 45.8 \text{ min}$
M3:	$R^2 = 0.9924$	$k_{eff} = 1.69 \cdot 10^{-2} \text{ L mol}^{-1} \text{ s}^{-1}$	$t_{1/2} = 45.4 \text{ min}$
Avg.:		$1.68 \cdot 10^{-2} \text{ L mol}^{-1} \text{ s}^{-1}$	$45.7 \pm 0.2 \text{ min}$



**Figure 8.40.** Time vs. conversion plot of **5a** with 1.2 equiv Et<sub>3</sub>N (**2a**) and catalyst **3g** with 2 mol% catalyst loading.

M1:	$R^2 = 0.9896$	$k_{eff} = 4.13 \cdot 10^{-2} \text{ L mol}^{-1} \text{ s}^{-1}$	$t_{1/2} = 18.6 \text{ min}$
M2:	$R^2 = 0.9937$	$k_{eff} = 3.81 \cdot 10^{-2} \text{ L mol}^{-1} \text{ s}^{-1}$	$t_{1/2} = 20.1 \text{ min}$
M3:	$R^2 = 0.9894$	$k_{eff} = 3.79 \cdot 10^{-2} \text{ L mol}^{-1} \text{ s}^{-1}$	$t_{1/2} = 20.3 \text{ min}$
Avg.:		$3.91 \cdot 10^{-2} \text{ L mol}^{-1} \text{ s}^{-1}$	$19.6 \pm 0.8 \text{ min}$

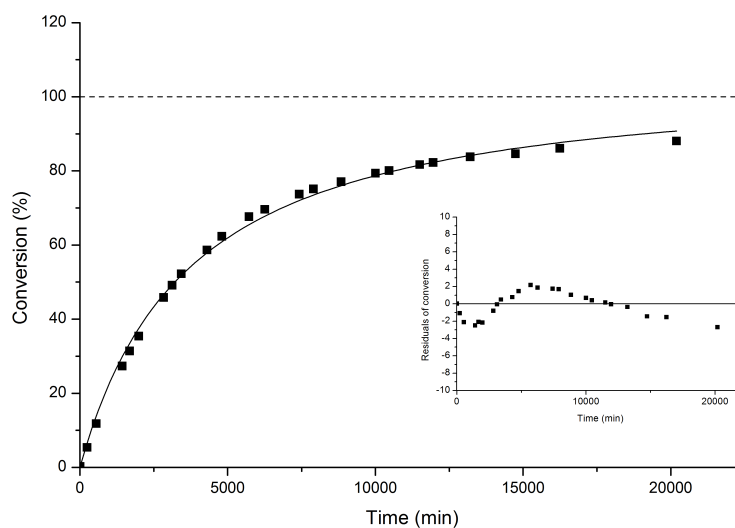


**Figure 8.41.** Time vs. conversion plot of **5a** with 1.2 equiv  $\text{Et}_3\text{N}$  (**2a**) and catalyst **3g** with 3 mol% catalyst loading.

M1:	$R^2 = 0.9925$	$k_{\text{eff}} = 5.52 \cdot 10^{-2} \text{ L mol}^{-1} \text{ s}^{-1}$	$t_{1/2} = 13.9 \text{ min}$
M2:	$R^2 = 0.9810$	$k_{\text{eff}} = 5.58 \cdot 10^{-2} \text{ L mol}^{-1} \text{ s}^{-1}$	$t_{1/2} = 13.8 \text{ min}$
M3:	$R^2 = 0.9756$	$k_{\text{eff}} = 6.16 \cdot 10^{-2} \text{ L mol}^{-1} \text{ s}^{-1}$	$t_{1/2} = 12.5 \text{ min}$
Avg.:		$3.91 \cdot 10^{-2} \text{ L mol}^{-1} \text{ s}^{-1}$	$13.4 \pm 0.6 \text{ min}$

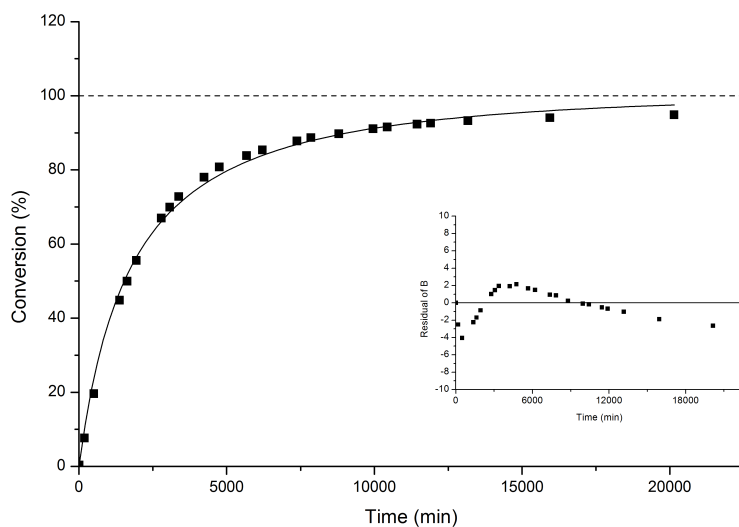
## 8.2.3 Variation of Catalysts and Catalyst Loadings for a Secondary Alcohol

This data and plots are used for the results shown and discussed in Chapter 2.2.2. The first plots are with different catalyst **3a**, **3b**, **3c**, **3e**, and **3g** at catalyst loadings of 4 mol%, 10 mol%, 20 mol%, and 30 mol%.



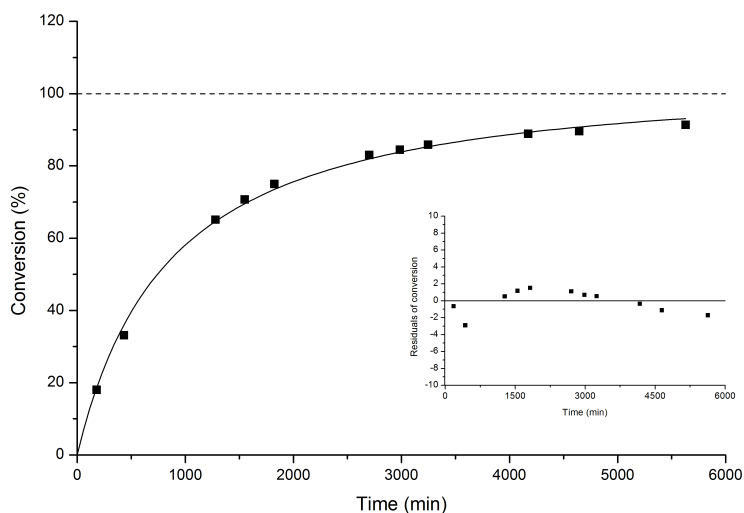
**Figure 8.42.** Time vs. conversion plot of **5b** with 1.2 equiv  $\text{Et}_3\text{N}$  (**2a**) and DMAP (**3a**) with 4 mol% catalyst loading.

M1:	$R^2 = 0.9968$	$k_{\text{eff}} = 2.40 \cdot 10^{-4} \text{ L mol}^{-1} \text{ s}^{-1}$	$t_{1/2} = 3199.1 \text{ min}$
M2:	$R^2 = 0.9943$	$k_{\text{eff}} = 2.45 \cdot 10^{-4} \text{ L mol}^{-1} \text{ s}^{-1}$	$t_{1/2} = 3132.8 \text{ min}$
Avg.:		$2.43 \cdot 10^{-4} \text{ L mol}^{-1} \text{ s}^{-1}$	$3165.6 \pm 33.1 \text{ min}$



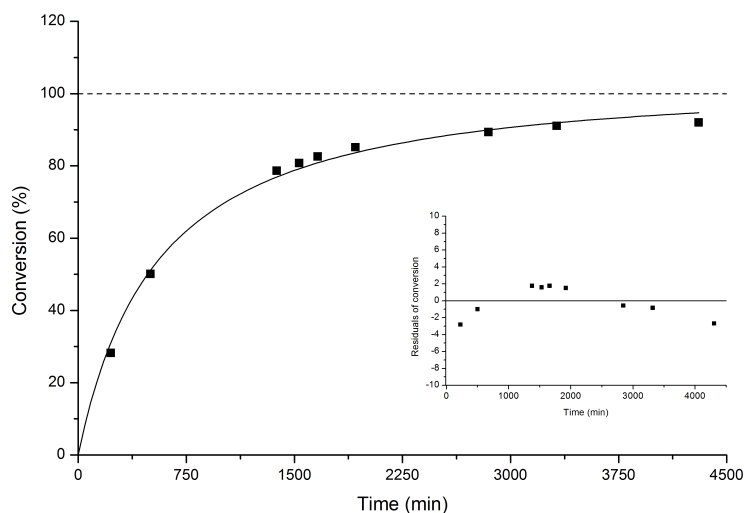
**Figure 8.43.** Time vs. conversion plot of **5b** with 1.2 equiv Et<sub>3</sub>N (**2a**) and DMAP (**3a**) with 10 mol% catalyst loading.

M1:	$R^2 = 0.9961$	$k_{eff} = 5.03 \cdot 10^{-4} \text{ L mol}^{-1} \text{ s}^{-1}$	$t_{1/2} = 1530.2 \text{ min}$
M2:	$R^2 = 0.9966$	$k_{eff} = 5.08 \cdot 10^{-4} \text{ L mol}^{-1} \text{ s}^{-1}$	$t_{1/2} = 1512.0 \text{ min}$
M3:	$R^2 = 0.9968$	$k_{eff} = 4.94 \cdot 10^{-4} \text{ L mol}^{-1} \text{ s}^{-1}$	$t_{1/2} = 1553.8 \text{ min}$
Avg.:		$5.02 \cdot 10^{-4} \text{ L mol}^{-1} \text{ s}^{-1}$	$1530.2 \pm 17.5 \text{ min}$



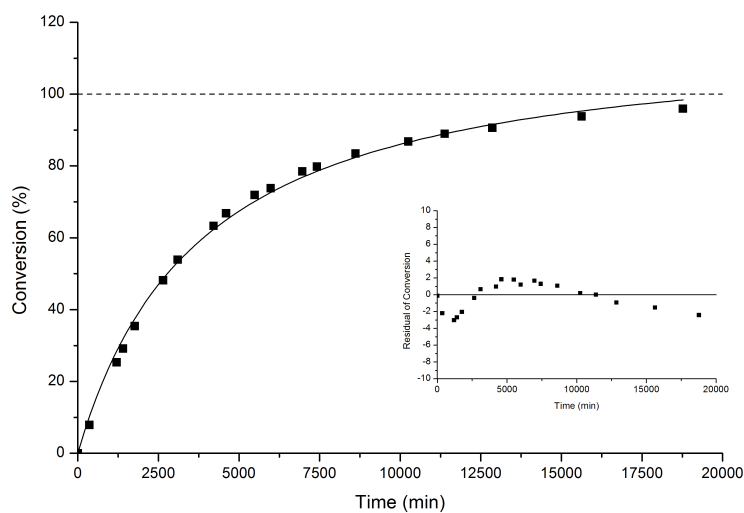
**Figure 8.44.** Time vs. conversion plot of **5b** with 1.2 equiv Et<sub>3</sub>N (**2a**) and DMAP (**3a**) with 20 mol% catalyst loading.

M1:	$R^2 = 0.9964$	$k_{eff} = 1.04 \cdot 10^{-3} \text{ L mol}^{-1} \text{ s}^{-1}$	$t_{1/2} = 738.4 \text{ min}$
M2:	$R^2 = 0.9975$	$k_{eff} = 1.06 \cdot 10^{-3} \text{ L mol}^{-1} \text{ s}^{-1}$	$t_{1/2} = 724.4 \text{ min}$
M3:	$R^2 = 0.9972$	$k_{eff} = 1.07 \cdot 10^{-3} \text{ L mol}^{-1} \text{ s}^{-1}$	$t_{1/2} = 717.4 \text{ min}$
Avg.:		$1.06 \cdot 10^{-3} \text{ L mol}^{-1} \text{ s}^{-1}$	$726.7 \pm 8.6 \text{ min}$



**Figure 8.45.** Time vs. conversion plot of **5b** with 1.2 equiv  $\text{Et}_3\text{N}$  (**2a**) and DMAP (**3a**) with 30 mol% catalyst loading.

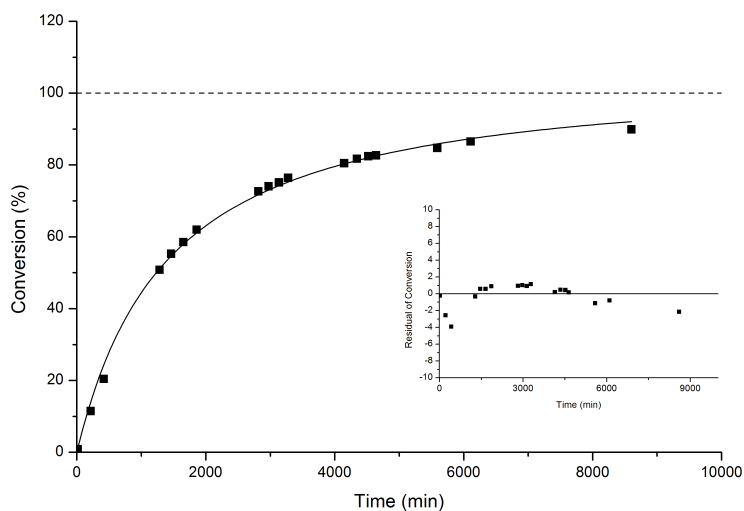
M1:	$R^2 = 0.9915$	$k_{\text{eff}} = 1.60 \cdot 10^{-3} \text{ L mol}^{-1} \text{ s}^{-1}$	$t_{1/2} = 479.9 \text{ min}$
M2:	$R^2 = 0.9940$	$k_{\text{eff}} = 1.66 \cdot 10^{-3} \text{ L mol}^{-1} \text{ s}^{-1}$	$t_{1/2} = 462.6 \text{ min}$
M3:	$R^2 = 0.9939$	$k_{\text{eff}} = 1.69 \cdot 10^{-3} \text{ L mol}^{-1} \text{ s}^{-1}$	$t_{1/2} = 454.4 \text{ min}$
Avg.:		$1.63 \cdot 10^{-3} \text{ L mol}^{-1} \text{ s}^{-1}$	$471.1 \pm 10.7 \text{ min}$



**Figure 8.46.** Time vs. conversion plot of **5b** with 1.2 equiv  $\text{Et}_3\text{N}$  (**2a**) and PPY (**3b**) with 4 mol% catalyst loading.

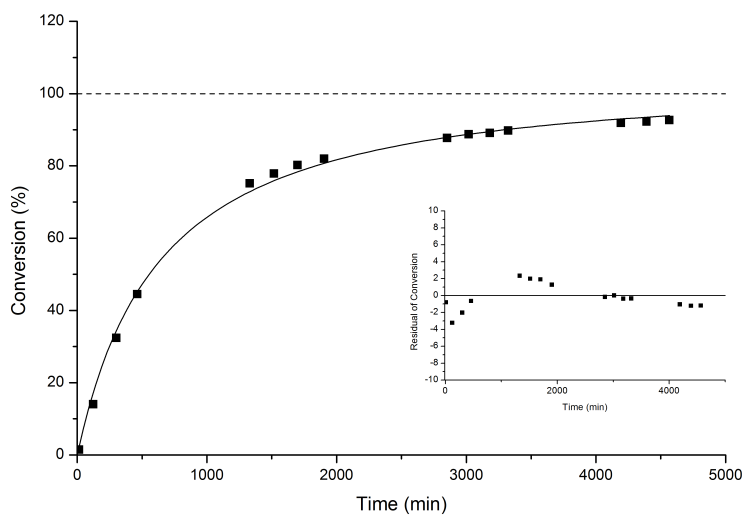
M1:	$R^2 = 0.9959$	$k_{\text{eff}} = 2.50 \cdot 10^{-4} \text{ L mol}^{-1} \text{ s}^{-1}$	$t_{1/2} = 3070.9 \text{ min}$
M2:	$R^2 = 0.9967$	$k_{\text{eff}} = 2.34 \cdot 10^{-4} \text{ L mol}^{-1} \text{ s}^{-1}$	$t_{1/2} = 3278.7 \text{ min}$
M3:	$R^2 = 0.9962$	$k_{\text{eff}} = 2.40 \cdot 10^{-4} \text{ L mol}^{-1} \text{ s}^{-1}$	$t_{1/2} = 3203.3 \text{ min}$
Avg.:		$2.41 \cdot 10^{-4} \text{ L mol}^{-1} \text{ s}^{-1}$	$3182.0 \pm 85.7 \text{ min}$





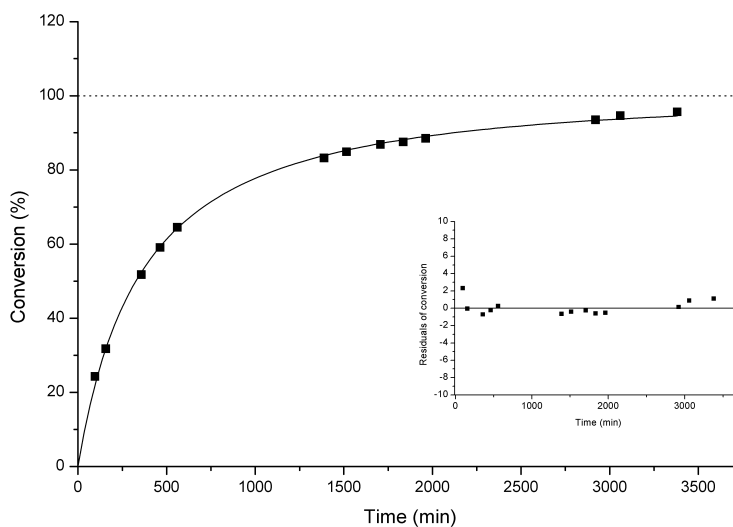
**Figure 8.47.** Time vs. conversion plot of **5b** with 1.2 equiv Et<sub>3</sub>N (**2a**) and PPY (**3b**) with 10 mol% catalyst loading.

M1:	$R^2 = 0.9972$	$k_{eff} = 6.23 \cdot 10^{-4} \text{ L mol}^{-1} \text{ s}^{-1}$	$t_{1/2} = 1232.4 \text{ min}$
M2:	$R^2 = 0.9972$	$k_{eff} = 6.49 \cdot 10^{-4} \text{ L mol}^{-1} \text{ s}^{-1}$	$t_{1/2} = 1183.3 \text{ min}$
M3:	$R^2 = 0.9970$	$k_{eff} = 6.26 \cdot 10^{-4} \text{ L mol}^{-1} \text{ s}^{-1}$	$t_{1/2} = 1227.2 \text{ min}$
Avg.:		$6.33 \cdot 10^{-4} \text{ L mol}^{-1} \text{ s}^{-1}$	$1213.9 \pm 22.0 \text{ min}$



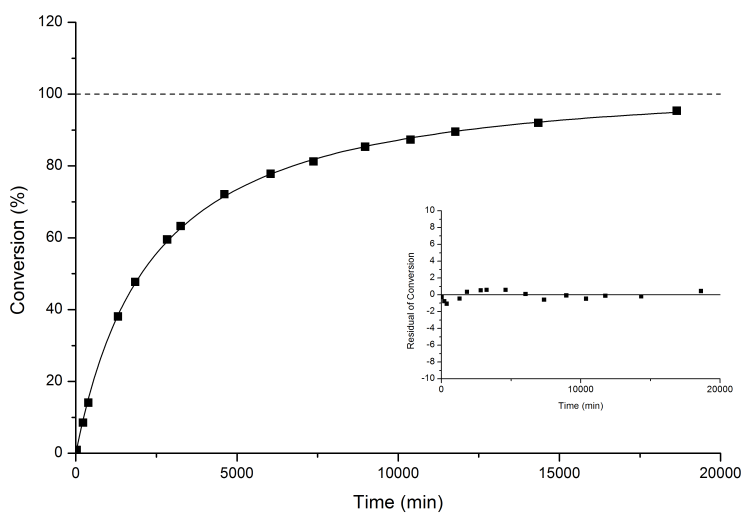
**Figure 8.48.** Time vs. conversion plot of **5b** with 1.2 equiv Et<sub>3</sub>N (**2a**) and PPY (**3b**) with 20 mol% catalyst loading.

M1:	$R^2 = 0.9970$	$k_{eff} = 1.41 \cdot 10^{-3} \text{ L mol}^{-1} \text{ s}^{-1}$	$t_{1/2} = 544.6 \text{ min}$
M2:	$R^2 = 0.9972$	$k_{eff} = 1.46 \cdot 10^{-3} \text{ L mol}^{-1} \text{ s}^{-1}$	$t_{1/2} = 526.0 \text{ min}$
M3:	$R^2 = 0.9972$	$k_{eff} = 1.39 \cdot 10^{-3} \text{ L mol}^{-1} \text{ s}^{-1}$	$t_{1/2} = 552.4 \text{ min}$
Avg.:		$1.42 \cdot 10^{-3} \text{ L mol}^{-1} \text{ s}^{-1}$	$540.8 \pm 11.1 \text{ min}$



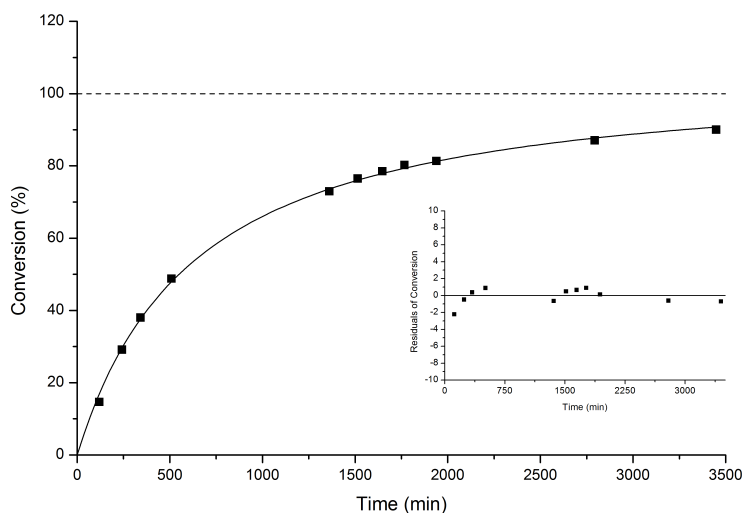
**Figure 8.49.** Time vs. conversion plot of **5b** with 1.2 equiv Et<sub>3</sub>N (**2a**) and PPY (**3b**) with 30 mol% catalyst loading.

M1:	$R^2 = 0.9986$	$k_{eff} = 2.48 \cdot 10^{-3} \text{ L mol}^{-1} \text{ s}^{-1}$	$t_{1/2} = 309.6 \text{ min}$
M2:	$R^2 = 0.9967$	$k_{eff} = 1.86 \cdot 10^{-3} \text{ L mol}^{-1} \text{ s}^{-1}$	$t_{1/2} = 412.8 \text{ min}$
M3:	$R^2 = 0.9986$	$k_{eff} = 2.44 \cdot 10^{-3} \text{ L mol}^{-1} \text{ s}^{-1}$	$t_{1/2} = 314.7 \text{ min}$
Avg.:		$1.42 \cdot 10^{-3} \text{ L mol}^{-1} \text{ s}^{-1}$	$339.8 \pm 47.5 \text{ min}$



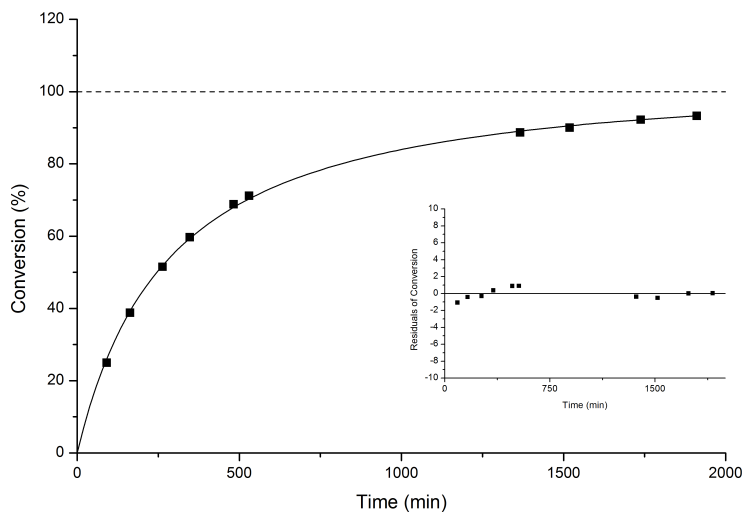
**Figure 8.50.** Time vs. conversion plot of **5b** with 1.2 equiv Et<sub>3</sub>N (**2a**) and catalyst **3c** with 4 mol% catalyst loading.

M1:	$R^2 = 0.9998$	$k_{eff} = 3.76 \cdot 10^{-4} \text{ L mol}^{-1} \text{ s}^{-1}$	$t_{1/2} = 2040.7 \text{ min}$
M2:	$R^2 = 0.9996$	$k_{eff} = 3.77 \cdot 10^{-4} \text{ L mol}^{-1} \text{ s}^{-1}$	$t_{1/2} = 2038.8 \text{ min}$
M3:	$R^2 = 0.9997$	$k_{eff} = 3.79 \cdot 10^{-4} \text{ L mol}^{-1} \text{ s}^{-1}$	$t_{1/2} = 2023.9 \text{ min}$
Avg.:		$3.77 \cdot 10^{-4} \text{ L mol}^{-1} \text{ s}^{-1}$	$1457.8 \pm 35.5 \text{ min}$



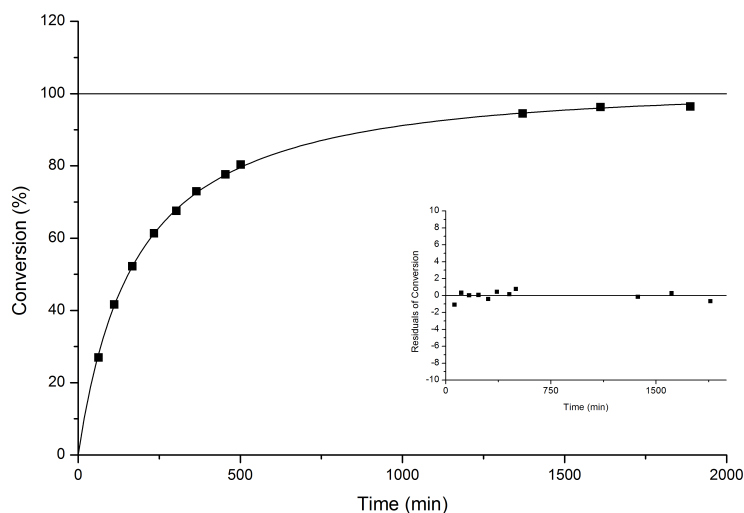
**Figure 8.51.** Time vs. conversion plot of **5b** with 1.2 equiv  $\text{Et}_3\text{N}$  (**2a**) and catalyst **3c** with 10 mol% catalyst loading.

M1:	$R^2 = 0.9996$	$k_{\text{eff}} = 1.51 \cdot 10^{-3} \text{ L mol}^{-1} \text{ s}^{-1}$	$t_{1/2} = 508.5 \text{ min}$
M2:	$R^2 = 0.9990$	$k_{\text{eff}} = 1.46 \cdot 10^{-3} \text{ L mol}^{-1} \text{ s}^{-1}$	$t_{1/2} = 526.0 \text{ min}$
M3:	$R^2 = 0.9985$	$k_{\text{eff}} = 1.40 \cdot 10^{-3} \text{ L mol}^{-1} \text{ s}^{-1}$	$t_{1/2} = 548.5 \text{ min}$
M4:	$R^2 = 0.9991$	$k_{\text{eff}} = 1.47 \cdot 10^{-3} \text{ L mol}^{-1} \text{ s}^{-1}$	$t_{1/2} = 522.4 \text{ min}$
Avg.:		$1.46 \cdot 10^{-3} \text{ L mol}^{-1} \text{ s}^{-1}$	$526.0 \pm 14.3 \text{ min}$



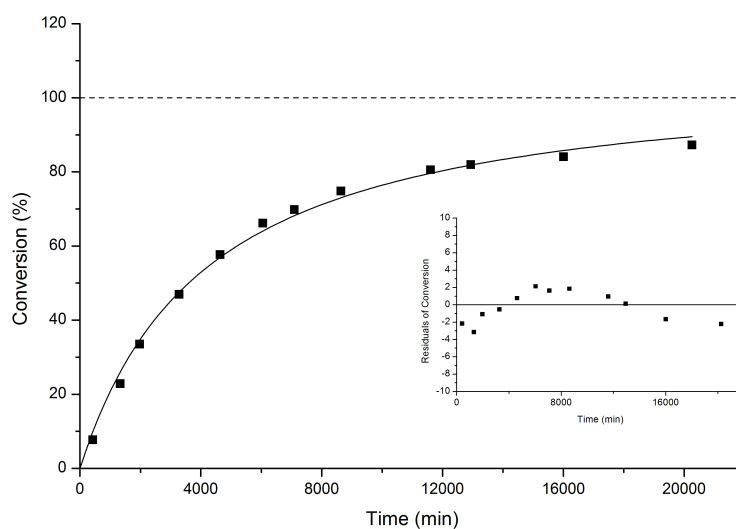
**Figure 8.52.** Time vs. conversion plot of **5b** with 1.2 equiv  $\text{Et}_3\text{N}$  (**2a**) and catalyst **3c** with 20 mol% catalyst loading.

M1:	$R^2 = 0.9978$	$k_{\text{eff}} = 2.51 \cdot 10^{-3} \text{ L mol}^{-1} \text{ s}^{-1}$	$t_{1/2} = 305.9 \text{ min}$
M2:	$R^2 = 0.9993$	$k_{\text{eff}} = 3.04 \cdot 10^{-3} \text{ L mol}^{-1} \text{ s}^{-1}$	$t_{1/2} = 252.6 \text{ min}$
M3:	$R^2 = 0.9992$	$k_{\text{eff}} = 3.14 \cdot 10^{-3} \text{ L mol}^{-1} \text{ s}^{-1}$	$t_{1/2} = 244.6 \text{ min}$
M4:	$R^2 = 0.9988$	$k_{\text{eff}} = 3.06 \cdot 10^{-3} \text{ L mol}^{-1} \text{ s}^{-1}$	$t_{1/2} = 250.9 \text{ min}$
Avg.:		$2.94 \cdot 10^{-3} \text{ L mol}^{-1} \text{ s}^{-1}$	$261.4.0 \pm 24.7 \text{ min}$



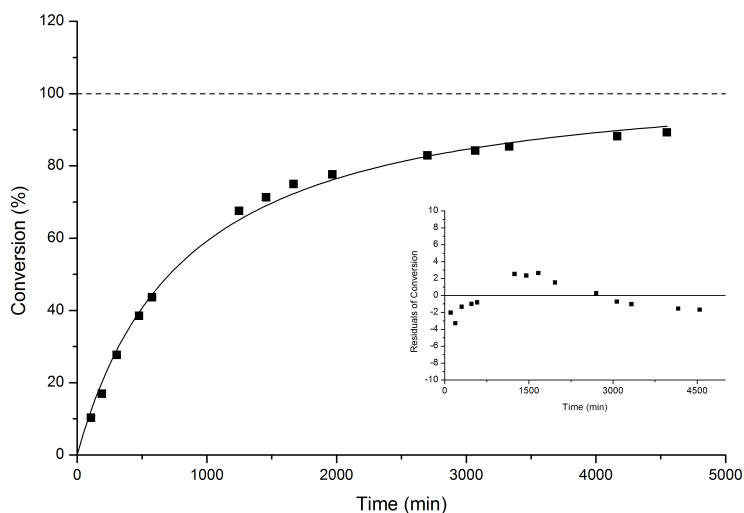
**Figure 8.53.** Time vs. conversion plot of **5b** with 1.2 equiv  $\text{Et}_3\text{N}$  (**2a**) and catalyst **3c** with 30 mol% catalyst loading.

M1:	$R^2 = 0.9980$	$k_{\text{eff}} = 4.32 \cdot 10^{-3} \text{ L mol}^{-1} \text{ s}^{-1}$	$t_{1/2} = 177.8 \text{ min}$
M2:	$R^2 = 0.9988$	$k_{\text{eff}} = 5.00 \cdot 10^{-3} \text{ L mol}^{-1} \text{ s}^{-1}$	$t_{1/2} = 153.6 \text{ min}$
M3:	$R^2 = 0.9994$	$k_{\text{eff}} = 5.00 \cdot 10^{-3} \text{ L mol}^{-1} \text{ s}^{-1}$	$t_{1/2} = 153.6 \text{ min}$
M4:	$R^2 = 0.9993$	$k_{\text{eff}} = 4.89 \cdot 10^{-3} \text{ L mol}^{-1} \text{ s}^{-1}$	$t_{1/2} = 157.0 \text{ min}$
Avg.:		$4.80 \cdot 10^{-3} \text{ L mol}^{-1} \text{ s}^{-1}$	$159.9 \pm 10.1 \text{ min}$



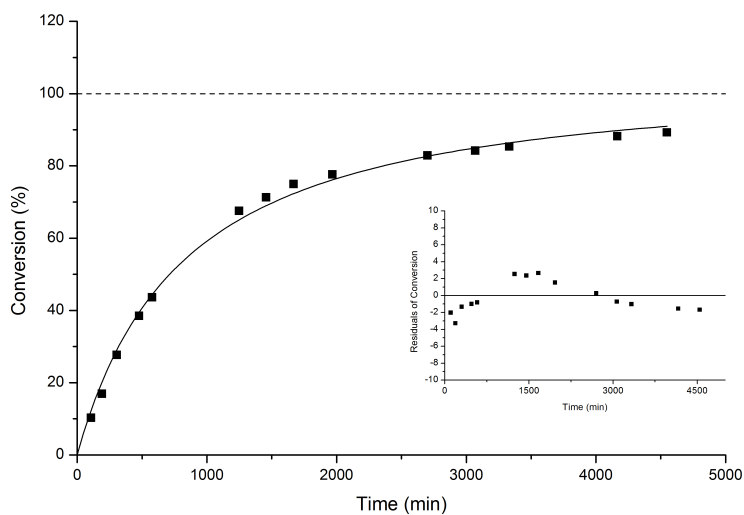
**Figure 8.54.** Time vs. conversion plot of **5b** with 1.2 equiv  $\text{Et}_3\text{N}$  (**2a**) and *N*-methylimidazole (**3e**) with 4 mol% catalyst loading.

M1:	$R^2 = 0.9948$	$k_{\text{eff}} = 2.13 \cdot 10^{-4} \text{ L mol}^{-1} \text{ s}^{-1}$	$t_{1/2} = 3611.0 \text{ min}$
M2:	$R^2 = 0.9944$	$k_{\text{eff}} = 2.12 \cdot 10^{-4} \text{ L mol}^{-1} \text{ s}^{-1}$	$t_{1/2} = 3630.7 \text{ min}$
Avg.:		$2.12 \cdot 10^{-3} \text{ L mol}^{-1} \text{ s}^{-1}$	$3620.8 \pm 9.8 \text{ min}$



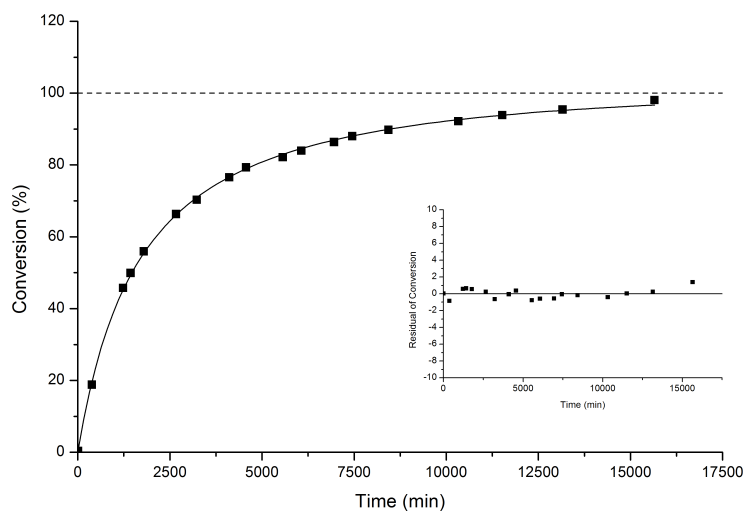
**Figure 8.55.** Time vs. conversion plot of **5b** with 1.2 equiv Et<sub>3</sub>N (**2a**) and *N*-methylimidazole (**3e**) with 20 mol% catalyst loading.

M1:	$R^2 = 0.9968$	$k_{eff} = 9.90 \cdot 10^{-4} \text{ L mol}^{-1} \text{ s}^{-1}$	$t_{1/2} = 775.9 \text{ min}$
M2:	$R^2 = 0.9937$	$k_{eff} = 9.17 \cdot 10^{-4} \text{ L mol}^{-1} \text{ s}^{-1}$	$t_{1/2} = 837.6 \text{ min}$
M3:	$R^2 = 0.9951$	$k_{eff} = 1.08 \cdot 10^{-3} \text{ L mol}^{-1} \text{ s}^{-1}$	$t_{1/2} = 711.0 \text{ min}$
M4:	$R^2 = 0.9937$	$k_{eff} = 1.11 \cdot 10^{-3} \text{ L mol}^{-1} \text{ s}^{-1}$	$t_{1/2} = 691.8 \text{ min}$
Avg.:		$1.03 \cdot 10^{-3} \text{ L mol}^{-1} \text{ s}^{-1}$	$749.8 \pm 57.4 \text{ min}$



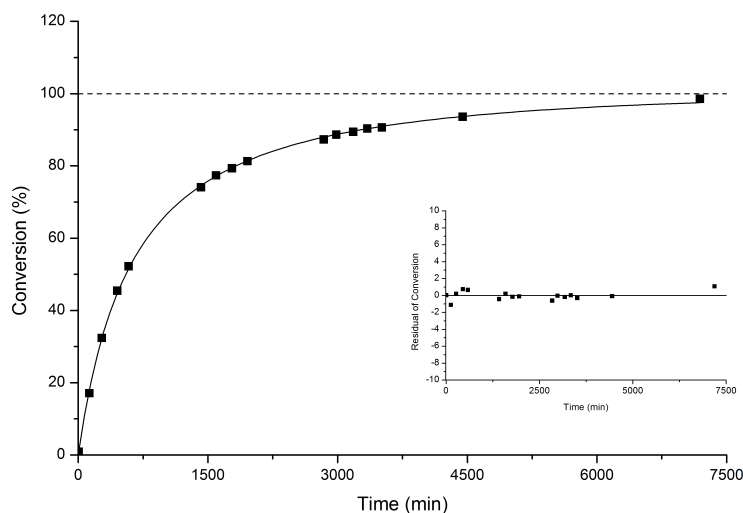
**Figure 8.56.** Time vs. conversion plot of **5b** with 1.2 equiv Et<sub>3</sub>N (**2a**) and *N*-methylimidazole (**3e**) with 30 mol% catalyst loading.

M1:	$R^2 = 0.9966$	$k_{eff} = 1.77 \cdot 10^{-3} \text{ L mol}^{-1} \text{ s}^{-1}$	$t_{1/2} = 433.8 \text{ min}$
M2:	$R^2 = 0.9960$	$k_{eff} = 1.66 \cdot 10^{-3} \text{ L mol}^{-1} \text{ s}^{-1}$	$t_{1/2} = 462.6 \text{ min}$
M3:	$R^2 = 0.9949$	$k_{eff} = 1.77 \cdot 10^{-3} \text{ L mol}^{-1} \text{ s}^{-1}$	$t_{1/2} = 433.8 \text{ min}$
Avg.:		$1.03 \cdot 10^{-3} \text{ L mol}^{-1} \text{ s}^{-1}$	$443.0 \pm 13.6 \text{ min}$



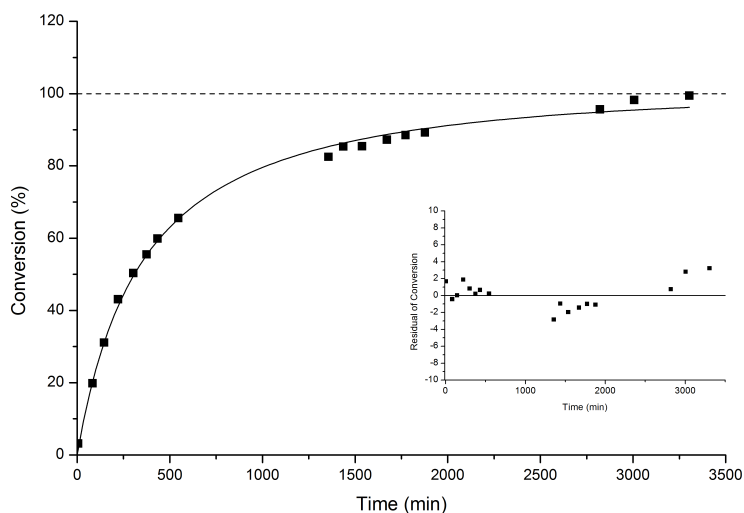
**Figure 8.57.** Time vs. conversion plot of **5b** with 1.2 equiv Et<sub>3</sub>N (**2a**) and catalyst **3g** with 4 mol% catalyst loading.

M1:	$R^2 = 0.9995$	$k_{eff} = 5.19 \cdot 10^{-4} \text{ L mol}^{-1} \text{ s}^{-1}$	$t_{1/2} = 1479.7 \text{ min}$
M2:	$R^2 = 0.9993$	$k_{eff} = 5.16 \cdot 10^{-4} \text{ L mol}^{-1} \text{ s}^{-1}$	$t_{1/2} = 1487.7 \text{ min}$
M3:	$R^2 = 0.9995$	$k_{eff} = 5.45 \cdot 10^{-4} \text{ L mol}^{-1} \text{ s}^{-1}$	$t_{1/2} = 1408.6 \text{ min}$
Avg.:		$5.27 \cdot 10^{-4} \text{ L mol}^{-1} \text{ s}^{-1}$	$1457.8 \pm 35.5 \text{ min}$



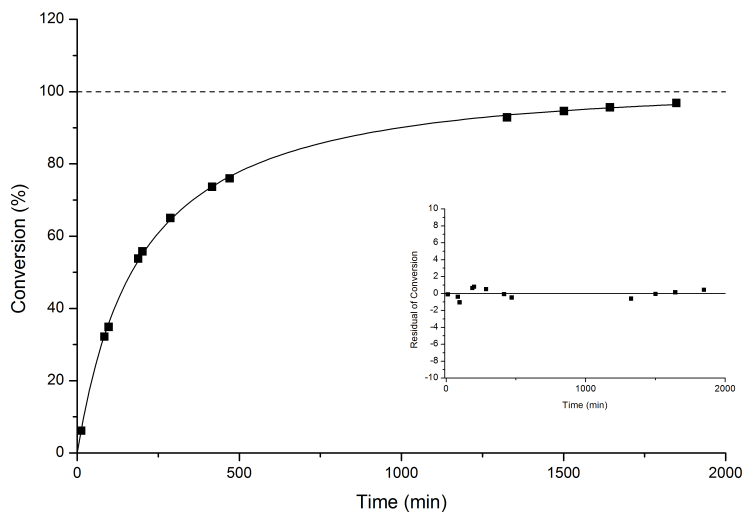
**Figure 8.58.** Time vs. conversion plot of **5b** with 1.2 equiv Et<sub>3</sub>N (**2a**) and catalyst **3g** with 10 mol% catalyst loading.

M1:	$R^2 = 0.9997$	$k_{eff} = 1.40 \cdot 10^{-3} \text{ L mol}^{-1} \text{ s}^{-1}$	$t_{1/2} = 548.5 \text{ min}$
M2:	$R^2 = 0.9994$	$k_{eff} = 1.34 \cdot 10^{-3} \text{ L mol}^{-1} \text{ s}^{-1}$	$t_{1/2} = 573.1 \text{ min}$
M3:	$R^2 = 0.9995$	$k_{eff} = 1.40 \cdot 10^{-3} \text{ L mol}^{-1} \text{ s}^{-1}$	$t_{1/2} = 548.5 \text{ min}$
Avg.:		$1.38 \cdot 10^{-3} \text{ L mol}^{-1} \text{ s}^{-1}$	$556.4 \pm 11.6 \text{ min}$



**Figure 8.59.** Time vs. conversion plot of **5b** with 1.2 equiv Et<sub>3</sub>N (**2a**) and catalyst **3g** with 20 mol% catalyst loading.

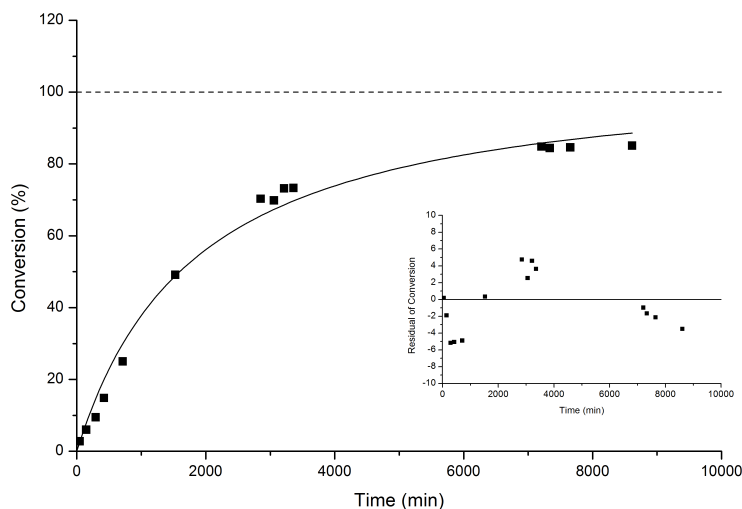
M1:	$R^2 = 0.9966$	$k_{eff} = 2.50 \cdot 10^{-3} \text{ L mol}^{-1} \text{ s}^{-1}$	$t_{1/2} = 307.2 \text{ min}$
M2:	$R^2 = 0.9991$	$k_{eff} = 2.74 \cdot 10^{-3} \text{ L mol}^{-1} \text{ s}^{-1}$	$t_{1/2} = 280.3 \text{ min}$
M3:	$R^2 = 0.9975$	$k_{eff} = 3.03 \cdot 10^{-3} \text{ L mol}^{-1} \text{ s}^{-1}$	$t_{1/2} = 253.4 \text{ min}$
Avg.:		$2.76 \cdot 10^{-3} \text{ L mol}^{-1} \text{ s}^{-1}$	$278.6 \pm 21.6 \text{ min}$



**Figure 8.60.** Time vs. conversion plot of **5b** with 1.2 equiv Et<sub>3</sub>N (**2a**) and catalyst **3g** with 30 mol% catalyst loading.

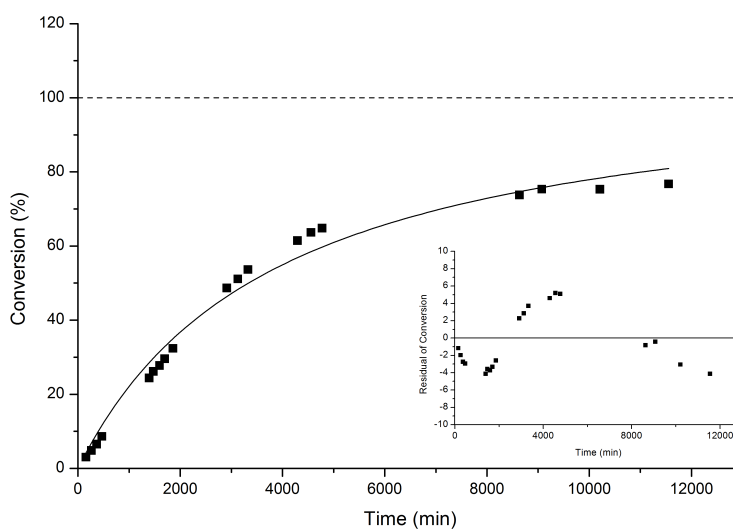
M1:	$R^2 = 0.9996$	$k_{eff} = 4.61 \cdot 10^{-3} \text{ L mol}^{-1} \text{ s}^{-1}$	$t_{1/2} = 166.6 \text{ min}$
M2:	$R^2 = 0.9984$	$k_{eff} = 4.19 \cdot 10^{-3} \text{ L mol}^{-1} \text{ s}^{-1}$	$t_{1/2} = 183.3 \text{ min}$
M3:	$R^2 = 0.9994$	$k_{eff} = 4.36 \cdot 10^{-3} \text{ L mol}^{-1} \text{ s}^{-1}$	$t_{1/2} = 176.1 \text{ min}$
M4:	$R^2 = 0.9966$	$k_{eff} = 4.24 \cdot 10^{-3} \text{ L mol}^{-1} \text{ s}^{-1}$	$t_{1/2} = 181.1 \text{ min}$
Avg.:		$4.26 \cdot 10^{-3} \text{ L mol}^{-1} \text{ s}^{-1}$	$180.1 \pm 3.0 \text{ min}$

## 8.2.4 Silylation with Phosphane Catalysts



**Figure 8.61.** Time vs. conversion plot of **5a** with 1.2 equiv Et<sub>3</sub>N (**2a**) and PPh<sub>3</sub> (**17a**) with 1 mol% catalyst loading.

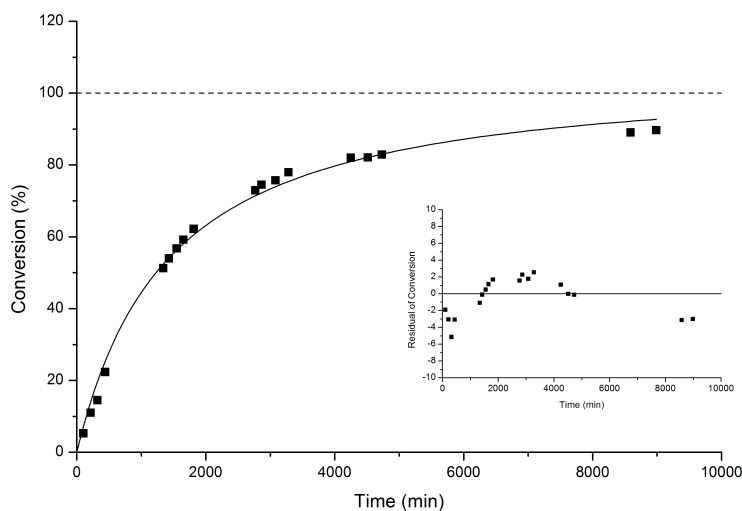
M1:	$R^2 = 0.9861$	$k_{eff} = 4.34 \cdot 10^{-4} \text{ L mol}^{-1} \text{ s}^{-1}$	$t_{1/2} = 1767.7 \text{ min}$
M2:	$R^2 = 0.9932$	$k_{eff} = 4.37 \cdot 10^{-4} \text{ L mol}^{-1} \text{ s}^{-1}$	$t_{1/2} = 1756.1 \text{ min}$
M3:	$R^2 = 0.9872$	$k_{eff} = 4.83 \cdot 10^{-4} \text{ L mol}^{-1} \text{ s}^{-1}$	$t_{1/2} = 1589.5 \text{ min}$
Avg.:		$4.52 \cdot 10^{-4} \text{ L mol}^{-1} \text{ s}^{-1}$	$1700.7 \pm 81.7 \text{ min}$



**Figure 8.62.** Time vs. conversion plot of **5a** with 1.2 equiv Et<sub>3</sub>N (**2a**) and P(OMe)<sub>2</sub><sub>3</sub> (**17b**) with 1 mol% catalyst loading.

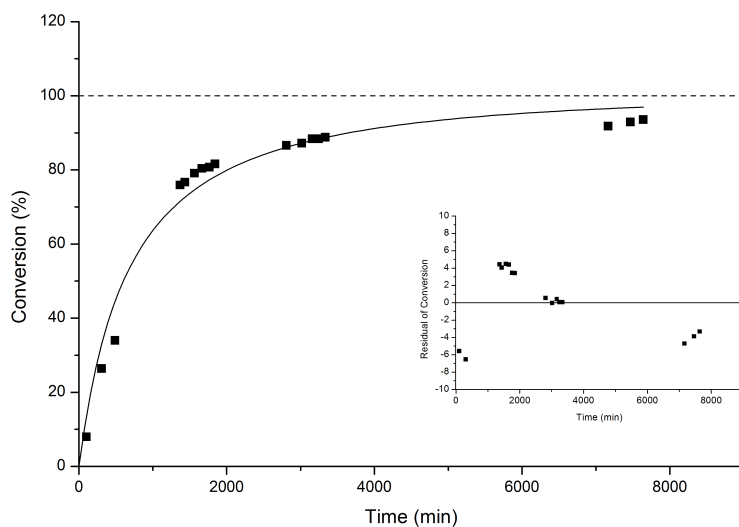
M1:	$R^2 = 0.9819$	$k_{eff} = 2.31 \cdot 10^{-4} \text{ L mol}^{-1} \text{ s}^{-1}$	$t_{1/2} = 3320.7 \text{ min}$
M2:	$R^2 = 0.9823$	$k_{eff} = 2.23 \cdot 10^{-4} \text{ L mol}^{-1} \text{ s}^{-1}$	$t_{1/2} = 3446.4 \text{ min}$
Avg.:		$2.27 \cdot 10^{-4} \text{ L mol}^{-1} \text{ s}^{-1}$	$3382.4 \pm 62.8 \text{ min}$





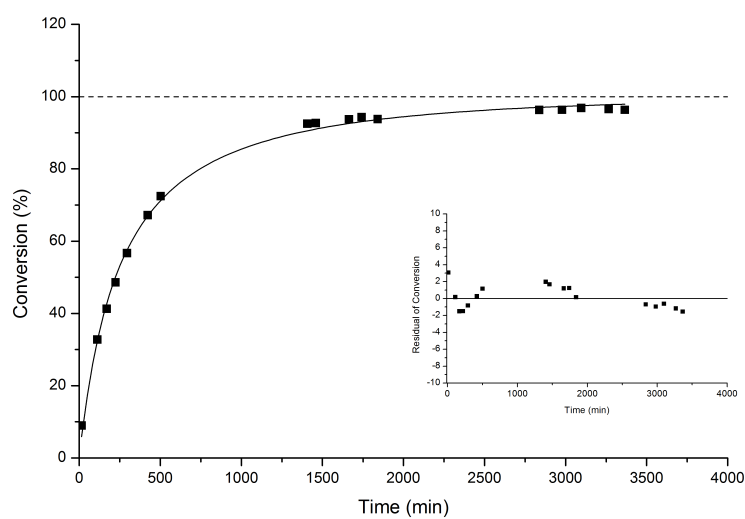
**Figure 8.63.** Time vs. conversion plot of **5a** with 1.2 equiv **Et<sub>3</sub>N** (**2a**) and **P(Tol)<sub>3</sub>** (**17c**) with 1 mol% catalyst loading.

M1:	$R^2 = 0.9927$	$k_{eff} = 6.52 \cdot 10^{-4} \text{ L mol}^{-1} \text{ s}^{-1}$	$t_{1/2} = 1177.7 \text{ min}$
M2:	$R^2 = 0.9926$	$k_{eff} = 6.26 \cdot 10^{-4} \text{ L mol}^{-1} \text{ s}^{-1}$	$t_{1/2} = 1226.7 \text{ min}$
Avg.:		$6.39 \cdot 10^{-4} \text{ L mol}^{-1} \text{ s}^{-1}$	$1201.5 \pm 24.3 \text{ min}$



**Figure 8.64.** Time vs. conversion plot of **5a** with 1.2 equiv **Et<sub>3</sub>N** (**2a**) and **P(pOMePh)<sub>3</sub>** (**17d**) with 1 mol% catalyst loading.

M1:	$R^2 = 0.9662$	$k_{eff} = 1.30 \cdot 10^{-3} \text{ L mol}^{-1} \text{ s}^{-1}$	$t_{1/2} = 590.7 \text{ min}$
M2:	$R^2 = 0.9684$	$k_{eff} = 1.36 \cdot 10^{-3} \text{ L mol}^{-1} \text{ s}^{-1}$	$t_{1/2} = 564.6 \text{ min}$
Avg.:		$1.33 \cdot 10^{-3} \text{ L mol}^{-1} \text{ s}^{-1}$	$577.4 \pm 13.0 \text{ min}$

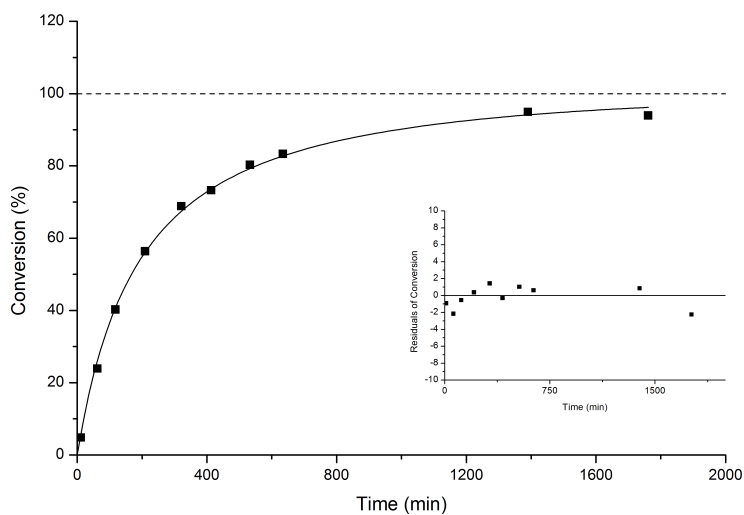


**Figure 8.65.** Time vs. conversion plot of **5a** with 1.2 equiv  $\text{Et}_3\text{N}$  (**2a**) and  $\text{P}(\text{NMe}_2)_3$  (**17e**) with 1 mol% catalyst loading.

M1:	$R^2 = 0.9977$	$k_{\text{eff}} = 3.34 \cdot 10^{-3} \text{ L mol}^{-1} \text{ s}^{-1}$	$t_{1/2} = 229.9 \text{ min}$
M2:	$R^2 = 0.9973$	$k_{\text{eff}} = 3.48 \cdot 10^{-3} \text{ L mol}^{-1} \text{ s}^{-1}$	$t_{1/2} = 220.7 \text{ min}$
Avg.:		$3.41 \cdot 10^{-3} \text{ L mol}^{-1} \text{ s}^{-1}$	$225.2 \pm 4.6 \text{ min}$

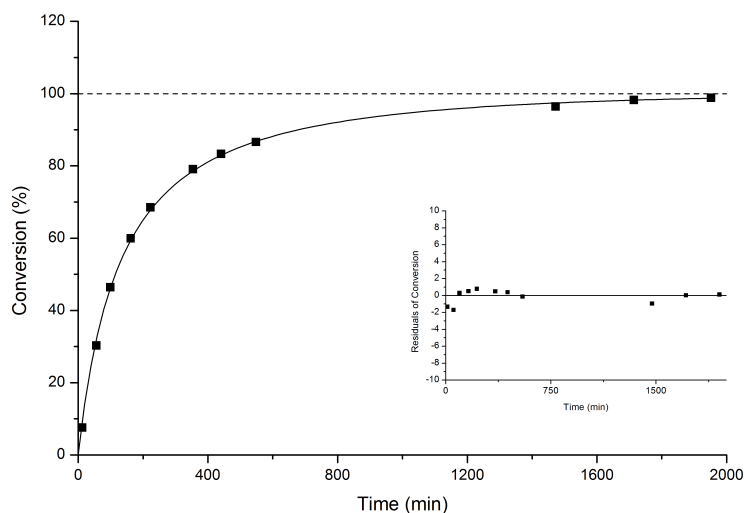
8.2.5 Silylation of *para*-Substituted Secondary Alcohols

For the results discussed in Chapter 2.6.2 the time-conversion plots will be depicted on the following pages.



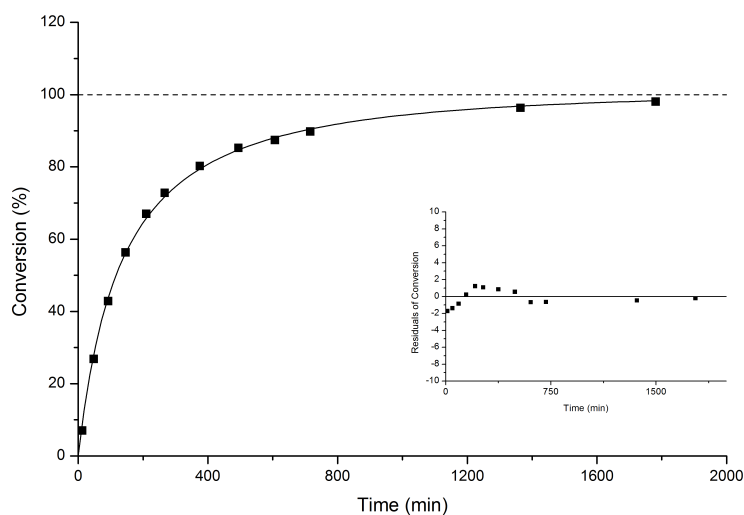
**Figure 8.66.** Time vs. conversion plot of **13** (*p*-Br) with 1.2 equiv Et<sub>3</sub>N (**2a**) and catalyst **3c** with 30 mol% catalyst loading.

M1:	$R^2 = 0.9979$	$k_{eff} = 4.59 \cdot 10^{-3} \text{ L mol}^{-1} \text{ s}^{-1}$	$t_{1/2} = 167.3 \text{ min}$
M2:	$R^2 = 0.9965$	$k_{eff} = 4.75 \cdot 10^{-3} \text{ L mol}^{-1} \text{ s}^{-1}$	$t_{1/2} = 161.7 \text{ min}$
Avg.:		$4.67 \cdot 10^{-3} \text{ L mol}^{-1} \text{ s}^{-1}$	$164.4 \pm 2.8 \text{ min}$



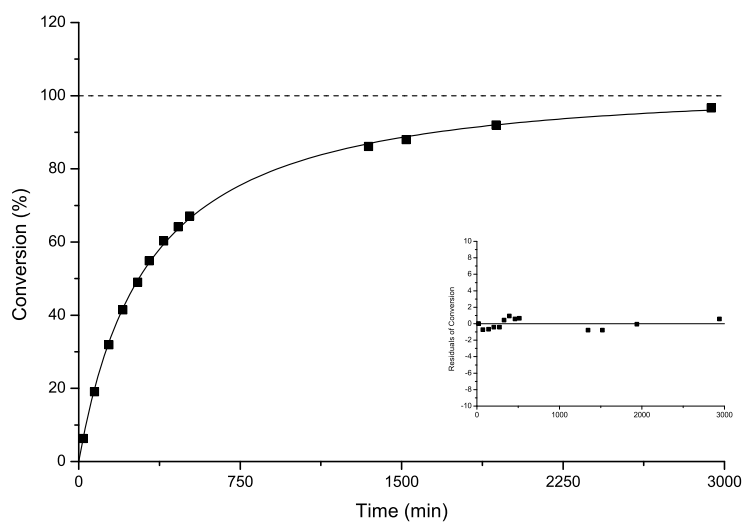
**Figure 8.67.** Time vs. conversion plot of **15b** (*p*-OMe) with 1.2 equiv Et<sub>3</sub>N (**2a**) and catalyst **3c** with 30 mol% catalyst loading.

M1:	$R^2 = 0.9991$	$k_{eff} = 6.74 \cdot 10^{-3} \text{ L mol}^{-1} \text{ s}^{-1}$	$t_{1/2} = 113.9 \text{ min}$
M2:	$R^2 = 0.9979$	$k_{eff} = 6.63 \cdot 10^{-3} \text{ L mol}^{-1} \text{ s}^{-1}$	$t_{1/2} = 115.8 \text{ min}$
M3:	$R^2 = 0.9979$	$k_{eff} = 6.77 \cdot 10^{-3} \text{ L mol}^{-1} \text{ s}^{-1}$	$t_{1/2} = 113.4 \text{ min}$
Avg.:		$6.71 \cdot 10^{-3} \text{ L mol}^{-1} \text{ s}^{-1}$	$114.4 \pm 1.0 \text{ min}$



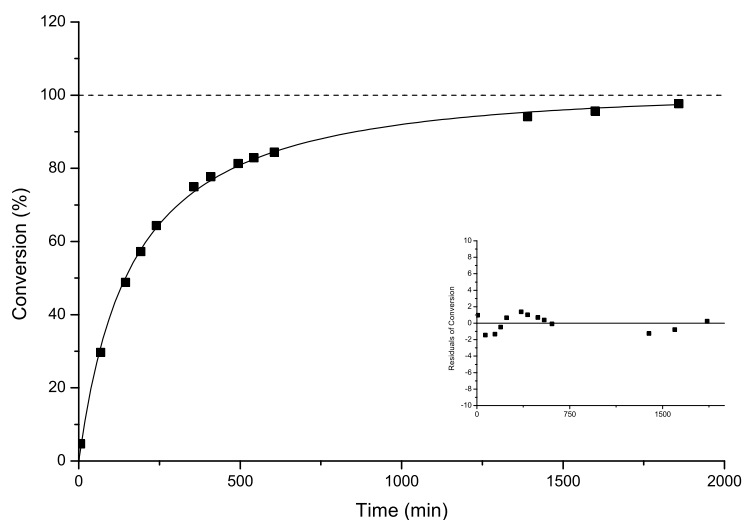
**Figure 8.68.** Time vs. conversion plot of **11** (*p*-Me) with 1.2 equiv Et<sub>3</sub>N (**2a**) and catalyst **3c** with 30 mol% catalyst loading.

M1:	$R^2 = 0.9987$	$k_{eff} = 6.62 \cdot 10^{-3} \text{ L mol}^{-1} \text{ s}^{-1}$	$t_{1/2} = 116.0 \text{ min}$
M2:	$R^2 = 0.9965$	$k_{eff} = 6.77 \cdot 10^{-3} \text{ L mol}^{-1} \text{ s}^{-1}$	$t_{1/2} = 118.7 \text{ min}$
Avg.:		$6.55 \cdot 10^{-3} \text{ L mol}^{-1} \text{ s}^{-1}$	$117.3 \pm 1.3 \text{ min}$



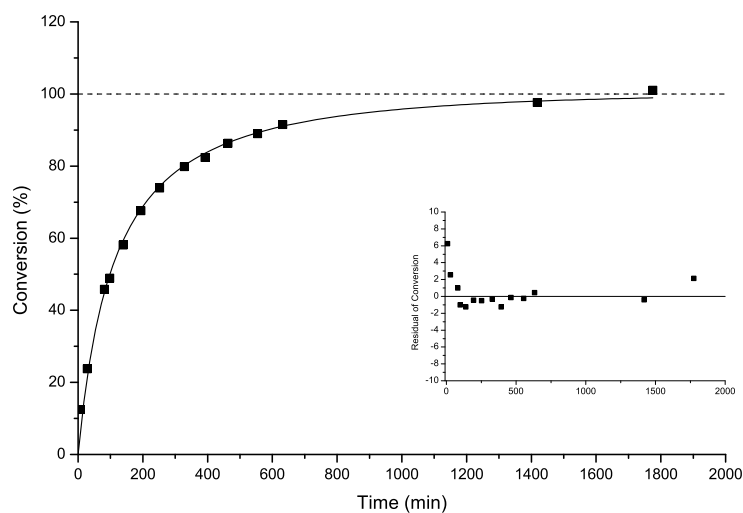
**Figure 8.69.** Time vs. conversion plot of **14** (*p*-CN) with 1.2 equiv Et<sub>3</sub>N (**2a**) and catalyst **3c** with 30 mol% catalyst loading.

M1:	$R^2 = 0.9995$	$k_{eff} = 2.77 \cdot 10^{-3} \text{ L mol}^{-1} \text{ s}^{-1}$	$t_{1/2} = 277.2 \text{ min}$
M2:	$R^2 = 0.9994$	$k_{eff} = 2.69 \cdot 10^{-3} \text{ L mol}^{-1} \text{ s}^{-1}$	$t_{1/2} = 285.5 \text{ min}$
M3:	$R^2 = 0.9995$	$k_{eff} = 2.76 \cdot 10^{-3} \text{ L mol}^{-1} \text{ s}^{-1}$	$t_{1/2} = 278.2 \text{ min}$
Avg.:		$2.74 \cdot 10^{-3} \text{ L mol}^{-1} \text{ s}^{-1}$	$280.3 \pm 3.7 \text{ min}$



**Figure 8.70.** Time vs. conversion plot of **12** (*p*-F) with 1.2 equiv Et<sub>3</sub>N (**2a**) and catalyst **3c** with 30 mol% catalyst loading.

M1:	$R^2 = 0.9982$	$k_{eff} = 4.85 \cdot 10^{-3} \text{ L mol}^{-1} \text{ s}^{-1}$	$t_{1/2} = 158.3 \text{ min}$
M2:	$R^2 = 0.9986$	$k_{eff} = 4.75 \cdot 10^{-3} \text{ L mol}^{-1} \text{ s}^{-1}$	$t_{1/2} = 161.7 \text{ min}$
M3:	$R^2 = 0.9985$	$k_{eff} = 5.35 \cdot 10^{-3} \text{ L mol}^{-1} \text{ s}^{-1}$	$t_{1/2} = 143.5 \text{ min}$
Avg.:		$4.98 \cdot 10^{-3} \text{ L mol}^{-1} \text{ s}^{-1}$	$154.7 \pm 7.9 \text{ min}$

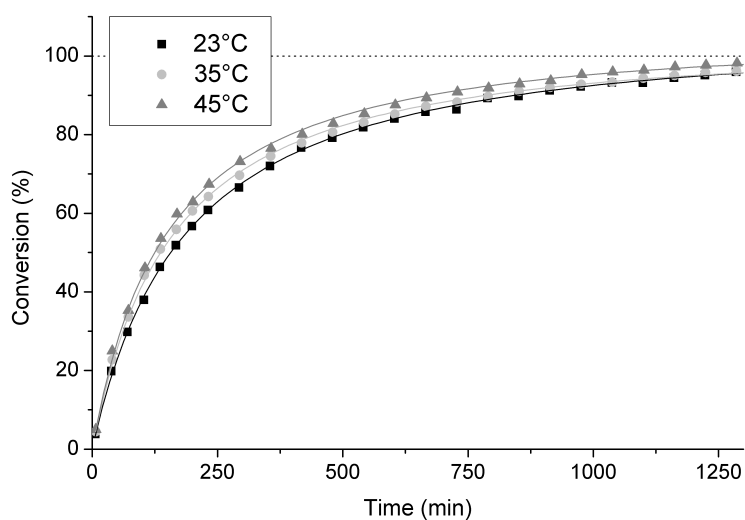


**Figure 8.71.** Time vs. conversion plot of **16** (*p*-NMe<sub>2</sub>) with 1.2 equiv Et<sub>3</sub>N (**2a**) and catalyst **3c** with 30 mol% catalyst loading.

M1:	$R^2 = 0.9948$	$k_{eff} = 7.68 \cdot 10^{-3} \text{ L mol}^{-1} \text{ s}^{-1}$	$t_{1/2} = 100.0 \text{ min}$
M2:	$R^2 = 0.9937$	$k_{eff} = 7.84 \cdot 10^{-3} \text{ L mol}^{-1} \text{ s}^{-1}$	$t_{1/2} = 97.9 \text{ min}$
M3:	$R^2 = 0.9961$	$k_{eff} = 7.88 \cdot 10^{-3} \text{ L mol}^{-1} \text{ s}^{-1}$	$t_{1/2} = 97.4 \text{ min}$
Avg.:		$7.80 \cdot 10^{-3} \text{ L mol}^{-1} \text{ s}^{-1}$	$98.4 \pm 1.1 \text{ min}$

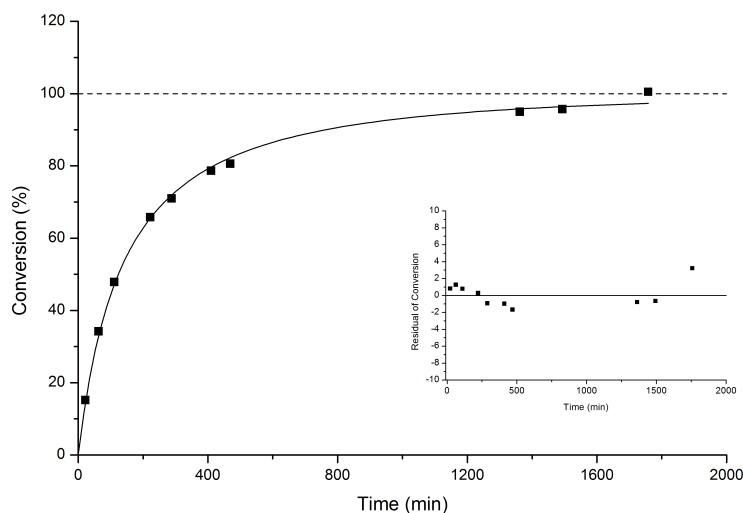
### 8.2.6 Variation of Temperature and Solvents

Kinetic measurements have been performed at different temperatures (23 °C, 35 °C, and 45 °C) for the silylation of **5b** in CDCl<sub>3</sub> with catalyst **3g** (30 mol% catalyst loading) in melted NMR tubes. In addition the kinetic measurements in various solvents will be displayed here.



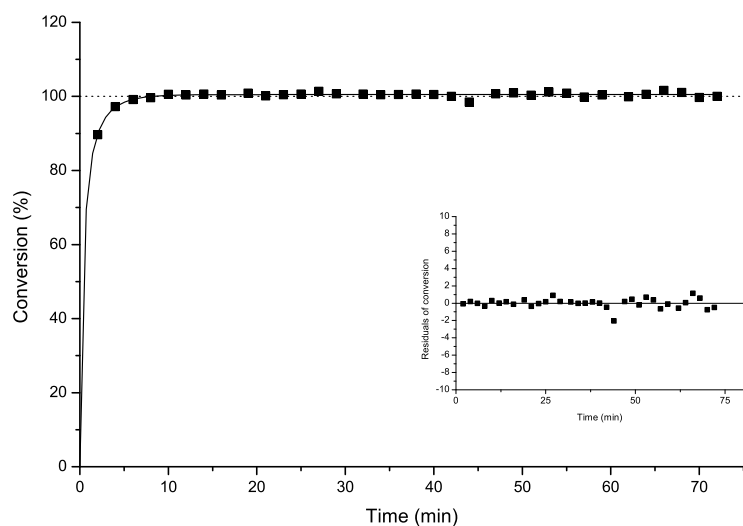
**Figure 8.72.** Time vs. conversion plot of **5b** with 1.2 equiv Et<sub>3</sub>N (**2a**) and catalyst **3g** with 30 mol% catalyst loading.

M1 (23 °C):	$R^2 = 0.9996$	$k_{eff} = 4.72 \cdot 10^{-3} \text{ L mol}^{-1} \text{ s}^{-1}$	$t_{1/2} = 162.7 \text{ min}$
M2 (35 °C):	$R^2 = 0.9994$	$k_{eff} = 5.59 \cdot 10^{-3} \text{ L mol}^{-1} \text{ s}^{-1}$	$t_{1/2} = 137.4 \text{ min}$
M3 (45 °C):	$R^2 = 0.9989$	$k_{eff} = 5.95 \cdot 10^{-3} \text{ L mol}^{-1} \text{ s}^{-1}$	$t_{1/2} = 129.1 \text{ min}$



**Figure 8.73.** Time vs. conversion plot of **5h** with 1.2 equiv **Et<sub>3</sub>N (2a)**, and **3c** as catalyst with 30 mol% catalyst loading in **CH<sub>2</sub>Cl<sub>2</sub>**.

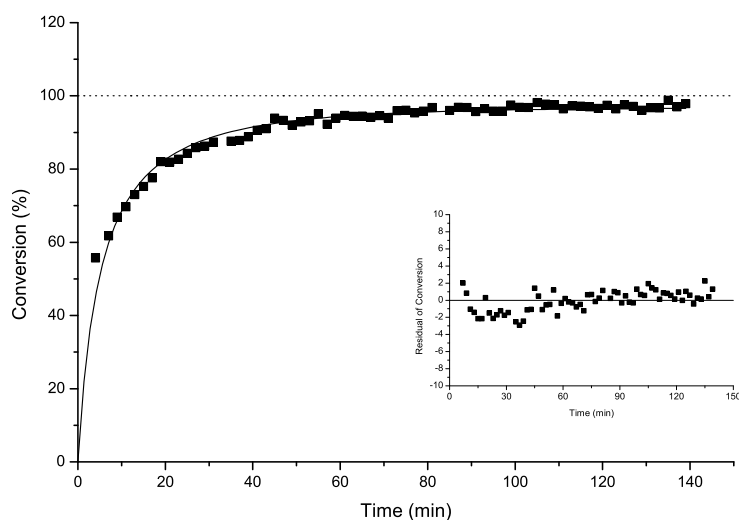
M1:	$R^2 = 0.9970$	$k_{eff} = 6.31 \cdot 10^{-3} \text{ L mol}^{-1} \text{ s}^{-1}$	$t_{1/2} = 116.2 \text{ min}$
M2:	$R^2 = 0.9993$	$k_{eff} = 6.76 \cdot 10^{-3} \text{ L mol}^{-1} \text{ s}^{-1}$	$t_{1/2} = 114.8 \text{ min}$
Avg.:		$6.65 \cdot 10^{-4} \text{ L mol}^{-1} \text{ s}^{-1}$	$115.5 \pm 0.7 \text{ min}$



**Figure 8.74.** Time vs. conversion plot of **5a** with 1.2 equiv **Et<sub>3</sub>N (2a)**, and no catalyst **DMF-d<sub>7</sub>**.

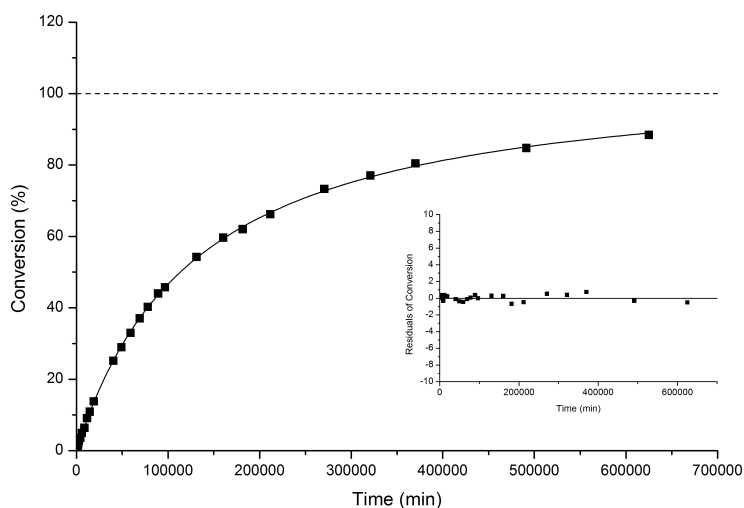
M1:	$R^2 = 0.9216$	$k_{eff} = 2.18 \text{ L mol}^{-1} \text{ s}^{-1}$	$t_{1/2} = 0.4 \text{ min}$
M2:	$R^2 = 0.8976$	$k_{eff} = 3.15 \text{ L mol}^{-1} \text{ s}^{-1}$	$t_{1/2} = 0.2 \text{ min}$
Avg.:		$2.85 \text{ L mol}^{-1} \text{ s}^{-1}$	$0.3 \pm 0.1 \text{ min}$





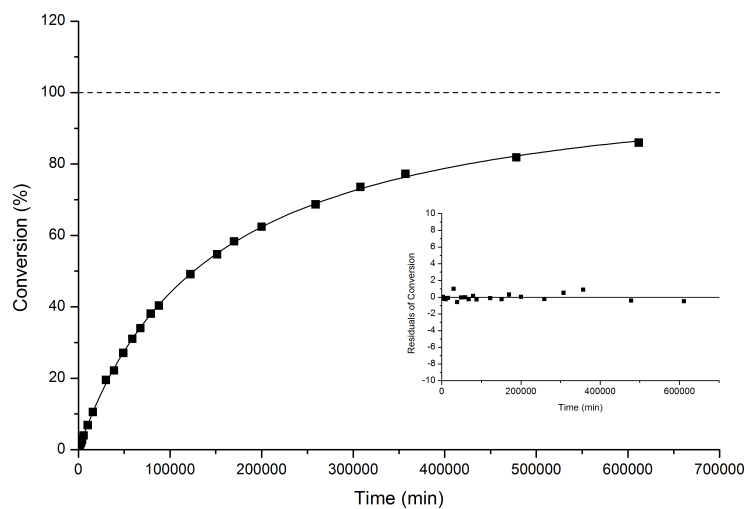
**Figure 8.75.** Time vs. conversion plot of **5b** with 1.2 equiv  $\text{Et}_3\text{N}$  (**2a**), and no catalyst loading  $\text{DMF-d}_7$ .

M1:	$R^2 = 0.9620$	$k_{\text{eff}} = 1.70 \cdot 10^{-1} \text{ L mol}^{-1} \text{ s}^{-1}$	$t_{1/2} = 4.5 \text{ min}$
M2:	$R^2 = 0.9576$	$k_{\text{eff}} = 1.15 \cdot 10^{-1} \text{ L mol}^{-1} \text{ s}^{-1}$	$t_{1/2} = 6.7 \text{ min}$
Avg.:		$1.43 \cdot 10^{-1} \text{ L mol}^{-1} \text{ s}^{-1}$	$5.4 \pm 1.1 \text{ min}$



**Figure 8.76.** Time vs. conversion plot of **5c** with 1.2 equiv  $\text{Et}_3\text{N}$  (**2a**), and no catalyst in  $\text{DMF-d}_7$ .

M1:	$R^2 = 0.9998$	$k_{\text{eff}} = 6.80 \cdot 10^{-6} \text{ L mol}^{-1} \text{ s}^{-1}$	$t_{1/2} = 112901.6 \text{ min}$
M2:	$R^2 = 0.9998$	$k_{\text{eff}} = 6.83 \cdot 10^{-6} \text{ L mol}^{-1} \text{ s}^{-1}$	$t_{1/2} = 112500.3 \text{ min}$
Avg.:		$6.81 \cdot 10^{-6} \text{ L mol}^{-1} \text{ s}^{-1}$	$112700.9 \pm 283.7 \text{ min}$

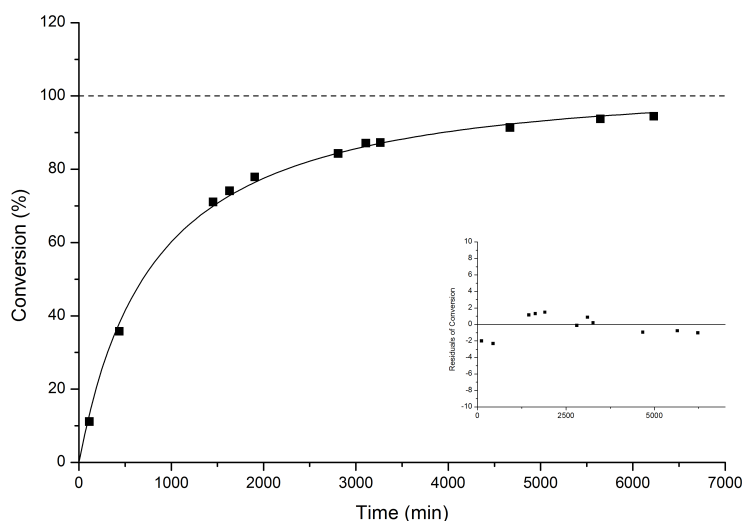


**Figure 8.77.** Time vs. conversion plot of **5c** with 1.2 equiv  $\text{Et}_3\text{N}$  (**2a**), and catalyst **3c** with 30 mol% catalyst loading in  $\text{DMF-d}_7$ .

M1:	$R^2 = 0.9992$	$k_{\text{eff}} = 5.99 \cdot 10^{-6} \text{ L mol}^{-1} \text{ s}^{-1}$	$t_{1/2} = 128030.8 \text{ min}$
M2:	$R^2 = 0.9997$	$k_{\text{eff}} = 5.97 \cdot 10^{-6} \text{ L mol}^{-1} \text{ s}^{-1}$	$t_{1/2} = 128474.4 \text{ min}$
Avg.:		<b><math>5.99 \cdot 10^{-6} \text{ L mol}^{-1} \text{ s}^{-1}</math></b>	<b><math>128252.6 \pm 313.7 \text{ min}</math></b>

8.2.7 Variation of Silyl Reagent in  $\text{CDCl}_3$  and  $\text{DMF-d}_7$ 

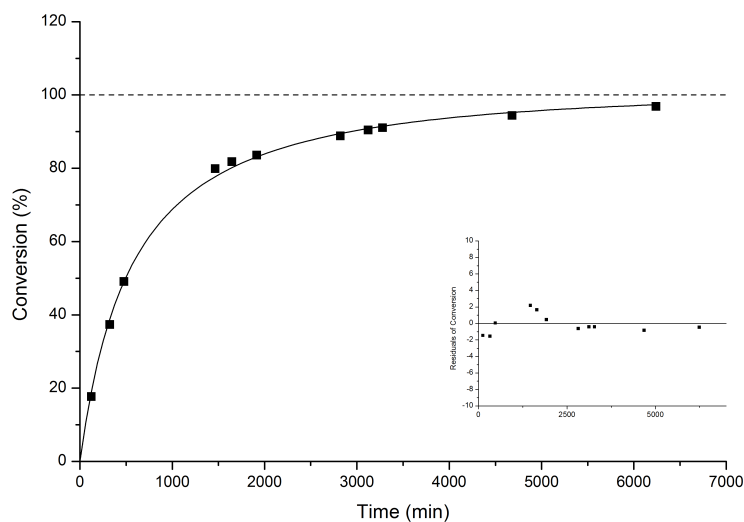
For the results discussed in Chapter 3 the time vs. conversion plots will be depicted on the following pages starting with measurements in  $\text{CDCl}_3$ . The measurements for TBSCl (**1a**) have already been depicted on previous pages.



**Figure 8.78.** Time vs. conversion plot of primary alcohol **5a** and TBSCN (**1c**) with 1.2 equiv  $\text{Et}_3\text{N}$  (**2a**), and catalyst **3a** with 1 mol% catalyst loading in  $\text{CDCl}_3$ .

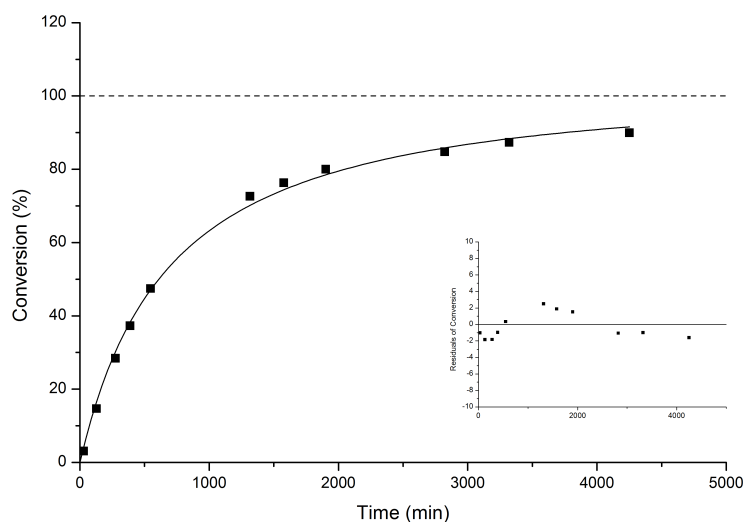
M1:	$R^2 = 0.9971$	$k_{\text{eff}} = 1.10 \cdot 10^{-3} \text{ L mol}^{-1} \text{ s}^{-1}$	$t_{1/2} = 698.1 \text{ min}$
M2:	$R^2 = 0.9969$	$k_{\text{eff}} = 1.10 \cdot 10^{-3} \text{ L mol}^{-1} \text{ s}^{-1}$	$t_{1/2} = 698.1 \text{ min}$
M3:	$R^2 = 0.9917$	$k_{\text{eff}} = 1.12 \cdot 10^{-3} \text{ L mol}^{-1} \text{ s}^{-1}$	$t_{1/2} = 685.6 \text{ min}$
Avg.:		$1.96 \cdot 10^{-3} \text{ L mol}^{-1} \text{ s}^{-1}$	$693.9 \pm 5.9 \text{ min}$

## 8.2 Data of Direct Rate Measurements



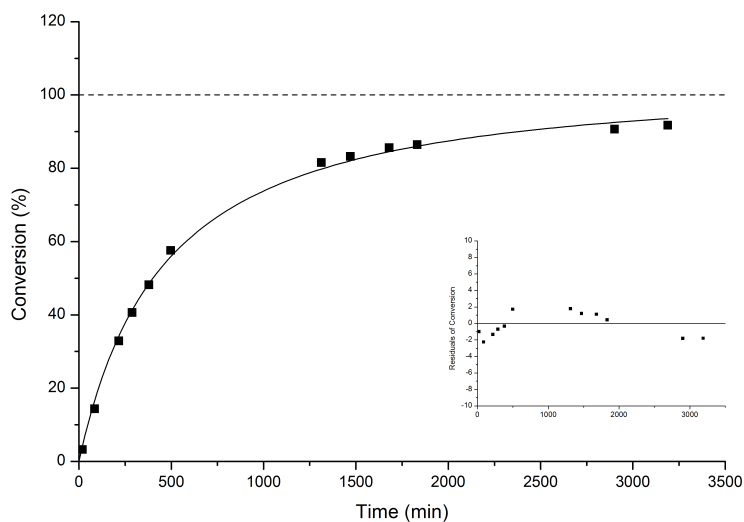
**Figure 8.79.** Time vs. conversion plot of primary alcohol **5a** and TBSCN (**1c**) with 1.2 equiv Et<sub>3</sub>N (**2a**), and catalyst **3a** with 2 mol% catalyst loading in CDCl<sub>3</sub>.

M1:	$R^2 = 0.9978$	$k_{eff} = 1.56 \cdot 10^{-3} \text{ L mol}^{-1} \text{ s}^{-1}$	$t_{1/2} = 492.2 \text{ min}$
M2:	$R^2 = 0.9978$	$k_{eff} = 1.57 \cdot 10^{-3} \text{ L mol}^{-1} \text{ s}^{-1}$	$t_{1/2} = 489.1 \text{ min}$
M3:	$R^2 = 0.9979$	$k_{eff} = 1.58 \cdot 10^{-3} \text{ L mol}^{-1} \text{ s}^{-1}$	$t_{1/2} = 486.0 \text{ min}$
Avg.:		$1.57 \cdot 10^{-3} \text{ L mol}^{-1} \text{ s}^{-1}$	$489.1 \pm 2.5 \text{ min}$



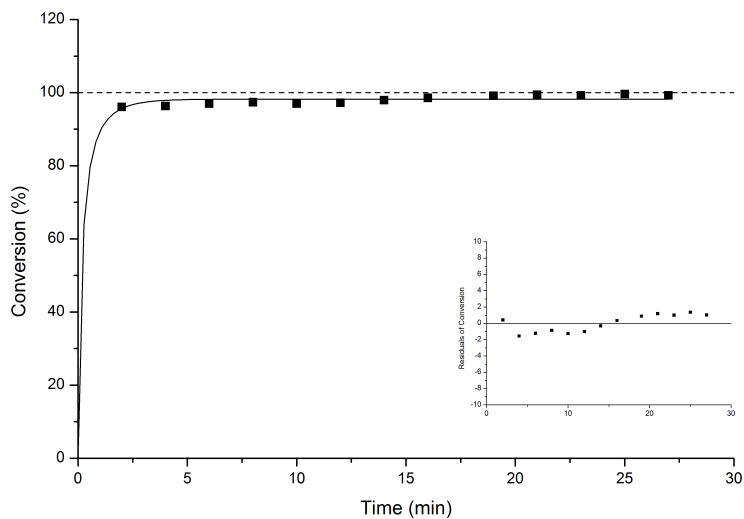
**Figure 8.80.** Time vs. conversion plot of primary alcohol **5a** and TBSCN (**1c**) with 1.2 equiv Et<sub>3</sub>N (**2a**), and catalyst **3a** with 3 mol% catalyst loading in CDCl<sub>3</sub>.

M1:	$R^2 = 0.9959$	$k_{eff} = 1.20 \cdot 10^{-3} \text{ L mol}^{-1} \text{ s}^{-1}$	$t_{1/2} = 639.9 \text{ min}$
M2:	$R^2 = 0.9971$	$k_{eff} = 1.28 \cdot 10^{-3} \text{ L mol}^{-1} \text{ s}^{-1}$	$t_{1/2} = 599.9 \text{ min}$
M3:	$R^2 = 0.9975$	$k_{eff} = 1.20 \cdot 10^{-3} \text{ L mol}^{-1} \text{ s}^{-1}$	$t_{1/2} = 639.9 \text{ min}$
Avg.:		$1.24 \cdot 10^{-3} \text{ L mol}^{-1} \text{ s}^{-1}$	$619.3 \pm 18.9 \text{ min}$



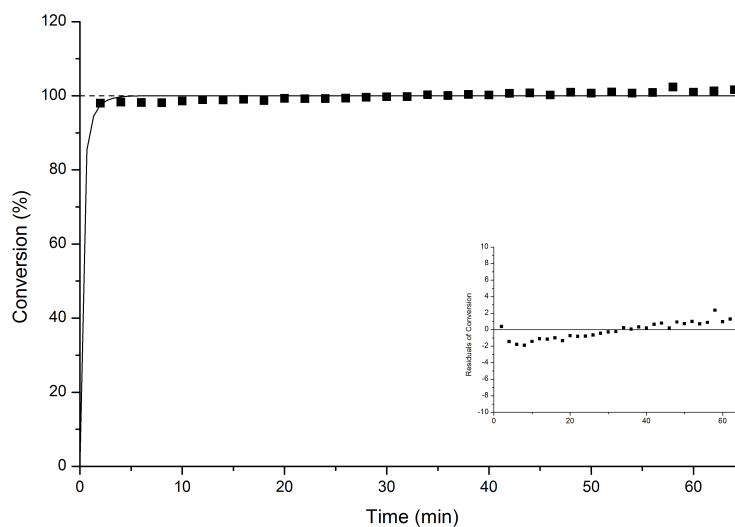
**Figure 8.81.** Time vs. conversion plot of primary alcohol **5a** and TBSCN (**1c**) with 1.2 equiv Et<sub>3</sub>N (**2a**), and catalyst **3a** with 4 mol% catalyst loading in CDCl<sub>3</sub>.

M1:	$R^2 = 0.9975$	$k_{eff} = 1.92 \cdot 10^{-3} \text{ L mol}^{-1} \text{ s}^{-1}$	$t_{1/2} = 399.9 \text{ min}$
M2:	$R^2 = 0.9901$	$k_{eff} = 1.99 \cdot 10^{-3} \text{ L mol}^{-1} \text{ s}^{-1}$	$t_{1/2} = 385.9 \text{ min}$
M3:	$R^2 = 0.9968$	$k_{eff} = 1.87 \cdot 10^{-3} \text{ L mol}^{-1} \text{ s}^{-1}$	$t_{1/2} = 410.6 \text{ min}$
Avg.:		$1.93 \cdot 10^{-3} \text{ L mol}^{-1} \text{ s}^{-1}$	$398.6 \pm 10.1 \text{ min}$



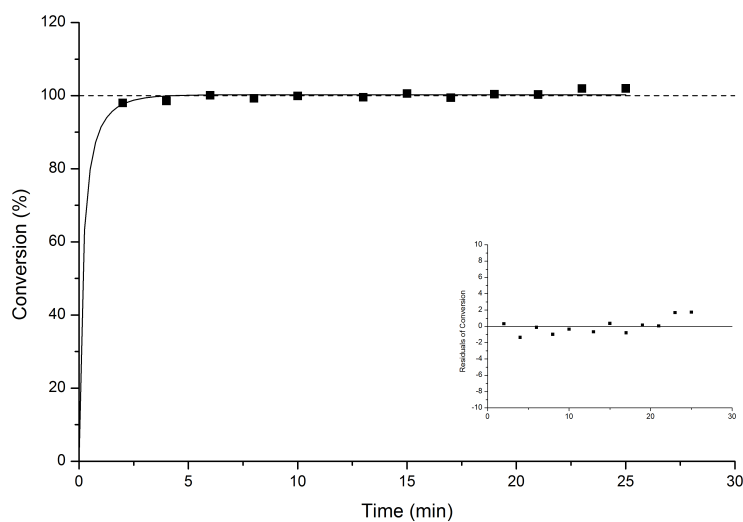
**Figure 8.82.** Time vs. conversion plot of secondary alcohol **5b** and TBSOTf (**1b**) with 1.2 equiv Et<sub>3</sub>N (**2a**), and no catalyst in CDCl<sub>3</sub>.

M1:	$R^2 = 0.3341$	$k_{eff} = 2.97 \text{ L mol}^{-1} \text{ s}^{-1}$	$t_{1/2} = 0.258 \text{ min}$
M2:	$R^2 = 0.3304$	$k_{eff} = 5.35 \text{ L mol}^{-1} \text{ s}^{-1}$	$t_{1/2} = 0.144 \text{ min}$
M3:	$R^2 = 0.2043$	$k_{eff} = 4.92 \text{ L mol}^{-1} \text{ s}^{-1}$	$t_{1/2} = 0.156 \text{ min}$
Avg.:		$4.42 \text{ L mol}^{-1} \text{ s}^{-1}$	$0.174 \pm 0.051 \text{ min}$



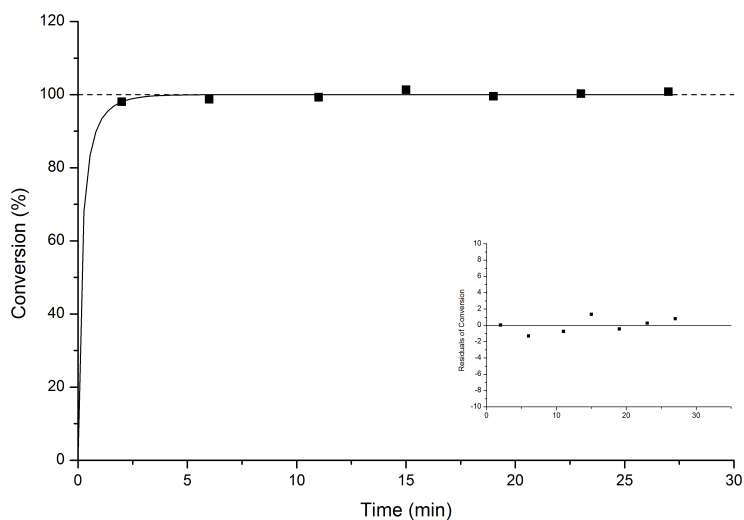
**Figure 8.83.** Time vs. conversion plot of secondary alcohol **5b** and TBSOTf (**1b**) with 1.2 equiv Et<sub>3</sub>N (**2a**), and catalyst **3a** with 10 mol% catalyst loading in CDCl<sub>3</sub>.

M1:	$R^2 = 0.1197$	$k_{eff} = 5.49 \text{ L mol}^{-1} \text{ s}^{-1}$	$t_{1/2} = 0.140 \text{ min}$
M2:	$R^2 = 0.0862$	$k_{eff} = 5.10 \text{ L mol}^{-1} \text{ s}^{-1}$	$t_{1/2} = 0.151 \text{ min}$
Avg.:		<b><math>5.30 \text{ L mol}^{-1} \text{ s}^{-1}</math></b>	<b><math>0.143 \pm 0.001 \text{ min}</math></b>



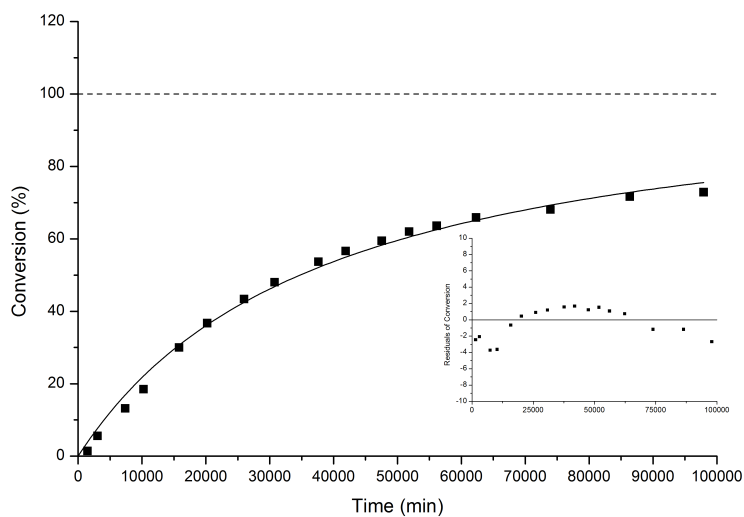
**Figure 8.84.** Time vs. conversion plot of secondary alcohol **5b** and TBSOTf (**1b**) with 1.2 equiv Et<sub>3</sub>N (**2a**), and catalyst **3a** with 20 mol% catalyst loading in CDCl<sub>3</sub>.

M1:	$R^2 = 0.2780$	$k_{eff} = 4.97 \text{ L mol}^{-1} \text{ s}^{-1}$	$t_{1/2} = 0.154 \text{ min}$
M2:	$R^2 = 0.1758$	$k_{eff} = 4.85 \text{ L mol}^{-1} \text{ s}^{-1}$	$t_{1/2} = 0.158 \text{ min}$
M3:	$R^2 = 0.1758$	$k_{eff} = 6.31 \text{ L mol}^{-1} \text{ s}^{-1}$	$t_{1/2} = 0.122 \text{ min}$
Avg.:		<b><math>5.38 \text{ L mol}^{-1} \text{ s}^{-1}</math></b>	<b><math>0.143 \pm 0.017 \text{ min}</math></b>



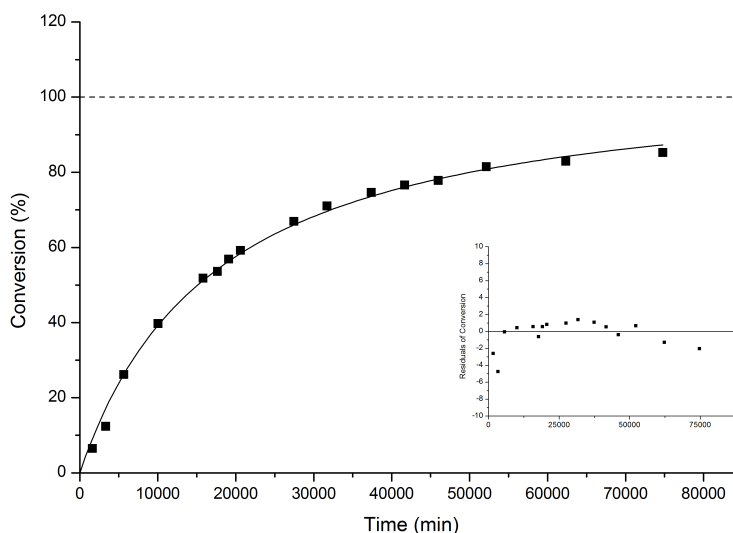
**Figure 8.85.** Time vs. conversion plot of secondary alcohol **5b** and TBSOTf (**1b**) with 1.2 equiv Et<sub>3</sub>N (**2a**), and catalyst **3a** with 30 mol% catalyst loading in CDCl<sub>3</sub>.

M1:	$R^2 = 0.1333$	$k_{eff} = 4.63 \text{ L mol}^{-1} \text{ s}^{-1}$	$t_{1/2} = 0.166 \text{ min}$
M2:	$R^2 = 0.2728$	$k_{eff} = 5.57 \text{ L mol}^{-1} \text{ s}^{-1}$	$t_{1/2} = 0.138 \text{ min}$
Avg.:		<b><math>5.10 \text{ L mol}^{-1} \text{ s}^{-1}</math></b>	<b><math>0.151 \pm 0.014 \text{ min}</math></b>



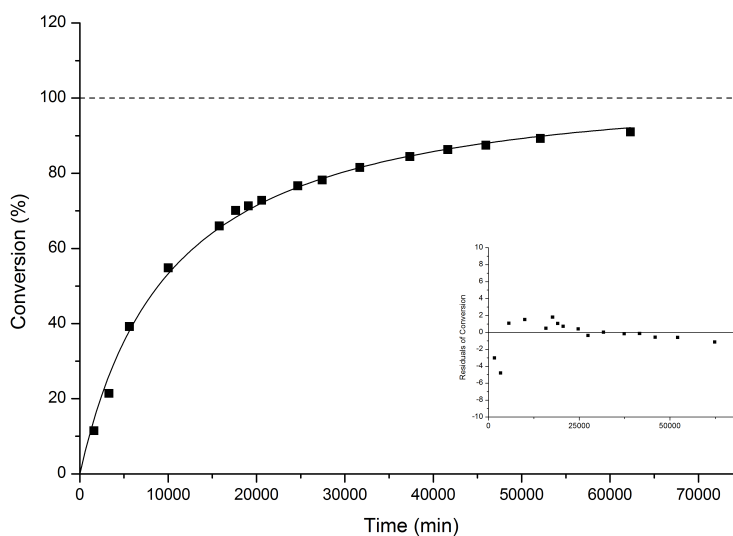
**Figure 8.86.** Time vs. conversion plot of secondary alcohol **5b** and TBSCN (**1c**) with 1.2 equiv Et<sub>3</sub>N (**2a**), and catalyst **3a** with 10 mol% catalyst loading in CDCl<sub>3</sub>.

M1:	$R^2 = 0.9903$	$k_{eff} = 2.28 \cdot 10^{-5} \text{ L mol}^{-1} \text{ s}^{-1}$	$t_{1/2} = 33634.8 \text{ min}$
M2:	$R^2 = 0.9927$	$k_{eff} = 2.34 \cdot 10^{-5} \text{ L mol}^{-1} \text{ s}^{-1}$	$t_{1/2} = 32810.4 \text{ min}$
M3:	$R^2 = 0.9932$	$k_{eff} = 2.24 \cdot 10^{-5} \text{ L mol}^{-1} \text{ s}^{-1}$	$t_{1/2} = 34212.9 \text{ min}$
Avg.:		<b><math>2.29 \cdot 10^{-5} \text{ L mol}^{-1} \text{ s}^{-1}</math></b>	<b><math>33542.8 \pm 575.5 \text{ min}</math></b>



**Figure 8.87.** Time vs. conversion plot of secondary alcohol **5b** and TBSCN (**1c**) with 1.2 equiv Et<sub>3</sub>N (**2a**), and catalyst **3a** with 20 mol% catalyst loading in CDCl<sub>3</sub>.

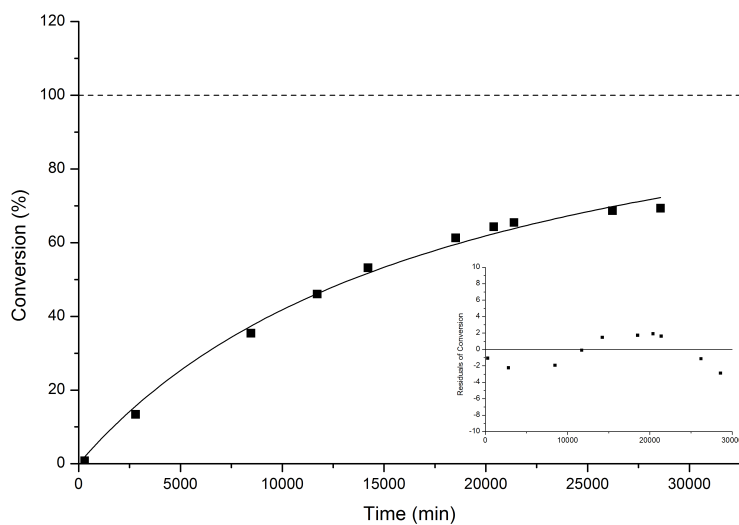
M1:	$R^2 = 0.9952$	$k_{eff} = 5.10 \cdot 10^{-5} \text{ L mol}^{-1} \text{ s}^{-1}$	$t_{1/2} = 15055.0 \text{ min}$
M2:	$R^2 = 0.9938$	$k_{eff} = 5.44 \cdot 10^{-5} \text{ L mol}^{-1} \text{ s}^{-1}$	$t_{1/2} = 14098.8 \text{ min}$
Avg.:		$5.27 \cdot 10^{-5} \text{ L mol}^{-1} \text{ s}^{-1}$	$14561.2 \pm 478.1 \text{ min}$



**Figure 8.88.** Time vs. conversion plot of secondary alcohol **5b** and TBSCN (**1c**) with 1.2 equiv Et<sub>3</sub>N (**2a**), and catalyst **3a** with 30 mol% catalyst loading in CDCl<sub>3</sub>.

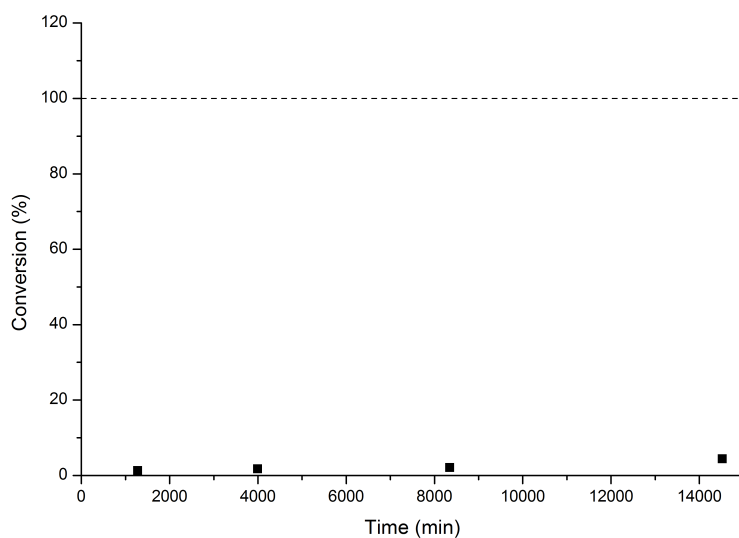
M1:	$R^2 = 0.9947$	$k_{eff} = 8.69 \cdot 10^{-5} \text{ L mol}^{-1} \text{ s}^{-1}$	$t_{1/2} = 8832.5 \text{ min}$
M2:	$R^2 = 0.9922$	$k_{eff} = 8.65 \cdot 10^{-5} \text{ L mol}^{-1} \text{ s}^{-1}$	$t_{1/2} = 8878.4 \text{ min}$
Avg.:		$8.67 \cdot 10^{-5} \text{ L mol}^{-1} \text{ s}^{-1}$	$8855.4 \pm 23.0 \text{ min}$





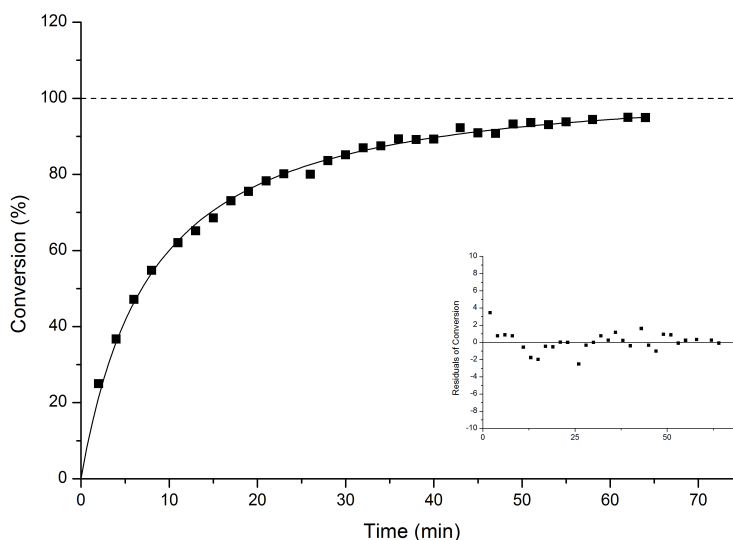
**Figure 8.89.** Time vs. conversion plot of secondary alcohol **5b** and MTBSTFA (**1d**) with 1.2 equiv Et<sub>3</sub>N (**2a**), and catalyst **3a** with 30 mol% catalyst loading in CDCl<sub>3</sub>.

M1:	$R^2 = 0.9924$	$k_{eff} = 4.91 \cdot 10^{-5} \text{ L mol}^{-1} \text{ s}^{-1}$	$t_{1/2} = 15637.6 \text{ min}$
M2:	$R^2 = 0.9934$	$k_{eff} = 4.88 \cdot 10^{-5} \text{ L mol}^{-1} \text{ s}^{-1}$	$t_{1/2} = 15727.2 \text{ min}$
Avg.:		$4.90 \cdot 10^{-5} \text{ L mol}^{-1} \text{ s}^{-1}$	$15687.3 \pm 48.1 \text{ min}$



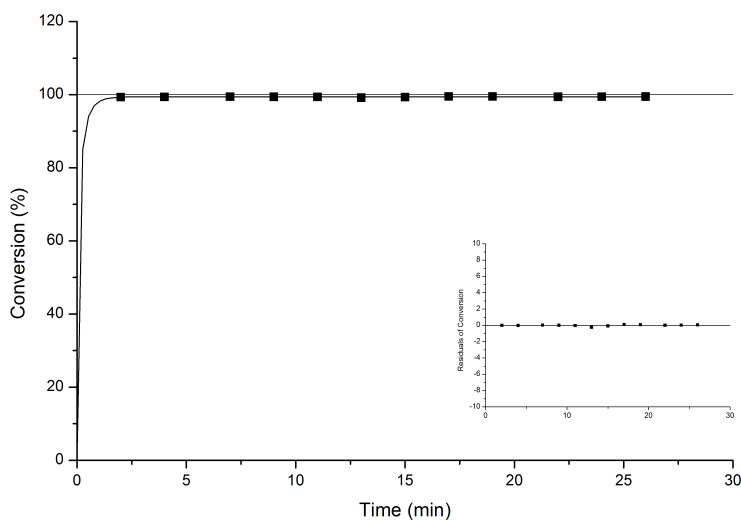
**Figure 8.90.** Time vs. conversion plot of secondary alcohol **5b** and TBS-IMI (**1e**) with 1.2 equiv Et<sub>3</sub>N (**2a**), and catalyst **3a** with 30 mol% catalyst loading in CDCl<sub>3</sub>.

M1:	$R^2 = \text{n.d.}$	$k_{eff} = 4.15 \cdot 10^{-6} \text{ L mol}^{-1} \text{ s}^{-1}$	$t_{1/2} = 185035 \text{ min}$
M2:	$R^2 = \text{n.d.}$	$k_{eff} = 4.04 \cdot 10^{-5} \text{ L mol}^{-1} \text{ s}^{-1}$	$t_{1/2} = 190073 \text{ min}$
Avg.:		$4.10 \cdot 10^{-6} \text{ L mol}^{-1} \text{ s}^{-1}$	$1.87 \cdot 10^{+6} \pm 2519 \text{ min}$



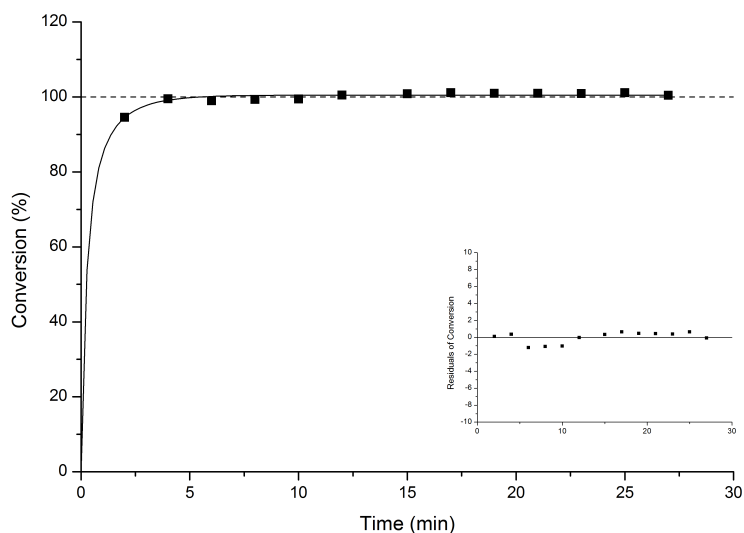
**Figure 8.91.** Time vs. conversion plot of secondary alcohol **5b** with 1.2 equiv  $\text{Et}_3\text{N}$  (**2a**) and DMAP (**3a**) with 30 mol% catalyst loading in  $\text{DMF-d}_7$ .

M1:	$R^2 = 0.9927$	$k_{\text{eff}} = 1.05 \cdot 10^{-1} \text{ L mol}^{-1} \text{ s}^{-1}$	$t_{1/2} = 7.3 \text{ min}$
M2:	$R^2 = 0.9961$	$k_{\text{eff}} = 1.12 \cdot 10^{-1} \text{ L mol}^{-1} \text{ s}^{-1}$	$t_{1/2} = 6.9 \text{ min}$
Avg.:		$1.09 \cdot 10^{-1} \text{ L mol}^{-1} \text{ s}^{-1}$	$7.1 \pm 0.2 \text{ min}$



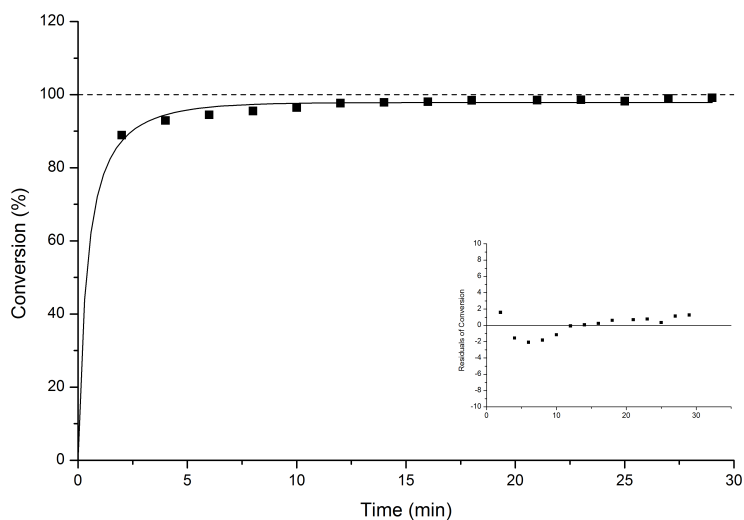
**Figure 8.92.** Time vs. conversion plot of secondary alcohol **5b** and TBSOTf (**1b**) with 1.2 equiv  $\text{Et}_3\text{N}$  (**2a**), and catalyst **3a** with 0 mol% catalyst loading in  $\text{DMF-d}_7$ .

M1:	$R^2 = 0.3241$	$k_{\text{eff}} = 1.16 \cdot 10^{+1} \text{ L mol}^{-1} \text{ s}^{-1}$	$t_{1/2} = 0.066 \text{ min}$
M2:	$R^2 = 0.3305$	$k_{\text{eff}} = 1.31 \cdot 10^{+1} \text{ L mol}^{-1} \text{ s}^{-1}$	$t_{1/2} = 0.059 \text{ min}$
Avg.:		$1.23 \cdot 10^{+1} \text{ L mol}^{-1} \text{ s}^{-1}$	$0.062 \pm 0.004 \text{ min}$



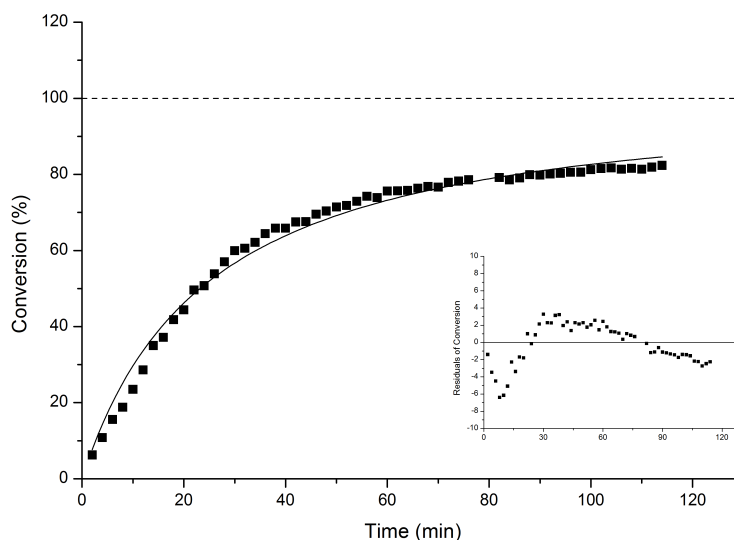
**Figure 8.93.** Time vs. conversion plot of secondary alcohol **5b** and TBSOTf (**1b**) with 1.2 equiv Et<sub>3</sub>N (**2a**), and catalyst **3a** with 15 mol% catalyst loading in DMF-d<sub>7</sub>.

M1:	$R^2 = 0.7241$	$k_{eff} = 4.06 \text{ L mol}^{-1} \text{ s}^{-1}$	$t_{1/2} = 0.189 \text{ min}$
M2:	$R^2 = 0.8465$	$k_{eff} = 3.21 \text{ L mol}^{-1} \text{ s}^{-1}$	$t_{1/2} = 0.239 \text{ min}$
Avg.:		<b><math>3.64 \text{ L mol}^{-1} \text{ s}^{-1}</math></b>	<b><math>0.211 \pm 0.025 \text{ min}</math></b>



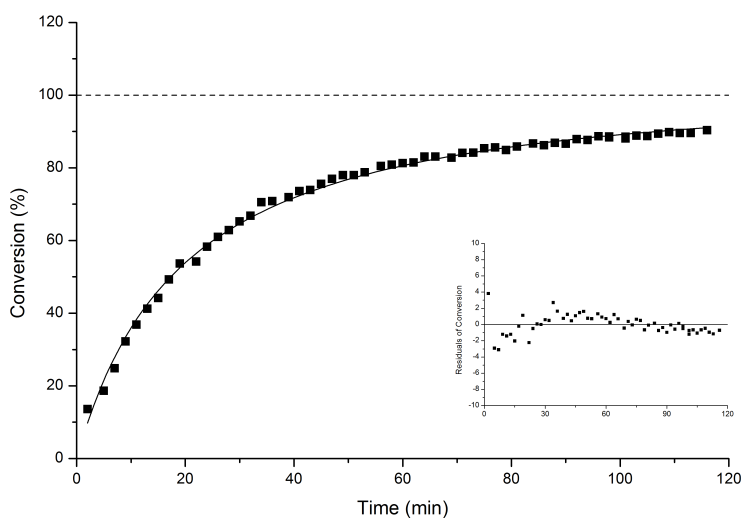
**Figure 8.94.** Time vs. conversion plot of secondary alcohol **5b** and TBSOTf (**1b**) with 1.2 equiv Et<sub>3</sub>N (**2a**), and catalyst **3a** with 30 mol% catalyst loading in DMF-d<sub>7</sub>.

M1:	$R^2 = 0.8243$	$k_{eff} = 2.14 \text{ L mol}^{-1} \text{ s}^{-1}$	$t_{1/2} = 0.353 \text{ min}$
M2:	$R^2 = 0.9215$	$k_{eff} = 2.99 \text{ L mol}^{-1} \text{ s}^{-1}$	$t_{1/2} = 0.256 \text{ min}$
Avg.:		<b><math>2.59 \text{ L mol}^{-1} \text{ s}^{-1}</math></b>	<b><math>0.297 \pm 0.049 \text{ min}</math></b>



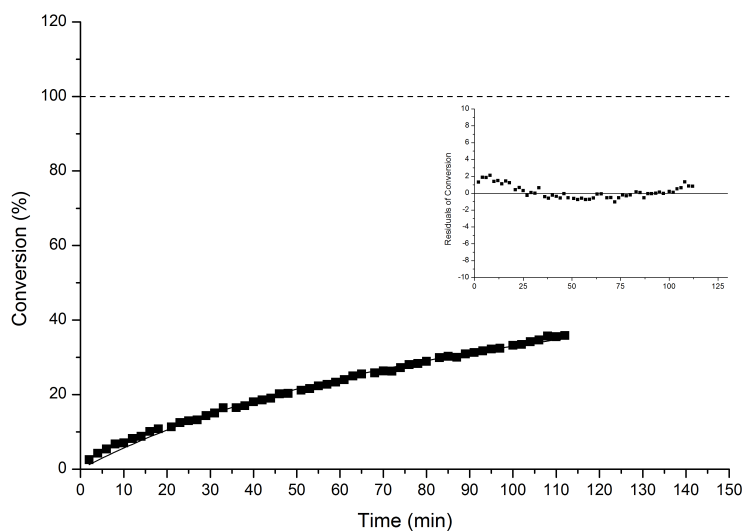
**Figure 8.95.** Time vs. conversion plot of secondary alcohol **5b** and TBSCN (**1c**) with 1.2 equiv Et<sub>3</sub>N (**2a**), and catalyst **3a** with 0 mol% catalyst loading in DMF-d<sub>7</sub>.

M1:	$R^2 = 0.9861$	$k_{\text{eff}} = 3.62 \cdot 10^{-2} \text{ L mol}^{-1} \text{ s}^{-1}$	$t_{1/2} = 21.2 \text{ min}$
M2:	$R^2 = 0.9910$	$k_{\text{eff}} = 3.80 \cdot 10^{-2} \text{ L mol}^{-1} \text{ s}^{-1}$	$t_{1/2} = 20.2 \text{ min}$
Avg.:		$3.71 \cdot 10^{-2} \text{ L mol}^{-1} \text{ s}^{-1}$	$20.7 \pm 0.5 \text{ min}$



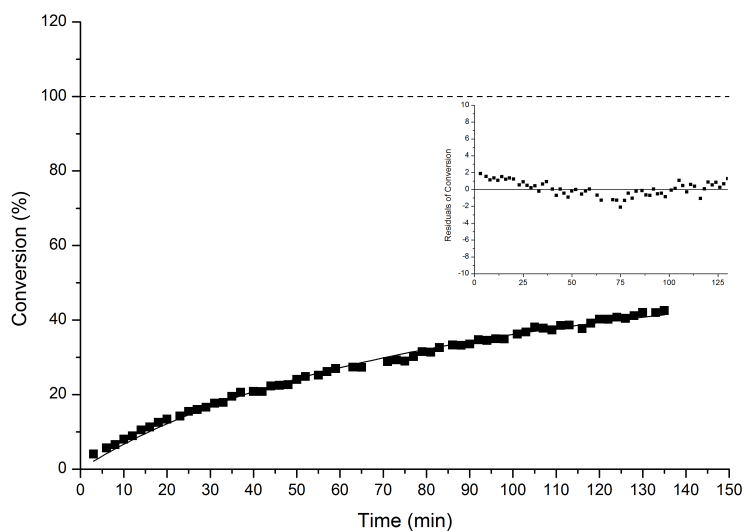
**Figure 8.96.** Time vs. conversion plot of secondary alcohol **5b** and TBSCN (**1c**) with 1.2 equiv Et<sub>3</sub>N (**2a**), and catalyst **3a** with 30 mol% catalyst loading in DMF-d<sub>7</sub>.

M1:	$R^2 = 0.9960$	$k_{\text{eff}} = 4.52 \cdot 10^{-2} \text{ L mol}^{-1} \text{ s}^{-1}$	$t_{1/2} = 17.0 \text{ min}$
M2:	$R^2 = 0.9848$	$k_{\text{eff}} = 3.38 \cdot 10^{-2} \text{ L mol}^{-1} \text{ s}^{-1}$	$t_{1/2} = 22.7 \text{ min}$
Avg.:		$3.95 \cdot 10^{-2} \text{ L mol}^{-1} \text{ s}^{-1}$	$19.4 \pm 2.9 \text{ min}$



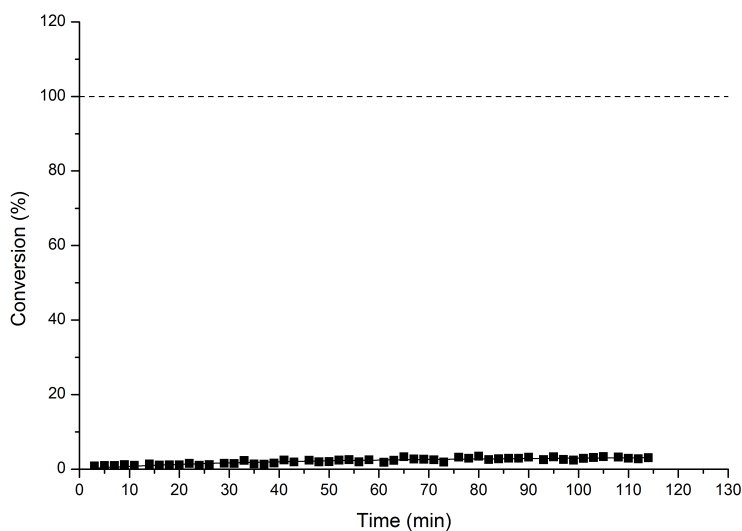
**Figure 8.97.** Time vs. conversion plot of secondary alcohol **5b** and MTBSTFA (**1d**) with 1.2 equiv  $\text{Et}_3\text{N}$  (**2a**), and catalyst **3a** with 0 mol% catalyst loading in  $\text{DMF-d}_7$ .

M1:	$R^2 = 0.9816$	$k_{\text{eff}} = 9.35 \cdot 10^{-3} \text{ L mol}^{-1} \text{ s}^{-1}$	$t_{1/2} = 82.1 \text{ min}$
M2:	$R^2 = 0.9778$	$k_{\text{eff}} = 2.17 \cdot 10^{-2} \text{ L mol}^{-1} \text{ s}^{-1}$	$t_{1/2} = 35.3 \text{ min}$
Avg.:		$1.56 \cdot 10^{-2} \text{ L mol}^{-1} \text{ s}^{-1}$	$49.4 \pm 23.4 \text{ min}$



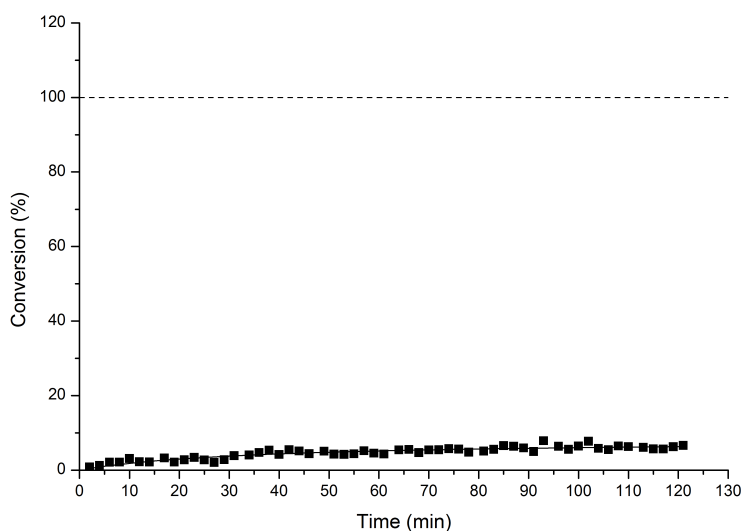
**Figure 8.98.** Time vs. conversion plot of secondary alcohol **5b** and MTBSTFA (**1d**) with 1.2 equiv  $\text{Et}_3\text{N}$  (**2a**), and catalyst **3a** with 30 mol% catalyst loading in  $\text{DMF-d}_7$ .

M1:	$R^2 = 0.9879$	$k_{\text{eff}} = 7.81 \cdot 10^{-3} \text{ L mol}^{-1} \text{ s}^{-1}$	$t_{1/2} = 98.3 \text{ min}$
M2:	$R^2 = 0.9804$	$k_{\text{eff}} = 1.34 \cdot 10^{-2} \text{ L mol}^{-1} \text{ s}^{-1}$	$t_{1/2} = 57.4 \text{ min}$
Avg.:		$1.06 \cdot 10^{-2} \text{ L mol}^{-1} \text{ s}^{-1}$	$72.6 \pm 20.4 \text{ min}$



**Figure 8.99.** Time vs. conversion plot of secondary alcohol **5b** and TBS-Imi (**1e**) with 1.2 equiv Et<sub>3</sub>N (**2a**), and catalyst **3a** with 0 mol% catalyst loading in DMF-d<sub>7</sub>.

M1:	$R^2 = \text{n.d.}$	$k_{\text{eff}} = 7.54 \cdot 10^{-4} \text{ L mol}^{-1} \text{ s}^{-1}$	$t_{1/2} = 1018.4 \text{ min}$
M2:	$R^2 = \text{n.d.}$	$k_{\text{eff}} = 7.79 \cdot 10^{-4} \text{ L mol}^{-1} \text{ s}^{-1}$	$t_{1/2} = 985.7 \text{ min}$
Avg.:		$7.67 \cdot 10^{-4} \text{ L mol}^{-1} \text{ s}^{-1}$	$1001.8 \pm 16.3 \text{ min}$



**Figure 8.100.** Time vs. conversion plot of secondary alcohol **5b** and TBS-Imi (**1e**) with 1.2 equiv Et<sub>3</sub>N (**2a**), and catalyst **3a** with 30 mol% catalyst loading in DMF-d<sub>7</sub>.

M1:	$R^2 = \text{n.d.}$	$k_{\text{eff}} = 9.03 \cdot 10^{-4} \text{ L mol}^{-1} \text{ s}^{-1}$	$t_{1/2} = 850.4 \text{ min}$
M2:	$R^2 = \text{n.d.}$	$k_{\text{eff}} = 1.19 \cdot 10^{-3} \text{ L mol}^{-1} \text{ s}^{-1}$	$t_{1/2} = 645.3 \text{ min}$
Avg.:		$1.05 \cdot 10^{-3} \text{ L mol}^{-1} \text{ s}^{-1}$	$733.8 \pm 102.5 \text{ min}$

## 8.3 Computational Methods

Silyl Cation Affinities (SCA) of *N*-heterocyclic bases have been calculated as the reaction enthalpy at 298.15 K and 1 atm pressure for the exchange reaction of the TBS-group. All geometry optimizations and vibrational frequency calculations have been performed using the MPW1K hybrid functional in combination with the 6-31+G(d) basis set. The conformational space of flexible *N*-heterocycles and the corresponding TBS-compounds has been searched using the MM3\* force field and the systematic search routine implemented in MACROMODEL 9.7.<sup>[154]</sup> All stationary points located at force field level have then been reoptimized at MPW1K/6-31+G(d) level as described before. Thermochemical corrections to 298.15 K have been calculated for all minima from unscaled vibrational frequencies obtained at this same level and have been combined with single point energies calculated at the MP2(FC)/G3MP2large//MPW1K/6-31+G(d) level to yield enthalpies  $H_{298}$  at 298.15 K. In conformationally flexible systems enthalpies have been calculated as Boltzmann-averaged values over all available conformers. All quantum mechanical calculations have been performed with Gaussian 03 or Gaussian 09.

### 8.3.1 Data for SCA and MCA Calculations for Various Catalysts

In the following tables the energies (in Hartree) of the quantum chemical calculations will be depicted for all compounds. The following abbreviation will be used in the tables: ‘\_sil\_’ for TBS-adducts, ‘\_me\_’ for methyl-adducts and for protonated catalysts ‘\_H\_’.

**Table 8.1.** Data for pyridine-based *N*-heterocycles and their TBS adducts (gas phase data).

System	MPW1K/6-31+G(d)		MP2(FC)/G3MP2large//MPW1K/6-31+G(d)		
	$E_{\text{tot}}$	$H_{298}$	$E_{\text{tot}}$	$H_{298}$	$\langle H_{298} \rangle$
Pyridine					
_01	−248.216536	−248.119565	−247.744655	−247.647834	
_sil_01	−775.187914	−774.873082	−773.738298	−773.423466	
_me_01	−287.893166	−287.751587	−287.327482	−287.185903	
20a					
_01	−287.528646	−287.401608	−286.968182	−286.841144	
_sil_01	−814.505462	−814.161527	−812.966605	−812.622670	
_me_01	−327.211625	−327.040078	−326.556484	−326.384937	
3d					
_01	−226.153472	−226.074909	−225.762930	−225.684367	
					−751.467619
_sil_01	−753.134927	−752.838383	−751.764361	−751.467817	
_sil_02	−753.131049	−752.835507	−751.760515	−751.464974	
_sil_03	−753.130000	−752.834435	−751.759647	−751.464082	
_me_01	−265.837290	−265.714056	−265.350950	−265.227716	

### 8.3 Computational Methods

**Table 8.1.** Continuation.

System	MPW1K/6-31+G(d)		MP2(FC)/G3MP2large//MPW1K/6-31+G(d)		
	E <sub>tot</sub>	H <sub>298</sub>	E <sub>tot</sub>	H <sub>298</sub>	<H <sub>298</sub> >
<hr/>					
<b>3e</b>					
_01	−265.456724	−265.347809	−264.975577	−264.866661	<b>−790.656154</b>
_sil_01	−792.443467	−792.116681	−790.983131	−790.656345	
_sil_02	−792.439557	−792.113750	−790.979255	−790.653448	
_sil_03	−792.438621	−792.112754	−790.978432	−790.652565	
_me_01	−305.146849	−304.993315	−304.570358	−304.416824	
<hr/>					
<b>3a</b>					
_01	−382.158062	−381.981128	−381.426958	−381.250024	<b>−420.8124204</b>
_sil_01	−909.151934	−908.756685	−907.442627	−907.047378	
_me_01	−421.860101	−421.910636	−421.638221	−420.812338	
_me_02	−421.858673	−421.909125	−421.638663	−420.812491	
_H_01	−372.554571	−382.362750	−381.817451	−381.625695	
<hr/>					
<b>3b</b>					
_01	−459.576289	−459.360534	−458.679678	−458.463923	<b>−592.0711206</b>
_sil_1	−986.573129	−986.138905	−984.698451	−984.264227	
_me_01	−499.281805	−499.022005	−498.290172	−498.030372	
_H_01	−459.976693	−459.746006	−459.073923	−458.843236	
<hr/>					
<b>3f</b>					
_01	−593.515444	−593.220176	−592.367220	−592.071951	<b>−1117.878506</b>
_02	−593.514749	−593.219530	−592.366124	−592.070905	
_04	−593.514069	−593.218961	−592.365843	−592.069775	
_05	−593.513869	−593.218551	−592.365294	−592.069496	
_06	−593.513225	−593.218495	−592.364870	−592.069289	
_07	−593.513290	−593.217691	−592.364823	−592.068940	
_09	−593.512170	−593.218216	−592.364014	−592.068105	
_08	−593.511963	−593.216797	−592.363474	−592.068308	
_10	−593.512460	−593.216777	−592.363498	−592.067724	
_03	−593.520404	−593.217522	−592.362662	−592.070565	
_sil_02	−1120.517043	−1120.003531	−1118.392797	−1117.879117	
_sil_01	−1120.517107	−1120.003453	−1118.392735	−1117.879125	
_sil_03	−1120.517123	−1120.003337	−1118.392800	−1117.879085	
_sil_06	−1120.517215	−1120.003369	−1118.392839	−1117.878973	
_sil_05	−1120.517157	−1120.003370	−1118.392860	−1117.878980	
_sil_04	−1120.517327	−1120.003273	−1118.392886	−1117.879001	
_sil_07	−1120.516958	−1120.003055	−1118.392503	−1117.878600	
_sil_08	−1120.516185	−1120.002749	−1118.391414	−1117.878229	
_sil_09	−1120.516185	−1120.002748	−1118.391414	−1117.878227	



Table 8.1. Continuation.

System	MPW1K/6-31+G(d)		MP2(FC)/G3MP2large//MPW1K/6-31+G(d)		
	E <sub>tot</sub>	H <sub>298</sub>	E <sub>tot</sub>	H <sub>298</sub>	<H <sub>298</sub> >
_sil_10	-1120.515987	-1120.002623	-1118.391262	-1117.878126	<b>-631.6442506</b>
_me_01	-633.227838	-632.887404	-631.985176	-631.644743	
_me_02	-633.227775	-632.887284	-631.985338	-631.644846	
_me_03	-633.227306	-632.886659	-631.984068	-631.643421	
_me_04	-633.226990	-632.886306	-631.983917	-631.643233	
_me_05	-633.226982	-632.886312	-631.983908	-631.643238	
_me_06	-633.226850	-632.886394	-631.984115	-631.643659	
_me_07	-633.226633	-632.886250	-631.984179	-631.643795	
_me_08	-633.225277	-632.884611	-631.982431	-631.641765	
_me_09	-633.224440	-632.883542	-631.980909	-631.640010	
_me_10	-633.224263	-632.883600	-631.981412	-631.640749	
_me_11	-633.220156	-632.879920	-631.976484	-631.636248	
_me_12	-633.219692	-632.879400	-631.976149	-631.635857	
_me_13	-633.216863	-632.876383	-631.972859	-631.632379	
<b>3g</b>					<b>-747.667541</b>
_01	-749.543575	-749.148245	-748.063656	-747.668326	<b>-1273.478667</b>
_02	-749.542960	-749.147756	-748.063146	-747.667870	
_03	-749.543032	-749.147263	-748.063178	-747.667482	
_06	-749.542525	-749.147727	-748.062300	-747.667306	
_05	-749.542673	-749.147078	-748.062900	-747.667305	
_04	-749.542673	-749.147079	-748.062900	-747.667131	
_08	-749.541623	-749.147208	-748.062543	-747.667224	
_07	-749.542896	-749.147271	-748.061576	-747.667226	
_10	-749.541563	-749.146870	-748.060705	-747.666038	
_09	-749.541562	-749.146877	-748.060723	-747.666012	
_sil_01	-1276.549133	-1275.935258	-1274.093314	-1273.479438	
_sil_02	-1276.549017	-1275.935032	-1274.093238	-1273.479253	
_sil_04	-1276.547385	-1275.933543	-1274.092015	-1273.477974	
_sil_03	-1276.547539	-1275.933447	-1274.091911	-1273.478019	
_sil_05	-1276.546803	-1275.932975	-1274.091144	-1273.477316	
_sil_06	-1276.546646	-1275.932891	-1274.090807	-1273.477053	
_sil_08	-1276.546425	-1275.932478	-1274.090943	-1273.476866	
_sil_10	-1276.546205	-1275.932653	-1274.090518	-1273.476634	
_sil_09	-1276.546305	-1275.932311	-1274.090938	-1273.476824	
_sil_07	-1276.546503	-1275.932522	-1274.090317	-1273.476918	
					<b>-787.2445322</b>
_me_01	-789.260264	-788.819689	-787.685822	-787.245247	
_me_02	-789.258550	-788.817855	-787.684553	-787.243859	

### 8.3 Computational Methods

**Table 8.1.** Continuation.

System	MPW1K/6-31+G(d)		MP2(FC)/G3MP2large//MPW1K/6-31+G(d)		
	E <sub>tot</sub>	H <sub>298</sub>	E <sub>tot</sub>	H <sub>298</sub>	<H <sub>298</sub> >
_me_03	−789.257797	−788.817415	−787.683481	−787.243099	
_me_04	−789.257619	−788.816883	−787.683635	−787.242898	
_me_05	−789.257322	−788.816937	−787.682996	−787.242611	
_me_06	−789.256515	−788.815926	−787.682233	−787.241644	
_me_07	−789.255785	−788.815377	−787.681816	−787.241408	
_me_08	−789.255644	−788.815048	−787.681686	−787.241090	
<b>3c</b>					<b>−535.691026</b>
_01	−537.001964	−536.747721	−535.945525	−535.691281	
_02	−537.001229	−536.747037	−535.944503	−535.690311	
					<b>−1061.495439</b>
_sil_03	−1064.003068	−1063.529531	−1061.968238	−1061.495502	
_sil_01	−1064.002315	−1063.529522	−1061.968209	−1061.495455	
_sil_02	−1064.002384	−1063.530332	−1061.968238	−1061.495347	
					<b>−575.2623129</b>
_me_01	−576.712746	−576.414228	−575.561076	−575.262558	
_me_02	−576.712060	−576.412522	−575.560456	−575.260918	
_H_01	−537.407327	−537.137881	−536.344020	−536.074574	
DMF	−248.441155	−248.328105	−248.016399	−247.903350	
					<b>−773.677155</b>
_sil_01	−775.413826	−775.082896	−774.008128	−773.677198	
_sil_02	−775.413819	−775.082871	−774.008123	−773.677176	
_sil_03	−775.413803	−775.082855	−774.008095	−773.677146	
_sil_04	−775.413797	−775.082841	−774.008107	−773.677152	
_sil_05	−775.413793	−775.082902	−774.008033	−773.677142	
_sil_06	−775.413789	−775.082826	−774.008120	−773.677157	
_sil_07	−775.413781	−775.082823	−774.008132	−773.677175	
_sil_08	−775.413776	−775.082804	−774.008088	−773.677116	
_sil_09	−775.413773	−775.082818	−774.008136	−773.677181	
_sil_10	−775.413770	−775.082849	−774.008023	−773.677102	
<b>20f</b>					<b>−1219.867052</b>
_01	−1222.737200	−1222.190818	−1220.413369	−1219.866987	
_02	−1222.737143	−1222.190746	−1220.413506	−1219.867109	
<b>20f-in</b>					<b>−1745.664882</b>
_01	−1749.711318	−1748.944019	−1746.432743	−1745.665445	
_02	−1749.710862	−1748.943682	−1746.432493	−1745.665313	
_03	−1749.710639	−1748.944104	−1746.430822	−1745.664287	
_04	−1749.710638	−1748.944107	−1746.430810	−1745.664279	
_05	−1749.710629	−1748.944110	−1746.430800	−1745.664281	
_06	−1749.709443	−1748.942912	−1746.429731	−1745.663200	
_07	−1749.708962	−1748.941550	−1746.430877	−1745.663464	

Table 8.1. Continuation.

System	MPW1K/6-31+G(d)		MP2(FC)/G3MP2large//MPW1K/6-31+G(d)		
	E <sub>tot</sub>	H <sub>298</sub>	E <sub>tot</sub>	H <sub>298</sub>	<H <sub>298</sub> >
_08	-1749.708380	-1748.941896	-1746.428649	-1745.662165	
<b>20f-out</b>					<b>-1745.665462</b>
_01	-1749.716117	-1748.948609	-1746.432676	-1745.665168	
_02	-1749.715559	-1748.949022	-1746.431955	-1745.665539	
_03	-1749.715552	-1748.949024	-1746.432053	-1745.665576	
_04	-1749.715533	-1748.949014	-1746.432104	-1745.665585	
_05	-1749.715525	-1748.949025	-1746.432073	-1745.660001	
_06	-1749.713572	-1748.946180	-1746.426503	-1745.659127	
_07	-1749.713569	-1748.946193	-1746.426519	-1745.658529	
_08	-1749.712991	-1748.946631	-1746.425906	-1745.659494	
_09	-1749.712972	-1748.946611	-1746.425854	-1745.659446	
_10	-1749.712947	-1748.946638	-1746.425807	-1745.659458	
_11	-1749.712873	-1748.946565	-1746.425766	-1745.659023	
_12	-1749.712758	-1748.945548	-1746.425331	-1745.658440	
_13	-1749.712488	-1748.945205	-1746.425650	-1745.664672	
<b>20f-in</b>					<b>-1259.438536</b>
_me_01	-1262.445595	-1261.852158	-1260.031715	-1259.438278	
_me_02	-1262.445113	-1261.852679	-1260.031145	-1259.438712	
_me_03	-1262.445105	-1261.852674	-1260.031135	-1259.438704	
_me_04	-1262.445099	-1261.852668	-1260.031137	-1259.438706	
_me_05	-1262.444547	-1261.851070	-1260.030893	-1259.437416	
_me_06	-1262.441552	-1261.848224	-1260.027175	-1259.433846	
_me_07	-1262.440237	-1261.846862	-1260.026580	-1259.433204	
_me_08	-1262.439680	-1261.847317	-1260.025957	-1259.433594	
<b>20f-out</b>					<b>-1259.438308</b>
_me_01	-1262.447726	-1261.853979	-1260.032155	-1259.438408	
_me_02	-1262.444579	-1261.851040	-1260.028692	-1259.435153	
<b>20d</b>					<b>-630.1019043</b>
_01	-631.629357	-631.326103	-630.405947	-630.102694	
_02	-631.628184	-631.324882	-630.404545	-630.101243	
_03	-631.627746	-631.324338	-630.403967	-630.100560	
_04	-631.627688	-631.324176	-630.403701	-630.100190	
_05	-631.626985	-631.323564	-630.402985	-630.099563	
_06	-631.626861	-631.323545	-630.403158	-630.099842	
_07	-631.626846	-631.323874	-630.402575	-630.099603	
_08	-631.625809	-631.322726	-630.402361	-630.099278	
_09	-631.625165	-631.322272	-630.400220	-630.097327	
_10	-631.624535	-631.321302	-630.400918	-630.097685	
					<b>-1155.91099</b>
_sil_01	-1158.632604	-1158.110642	-1156.433360	-1155.911399	

### 8.3 Computational Methods

**Table 8.1.** Continuation.

System	MPW1K/6-31+G(d)		MP2(FC)/G3MP2large//MPW1K/6-31+G(d)		
	E <sub>tot</sub>	H <sub>298</sub>	E <sub>tot</sub>	H <sub>298</sub>	<H <sub>298</sub> >
_sil_02	−1158.632512	−1158.110620	−1156.433211	−1155.911319	
_sil_03	−1158.632448	−1158.110520	−1156.433398	−1155.911470	
_sil_04	−1158.632401	−1158.110545	−1156.433299	−1155.911443	
_sil_05	−1158.631981	−1158.109978	−1156.431951	−1155.909948	
_sil_06	−1158.631882	−1158.109922	−1156.431773	−1155.909813	
_sil_07	−1158.631676	−1158.109628	−1156.431642	−1155.909593	
_sil_08	−1158.631589	−1158.109575	−1156.431549	−1155.909535	
_sil_09	−1158.631471	−1158.109549	−1156.432103	−1155.910181	
_sil_10	−1158.631443	−1158.109581	−1156.432344	−1155.910482	
_sil_11	−1158.631414	−1158.109460	−1156.432138	−1155.910184	
_sil_12	−1158.631360	−1158.109470	−1156.432321	−1155.910431	
_sil_13	−1158.627725	−1158.107317	−1156.426078	−1155.905670	
					−669.6766507
_me_01	−671.343411	−670.994868	−670.025807	−669.677264	
_me_02	−671.343351	−670.994831	−670.025530	−669.677010	
_me_03	−671.342834	−670.994084	−670.024437	−669.675686	
_me_04	−671.342580	−670.993804	−670.024268	−669.675493	
_me_05	−671.342421	−670.993836	−670.024620	−669.676036	
_me_06	−671.342385	−670.993760	−670.024437	−669.675812	
_me_07	−671.342385	−670.993762	−670.024436	−669.675814	
_me_08	−671.336066	−670.987734	−670.017190	−669.668859	
_me_09	−671.335698	−670.987296	−670.016882	−669.668480	
20c					−646.133931
_01	−647.641301	−647.350260	−646.425358	−646.134317	
_02	−647.639919	−647.348777	−646.424219	−646.133077	
_03	−647.638258	−647.347380	−646.422391	−646.131513	
_04	−647.636461	−647.345566	−646.420186	−646.129291	
_05	−647.634679	−647.344015	−646.418913	−646.128248	
_06	−647.632356	−647.341818	−646.415416	−646.124878	
					−1171.945366
_sil_01	−1174.645543	−1174.135913	−1172.455193	−1171.945562	
_sil_02	−1174.645412	−1174.135801	−1172.454980	−1171.945370	
_sil_03	−1174.645190	−1174.135564	−1172.454722	−1171.945096	
_sil_04	−1174.640681	−1174.131387	−1172.449267	−1171.939973	
_sil_05	−1174.640668	−1174.131324	−1172.449072	−1171.939728	
_sil_06	−1174.640058	−1174.130677	−1172.448075	−1171.938694	
_sil_07	−1174.639923	−1174.130581	−1172.448035	−1171.938692	
_sil_08	−1174.635062	−1174.126043	−1172.442505	−1171.933486	
_sil_09	−1174.633779	−1174.124798	−1172.440363	−1171.931382	
					−685.7112018

Table 8.1. Continuation.

System	MPW1K/6-31+G(d)		MP2(FC)/G3MP2large//MPW1K/6-31+G(d)		
	E <sub>tot</sub>	H <sub>298</sub>	E <sub>tot</sub>	H <sub>298</sub>	<H <sub>298</sub> >
_me_01	−687.356547	−687.020268	−686.047693	−685.711414	
_me_02	−687.356141	−687.019844	−686.047139	−685.710842	
_me_03	−687.351485	−687.015465	−686.041604	−685.705583	
_me_04	−687.350750	−687.014722	−686.040371	−685.704343	
_me_05	−687.345279	−687.009539	−686.034890	−685.699150	
_me_06	−687.343661	−687.008986	−686.032157	−685.697482	
<b>20e</b>					<b>−1017.321613</b>
_01	−1019.859807	−1019.348442	−1017.833861	−1017.322495	
_02	−1019.858765	−1019.346393	−1017.832393	−1017.320020	
_03	−1019.858753	−1019.346391	−1017.832508	−1017.320147	
_04	−1019.858689	−1019.346309	−1017.832338	−1017.319958	
_05	−1019.858639	−1019.346431	−1017.833532	−1017.321325	
_06	−1019.858621	−1019.346222	−1017.832043	−1017.319644	
_07	−1019.858570	−1019.346392	−1017.833308	−1017.321131	
_08	−1019.858542	−1019.346327	−1017.833401	−1017.321187	
_09	−1019.858404	−1019.346218	−1017.833033	−1017.320847	
					<b>−1543.135537</b>
_sil_01	−1546.865650	−1546.134812	−1543.866077	−1543.135239	
_sil_02	−1546.865643	−1546.134810	−1543.866080	−1543.135247	
_sil_03	−1546.865640	−1546.134813	−1543.866085	−1543.135257	
_sil_04	−1546.865628	−1546.134811	−1543.865807	−1543.134990	
_sil_05	−1546.865623	−1546.134794	−1543.866366	−1543.135537	
_sil_06	−1546.865612	−1546.134882	−1543.866105	−1543.135375	
_sil_07	−1546.865606	−1546.134773	−1543.866226	−1543.135393	
_sil_08	−1546.865601	−1546.134767	−1543.866320	−1543.135486	
_sil_09	−1546.865596	−1546.135728	−1543.866292	−1543.136424	
_sil_10	−1546.865594	−1546.134804	−1543.866213	−1543.135422	
_sil_11	−1546.865587	−1546.134805	−1543.866234	−1543.135452	
_sil_12	−1546.865579	−1546.134706	−1543.866221	−1543.135349	
_sil_13	−1546.865574	−1546.134713	−1543.866198	−1543.135336	
_sil_14	−1546.865554	−1546.134787	−1543.866324	−1543.135557	
_sil_15	−1546.865544	−1546.134769	−1543.866065	−1543.135290	
_sil_16	−1546.865535	−1546.134740	−1543.865971	−1543.135176	
_sil_17	−1546.865526	−1546.135735	−1543.865931	−1543.136140	
_sil_18	−1546.865521	−1546.134743	−1543.865980	−1543.135201	
_sil_19	−1546.865482	−1546.134666	−1543.865716	−1543.134900	
_sil_20	−1546.865478	−1546.134625	−1543.865923	−1543.135070	
_sil_21	−1546.865437	−1546.134771	−1543.866079	−1543.135413	
_sil_22	−1546.865435	−1546.134780	−1543.866060	−1543.135405	
_sil_23	−1546.865427	−1546.134672	−1543.866067	−1543.135312	

### 8.3 Computational Methods

**Table 8.1.** Continuation.

System	MPW1K/6-31+G(d)		MP2(FC)/G3MP2large//MPW1K/6-31+G(d)		
	E <sub>tot</sub>	H <sub>298</sub>	E <sub>tot</sub>	H <sub>298</sub>	<H <sub>298</sub> >
					<b>−1056.899569</b>
_me_01	−1059.577051	−1059.019593	−1057.457276	−1056.899818	
_me_02	−1059.577049	−1059.019597	−1057.457276	−1056.899825	
_me_03	−1059.577042	−1059.019463	−1057.457237	−1056.899658	
_me_04	−1059.577041	−1059.019463	−1057.457233	−1056.899655	
_me_05	−1059.577029	−1059.019492	−1057.457206	−1056.899668	
_me_06	−1059.577026	−1059.019501	−1057.457215	−1056.899690	
_me_07	−1059.577015	−1059.019533	−1057.457108	−1056.899626	
_me_08	−1059.577013	−1059.019429	−1057.457256	−1056.899672	
_me_09	−1059.577000	−1059.019447	−1057.457072	−1056.899518	
_me_10	−1059.576987	−1059.019458	−1057.457113	−1056.899584	
_me_11	−1059.576982	−1059.019430	−1057.457004	−1056.899451	
_me_12	−1059.576926	−1059.019455	−1057.456973	−1056.899502	
_me_13	−1059.576899	−1059.019392	−1057.457126	−1056.899619	
_me_14	−1059.576849	−1059.019332	−1057.456962	−1056.899445	
_me_15	−1059.576835	−1059.019281	−1057.456915	−1056.899361	
_me_16	−1059.576831	−1059.019309	−1057.456973	−1056.899451	
_me_17	−1059.576813	−1059.019231	−1057.456776	−1056.899194	
_me_18	−1059.576808	−1059.019232	−1057.456770	−1056.899194	
_me_19	−1059.576772	−1059.019219	−1057.456751	−1056.899198	
<b>20b</b>					
_01	−609.524002	−609.242767	−608.385763	−608.104528	
					<b>−1133.907697</b>
_sil_01	−1136.525526	−1136.025854	−1134.407434	−1133.907762	
_sil_02	−1136.525468	−1136.025705	−1134.407384	−1133.907621	
_me_01	−649.235795	−648.909439	−648.000337	−647.673981	

**Table 8.2.** Data for pyridine-based *N*-heterocycles and their TBS adducts. Gas phase calculation with additional PCM values in CHCl<sub>3</sub>.

System	MP2(FC)/G3MP2large// MPW1K/6-31+G(d)		PCM/UAHF/MPW1K/6-31+G(d)	
	E <sub>tot</sub>	ΔG <sub>solv</sub>	ΔH <sub>298</sub>	<H <sub>298</sub> >
Pyridine				
_01	−247.647834	−0.003588853	−247.651423	
_sil_01	−773.423466	−0.041269609	−773.464736	
_me_01	−287.185903	−0.056548318	−287.242452	
<b>20a</b>				
_01	−286.841144	−0.003423044	−286.844567	

Table 8.2. Continuation.

System	MP2(FC)/G3MP2large// MPW1K/6-31+G(d)	PCM/UAHF/MPW1K/6-31+G(d)		
	$E_{\text{tot}}$	$\Delta G_{\text{solv}}$	$\Delta H_{298}$	$\langle H_{298} \rangle$
_sil_01	−812.622670	−0.045262904	−812.667933	
_me_01	−326.384937	−0.054158908	−326.439096	
<hr/>				
<b>3d</b>				
_01	−225.684367	−0.007441933	−225.691809	
				−751.467619
_sil_01	−751.467817	−0.046928852	−751.514746	
_sil_02	−751.464974	−0.046961179	−751.511935	
_sil_03	−751.464082	−0.047198284	−751.511280	
_me_01	−265.227716	−0.061512458	−265.289229	
<hr/>				
<b>3e</b>				
_01	−264.866661	−0.006199577	−264.872861	
				−790.656154
_sil_01	−790.656345	−0.042377133	−790.698722	
_sil_02	−790.653448	−0.042249710	−790.695698	
_sil_03	−790.652565	−0.042781461	−790.695346	
_me_01	−304.416824	−0.056448395	−304.473272	
<hr/>				
<b>3a</b>				
_01	−381.250024	−0.005888762	−381.255913	
_sil_01	−907.047378	−0.038258696	−907.085637	
				−420.812420
_me_01	−420.812338	−0.050534233	−420.862872	
_me_02	−420.812491	−0.050451839	−420.862943	
_H_01	−381.817450	−0.054578438	−381.680208	
<hr/>				
<b>3b</b>				
_01	−458.463923	−0.007244452	−458.471168	
_sil_1	−984.264227	−0.038318889	−984.302546	
_me_01	−498.030372	−0.049122860	−498.079495	
_H_01	−459.073923	−0.052986984	−458.896223	
<hr/>				
<b>3f</b>				−592.071121
_01	−592.071951	−0.00677571	−592.078727	
_02	−592.070905	−0.00678336	−592.077688	
_04	−592.069775	−0.006986736	−592.076762	
_05	−592.069496	−0.006948848	−592.076445	
_06	−592.069289	−0.006989972	−592.076279	
_07	−592.068940	−0.006018229	−592.074958	
_09	−592.068105	−0.006785078	−592.074890	
_08	−592.068308	−0.005963194	−592.074271	
_10	−592.067724	−0.006061872	−592.073786	
_03	−592.070565	−0.000491426	−592.071056	

### 8.3 Computational Methods

**Table 8.2.** Continuation.

System	MP2(FC)/G3MP2large// MPW1K/6-31+G(d)	PCM/UAHF/MPW1K/6-31+G(d)		
	E <sub>tot</sub>	$\Delta G_{\text{solv}}$	$\Delta H_{298}$	$\langle H_{298} \rangle$
				<b>−1117.878506</b>
_sil_02	−1117.879117	−0.03485935	−1117.913976	
_sil_01	−1117.879125	−0.03471492	−1117.913840	
_sil_03	−1117.879085	−0.03467924	−1117.913764	
_sil_06	−1117.878973	−0.03471981	−1117.913693	
_sil_05	−1117.878980	−0.03469664	−1117.913677	
_sil_04	−1117.879001	−0.03466109	−1117.913662	
_sil_07	−1117.878600	−0.03455587	−1117.913156	
_sil_08	−1117.878229	−0.03467415	−1117.912903	
_sil_09	−1117.878227	−0.03467409	−1117.912901	
_sil_10	−1117.878126	−0.03469784	−1117.912824	
				<b>−631.644251</b>
_me_01	−631.644743	−0.047285965	−631.692029	
_me_02	−631.644846	−0.047351874	−631.692198	
_me_03	−631.643421	−0.04705067	−631.690472	
_me_04	−631.643233	−0.047119435	−631.690353	
_me_05	−631.643238	−0.0471106	−631.690349	
_me_06	−631.643659	−0.047342443	−631.691002	
_me_07	−631.643795	−0.047437291	−631.691233	
_me_08	−631.641765	−0.046938925	−631.688704	
_me_09	−631.640010	−0.046701214	−631.686712	
_me_10	−631.640749	−0.046950874	−631.687700	
_me_11	−631.636248	−0.047835983	−631.684084	
_me_12	−631.635857	−0.047869688	−631.683726	
_me_13	−631.632379	−0.04749021	−631.679870	
<b>3g</b>				<b>−747.667541</b>
_01	−747.668326	−0.004441183	−747.672767	
_02	−747.667870	−0.004389472	−747.672259	
_03	−747.667482	−0.004575526	−747.672058	
_06	−747.667306	−0.004555183	−747.671861	
_05	−747.667305	−0.004534879	−747.671840	
_04	−747.667131	−0.004533863	−747.671665	
_08	−747.667224	−0.003405002	−747.670629	
_07	−747.667226	−0.003295993	−747.670522	
_10	−747.666038	−0.003294399	−747.669332	
_09	−747.666012	−0.003293909	−747.669306	
				<b>−1273.478667</b>
_sil_01	−1273.479438	−0.03010476	−1273.509543	
_sil_02	−1273.479253	−0.03027728	−1273.509530	



Table 8.2. Continuation.

System	MP2(FC)/G3MP2large// MPW1K/6-31+G(d)	PCM/UAHF/MPW1K/6-31+G(d)		
	$E_{\text{tot}}$	$\Delta G_{\text{solv}}$	$\Delta H_{298}$	$\langle H_{298} \rangle$
_sil_04	−1273.477974	−0.03102941	−1273.509003	
_sil_03	−1273.478019	−0.03076112	−1273.508780	
_sil_05	−1273.477316	−0.03028413	−1273.507600	
_sil_06	−1273.477053	−0.03033832	−1273.507391	
_sil_08	−1273.476866	−0.03022415	−1273.507090	
_sil_10	−1273.476634	−0.0303826	−1273.507017	
_sil_09	−1273.476824	−0.03018489	−1273.507009	
_sil_07	−1273.476918	−0.02986133	−1273.506779	
				−787.244532
_me_01	−787.245247	−0.044351415	−787.289598	
_me_02	−787.243859	−0.044777933	−787.288636	
_me_03	−787.243099	−0.044430608	−787.287529	
_me_04	−787.242898	−0.044089637	−787.286988	
_me_05	−787.242611	−0.044580268	−787.287191	
_me_06	−787.241644	−0.044835031	−787.286479	
_me_07	−787.241408	−0.044827202	−787.286235	
_me_08	−787.241090	−0.044280225	−787.285370	
3c				−535.691026
_01	−535.691281	−0.008780639	−535.700062	
_02	−535.690311	−0.009046961	−535.699358	
				−1061.495439
_sil_03	−1061.495502	−0.03920786	−1061.534710	
_sil_01	−1061.495455	−0.03925046	−1061.534705	
_sil_02	−1061.495347	−0.03917397	−1061.534521	
				−575.262313
_me_01	−575.262558	−0.048568514	−575.311127	
_me_02	−575.260918	−0.048606049	−575.309524	
_H_01	−536.344020	−0.052185255	−536.126759	
DMF	−247.903350	−0.005161118	−247.908511	
				−773.677155
_sil_01	−773.677198	−0.051393685	−773.728591	
_sil_02	−773.677176	−0.051364491	−773.728540	
_sil_03	−773.677146	−0.051302372	−773.728449	
_sil_04	−773.677152	−0.051361849	−773.728513	
_sil_05	−773.677142	−0.051453328	−773.728595	
_sil_06	−773.677157	−0.051246756	−773.728404	
_sil_07	−773.677175	−0.051242561	−773.728417	
_sil_08	−773.677116	−0.051362814	−773.728479	
_sil_09	−773.677181	−0.051278487	−773.728460	

### 8.3 Computational Methods

**Table 8.2.** Continuation.

System	MP2(FC)/G3MP2large// MPW1K/6-31+G(d)	PCM/UAHF/MPW1K/6-31+G(d)		
	$E_{\text{tot}}$	$\Delta G_{\text{solv}}$	$\Delta H_{298}$	$\langle H_{298} \rangle$
<i>_sil_10</i>	−773.677102	−0.051395053	−773.728497	
<b>20f</b>				<b>−1219.867052</b>
<i>_01</i>	−1219.866987	−0.00776147	−1219.874749	
<i>_02</i>	−1219.867109	−0.00768068	−1219.874789	
<b>20f-in</b>				<b>−1745.664882</b>
<i>_01</i>	−1745.665445	−0.0365691	−1745.702014	
<i>_02</i>	−1745.665313	−0.0365439	−1745.701857	
<i>_03</i>	−1745.664287	−0.03553876	−1745.699826	
<i>_04</i>	−1745.664279	−0.03553676	−1745.699816	
<i>_05</i>	−1745.664281	−0.03553464	−1745.699815	
<i>_06</i>	−1745.663200	−0.03568828	−1745.698888	
<i>_07</i>	−1745.663464	−0.03582439	−1745.699289	
<i>_08</i>	−1745.662165	−0.03655233	−1745.698717	
<b>20f-out</b>				<b>−1745.665462</b>
<i>_01</i>	−1745.665168	−0.03783744	−1745.703005	
<i>_02</i>	−1745.665539	−0.03780967	−1745.703349	
<i>_03</i>	−1745.665576	−0.03781778	−1745.703394	
<i>_04</i>	−1745.665585	−0.03780553	−1745.703390	
<i>_05</i>	−1745.660001	−0.03779106	−1745.697792	
<i>_06</i>	−1745.659127	−0.03812598	−1745.697253	
<i>_07</i>	−1745.658529	−0.03812271	−1745.696652	
<i>_08</i>	−1745.659494	−0.03812075	−1745.697615	
<i>_09</i>	−1745.659446	−0.03810489	−1745.697551	
<i>_10</i>	−1745.659458	−0.03814664	−1745.697604	
<i>_11</i>	−1745.659023	−0.038132	−1745.697155	
<i>_12</i>	−1745.658440	−0.03819427	−1745.696634	
<i>_13</i>	−1745.664672	−0.03802606	−1745.702698	
<b>20f-in</b>				<b>−1259.438536</b>
<i>_me_01</i>	−1259.438278	−0.03802758	−1259.476306	
<i>_me_02</i>	−1259.438712	−0.03798358	−1259.476695	
<i>_me_03</i>	−1259.438704	−0.03798057	−1259.476685	
<i>_me_04</i>	−1259.438706	−0.03797877	−1259.476685	
<i>_me_05</i>	−1259.437416	−0.03759596	−1259.475012	
<i>_me_06</i>	−1259.433846	−0.03817111	−1259.472018	
<i>_me_07</i>	−1259.433204	−0.03824395	−1259.471448	
<i>_me_08</i>	−1259.433594	−0.03816251	−1259.471757	
<b>"20f-out "</b>				<b>−1259.438308</b>
<i>_me_01</i>	−1259.438408	−0.04110669	−1259.479515	

Table 8.2. Continuation.

System	MP2(FC)/G3MP2large// MPW1K/6-31+G(d)	PCM/UAHF/MPW1K/6-31+G(d)		
	$E_{\text{tot}}$	$\Delta G_{\text{solv}}$	$\Delta H_{298}$	$\langle H_{298} \rangle$
_me_02	-1259.435153	-0.0417951	-1259.476948	
<b>20d</b>				<b>-630.101904</b>
_01	-630.102694	-0.006264526	-630.108958	
_02	-630.101243	-0.00620357	-630.107446	
_03	-630.100560	-0.00656935	-630.107129	
_04	-630.100190	-0.006287947	-630.106478	
_05	-630.099563	-0.006510991	-630.106074	
_06	-630.099842	-0.006471662	-630.106314	
_07	-630.099603	-0.006047833	-630.105651	
_08	-630.099278	-0.00623052	-630.105509	
_09	-630.097327	-0.006342843	-630.103670	
_10	-630.097685	-0.006212386	-630.103898	
		0		<b>-1155.910990</b>
_sil_01	-1155.911399	-0.04184988	-1155.953249	
_sil_02	-1155.911319	-0.04190475	-1155.953223	
_sil_03	-1155.911470	-0.04189613	-1155.953366	
_sil_04	-1155.911443	-0.04190715	-1155.953350	
_sil_05	-1155.909948	-0.04158879	-1155.951537	
_sil_06	-1155.909813	-0.04160346	-1155.951416	
_sil_07	-1155.909593	-0.04152065	-1155.951114	
_sil_08	-1155.909535	-0.04152859	-1155.951063	
_sil_09	-1155.910181	-0.04201541	-1155.952196	
_sil_10	-1155.910482	-0.04200085	-1155.952483	
_sil_11	-1155.910184	-0.04191697	-1155.952101	
_sil_12	-1155.910431	-0.04187324	-1155.952304	
_sil_13	-1155.905670	-0.04182291	-1155.947493	
				<b>-669.676651</b>
_me_01	-669.677264	-0.047326586	-669.724591	
_me_02	-669.677010	-0.047330549	-669.724340	
_me_03	-669.675686	-0.047112111	-669.722799	
_me_04	-669.675493	-0.047077888	-669.722571	
_me_05	-669.676036	-0.047336517	-669.723372	
_me_06	-669.675812	-0.04737082	-669.723183	
_me_07	-669.675814	-0.047370012	-669.723184	
_me_08	-669.668859	-0.047955407	-669.716814	
_me_09	-669.668480	-0.047903197	-669.716383	
<b>20c</b>				<b>-646.133931</b>
_01	-646.134317	-0.007307173	-646.141624	
_02	-646.133077	-0.007599943	-646.140677	

**Table 8.2.** Continuation.

System	MP2(FC)/G3MP2large// MPW1K/6-31+G(d)	PCM/UAHF/MPW1K/6-31+G(d)		
	$E_{\text{tot}}$	$\Delta G_{\text{solv}}$	$\Delta H_{298}$	$\langle H_{298} \rangle$
_03	−646.131513	−0.007253136	−646.138766	
_04	−646.129291	−0.007547939	−646.136839	
_05	−646.128248	−0.007117596	−646.135366	
_06	−646.124878	−0.007357063	−646.132236	
				<b>−1171.945366</b>
_sil_01	−1171.945562	−0.04216327	−1171.987725	
_sil_02	−1171.945370	−0.0422221	−1171.987592	
_sil_03	−1171.945096	−0.04231359	−1171.987410	
_sil_04	−1171.939973	−0.04236825	−1171.982341	
_sil_05	−1171.939728	−0.04237452	−1171.982103	
_sil_06	−1171.938694	−0.04248986	−1171.981184	
_sil_07	−1171.938692	−0.04250373	−1171.981196	
_sil_08	−1171.933486	−0.04238634	−1171.975872	
_sil_09	−1171.931382	−0.04250579	−1171.973887	
				<b>−685.711202</b>
_me_01	−685.711414	−0.04774796	−685.759162	
_me_02	−685.710842	−0.047861011	−685.758703	
_me_03	−685.705583	−0.048118535	−685.753702	
_me_04	−685.704343	−0.048193175	−685.752536	
_me_05	−685.699150	−0.048172879	−685.747323	
_me_06	−685.697482	−0.048462598	−685.745945	
<b>20e</b>				<b>−1017.321613</b>
_01	−1017.322495	−0.00617871	−1017.328674	
_02	−1017.320020	−0.00671831	−1017.326739	
_03	−1017.320147	−0.00658572	−1017.326732	
_04	−1017.319958	−0.00658149	−1017.326539	
_05	−1017.321325	−0.00624308	−1017.327568	
_06	−1017.319644	−0.00671642	−1017.326360	
_07	−1017.321131	−0.0064097	−1017.327540	
_08	−1017.321187	−0.0062661	−1017.327453	
_09	−1017.320847	−0.00642801	−1017.327275	
				<b>−1543.135537</b>
_sil_01	−1543.135239	−0.03946999	−1543.174709	
_sil_02	−1543.135247	−0.03945239	−1543.174700	
_sil_03	−1543.135257	−0.03943999	−1543.174697	
_sil_04	−1543.134990	−0.03958676	−1543.174577	
_sil_05	−1543.135537	−0.03951477	−1543.175052	
_sil_06	−1543.135375	−0.03949899	−1543.174874	

Table 8.2. Continuation.

System	MP2(FC)/G3MP2large// MPW1K/6-31+G(d)	PCM/UAHF/MPW1K/6-31+G(d)		
	$E_{\text{tot}}$	$\Delta G_{\text{solv}}$	$\Delta H_{298}$	$\langle H_{298} \rangle$
_sil_07	−1543.135393	−0.03938514	−1543.174778	
_sil_08	−1543.135486	−0.03937098	−1543.174856	
_sil_09	−1543.136424	−0.03937975	−1543.175804	
_sil_10	−1543.135422	−0.03936237	−1543.174785	
_sil_11	−1543.135452	−0.03933706	−1543.174789	
_sil_12	−1543.135349	−0.03931103	−1543.174660	
_sil_13	−1543.135336	−0.0393574	−1543.174694	
_sil_14	−1543.135557	−0.03924012	−1543.174797	
_sil_15	−1543.135290	−0.03927273	−1543.174563	
_sil_16	−1543.135176	−0.03945328	−1543.174629	
_sil_17	−1543.136140	−0.03928288	−1543.175423	
_sil_18	−1543.135201	−0.03928845	−1543.174490	
_sil_19	−1543.134900	−0.03951529	−1543.174415	
_sil_20	−1543.135070	−0.0393405	−1543.174411	
_sil_21	−1543.135413	−0.03944439	−1543.174858	
_sil_22	−1543.135405	−0.03943887	−1543.174844	
_sil_23	−1543.135312	−0.03929213	−1543.174604	
				−1056.899569
_me_01	−1056.899818	−0.04347056	−1056.943289	
_me_02	−1056.899825	−0.04347172	−1056.943296	
_me_03	−1056.899658	−0.04358207	−1056.943240	
_me_04	−1056.899655	−0.04357785	−1056.943233	
_me_05	−1056.899668	−0.04350245	−1056.943171	
_me_06	−1056.899690	−0.04350226	−1056.943192	
_me_07	−1056.899626	−0.04359551	−1056.943221	
_me_08	−1056.899672	−0.043605	−1056.943277	
_me_09	−1056.899518	−0.04374024	−1056.943259	
_me_10	−1056.899584	−0.04360842	−1056.943193	
_me_11	−1056.899451	−0.04365174	−1056.943103	
_me_12	−1056.899502	−0.04363359	−1056.943135	
_me_13	−1056.899619	−0.04347742	−1056.943096	
_me_14	−1056.899445	−0.04354881	−1056.942994	
_me_15	−1056.899361	−0.04354659	−1056.942907	
_me_16	−1056.899451	−0.04361547	−1056.943066	
_me_17	−1056.899194	−0.04372819	−1056.942923	
_me_18	−1056.899194	−0.04373316	−1056.942928	
_me_19	−1056.899198	−0.04365395	−1056.942852	
<b>20b</b>				
_01	−608.104528	−0.006058769	−608.110587	

### 8.3 Computational Methods

**Table 8.2.** Continuation.

System	MP2(FC)/G3MP2large// MPW1K/6-31+G(d)	PCM/UAHF/MPW1K/6-31+G(d)		
	E <sub>tot</sub>	$\Delta G_{\text{solv}}$	$\Delta H_{298}$	$\langle H_{298} \rangle$
				<b>−1133.907697</b>
_sil_01	−1133.907762	−0.04043705	−1133.948199	
_sil_02	−1133.907621	−0.04041168	−1133.948033	
_me_01	−647.673981	−0.045865804	−647.719847	

**Table 8.3.** Silyl- and methyl cation affinities (in kJ/mol) of pyridine-based *N*-heterocyclic compounds relative to pyridine (gas and solution phase data).

System	Silyl cation affinities		Methyl cation affinities	
	$\Delta H_{298}$	$\Delta H_{298}$ (sol)	$\Delta H_{298}$	$\Delta H_{298}$ (sol)
Pyridine	0	0	0	0
DMF	+4.8	−17.5	n.d.	n.d.
<b>20a</b>	−15.5	−26.4	−15.0	−9.2
<b>20f-in</b>	−58.3	−35.3	−87.7	−28.2
<b>20f-out</b>	−59.8	−39.7	−87.1	−35.6
<b>3a</b>	−57.0	−43.1	−63.9	−41.9
<b>3b</b>	−64.8	−47.4	−74.5	−45.4
<b>3c</b>	−75.6	−56.5	−87.2	−52.5
<b>3f</b>	−83.4	−58.5	−92.1	−59.2
<b>3g</b>	−93.2	−62.0	−102.2	−67.7
<b>20b</b>	−72.3	−63.6	−82.4	−47.9
<b>20d</b>	−87.8	−82.5	−96.3	−65.1
<b>20c</b>	−94.0	−86.7	−102.9	−70.1
<b>20e</b>	−100.5	−88.8	−104.7	−63.9

**Table 8.4.** Data for phosphane-based catalysts and their TBS adducts (gas phase data).

System	MPW1K/6-31+G(d)		MP2(FC)/G3MP2large//MPW1K/6-31+G(d)		
	E <sub>tot</sub>	H <sub>298</sub>	E <sub>tot</sub>	H <sub>298</sub>	$\langle H_{298} \rangle$
PPh <sub>3</sub> ( <b>17a</b> )					<b>−1033.987279</b>
_01	−1036.132096	−1035.832985	−1034.286365	−1033.987253	
_02	−1036.132010	−1035.832936	−1034.286378	−1033.987304	
					<b>−1559.764848</b>
_sil_01	−1563.097437	−1562.580497	−1560.281584	−1559.764644	
_sil_02	−1563.097430	−1562.580426	−1560.281564	−1559.764560	
_sil_03	−1563.097393	−1562.581275	−1560.281515	−1559.765396	

Table 8.4. Continuation.

System	MPW1K/6-31+G(d)		MP2(FC)/G3MP2large//MPW1K/6-31+G(d)		
	E <sub>tot</sub>	H <sub>298</sub>	E <sub>tot</sub>	H <sub>298</sub>	<H <sub>298</sub> >
_sil_04	-1563.096934	-1562.580765	-1560.280971	-1559.764802	
_sil_05	-1563.096852	-1562.580636	-1560.280981	-1559.764765	
_sil_06	-1563.096206	-1562.578978	-1560.280085	-1559.762857	
_sil_07	-1563.096199	-1562.578987	-1560.280088	-1559.762875	
					-1034.353546
_H_01	-1036.515109	-1036.514898	-1036.514059	-1034.3537413	
_H_02	-1036.204454	-1036.204281	-1036.204253	-1034.3535261	
_H_03	-1034.664396	-1034.664143	-1034.663047	-1034.3532412	
P(OMe) <sub>3</sub> (17b)					-685.571954
_01	-686.675145	-686.530787	-685.716627	-685.572269	
_02	-686.673138	-686.528877	-685.715263	-685.571001	
_03	-686.670866	-686.526596	-685.712615	-685.568344	
_04	-686.668255	-686.524075	-685.710486	-685.566306	
					-1211.333542
_sil_01	-1213.629704	-1213.267446	-1211.696318	-1211.334061	
_sil_02	-1213.629186	-1213.266967	-1211.695702	-1211.333483	
_sil_03	-1213.629029	-1213.266831	-1211.695362	-1211.333164	
_sil_04	-1213.629005	-1213.266749	-1211.695433	-1211.333177	
_sil_05	-1213.627798	-1213.265583	-1211.694640	-1211.332424	
					-685.924863
_H_01	-687.032334	-686.875401	-686.082173	-685.925240	
_H_02	-687.030906	-686.874085	-686.080856	-685.924035	
_H_03	-687.028576	-686.871772	-686.079501	-685.922697	
PpTol <sub>3</sub> (17c)					-1151.566315
_01	-1154.064300	-1153.675995	-1151.954273	-1151.565968	
_02	-1154.064240	-1153.674978	-1151.954221	-1151.564959	
_03	-1154.064222	-1153.675912	-1151.954054	-1151.565744	
_04	-1154.064172	-1153.676816	-1151.954071	-1151.566715	
_05	-1154.064163	-1153.676803	-1151.953958	-1151.565633	
_06	-1154.064125	-1153.675838	-1151.95398	-1151.566620	
_07	-1154.064086	-1153.676765	-1151.954021	-1151.565761	
_08	-1154.064073	-1153.675826	-1151.954104	-1151.563435	
_09	-1154.061704	-1153.673403	-1151.951278	-1151.562977	
					-1677.349936
_sil_01	-1681.036310	-1680.430931	-1677.955725	-1677.350346	
_sil_02	-1681.036250	-1680.430986	-1677.955768	-1677.350504	
_sil_03	-1681.036203	-1680.428916	-1677.955746	-1677.348459	
_sil_04	-1681.036150	-1680.428915	-1677.955701	-1677.348466	
_sil_05	-1681.034947	-1680.427603	-1677.954354	-1677.347010	
_sil_06	-1681.034881	-1680.429424	-1677.954287	-1677.348830	

### 8.3 Computational Methods

**Table 8.4.** Continuation.

System	MPW1K/6-31+G(d)		MP2(FC)/G3MP2large//MPW1K/6-31+G(d)		
	E <sub>tot</sub>	H <sub>298</sub>	E <sub>tot</sub>	H <sub>298</sub>	<H <sub>298</sub> >
_sil_07	−1681.034734	−1680.429414	−1677.954217	−1677.348897	
_sil_08	−1681.034720	−1680.428447	−1677.954162	−1677.347889	
					<b>−1151.941045</b>
_H_01	−1154.455950	−1154.057086	−1152.339939	−1151.941075	
_H_02	−1154.455831	−1154.056000	−1152.339809	−1151.939978	
_H_03	−1154.455655	−1154.055848	−1152.339733	−1151.939926	
_H_04	−1154.455562	−1154.056637	−1152.339692	−1151.940767	
_H_05	−1154.455374	−1154.057510	−1152.339414	−1151.941550	
P(PhOMe) <sub>3</sub> (17d)					<b>−1376.847679</b>
_01	−1379.598832	−1379.190401	−1377.256087	−1376.847656	
_02	−1379.598824	−1379.190405	−1377.255965	−1376.847546	
_03	−1379.598822	−1379.190435	−1377.256006	−1376.847619	
_04	−1379.598818	−1379.190426	−1377.255942	−1376.847549	
_05	−1379.598802	−1379.190352	−1377.256064	−1376.847614	
_06	−1379.598788	−1379.190394	−1377.255981	−1376.847586	
_07	−1379.598784	−1379.190406	−1377.256102	−1376.847724	
_08	−1379.598777	−1379.190390	−1377.256078	−1376.847691	
_09	−1379.598765	−1379.190376	−1377.256098	−1376.847709	
_10	−1379.598755	−1379.190453	−1377.256102	−1376.847800	
_11	−1379.598754	−1379.190450	−1377.256093	−1376.847788	
_12	−1379.598750	−1379.190400	−1377.255908	−1376.847557	
_13	−1379.598746	−1379.190421	−1377.256049	−1376.847724	
_14	−1379.598739	−1379.190419	−1377.256099	−1376.847779	
_15	−1379.598733	−1379.190407	−1377.256080	−1376.847754	
_16	−1379.598730	−1379.190333	−1377.256119	−1376.847723	
_17	−1379.598726	−1379.190313	−1377.255994	−1376.847581	
_18	−1379.598643	−1379.190309	−1377.256027	−1376.847693	
					<b>−1902.635471</b>
_sil_01	−1906.575607	−1905.94909	−1903.262528	−1902.636012	
_sil_02	−1906.575196	−1905.948753	−1903.262419	−1902.635976	
_sil_03	−1906.575110	−1905.948665	−1903.262324	−1902.635879	
_sil_04	−1906.575109	−1905.948665	−1903.262322	−1902.635878	
_sil_05	−1906.575025	−1905.94856	−1903.262217	−1902.635753	
_sil_06	−1906.574809	−1905.948353	−1903.262141	−1902.635685	
_sil_07	−1906.574724	−1905.948338	−1903.26201	−1902.635624	
_sil_08	−1906.574605	−1905.948191	−1903.261949	−1902.635535	
_sil_09	−1906.574460	−1905.947998	−1903.261789	−1902.635327	
_sil_10	−1906.574239	−1905.947629	−1903.261131	−1902.634522	
_sil_11	−1906.573905	−1905.947328	−1903.260938	−1902.634361	
_sil_12	−1906.573900	−1905.94733	−1903.260938	−1902.634367	



**Table 8.4.** Continuation.

System	MPW1K/6-31+G(d)		MP2(FC)/G3MP2large//MPW1K/6-31+G(d)		
	E <sub>tot</sub>	H <sub>298</sub>	E <sub>tot</sub>	H <sub>298</sub>	<H <sub>298</sub> >
_sil_13	−1906.573765	−1905.947232	−1903.260704	−1902.634170	
_sil_14	−1906.573765	−1905.94723	−1903.260703	−1902.634168	
_sil_15	−1906.573714	−1905.947164	−1903.260764	−1902.634215	
_sil_16	−1906.573712	−1905.947164	−1903.260763	−1902.634215	
_sil_17	−1906.573492	−1905.946932	−1903.260488	−1902.633928	
_sil_18	−1906.573413	−1905.946887	−1903.260586	−1902.634061	
_sil_19	−1906.573332	−1905.946763	−1903.260425	−1902.633857	
_sil_20	−1906.573331	−1905.946764	−1903.260424	−1902.633857	
_sil_21	−1906.573016	−1905.946655	−1903.26023	−1902.633869	
					−1377.227763
_H_01	−1379.996295	−1379.576193	−1377.647903	−1377.227802	
_H_02	−1379.996125	−1379.576082	−1377.647766	−1377.227723	
_H_03	−1379.996120	−1379.576076	−1377.647743	−1377.227699	
_H_04	−1379.996049	−1379.576048	−1377.647902	−1377.227901	
_H_05	−1379.996034	−1379.575926	−1377.647710	−1377.227602	
_H_06	−1379.996029	−1379.575963	−1377.647808	−1377.227741	
_H_07	−1379.996016	−1379.575943	−1377.647816	−1377.227743	
_H_08	−1379.996008	−1379.575951	−1377.647789	−1377.227732	
_H_09	−1379.995988	−1379.575921	−1377.647809	−1377.227741	
_H_10	−1379.995965	−1379.575950	−1377.647746	−1377.227732	
_H_11	−1379.995901	−1379.575877	−1377.647705	−1377.227681	
_H_12	−1379.995864	−1379.575873	−1377.647798	−1377.227807	
_H_13	−1379.995798	−1379.575805	−1377.647772	−1377.227780	
_H_14	−1379.995296	−1379.576116	−1377.647085	−1377.227905	
P(NMe <sub>2</sub> ) <sub>3</sub> ( <b>17e</b> )					−743.459132
_01	−744.975610	−744.702368	−743.731282	−743.458040	
					−1269.235830
_sil_01	−1271.941308	−1271.448573	−1269.728810	−1269.236075	
_sil_02	−1271.938973	−1271.447636	−1269.725769	−1269.234432	

**Table 8.5.** Data for phophane-based catalysts and their TBS adducts. Gas phase calculation with additional PCM values in CHCl<sub>3</sub>.

System	MP2(FC)/G3MP2large//MPW1K/6-31+G(d)		PCM/UAHF/MPW1K/6-31+G(d)	
	E <sub>tot</sub>	ΔG <sub>solv</sub>	ΔH <sub>298</sub>	<H <sub>298</sub> >
<b>17a</b>				−1033.990302
_01	−1033.987253	−0.003023	−1033.990276	
_02	−1033.987304	−0.003023	−1033.990327	

### 8.3 Computational Methods

**Table 8.5:** Continuation.

System	MP2(FC)/G3MP2large// MPW1K/6-31+G(d)	PCM/UAHF/MPW1K/6-31+G(d)		
	E <sub>tot</sub>	$\Delta G_{\text{solv}}$	$\Delta H_{298}$	$\langle H_{298} \rangle$
				<b>−1559.802816</b>
_sil_01	−1559.764644	−0.037985	−1559.802629	
_sil_02	−1559.764560	−0.037938	−1559.802498	
_sil_03	−1559.765396	−0.037975	−1559.803371	
_sil_04	−1559.764802	−0.037907	−1559.802709	
_sil_05	−1559.764765	−0.037981	−1559.802746	
_sil_06	−1559.762857	−0.037884	−1559.800740	
_sil_07	−1559.762875	−0.037868	−1559.800743	
				<b>−1034.398931</b>
_H_01	−1036.514059	−0.04550433	−1034.399246	
_H_02	−1036.204253	−0.04526707	−1034.398793	
_H_03	−1034.663047	−0.04508009	−1034.398321	
<b>17b</b>				<b>−685.574313</b>
_01	−685.572269	−0.002263	−685.574533	
_02	−685.571001	−0.003255	−685.574256	
_03	−685.568344	−0.003214	−685.571559	
_04	−685.566306	−0.004328	−685.570634	
				<b>−1211.377321</b>
_sil_01	−1211.334061	−0.043602	−1211.377662	
_sil_02	−1211.333483	−0.043918	−1211.377401	
_sil_03	−1211.333164	−0.044019	−1211.377183	
_sil_04	−1211.333177	−0.043983	−1211.377160	
_sil_05	−1211.332424	−0.043535	−1211.375959	
				<b>−685.985225</b>
_H_01	−686.082173	−0.06041109	−685.985651	
_H_02	−686.080856	−0.05994741	−685.983982	
_H_03	−686.079501	−0.06130878	−685.984006	
<b>17c</b>				<b>−1151.569313</b>
_01	−1151.565968	−0.003121	−1151.569089	
_02	−1151.564959	−0.003130	−1151.568088	
_03	−1151.565744	−0.003132	−1151.568876	
_04	−1151.566715	−0.003136	−1151.569851	
_05	−1151.565633	−0.003129	−1151.568762	
_06	−1151.566620	−0.003128	−1151.569748	
_07	−1151.565761	−0.003129	−1151.568890	
_08	−1151.563435	−0.003140	−1151.566575	
_09	−1151.562977	−0.003331	−1151.566309	
				<b>−1677.385773</b>
_sil_01	−1677.350346	−0.035818	−1677.386164	

Table 8.5: Continuation.

System	MP2(FC)/G3MP2large// MPW1K/6-31+G(d)	PCM/UAHF/MPW1K/6-31+G(d)		
	$E_{\text{tot}}$	$\Delta G_{\text{solv}}$	$\Delta H_{298}$	$\langle H_{298} \rangle$
_sil_02	-1677.350504	-0.035841	-1677.386346	
_sil_03	-1677.348459	-0.035836	-1677.384295	
_sil_04	-1677.348466	-0.035816	-1677.384282	
_sil_05	-1677.347010	-0.035774	-1677.382784	
_sil_06	-1677.348830	-0.035771	-1677.384601	
_sil_07	-1677.348897	-0.035749	-1677.384646	
_sil_08	-1677.347889	-0.035754	-1677.383642	
				<b>-1151.983401</b>
_H_01	-1152.339939	-0.04224958	-1151.983325	
_H_02	-1152.339809	-0.04224460	-1151.982223	
_H_03	-1152.339733	-0.04210897	-1151.982035	
_H_04	-1152.339692	-0.04208896	-1151.982856	
_H_05	-1152.339414	-0.04241779	-1151.983968	
<b>17d</b>				<b>-1376.853637</b>
_01	-1376.847656	-0.005961	-1376.853617	
_02	-1376.847546	-0.005958	-1376.853504	
_03	-1376.847619	-0.005956	-1376.853575	
_04	-1376.847549	-0.005952	-1376.853501	
_05	-1376.847614	-0.005960	-1376.853574	
_06	-1376.847586	-0.005952	-1376.853539	
_07	-1376.847724	-0.005959	-1376.853683	
_08	-1376.847691	-0.005959	-1376.853650	
_09	-1376.847709	-0.005962	-1376.853671	
_10	-1376.847800	-0.005960	-1376.853760	
_11	-1376.847788	-0.005947	-1376.853735	
_12	-1376.847557	-0.005960	-1376.853517	
_13	-1376.847724	-0.005945	-1376.853670	
_14	-1376.847779	-0.005966	-1376.853745	
_15	-1376.847754	-0.005958	-1376.853711	
_16	-1376.847723	-0.005961	-1376.853683	
_17	-1376.847581	-0.005954	-1376.853535	
_18	-1376.847693	-0.005963	-1376.853656	
				<b>-1902.672434</b>
_sil_01	-1902.636012	-0.036845	-1902.672856	
_sil_02	-1902.635976	-0.036930	-1902.672906	
_sil_03	-1902.635879	-0.036952	-1902.672831	
_sil_04	-1902.635878	-0.036958	-1902.672836	
_sil_05	-1902.635753	-0.036888	-1902.672641	
_sil_06	-1902.635685	-0.037052	-1902.672737	

### 8.3 Computational Methods

**Table 8.5:** Continuation.

System	MP2(FC)/G3MP2large// MPW1K/6-31+G(d)	PCM/UAHF/MPW1K/6-31+G(d)		
	E <sub>tot</sub>	$\Delta G_{\text{solv}}$	$\Delta H_{298}$	$\langle H_{298} \rangle$
_sil_07	−1902.635624	−0.037038	−1902.672662	
_sil_08	−1902.635535	−0.037019	−1902.672553	
_sil_09	−1902.635327	−0.037131	−1902.672458	
_sil_10	−1902.634522	−0.036716	−1902.671238	
_sil_11	−1902.634361	−0.036856	−1902.671216	
_sil_12	−1902.634367	−0.036837	−1902.671205	
_sil_13	−1902.634170	−0.036820	−1902.670991	
_sil_14	−1902.634168	−0.036821	−1902.670989	
_sil_15	−1902.634215	−0.036851	−1902.671065	
_sil_16	−1902.634215	−0.036850	−1902.671065	
_sil_17	−1902.633928	−0.036916	−1902.670844	
_sil_18	−1902.634061	−0.036980	−1902.671040	
_sil_19	−1902.633857	−0.036994	−1902.670851	
_sil_20	−1902.633857	−0.036982	−1902.670839	
_sil_21	−1902.633869	−0.037053	−1902.670922	
				−1377.270443
_H_01	−1377.647903	−0.04279409	−1377.270596	
_H_02	−1377.647766	−0.04263685	−1377.270360	
_H_03	−1377.647743	−0.04268229	−1377.270381	
_H_04	−1377.647902	−0.04273656	−1377.270638	
_H_05	−1377.647710	−0.04264786	−1377.270250	
_H_06	−1377.647808	−0.04259486	−1377.270336	
_H_07	−1377.647816	−0.04261875	−1377.270362	
_H_08	−1377.647789	−0.04276313	−1377.270495	
_H_09	−1377.647809	−0.04281620	−1377.270557	
_H_10	−1377.647746	−0.04265207	−1377.270384	
_H_11	−1377.647705	−0.04283576	−1377.270517	
_H_12	−1377.647798	−0.04251116	−1377.270318	
_H_13	−1377.647772	−0.04271791	−1377.270498	
_H_14	−1377.647085	−0.04241389	−1377.270319	
17e				−743.459132
_01	−743.731282	−0.001092	−743.459132	
				−1269.278894
_sil_01	−1269.236075	−0.043064	−1269.279139	
_sil_02	−1269.234432	−0.043065	−1269.277497	

**Table 8.6.** Silyl cation affinities (in  $\text{kJ mol}^{-1}$ ) of phosphane-based catalysts relative to pyridine (gas and solution phase data).

System	Silyl cation affinities	
	$\Delta H_{298}$	$\Delta H_{298} \text{ (sol)}$
Pyridine	0	0
P(OMe) <sub>3</sub> ( <b>17b</b> )	+36.9	+27.1
PPh <sub>3</sub> ( <b>17a</b> )	−5.1	+2.1
P <i>p</i> Tol <sub>3</sub> ( <b>17c</b> )	−21.0	−8.3
P(PhOMe) <sub>3</sub> ( <b>17d</b> )	−4.3	−14.4
P(NMe <sub>2</sub> ) <sub>3</sub> ( <b>17e</b> )	−5.7	−16.9

**Table 8.7.** Data for phosphane- and pyridine-oxides as catalysts and their TBS adducts (gas phase data).

System	MPW1K/6-31+G(d)		MP2(FC)/G3MP2large//MPW1K/6-31+G(d)		
	E <sub>tot</sub>	H <sub>298</sub>	E <sub>tot</sub>	H <sub>298</sub>	<H <sub>298</sub> >
<b>18a</b>					<b>−1109.152507</b>
_01	−1111.359972	−1111.054926	−1109.457456	−1109.152410	
_02	−1111.359950	−1111.054949	−1109.457532	−1109.152531	
_03	−1111.359928	−1111.054961	−1109.457502	−1109.152534	
_04	−1111.359886	−1111.054867	−1109.457577	−1109.152558	
_05	−1111.359529	−1111.054506	−1109.457280	−1109.151900	
_06	−1111.359074	−1111.055037	−1109.456691	−1109.152199	
					<b>−1634.957870</b>
_sil_01	−1638.357787	−1637.835616	−1635.480040	−1634.957870	
					<b>−1034.353546</b>
_H_01	−1111.739152	−1036.514898	−1036.514059	−1034.3537413	
_H_02	−1111.737367	−1036.204281	−1036.204253	−1034.3535261	
<b>18b</b>					<b>−1226.733934</b>
_01	−1229.292980	−1228.897847	−1227.126029	−1226.730896	
_02	−1229.292963	−1228.899718	−1227.126110	−1226.732866	
_03	−1229.292854	−1228.898674	−1227.126209	−1226.732029	
_04	−1229.292694	−1228.899488	−1227.126170	−1226.732964	
_05	−1229.292368	−1228.901073	−1227.125653	−1226.734357	
_06	−1229.292163	−1228.900868	−1227.125524	−1226.734229	
					<b>−1752.545549</b>
_sil_01	−1756.297979	−1755.688479	−1753.155132	−1752.545631	
_sil_02	−1756.297228	−1755.687921	−1753.154781	−1752.545474	
_sil_03	−1756.297191	−1755.687869	−1753.154851	−1752.545529	
					<b>−1227.100523</b>
_H_01	−1229.680107	−1229.275432	−1227.505561	−1227.100886	

### 8.3 Computational Methods

**Table 8.7.** Continuation.

System	MPW1K/6-31+G(d)		MP2(FC)/G3MP2large//MPW1K/6-31+G(d)		
	E <sub>tot</sub>	H <sub>298</sub>	E <sub>tot</sub>	H <sub>298</sub>	<H <sub>298</sub> >
_H_02	−1229.679218	−1229.273500	−1227.504194	−1227.098476	
_H_03	−1229.678246	−1229.273686	−1227.503532	−1227.098972	
<b>18c</b>					<b>−1452.015052</b>
_01	−1454.829454	−1454.415110	−1452.429679	−1452.015335	
_02	−1454.829445	−1454.415071	−1452.429479	−1452.015105	
_03	−1454.829431	−1454.415074	−1452.429581	−1452.015224	
_04	−1454.829395	−1454.415129	−1452.429516	−1452.015250	
_05	−1454.829386	−1454.415144	−1452.429620	−1452.015378	
_06	−1454.829255	−1454.414901	−1452.429515	−1452.015162	
_07	−1454.829189	−1454.414886	−1452.429732	−1452.015429	
_08	−1454.829167	−1454.414892	−1452.429508	−1452.015233	
_09	−1454.829030	−1454.414653	−1452.429245	−1452.014868	
_10	−1454.829006	−1454.414886	−1452.429240	−1452.015120	
_11	−1454.829003	−1454.414634	−1452.429238	−1452.014869	
_12	−1454.828990	−1454.414636	−1452.429194	−1452.014840	
_13	−1454.828976	−1454.414645	−1452.429168	−1452.014837	
_14	−1454.828972	−1454.414648	−1452.429130	−1452.014806	
_15	−1454.828968	−1454.414656	−1452.429184	−1452.014873	
_16	−1454.828963	−1454.414650	−1452.429168	−1452.014854	
_17	−1454.828948	−1454.414568	−1452.429241	−1452.014861	
_18	−1454.828943	−1454.414645	−1452.429167	−1452.014868	
_19	−1454.828940	−1454.414581	−1452.429247	−1452.014888	
_20	−1454.828936	−1454.414636	−1452.429184	−1452.014884	
_21	−1454.828926	−1454.414647	−1452.429158	−1452.014879	
_22	−1454.828712	−1454.414395	−1452.428929	−1452.014612	
_23	−1454.828691	−1454.414388	−1452.428847	−1452.014543	
_24	−1454.828669	−1454.414329	−1452.428889	−1452.014549	
_25	−1454.828634	−1454.414300	−1452.428955	−1452.014621	
_26	−1454.828625	−1454.414279	−1452.429018	−1452.014672	
_27	−1454.828500	−1454.414223	−1452.428671	−1452.014394	
_28	−1454.828399	−1454.415119	−1452.428747	−1452.015467	
_29	−1454.828391	−1454.415113	−1452.428740	−1452.015462	
					<b>−1977.831341</b>
_sil_01	−1981.837699	−1981.206100	−1978.462752	−1977.831152	
_sil_02	−1981.837691	−1981.206089	−1978.462760	−1977.831157	
_sil_03	−1981.837631	−1981.206022	−1978.462741	−1977.831131	
_sil_04	−1981.837609	−1981.206029	−1978.462702	−1977.831122	
_sil_05	−1981.837405	−1981.205746	−1978.462571	−1977.830911	
_sil_06	−1981.837386	−1981.205736	−1978.462553	−1977.830903	
_sil_07	−1981.837379	−1981.205671	−1978.462483	−1977.830775	

Table 8.7. Continuation.

System	MPW1K/6-31+G(d)		MP2(FC)/G3MP2large//MPW1K/6-31+G(d)		
	E <sub>tot</sub>	H <sub>298</sub>	E <sub>tot</sub>	H <sub>298</sub>	<H <sub>298</sub> >
_sil_08	−1981.837304	−1981.206646	−1978.462516	−1977.831858	
_sil_09	−1981.837250	−1981.205600	−1978.462367	−1977.830717	
_sil_10	−1981.837080	−1981.206579	−1978.462380	−1977.831879	
_sil_11	−1981.836986	−1981.205482	−1978.462287	−1977.830783	
_sil_12	−1981.836952	−1981.206199	−1978.462148	−1977.831395	
_sil_13	−1981.836928	−1981.206445	−1978.462012	−1977.831529	
					−1452.387173
_H_01	−1455.221602	−1454.794696	−1452.814359	−1452.387453	
_H_02	−1455.221582	−1454.794696	−1452.814290	−1452.387404	
_H_03	−1455.221501	−1454.794586	−1452.814241	−1452.387326	
_H_04	−1455.221474	−1454.794548	−1452.814281	−1452.387356	
_H_05	−1455.221468	−1454.794525	−1452.814180	−1452.387237	
_H_06	−1455.221430	−1454.794519	−1452.814237	−1452.387326	
_H_07	−1455.221392	−1454.794519	−1452.814288	−1452.387415	
_H_08	−1455.221257	−1454.794382	−1452.814054	−1452.387180	
_H_09	−1455.221010	−1454.794137	−1452.813790	−1452.386916	
_H_10	−1455.220968	−1454.794133	−1452.813820	−1452.386985	
_H_11	−1455.220113	−1454.793167	−1452.812446	−1452.385499	
_H_12	−1455.219694	−1454.793900	−1452.811838	−1452.386044	
_H_13	−1455.219325	−1454.793455	−1452.811980	−1452.386110	
_H_14	−1455.219239	−1454.793451	−1452.811587	−1452.385799	
<b>18d</b>					−760.763343
_01	−761.925414	−761.774313	−760.914653	−760.763552	
_02	−761.925390	−761.774320	−760.914618	−760.763549	
_03	−761.924005	−761.772947	−760.913452	−760.762394	
_04	−761.921774	−761.770849	−760.911694	−760.760769	
					−1286.544021
_sil_01	−1288.901153	−1288.533056	−1286.912141	−1286.544044	
_sil_02	−1288.895160	−1288.526940	−1286.907152	−1286.538932	
					−761.096432
_H_01	−762.270915	−762.107590	−761.259836	−761.096511	
_H_02	−762.265569	−762.102475	−761.255294	−761.092199	
_H_03	−762.264597	−762.101458	−761.254251	−761.091111	
_H_04	−762.263207	−762.100061	−761.254222	−761.091077	
<b>19a</b>					−456.298890
_01	−457.287592	−457.105668	−456.481061	−456.299137	
_02	−457.284883	−457.104921	−456.477485	−456.297523	
					−982.107739
_sil_01	−984.295750	−983.895896	−982.507787	−982.107933	
_sil_02	−984.292666	−983.892757	−982.505634	−982.105725	

### 8.3 Computational Methods

**Table 8.7.** Continuation.

System	MPW1K/6-31+G(d)		MP2(FC)/G3MP2large//MPW1K/6-31+G(d)		
	E <sub>tot</sub>	H <sub>298</sub>	E <sub>tot</sub>	H <sub>298</sub>	<H <sub>298</sub> >
_H_01	−457.680624	−457.484564	−456.869134	−456.673074	
<b>19b</b>					−533.512527
_01	−534.705791	−534.485079	−533.733240	−533.512527	
					−1059.324571
_sil_01	−1061.717107	−1061.278324	−1059.763582	−1059.324799	
_sil_02	−1061.717073	−1061.278276	−1059.763563	−1059.324766	
_sil_03	−1061.714058	−1061.275291	−1059.761546	−1059.32278	
_sil_04	−1061.714041	−1061.275308	−1059.761457	−1059.322724	
_H_01	−535.102765	−534.8677822	−534.125545	−533.890602	
<b>19c</b>					−610.741844
_01	−612.132913	−611.873560	−611.001384	−610.742030	
_02	−612.131393	−611.872130	−610.999005	−610.739741	
					−1136.556635
_sil_01	−1139.147705	−1138.670135	−1137.034668	−1136.557098	
_sil_02	−1139.147110	−1138.669586	−1137.034009	−1136.556485	
_sil_03	−1139.147060	−1138.669559	−1137.033946	−1136.556446	
_sil_04	−1139.144081	−1138.666464	−1137.032274	−1136.554657	
_sil_05	−1139.143992	−1138.666366	−1137.032177	−1136.554551	
					−611.123221
_H_01	−612.534590	−612.260893	−611.397167	−611.123471	
_H_02	−612.533779	−612.260021	−611.396339	−611.122581	

**Table 8.8.** Data for phosphane- and pyridine-oxides as catalysts and their TBS adducts. Gas phase calculation with additional PCM values in CHCl<sub>3</sub>.

System	MP2(FC)/G3MP2large//MPW1K/6-31+G(d)		PCM/UAHF/MPW1K/6-31+G(d)	
	E <sub>tot</sub>	ΔG <sub>solv</sub>	ΔH <sub>298</sub>	<H <sub>298</sub> >
<b>18a</b>				−1109.158355
_01	−1109.152410	−0.005867	−1109.158277	
_02	−1109.152531	−0.005923	−1109.158455	
_03	−1109.152534	−0.005837	−1109.158371	
_04	−1109.152558	−0.005932	−1109.158490	
_05	−1109.151900	−0.006052	−1109.157952	
_06	−1109.152199	−0.006206	−1109.158405	
				−1634.995680
_sil_01	−1634.957870	−0.037810	−1634.995680	
				−1109.574077
_H_01	−1036.514059	−0.061762	−1109.574023	



Table 8.8. Continuation.

System	MP2(FC)/G3MP2large// MPW1K/6-31+G(d)	PCM/UAHF/MPW1K/6-31+G(d)		
	$E_{\text{tot}}$	$\Delta G_{\text{solv}}$	$\Delta H_{298}$	$\langle H_{298} \rangle$
_H_02	-1036.204253	-0.062901	-1109.574126	
<b>18b</b>				<b>-1226.740475</b>
_01	-1226.730896	-0.006097	-1226.736993	
_02	-1226.732866	-0.006172	-1226.739038	
_03	-1226.732029	-0.006250	-1226.738278	
_04	-1226.732964	-0.006346	-1226.739310	
_05	-1226.734357	-0.006478	-1226.740835	
_06	-1226.734229	-0.006552	-1226.740782	
				<b>-1752.581111</b>
_sil_01	-1752.545631	-0.035443	-1752.581074	
_sil_02	-1752.545474	-0.035613	-1752.581087	
_sil_03	-1752.545529	-0.035638	-1752.581168	
				<b>-1227.141057</b>
_H_01	-1227.505561	-0.0405743	-1227.141460	
_H_02	-1227.504194	-0.0408264	-1227.139302	
_H_03	-1227.503532	-0.0410305	-1227.140003	
<b>18c</b>				<b>-1452.023991</b>
_01	-1452.015335	-0.008648	-1452.023984	
_02	-1452.015105	-0.008584	-1452.023690	
_03	-1452.015224	-0.008562	-1452.023787	
_04	-1452.015250	-0.008563	-1452.023814	
_05	-1452.015378	-0.008654	-1452.024032	
_06	-1452.015162	-0.008835	-1452.023997	
_07	-1452.015429	-0.008877	-1452.024306	
_08	-1452.015233	-0.008829	-1452.024062	
_09	-1452.014868	-0.009032	-1452.023900	
_10	-1452.015120	-0.009044	-1452.024164	
_11	-1452.014869	-0.009009	-1452.023878	
_12	-1452.014840	-0.009029	-1452.023869	
_13	-1452.014837	-0.008996	-1452.023833	
_14	-1452.014806	-0.008976	-1452.023783	
_15	-1452.014873	-0.008979	-1452.023851	
_16	-1452.014854	-0.009030	-1452.023884	
_17	-1452.014861	-0.009033	-1452.023894	
_18	-1452.014868	-0.009019	-1452.023888	
_19	-1452.014888	-0.009062	-1452.023950	
_20	-1452.014884	-0.009029	-1452.023912	
_21	-1452.014879	-0.009006	-1452.023886	
_22	-1452.014612	-0.009208	-1452.023820	

### 8.3 Computational Methods

**Table 8.8.** Continuation.

System	MP2(FC)/G3MP2large// MPW1K/6-31+G(d)	PCM/UAHF/MPW1K/6-31+G(d)		
	E <sub>tot</sub>	$\Delta G_{\text{solv}}$	$\Delta H_{298}$	$\langle H_{298} \rangle$
_23	−1452.014543	−0.009110	−1452.023653	
_24	−1452.014549	−0.009221	−1452.023770	
_25	−1452.014621	−0.009196	−1452.023818	
_26	−1452.014672	−0.009282	−1452.023953	
_27	−1452.014394	−0.009093	−1452.023487	
_28	−1452.015467	−0.009086	−1452.024553	
_29	−1452.015462	−0.009072	−1452.024533	
				−1977.868048
_sil_01	−1977.831152	−0.036575	−1977.867727	
_sil_02	−1977.831157	−0.036565	−1977.867722	
_sil_03	−1977.831131	−0.036616	−1977.867747	
_sil_04	−1977.831122	−0.036613	−1977.867735	
_sil_05	−1977.830911	−0.036713	−1977.867625	
_sil_06	−1977.830903	−0.036741	−1977.867645	
_sil_07	−1977.830775	−0.036691	−1977.867465	
_sil_08	−1977.831858	−0.036685	−1977.868543	
_sil_09	−1977.830717	−0.036737	−1977.867454	
_sil_10	−1977.831879	−0.036685	−1977.868564	
_sil_11	−1977.830783	−0.036731	−1977.867514	
_sil_12	−1977.831395	−0.036847	−1977.868243	
_sil_13	−1977.831529	−0.036813	−1977.868342	
				−1452.428340
_H_01	−1452.814359	−0.041074	−1452.428527	
_H_02	−1452.814290	−0.040989	−1452.428393	
_H_03	−1452.814241	−0.041150	−1452.428476	
_H_04	−1452.814281	−0.041168	−1452.428524	
_H_05	−1452.814180	−0.041201	−1452.428438	
_H_06	−1452.814237	−0.041183	−1452.428509	
_H_07	−1452.814288	−0.041238	−1452.428653	
_H_08	−1452.814054	−0.041160	−1452.428340	
_H_09	−1452.813790	−0.041244	−1452.428160	
_H_10	−1452.813820	−0.041423	−1452.428408	
_H_11	−1452.812446	−0.041638	−1452.427138	
_H_12	−1452.811838	−0.041274	−1452.427318	
_H_13	−1452.811980	−0.041668	−1452.427779	
_H_14	−1452.811587	−0.041483	−1452.427282	
18d				−760.767228
_01	−760.763552	−0.003830	−760.7673819	
_02	−760.763549	−0.003838	−760.7673866	

Table 8.8. Continuation.

System	MP2(FC)/G3MP2large// MPW1K/6-31+G(d)	PCM/UAHF/MPW1K/6-31+G(d)		
	$E_{\text{tot}}$	$\Delta G_{\text{solv}}$	$\Delta H_{298}$	$\langle H_{298} \rangle$
_03	−760.762394	−0.004772	−760.7671659	
_04	−760.760769	−0.004997	−760.765766	
				−1286.587016
_sil_01	−1286.544044	−0.043008	−1286.587052	
_sil_02	−1286.538932	−0.043554	−1286.582486	
				−761.160145
_H_01	−761.259836	−0.063837	−761.160348	
_H_02	−761.255294	−0.064436	−761.156635	
_H_03	−761.254251	−0.064615	−761.155726	
_H_04	−761.254222	−0.066072	−761.157149	
<b>19a</b>				−456.308032
_01	−456.299137	−0.009158	−456.308295	
_02	−456.297523	−0.009549	−456.307072	
				−982.152161
_sil_01	−982.107933	−0.044412	−982.152345	
_sil_02	−982.105725	−0.044316	−982.1500413	
_H_01	−456.869135	−0.054885	−456.727960	
<b>19b</b>				−533.522123
_01	−533.512527	−0.009596	−533.522123	
				−1059.367933
_sil_01	−1059.324799	−0.043344	−1059.368144	
_sil_02	−1059.324766	−0.043355	−1059.368121	
_sil_03	−1059.32278	−0.043180	−1059.365960	
_sil_04	−1059.322724	−0.043267	−1059.365991	
_H_01	−534.125545	−0.053367	−533.943969	
<b>19c</b>				−610.751448
_01	−610.742030	−0.009669	−610.751699	
_02	−610.739741	−0.010417	−610.750158	
				−1136.600019
_sil_01	−1136.557098	−0.043370	−1136.600468	
_sil_02	−1136.556485	−0.043344	−1136.599829	
_sil_03	−1136.556446	−0.043326	−1136.599771	
_sil_04	−1136.554657	−0.043004	−1136.597661	
_sil_05	−1136.554551	−0.043038	−1136.597589	
				−611.175896
_H_01	−611.397167	−0.052670	−611.176141	
_H_02	−611.396339	−0.052714	−611.175295	

### 8.3 Computational Methods

**Table 8.9.** Data for imidazole-based N-heterocycles and their TBS adducts (gas phase data).

System	MPW1K/6-31+G(d)		MP2(FC)/G3MP2large//MPW1K/6-31+G(d)		
	E <sub>tot</sub>	H <sub>298</sub>	E <sub>tot</sub>	H <sub>298</sub>	<H <sub>298</sub> >
Pyridine					
_01	−248.216536	−248.119565	−247.744655	−247.647834	
_sil_01	−775.187914	−774.873082	−773.738298	−773.423466	
_me_01	−287.893166	−287.751587	−287.327482	−287.185903	
<b>3d/21a</b>					
_01	−226.153472	−226.074909	−225.762930	−225.684367	
					−751.467619
_sil_01	−753.134927	−752.838383	−751.764361	−751.467817	
_sil_02	−753.131049	−752.835507	−751.760515	−751.464974	
_sil_03	−753.130000	−752.834435	−751.759647	−751.464082	
_me_01	−265.837290	−265.714056	−265.350950	−265.227716	
<b>21b</b>					
_01	−265.469122	−265.360478	−264.988716	−264.880072	
					−790.667260
_sil_01	−792.452615	−792.125655	−790.994248	−790.667288	
_sil_02	−792.447831	−792.120872	−790.989367	−790.662407	
_me_01	−305.159006	−305.006512	−304.582867	−304.430373	
<b>21d</b>					
_01	−360.095688	−359.937625	−359.443919	−359.285856	
					−885.073907
_sil_01	−887.076278	−886.700033	−885.449529	−885.073284	
_sil_02	−887.076135	−886.700953	−885.449499	−885.074317	
_sil_03	−887.072606	−886.696445	−885.449499	−885.073339	
_me_01	−399.789500	−399.586528	−399.042054	−398.839082	
<b>21c</b>					
_01	−340.649878	−340.534778	−340.090624	−339.975524	
_02	−340.638820	−340.524032	−340.080751	−339.965963	
					−865.757326
_sil_01	−867.627693	−867.294772	−866.090325	−865.757403	
_sil_02	−867.624467	−867.291477	−866.086788	−865.753798	
					−379.518094
_me_01	−380.332662	−380.173100	−379.677666	−379.518104	
_me_02	−380.325015	−380.166251	−379.670138	−379.511374	
_me_03	−380.324165	−380.166339	−379.669056	−379.511231	
<b>3e/22a</b>					
_01	−265.456724	−265.347809	−264.975577	−264.866661	
					−790.656154
_sil_01	−792.443467	−792.116681	−790.983131	−790.656345	

Table 8.9. Continuation.

System	MPW1K/6-31+G(d)		MP2(FC)/G3MP2large//MPW1K/6-31+G(d)		
	E <sub>tot</sub>	H <sub>298</sub>	E <sub>tot</sub>	H <sub>298</sub>	<H <sub>298</sub> >
_sil_02	−792.439557	−792.113750	−790.979255	−790.653448	
_sil_03	−792.438621	−792.112754	−790.978432	−790.652565	
_me_01	−305.146849	−304.993315	−304.570358	−304.416824	
<hr/>					
<b>22b</b>					
_01	−304.771488	−304.632459	−304.201407	−304.062378	
					−829.854444
_sil_01	−831.758793	−831.401556	−830.211717	−829.854479	
_sil_02	−831.754331	−831.397060	−830.207172	−829.849901	
_me_01	−344.467066	−344.284343	−343.802033	−343.619310	
<hr/>					
<b>22d</b>					−398.469253
_01	−399.397886	−399.209207	−398.657932	−398.469253	
_02	−399.385719	−399.198879	−398.643469	−398.456629	
					−924.259258
_sil_01	−926.380445	−925.973967	−924.665841	−924.259363	
_sil_02	−926.377981	−925.971287	−924.662856	−924.256162	
_me_01	−439.092851	−438.859626	−438.256697	−438.023472	
<hr/>					
<b>22c</b>					
_01	−379.953240	−379.807610	−379.303700	−379.158070	
					−904.942400
_sil_01	−906.930635	−906.567401	−905.305782	−904.942548	
_sil_02	−906.930628	−906.567414	−905.305783	−904.942569	
_sil_03	−906.929536	−906.566314	−905.304303	−904.941081	
_sil_04	−906.926944	−906.563472	−905.301708	−904.938236	
					−418.703378
_me_01	−419.637002	−419.447101	−418.893458	−418.703557	
_me_01	−419.633686	−419.445441	−418.889443	−418.701199	
<hr/>					
<b>23a</b>					
_01	−379.767664	−379.638232	−379.075066	−378.945634	
					−904.730538
_sil_01	−906.747680	−906.400101	−905.078183	−904.730604	
_sil_02	−906.744158	−906.396526	−905.074441	−904.726809	
_me_01	−419.453937	−419.279719	−418.666273	−418.492055	
<hr/>					
<b>23b</b>					
_01	−419.084886	−418.925410	−418.302739	−418.143264	
_sil_01	−946.063500	−945.685419	−944.306840	−943.928758	
_me_01	−458.776830	−458.572432	−457.899628	−457.695230	
<hr/>					
<b>23d</b>					
_01	−513.715228	−513.506232	−512.761827	−512.552831	
_sil_01	−1040.688610	−1040.261082	−1038.764890	−1038.337362	

### 8.3 Computational Methods

**Table 8.9.** Continuation.

System	MPW1K/6-31+G(d)		MP2(FC)/G3MP2large//MPW1K/6-31+G(d)		
	E <sub>tot</sub>	H <sub>298</sub>	E <sub>tot</sub>	H <sub>298</sub>	<H <sub>298</sub> >
_me_01	−553.408983	−553.154907	−552.360775	−552.106699	
<b>23c</b>					−493.242172
_01	−494.268887	−494.102876	−493.408183	−493.242172	
_02	−494.256947	−494.091281	−493.397477	−493.231811	
					−1019.015091
_sil_01	−1021.240646	−1020.855578	−1019.401146	−1019.016078	
_sil_02	−1021.240153	−1020.855009	−1019.400019	−1019.014875	
_sil_03	−1021.239460	−1020.854281	−1019.399017	−1019.013838	
_sil_04	−1021.239434	−1020.854328	−1019.399560	−1019.014454	
_sil_05	−1021.239083	−1020.853992	−1019.399536	−1019.014445	
_sil_06	−1021.239022	−1020.853848	−1019.400284	−1019.015110	
_sil_07	−1021.238926	−1020.853798	−1019.399983	−1019.014856	
_sil_08	−1021.238863	−1020.853814	−1019.399418	−1019.014369	
_sil_09	−1021.238391	−1020.853157	−1019.399084	−1019.013850	
_sil_10	−1021.238220	−1020.852974	−1019.398497	−1019.013251	
_sil_11	−1021.238129	−1020.853031	−1019.398464	−1019.013366	
_sil_12	−1021.237622	−1020.852472	−1019.398528	−1019.013378	
					−532.786269
_me_01	−533.952450	−533.741898	−532.996824	−532.786272	
_me_02	−533.943252	−533.734463	−532.987714	−532.778925	
<b>24a</b>					
_01	−419.071755	−418.911849	−418.289589	−418.129683	
					−943.920093
_sil_01	−946.056379	−945.678387	−944.298150	−943.920158	
_sil_02	−946.052821	−945.674723	−944.294421	−943.916323	
_me_01	−458.763185	−458.558581	−457.886506	−457.681902	
<b>24b</b>					
_01	−458.387833	−458.197806	−457.516904	−457.326877	
_sil_01	−985.368654	−984.960094	−983.524331	−983.115771	
_me_01	−498.082572	−497.847688	−497.117441	−496.882557	
<b>24d</b>					
_01	−553.016047	−552.776308	−551.975620	−551.735880	
_sil_01	−1079.991137	−1079.533352	−1077.979778	−1077.521993	
_me_01	−592.711163	−592.42664	−591.575548	−591.291025	
<b>24c</b>					
_01	−533.573029	−533.376364	−532.623109	−532.426444	
					−1058.206863
_sil_01	−1060.543608	−1060.129073	−1058.621660	−1058.207124	
_sil_02	−1060.542953	−1060.128327	−1058.620646	−1058.206020	
					−571.970644

**Table 8.9.** Continuation.

System	MPW1K/6-31+G(d)		MP2(FC)/G3MP2large//MPW1K/6-31+G(d)		
	E <sub>tot</sub>	H <sub>298</sub>	E <sub>tot</sub>	H <sub>298</sub>	<H <sub>298</sub> >
_me_01	−573.254955	−573.014006	−572.211736	−571.970787	
_me_02	−573.251613	−573.012228	−572.207445	−571.968061	

**Table 8.10.** Data for imidazole-based *N*-heterocycles and their TBS adducts. Gas phase calculation with additional PCM values in CHCl<sub>3</sub>.

System	MP2(FC)/G3MP2large//MPW1K/6-31+G(d)		PCM/UAHF/MPW1K/6-31+G(d)		
	E <sub>tot</sub>	ΔG <sub>solv</sub>	ΔH <sub>298</sub>	<H <sub>298</sub> >	
Pyridin					
_01	−247.647834	−0.003589	−247.6514229		
_sil_01	−773.423466	−0.04170	−773.4647356		
_me_01	−287.185903	−0.056548	−287.2424517		
<b>3d/21a</b>					
_01	−225.684367	−0.007442	−225.6918086		
					−751.5145311
_sil_01	−751.467817	−0.046929	−751.5147459		
_sil_02	−751.464974	−0.046961	−751.5119352		
_sil_03	−751.464082	−0.047198	−751.5112803		
_me_01	−265.227716	−0.061512	−265.2892288		
<b>21b</b>					
_01	−264.880072	−0.006391	−264.8864632		
					−790.7172235
_sil_01	−790.667288	−0.049982	−790.7172694		
_sil_02	−790.662407	−0.054765	−790.7171726		
_me_01	−304.430373	−0.058089	−304.4884624		
<b>21d</b>					
_01	−359.285856	−0.006269	−359.292126		
					−885.1224115
_sil_01	−885.073284	−0.048328	−885.1216119		
_sil_02	−885.074317	−0.048513	−885.1228292		
_sil_03	−885.073339	−0.048521	−885.1218595		
_me_01	−398.839082	−0.054461	−398.8935423		
<b>21c</b>					−339.9806392
_01	−339.975524	−0.005125	−339.9806496		
_02	−339.965963	−0.008695	−339.9746574		
					−865.806688
_sil_01	−865.757403	−0.049351	−865.806754		
_sil_02	−865.753798	−0.049145	−865.8029429		

### 8.3 Computational Methods

**Table 8.10.** Continuation.

System	MP2(FC)/G3MP2large// MPW1K/6-31+G(d)	PCM/UAHF/MPW1K/6-31+G(d)		
	E <sub>tot</sub>	$\Delta G_{\text{solv}}$	$\Delta H_{298}$	$\langle H_{298} \rangle$
				<b>−379.5743274</b>
_me_01	−379.518104	−0.056237	−379.5743411	
_me_02	−379.511374	−0.056756	−379.5681305	
_me_03	−379.511231	−0.056321	−379.5675514	
<b>3e/22a</b>				
_01	−264.866661	−0.006199	−264.872861	
				<b>−790.698519</b>
_sil_01	−790.656345	−0.042377	−790.6987221	
_sil_02	−790.653448	−0.042250	−790.6956977	
_sil_03	−790.652565	−0.042781	−790.6953465	
_me_01	−304.416824	−0.056448	−304.4732721	
<b>22b</b>				
_01	−304.062378	−0.005440	−304.0678177	
				<b>−829.9009517</b>
_sil_01	−829.854479	−0.046505	−829.9009846	
_sil_02	−829.849901	−0.046411	−829.8963123	
_me_01	−343.619310	−0.053976	−343.6732858	
<b>22d</b>				<b>−398.4736925</b>
_01	−398.469253	−0.004439	−398.4736926	
_02	−398.456629	−0.005406	−398.4620346	
				<b>−924.3047831</b>
_sil_01	−924.259363	−0.045504	−924.3048664	
_sil_02	−924.256162	−0.045196	−924.3013582	
_me_01	−438.023472	−0.051252	−438.0747239	
<b>22c</b>				
_01	−379.158070	−0.003842	−379.1619121	
				<b>−904.9883294</b>
_sil_01	−904.942548	−0.045925	−904.9884729	
_sil_02	−904.942569	−0.045909	−904.9884783	
_sil_03	−904.941081	−0.045711	−904.9867926	
_sil_04	−904.938236	−0.045642	−904.9838783	
				<b>−418.7557329</b>
_me_01	−418.703557	−0.052392	−418.755949	
_me_01	−418.701199	−0.052768	−418.7539663	
<b>23a</b>				
_01	−378.945634	−0.006999	−378.952633	
				<b>−904.7754552</b>
_sil_01	−904.730604	−0.049144	−904.7797484	
_sil_02	−904.726809	−0.048603	−904.7754118	



Table 8.10. Continuation.

System	MP2(FC)/G3MP2large// MPW1K/6-31+G(d)	PCM/UAHF/MPW1K/6-31+G(d)		
	$E_{\text{tot}}$	$\Delta G_{\text{solv}}$	$\Delta H_{298}$	$\langle H_{298} \rangle$
_me_01	−418.492055	−0.057176	−418.5492314	
<b>23b</b>				
_01	−418.143264	−0.006561	−418.1498246	
_sil_01	−943.928758	−0.047610	−943.9763681	
_me_01	−457.695230	−0.052746	−457.7479764	
<b>23d</b>				
_01	−512.552831	−0.006899	−512.5597299	
_sil_01	−1038.337362	−0.046440	−1038.383802	
_me_01	−552.106699	−0.051839	−552.1585383	
<b>23c</b>				−493.2475093
_01	−493.242172	−0.005342	−493.247514	
_02	−493.231811	−0.008827	−493.2406388	
				−1019.06208
_sil_01	−1019.016078	−0.046963	−1019.063041	
_sil_02	−1019.014875	−0.047000	−1019.061876	
_sil_03	−1019.013838	−0.047044	−1019.060882	
_sil_04	−1019.014454	−0.047027	−1019.061481	
_sil_05	−1019.014445	−0.047128	−1019.061573	
_sil_06	−1019.015110	−0.047093	−1019.062203	
_sil_07	−1019.014856	−0.047083	−1019.061939	
_sil_08	−1019.014369	−0.047002	−1019.061371	
_sil_09	−1019.013850	−0.047072	−1019.060922	
_sil_10	−1019.013251	−0.047165	−1019.060416	
_sil_11	−1019.013366	−0.047199	−1019.060564	
_sil_12	−1019.013378	−0.047156	−1019.060534	
				−532.8392045
_me_01	−532.786272	−0.052937	−532.8392091	
_me_02	−532.778925	−0.053385	−532.8323104	
<b>24a</b>				
_01	−418.129683	−0.005778	−418.135461	
				−943.9655134
_sil_01	−943.920158	−0.045390	−943.9655484	
_sil_02	−943.916323	−0.044630	−943.9609527	
_me_01	−457.681902	−0.052746	−457.734648	
<b>24b</b>				
_01	−457.326877	−0.005420	−457.3322977	
_sil_01	−983.115771	−0.044366	−983.1601374	
_me_01	−496.882557	−0.050446	−496.9330028	
<b>24d</b>				

### 8.3 Computational Methods

**Table 8.10.** Continuation.

System	MP2(FC)/G3MP2large// MPW1K/6-31+G(d)	PCM/UAHF/MPW1K/6-31+G(d)		
	E <sub>tot</sub>	$\Delta G_{\text{solv}}$	$\Delta H_{298}$	$\langle H_{298} \rangle$
_01	−551.735880	−0.004810	−551.7406907	
_sil_01	−1077.521993	−0.043373	−1077.565366	
_me_01	−591.291025	−0.048828	−591.3398535	
<b>24c</b>				
_01	−532.426444	−0.004051	−532.4304954	
				−1058.250617
_sil_01	−1058.207124	−0.043754	−1058.250879	
_sil_02	−1058.206020	−0.043559	−1058.249578	
				−572.0197568
_me_01	−571.970787	−0.049170	−572.0199574	
_me_02	−571.968061	−0.049755	−572.0178156	

**Table 8.11.** Silyl- and methyl-cation affinities (in kJ mol<sup>−1</sup>) of imidazole-based *N*-heterocyclic compounds relative to pyridine (gas and solution phase data).

System	Silyl cation affinities		Methyl cation affinities	
	$\Delta H_{298}$	$\Delta H_{298}$ (sol)	$\Delta H_{298}$	$\Delta H_{298}$ (sol)
Pyridine	0	0	0	0
<b>23c</b>	+7.1	−3.3	−15.8	−1.7
<b>24c</b>	−12.6	−17.9	−16.1	+4.6
<b>3d/21a</b>	−20.0	−24.7	−13.9	−16.8
<b>23a</b>	−24.3	−25.0	−21.9	−14.6
<b>23d</b>	−23.4	−28.2	−41.5	−20.4
<b>24d</b>	−27.5	−29.8	−44.8	−21.4
<b>21b</b>	−30.3	−30.4	−32.1	−28.8
<b>3e/60a</b>	−36.4	−32.4	−31.8	−24.6
<b>21c</b>	−16.2	−33.4	−11.8	−7.0
<b>22c</b>	−22.8	−34.4	−19.0	−17.4
<b>23b</b>	−25.9	−34.7	−36.5	−18.7
<b>24b</b>	−34.8	−38.1	−46.2	−25.4
<b>21d</b>	−32.6	−42.5	−39.8	−27.3
<b>24a</b>	−38.8	−44.0	−37.1	−21.4
<b>22d</b>	−37.7	−46.7	−42.4	−26.3
<b>22b</b>	−43.1	−52.0	−49.5	−37.9

## 8.3.2 Data for the Various Leavings Groups

In the following tables the energies (in Hartree) of the quantum chemical calculations for the silyl reagents (Chapter 3.3) will be depicted for all compounds. The following abbreviation will be used in the tables: '\_a\_' for the anions, '\_H\_' for the protonated anion, and '\_aux\_' for the auxiliary base adduct.

**Table 8.12.** Data for various silyl reagents, corresponding anion, protonated anion, and auxiliary base adduct (gas phase data).

System	MPW1K/6-31+G(d)		MP2(FC)/G3MP2large//MPW1K/6-31+G(d)		
	E <sub>tot</sub>	H <sub>298</sub>	E <sub>tot</sub>	H <sub>298</sub>	<H <sub>298</sub> >
<b>TBSCl (1a)</b>					
_01	−987.420180	−987.202751	−985.934319	−985.716891	
_a_01	−460.276187	−460.273826	−459.770535	−459.768174	
_H_01	−460.802892	−460.792585	−460.302699	−460.292391	
_aux_01	−635.265133	−635.118645	−634.397798	−634.251311	
<b>TBSOTf (1b)</b>					<b>−1486.242562</b>
_01	−1488.456837	−1488.203145	−1486.496515	−1486.242823	
_02	−1488.455451	−1488.201786	−1486.495424	−1486.241759	
_a_01	−961.381927	−961.346825	−960.380846	−960.345744	
_H_01	−961.840083	−961.790878	−960.855869	−960.806663	
_aux_01	−1136.321386	−1136.136398	−1134.976816	−1134.791828	
<b>TBSCN (1c)</b>					
_01	−619.977791	−619.752387	−618.857927	−618.632524	
_a_01	−92.817228	−92.808869	−92.681217	−92.672858	
_H_01	−93.384897	−93.364434	−93.248191	−93.227728	
_aux_01	−267.830402	−267.677139	−267.328534	−267.175272	
<b>MTBSTFA (1d)</b>					<b>−1070.733885</b>
_01	−1072.662903	−1072.367468	−1071.029448	−1070.734012	
_02	−1072.658548	−1072.362809	−1071.026837	−1070.731098	
_a_01	−545.522667	−545.446119	−544.864137	−544.787589	<b>−544.787589</b>
_a_02	−545.505921	−545.429693	−544.848974	−544.772746	
_H_01	−546.086672	−545.995938	−545.423208	−545.332474	<b>−545.332471</b>
_H_02	−546.079856	−545.988150	−545.416836	−545.325129	
_aux_01	−720.527281	−720.302403	−719.503338	−719.278459	
<b>TBSImi (1e)</b>					<b>−751.097140</b>
_01	−752.743078	−752.460834	−751.379385	−751.097142	
_02	−752.743077	−752.460830	−751.379386	−751.097138	
_a_01	−225.582617	−225.518414	−225.199891	−225.135689	
_H_01	−226.153471	−226.074914	−225.762941	−225.684384	
_aux_01	−400.599879	−400.387971	−399.846963	−399.635055	
<b>TBSN<sub>3</sub> (1f)</b>					<b>−689.901829</b>

### 8.3 Computational Methods

**Table 8.12.** Continuation.

System	MPW1K/6-31+G(d)		MP2(FC)/G3MP2large//MPW1K/6-31+G(d)		
	E <sub>tot</sub>	H <sub>298</sub>	E <sub>tot</sub>	H <sub>298</sub>	<H <sub>298</sub> >
_01	−691.314247	−691.082779	−690.133221	−689.901753	
_02	−691.314104	−691.082487	−690.133512	−689.901894	
_a_01	−164.160981	−164.145990	−163.966021	−163.951030	
_H_01	−164.712883	−164.686394	−164.506718	−164.480230	
_aux_01	−339.160846	−339.000931	−338.592011	−338.432096	
<b>TBSOClO<sub>3</sub> (1g)</b>					<b>−1285.881346</b>
_01	−1287.805800	−1287.567884	−1286.119487	−1285.881572	
_02	−1287.803222	−1287.565218	−1286.117697	−1285.879693	
_a_01	−760.710805	−760.689910	−759.994724	−759.973830	
_H_01	−761.190301	−761.156741	−760.482554	−760.448993	
_aux_01	−935.673252	−935.503926	−934.598569	−934.429243	
<b>Me3N</b>					
_01	−174.433383	−174.302577	−174.067320	−173.936515	
<b>5b</b>					<b>−538.351667</b>
_01	−539.599653	−539.372802	−538.579167	−538.352316	
_02	−539.598979	−539.372055	−538.578495	−538.351571	
_03	−539.598168	−539.371234	−538.577429	−538.350495	
_04	−539.597667	−539.370947	−538.577029	−538.350309	
_05	−539.596649	−539.369859	−538.575661	−538.348871	
_06	−539.595512	−539.368823	−538.576732	−538.350044	
_07	−539.595179	−539.368411	−538.575238	−538.348470	
<b>7b</b>					<b>−1063.779233</b>
_01	−1066.202182	−1065.771607	−1064.209301	−1063.778726	
_02	−1066.201693	−1065.770970	−1064.210703	−1063.779979	
_03	−1066.201319	−1065.770848	−1064.208978	−1063.778507	
_04	−1066.201216	−1065.770565	−1064.209273	−1063.778622	
_05	−1066.200263	−1065.769619	−1064.208587	−1063.777943	
_06	−1066.199730	−1065.769097	−1064.208500	−1063.777867	
_07	−1066.197458	−1065.766864	−1064.205506	−1063.774912	

**Table 8.13.** Data for various silyl reagent, corresponding anion, protonated anion, and auxiliary base adduct (Gas phase calculation with additional SMD values in CHCl<sub>3</sub>).

System	MP2(FC)/G3MP2large// MPW1K/6-31+G(d)	SMD/MPW1K/6-31+G(d)		
	E <sub>tot</sub>	ΔG <sub>sol</sub>	ΔH <sub>298</sub>	<H <sub>298</sub> >
<b>TBSCl (1a)</b>				
_01	−985.716891	−0.008920	−985.725811	

Table 8.13. Continuation.

System	MP2(FC)/G3MP2large// MPW1K/6-31+G(d)	SMD/MPW1K/6-31+G(d)		
	$E_{\text{tot}}$	$\Delta G_{\text{sol}}$	$\Delta H_{298}$	$\langle H_{298} \rangle$
_a_01	−459.768174	−0.086198	−459.854372	
_H_01	−460.292391	−0.005357	−460.297748	
_aux_01	−634.251311	−0.029104	−634.280414	
<b>TBSOTf (1b)</b>				<b>−1486.251526</b>
_01	−1486.242823	−0.008960	−1486.251783	
_02	−1486.241759	−0.009027	−1486.250786	
_a_01	−960.345744	−0.061979	−960.407723	
_H_01	−960.806663	−0.006630	−960.813293	
_aux_01	−1134.791828	−0.025090	−1134.816918	
<b>TBSCN (1c)</b>				
_01	−618.632524	−0.008615	−618.641138	
_a_01	−92.672858	−0.084393	−92.757251	
_H_01	−93.227728	−0.004940	−93.232668	
_aux_01	−267.175272	−0.007549	−267.182821	
<b>MTBSTFA (1d)</b>				<b>−1070.744429</b>
_01	−1070.734012	−0.010640	−1070.744652	
_02	−1070.731098	−0.011651	−1070.742749	
_a_01	−544.787589	−0.069708	−544.857297	<b>−544.857297</b>
_a_02	−544.772746	−0.072107	−544.844852	
_H_01	−545.332474	−0.009110	−545.341584	<b>−545.341580</b>
_H_02	−545.325129	−0.009329	−545.334459	
_aux_01	−719.278459	−0.010000	−719.288459	
<b>TBSImi (1e)</b>				<b>−751.115369</b>
_01	−751.097142	−0.018229	−751.115371	
_02	−751.097138	−0.018229	−751.115368	
_a_01	−225.135689	−0.083254	−225.218943	
_H_01	−225.684384	−0.016972	−225.701356	
_aux_01	−399.635055	−0.020082	−399.655137	
<b>TBSN<sub>3</sub> (1f)</b>				<b>−689.905873</b>
_01	−689.901753	−0.004158	−689.905911	
_02	−689.901894	−0.003938	−689.905832	
_a_01	−163.951030	−0.075854	−164.026884	
_H_01	−164.480230	−0.000498	−164.480728	
_aux_01	−338.432096	−0.004678	−338.436774	
<b>TBSOCIO<sub>3</sub> (1g)</b>				<b>−1285.890204</b>
_01	−1285.881572	−0.008845	−1285.890417	
_02	−1285.879693	−0.008707	−1285.888400	
_a_01	−759.973830	−0.067365	−760.041195	
_H_01	−760.448993	−0.006532	−760.455525	

### 8.3 Computational Methods

**Table 8.13.** Continuation.

System	MP2(FC)/G3MP2large// MPW1K/6-31+G(d)	SMD/MPW1K/6-31+G(d)		
	$E_{\text{tot}}$	$\Delta G_{\text{sol}}$	$\Delta H_{298}$	$\langle H_{298} \rangle$
_aux_01	−934.429243	−0.028361	−934.457603	
Me3N				
_01	−173.936515	−0.006626	−173.943141	
<b>5b</b>				<b>−1063.798615</b>
_01	−538.352316	−0.018952	−1063.798766	
_02	−538.351571	−0.018269	−1063.799144	
_03	−538.350495	−0.018890	−1063.798405	
_04	−538.350309	−0.018851	−1063.798404	
_05	−538.348871	−0.019947	−1063.797463	
_06	−538.350044	−0.019521	−1063.797066	
_07	−538.348470	−0.020320	−1063.795670	
<b>7b</b>				<b>−538.370457</b>
_01	−1063.778726	−0.020040	−538.371267	
_02	−1063.779979	−0.019165	−538.369840	
_03	−1063.778507	−0.019898	−538.369385	
_04	−1063.778622	−0.019782	−538.369160	
_05	−1063.777943	−0.019520	−538.368818	
_06	−1063.777867	−0.019199	−538.3695649	
_07	−1063.774912	−0.020758	−538.3687899	

#### 8.3.3 Data for the Silyl Group Size

In the following tables the energies (in Hartree) of the quantum chemical calculations for the silyl groups size (Chapter 5.2) will be depicted for all compounds. The following abbreviation will be used in the tables: ‘\_py\_’ for the pyridine adducts, ‘\_cat\_’ for DMAP adducts, and ‘\_alc\_’ for the corresponding silylated alcohol **5b**.

**Table 8.14.** Data for several silyl chlorides, the intermediate with DMAP (\_cat) and their adducts with alcohol **5b** (\_alc) (gas phase data).

System	MPW1K/6-31+G(d)		MP2(FC)/G3MP2large//MPW1K/6-31+G(d)		
	$E_{\text{tot}}$	$H_{298}$	$E_{\text{tot}}$	$H_{298}$	$\langle H_{298} \rangle$
Pyridine					
_01	−248.216536	−248.119562	−247.744651	−247.647677	
DMAP (3a)					
_01	−382.158062	−381.981128	−381.426957	−381.250023	
_H	−382.554571	−382.362752	−381.817451	−381.625632	

Table 8.14. Continuation.

System	MPW1K/6-31+G(d)		MP2(FC)/G3MP2large//MPW1K/6-31+G(d)		
	E <sub>tot</sub>	H <sub>298</sub>	E <sub>tot</sub>	H <sub>298</sub>	<H <sub>298</sub> >
<b>5b</b>					<b>−538.3516667</b>
_01	−539.599653	−539.372802	−538.579167	−538.352316	
_02	−539.598979	−539.372055	−538.578495	−538.351571	
_03	−539.598168	−539.371234	−538.577429	−538.350495	
_04	−539.597667	−539.370947	−538.577029	−538.350309	
_05	−539.596649	−539.369859	−538.575661	−538.348871	
_06	−539.595512	−539.368823	−538.576732	−538.350044	
_07	−539.595179	−539.368411	−538.575238	−538.348470	
<b>TBS (1a)</b>					
_py_01	−775.187915	−774.873082	−773.738297	−773.423465	
_cat_01	−909.151934	−908.756686	−907.442626	−907.047378	
					<b>−1063.779233</b>
_alc_01	−1066.202182	−1065.771607	−1064.209301	−1063.778726	
_alc_02	−1066.201693	−1065.770970	−1064.210703	−1063.779979	
_alc_03	−1066.201319	−1065.770848	−1064.208978	−1063.778507	
_alc_04	−1066.201216	−1065.770565	−1064.209273	−1063.778622	
_alc_05	−1066.200263	−1065.769619	−1064.208587	−1063.777943	
_alc_06	−1066.199730	−1065.769097	−1064.208500	−1063.777867	
_alc_07	−1066.197458	−1065.766864	−1064.205506	−1063.774912	
<b>TMS (4a)</b>					
_py_01	−657.272917	−657.050856	−656.081655	−655.859595	
					<b>−789.4833696</b>
_cat_01	−791.237720	−790.934412	−789.786897	−789.483590	
_cat_02	−791.236315	−790.933929	−789.785311	−789.482925	
					<b>−946.2173061</b>
_alc_01	−948.2892492	−947.950469	−946.5554216	−946.216641	
_alc_02	−948.288701	−947.949777	−946.5567101	−946.217786	
_alc_03	−948.2858321	−947.946747	−946.555703	−946.216618	
_alc_04	−948.2852298	−947.94624	−946.5534332	−946.214443	
<b>TES (4e)</b>					<b>−773.4105078</b>
_pyr_01	−775.183040	−774.866424	−773.727785	−773.411169	
_pyr_02	−775.182454	−774.865821	−773.727008	−773.410375	
_pyr_03	−775.181628	−774.864793	−773.725761	−773.408926	
_pyr_04	−775.181307	−774.864773	−773.725844	−773.409310	
_pyr_05	−775.181211	−774.864508	−773.726158	−773.409455	
_pyr_06	−775.180801	−774.864107	−773.725191	−773.408497	
					<b>−907.0339445</b>
_cat_01	−909.146881	−908.749898	−907.431983	−907.035000	
_cat_02	−909.146333	−908.749322	−907.431210	−907.034199	
_cat_03	−909.145357	−908.748228	−907.429873	−907.032744	

**Table 8.14.** Continuation.

System	MPW1K/6-31+G(d)		MP2(FC)/G3MP2large//MPW1K/6-31+G(d)		
	E <sub>tot</sub>	H <sub>298</sub>	E <sub>tot</sub>	H <sub>298</sub>	<H <sub>298</sub> >
_cat_04	−909.145355	−908.748227	−907.429874	−907.032746	
_cat_05	−909.145347	−908.748270	−907.429869	−907.032792	
_cat_06	−909.145343	−908.748273	−907.429870	−907.032800	
_cat_07	−909.145139	−908.748178	−907.430024	−907.033063	
_cat_08	−909.145139	−908.748179	−907.430026	−907.033066	
_cat_09	−909.145065	−908.747983	−907.430389	−907.033307	
_cat_10	−909.145059	−908.747989	−907.430391	−907.033321	
_cat_11	−909.145058	−908.747991	−907.430392	−907.033324	
_cat_12	−909.144656	−908.747588	−907.429438	−907.032370	
_cat_13	−909.144547	−908.747507	−907.429052	−907.032012	
					<b>−1063.765228</b>
_alc_01	−1066.196016	−1065.763542	−1064.196722	−1063.764248	
_alc_02	−1066.195893	−1065.763543	−1064.196987	−1063.764637	
_alc_03	−1066.195876	−1065.763611	−1064.197302	−1063.765037	
_alc_04	−1066.195821	−1065.763401	−1064.197363	−1063.764943	
_alc_05	−1066.195630	−1065.763208	−1064.197743	−1063.765321	
_alc_06	−1066.195376	−1065.762863	−1064.198974	−1063.766461	
_alc_07	−1066.195374	−1065.762871	−1064.198706	−1063.766203	
_alc_08	−1066.195322	−1065.763024	−1064.197721	−1063.765423	
_alc_09	−1066.195258	−1065.762912	−1064.197856	−1063.765510	
_alc_10	−1066.195217	−1065.762938	−1064.197988	−1063.765709	
_alc_11	−1066.195183	−1065.762770	−1064.198915	−1063.766502	
_alc_12	−1066.195128	−1065.762713	−1064.196226	−1063.763811	
_alc_13	−1066.195102	−1065.762642	−1064.196215	−1063.763755	
_alc_14	−1066.195089	−1065.762537	−1064.198144	−1063.765592	
_alc_15	−1066.195041	−1065.762621	−1064.197846	−1063.765426	
_alc_16	−1066.195000	−1065.762521	−1064.196658	−1063.764179	
_alc_17	−1066.194959	−1065.762686	−1064.196077	−1063.763804	
_alc_18	−1066.194937	−1065.762686	−1064.196355	−1063.764104	
_alc_19	−1066.194786	−1065.762304	−1064.197180	−1063.764698	
_alc_20	−1066.194715	−1065.762321	−1064.195404	−1063.763010	
_alc_21	−1066.194702	−1065.762302	−1064.195642	−1063.763242	
_alc_22	−1066.194618	−1065.762194	−1064.196862	−1063.764438	
_alc_23	−1066.194603	−1065.762120	−1064.195725	−1063.763242	
_alc_24	−1066.194593	−1065.762125	−1064.196772	−1063.764304	
_alc_25	−1066.194564	−1065.762093	−1064.195412	−1063.762941	
_alc_26	−1066.194547	−1065.762120	−1064.195988	−1063.763561	
_alc_27	−1066.194530	−1065.762052	−1064.195692	−1063.763214	
_alc_28	−1066.194507	−1065.762135	−1064.194793	−1063.762421	
_alc_29	−1066.194472	−1065.762033	−1064.196839	−1063.764400	



Table 8.14. Continuation.

System	MPW1K/6-31+G(d)		MP2(FC)/G3MP2large//MPW1K/6-31+G(d)		
	E <sub>tot</sub>	H <sub>298</sub>	E <sub>tot</sub>	H <sub>298</sub>	<H <sub>298</sub> >
_alc_30	−1066.194443	−1065.761976	−1064.197897	−1063.765430	
_alc_31	−1066.194320	−1065.761904	−1064.196115	−1063.763699	
_alc_32	−1066.194241	−1065.761838	−1064.194235	−1063.761832	
_alc_33	−1066.194178	−1065.761600	−1064.196997	−1063.764419	
_alc_34	−1066.194115	−1065.761559	−1064.198612	−1063.766056	
_alc_35	−1066.194103	−1065.761706	−1064.196961	−1063.764564	
_alc_36	−1066.194065	−1065.761439	−1064.196710	−1063.764084	
_alc_37	−1066.194042	−1065.761560	−1064.197374	−1063.764892	
_alc_38	−1066.194036	−1065.761631	−1064.195637	−1063.763232	
_alc_39	−1066.194026	−1065.761690	−1064.194152	−1063.761816	
_alc_40	−1066.194013	−1065.761468	−1064.195179	−1063.762634	
_alc_41	−1066.193998	−1065.761431	−1064.197874	−1063.765307	
_alc_42	−1066.193976	−1065.761512	−1064.196362	−1063.763898	
_alc_43	−1066.193968	−1065.761417	−1064.198441	−1063.765890	
_alc_44	−1066.193937	−1065.761476	−1064.197768	−1063.765307	
_alc_45	−1066.193912	−1065.761254	−1064.196795	−1063.764137	
_alc_46	−1066.193898	−1065.761429	−1064.197060	−1063.764591	
_alc_47	−1066.193892	−1065.761436	−1064.195592	−1063.763136	
_alc_48	−1066.193885	−1065.761377	−1064.197636	−1063.765128	
_alc_49	−1066.193846	−1065.761242	−1064.196640	−1063.764036	
_alc_50	−1066.193830	−1065.761362	−1064.196818	−1063.764350	
_alc_51	−1066.193806	−1065.761348	−1064.196653	−1063.764195	
_alc_52	−1066.193701	−1065.761070	−1064.197276	−1063.764645	
_alc_53	−1066.193691	−1065.761252	−1064.196122	−1063.763683	
_alc_54	−1066.193558	−1065.761145	−1064.196846	−1063.764433	
_alc_55	−1066.193517	−1065.760945	−1064.193943	−1063.761371	
_alc_56	−1066.193452	−1065.760834	−1064.196395	−1063.763777	
_alc_57	−1066.193425	−1065.760900	−1064.195441	−1063.762916	
_alc_58	−1066.193218	−1065.760730	−1064.197323	−1063.764835	
_alc_59	−1066.193167	−1065.760603	−1064.195580	−1063.763016	
_alc_60	−1066.193155	−1065.760742	−1064.196057	−1063.763644	
_alc_61	−1066.192978	−1065.760530	−1064.194386	−1063.761938	
_alc_62	−1066.192947	−1065.760462	−1064.195686	−1063.763201	
_alc_63	−1066.192842	−1065.760305	−1064.194931	−1063.762394	
_alc_64	−1066.192789	−1065.760294	−1064.194558	−1063.762063	
_alc_65	−1066.192724	−1065.761430	−1064.195608	−1063.764314	
_alc_66	−1066.192709	−1065.760282	−1064.194562	−1063.762135	
_alc_67	−1066.192663	−1065.760141	−1064.196689	−1063.764167	
_alc_68	−1066.192611	−1065.760133	−1064.196862	−1063.764384	
_alc_69	−1066.192050	−1065.759357	−1064.194406	−1063.761713	

**Table 8.14.** Continuation.

System	MPW1K/6-31+G(d)		MP2(FC)/G3MP2large//MPW1K/6-31+G(d)		
	E <sub>tot</sub>	H <sub>298</sub>	E <sub>tot</sub>	H <sub>298</sub>	<H <sub>298</sub> >
_alc_70	−1066.191925	−1065.759397	−1064.195257	−1063.762729	
_alc_71	−1066.191780	−1065.759398	−1064.194895	−1063.762513	
_alc_72	−1066.191727	−1065.759239	−1064.195420	−1063.762932	
_alc_73	−1066.191670	−1065.758975	−1064.197446	−1063.764751	
_alc_74	−1066.191638	−1065.758973	−1064.195711	−1063.763046	
_alc_75	−1066.191571	−1065.759050	−1064.196505	−1063.763984	
_alc_76	−1066.191454	−1065.758794	−1064.196025	−1063.763365	
_alc_77	−1066.190824	−1065.758219	−1064.196102	−1063.763497	
_alc_78	−1066.190748	−1065.757929	−1064.195761	−1063.762942	
_alc_79	−1066.190736	−1065.758012	−1064.196560	−1063.763836	
_alc_80	−1066.190526	−1065.757833	−1064.196723	−1063.764030	
_alc_81	−1066.190452	−1065.757741	−1064.195579	−1063.762868	
_alc_82	−1066.189941	−1065.757141	−1064.194833	−1063.762033	
_alc_83	−1066.189890	−1065.757182	−1064.195537	−1063.762829	
_alc_84	−1066.189813	−1065.757150	−1064.195445	−1063.762782	
_alc_85	−1066.189747	−1065.756953	−1064.195060	−1063.762266	
_alc_86	−1066.189653	−1065.756980	−1064.194421	−1063.761748	
_alc_87	−1066.189517	−1065.756880	−1064.194945	−1063.762308	
_alc_88	−1066.189408	−1065.756502	−1064.195858	−1063.762952	
_alc_89	−1066.189203	−1065.756575	−1064.194511	−1063.761883	
TIPS (4b)					−890.9717993
_pyr_01	−893.092725	−892.684052	−891.381078	−890.972404	
_pyr_02	−893.091141	−892.682477	−891.379535	−890.970870	
_pyr_03	−893.091055	−892.682341	−891.379850	−890.971136	
_pyr_04	−893.090042	−892.681350	−891.378505	−890.969813	
_pyr_05	−893.089632	−892.680926	−891.377551	−890.968845	
_pyr_06	−893.088819	−892.680218	−891.377125	−890.968524	
					−1024.595232
_cat_01	−1027.056125	−1026.567009	−1025.084742	−1024.595626	
_cat_02	−1027.056085	−1026.567054	−1025.084772	−1024.595741	
_cat_03	−1027.054347	−1026.565359	−1025.083143	−1024.594155	
_cat_04	−1027.054343	−1026.565365	−1025.083141	−1024.594163	
_cat_05	−1027.054260	−1026.565319	−1025.083532	−1024.594591	
_cat_06	−1027.053262	−1026.564312	−1025.082099	−1024.593149	
_cat_07	−1027.052940	−1026.563905	−1025.081279	−1024.592244	
_cat_08	−1027.052083	−1026.563161	−1025.080883	−1024.591961	
					−1181.325438
_alc_01	−1184.104774	−1183.580435	−1181.850133	−1181.325794	
_alc_02	−1184.104651	−1183.580378	−1181.850383	−1181.326110	
_alc_03	−1184.104508	−1183.580336	−1181.849363	−1181.325192	

Table 8.14. Continuation.

System	MPW1K/6-31+G(d)		MP2(FC)/G3MP2large//MPW1K/6-31+G(d)		
	E <sub>tot</sub>	H <sub>298</sub>	E <sub>tot</sub>	H <sub>298</sub>	<H <sub>298</sub> >
_alc_04	-1184.104280	-1183.580084	-1181.850689	-1181.326493	
_alc_05	-1184.104113	-1183.579873	-1181.849484	-1181.325244	
_alc_06	-1184.103932	-1183.579751	-1181.849214	-1181.325033	
_alc_07	-1184.103869	-1183.579639	-1181.848838	-1181.324608	
_alc_08	-1184.103453	-1183.579242	-1181.850885	-1181.326674	
_alc_09	-1184.103392	-1183.579117	-1181.849446	-1181.325171	
_alc_10	-1184.103334	-1183.579190	-1181.849145	-1181.325001	
_alc_11	-1184.103241	-1183.579101	-1181.847587	-1181.323447	
_alc_12	-1184.103235	-1183.578924	-1181.850059	-1181.325748	
_alc_13	-1184.103229	-1183.578972	-1181.850216	-1181.325958	
_alc_14	-1184.103147	-1183.578809	-1181.849930	-1181.325592	
_alc_15	-1184.103131	-1183.578852	-1181.849276	-1181.324997	
_alc_16	-1184.103031	-1183.578852	-1181.847765	-1181.323586	
_alc_17	-1184.103011	-1183.578771	-1181.849218	-1181.324978	
_alc_18	-1184.102971	-1183.578750	-1181.848256	-1181.324034	
_alc_19	-1184.102852	-1183.578609	-1181.848014	-1181.323772	
_alc_20	-1184.102792	-1183.578564	-1181.848384	-1181.324156	
_alc_21	-1184.102792	-1183.578568	-1181.848378	-1181.324154	
_alc_22	-1184.102603	-1183.578361	-1181.847698	-1181.323456	
_alc_23	-1184.102596	-1183.578269	-1181.850020	-1181.325693	
_alc_24	-1184.102387	-1183.578125	-1181.848104	-1181.323842	
_alc_25	-1184.102314	-1183.577874	-1181.847598	-1181.323159	
_alc_26	-1184.102275	-1183.577904	-1181.848598	-1181.324227	
_alc_27	-1184.102235	-1183.577949	-1181.849708	-1181.325422	
_alc_28	-1184.102202	-1183.577836	-1181.848751	-1181.324385	
_alc_29	-1184.102176	-1183.577920	-1181.848637	-1181.324381	
_alc_30	-1184.102160	-1183.577939	-1181.847656	-1181.323435	
_alc_31	-1184.102151	-1183.577765	-1181.848483	-1181.324097	
_alc_32	-1184.102080	-1183.577861	-1181.848081	-1181.323862	
_alc_33	-1184.102079	-1183.577862	-1181.848084	-1181.323867	
_alc_34	-1184.102071	-1183.577860	-1181.848962	-1181.324751	
_alc_35	-1184.102020	-1183.577509	-1181.847273	-1181.322762	
_alc_36	-1184.102012	-1183.577632	-1181.848346	-1181.323967	
_alc_37	-1184.102010	-1183.577456	-1181.848065	-1181.323511	
_alc_38	-1184.102003	-1183.577807	-1181.847897	-1181.323701	
_alc_39	-1184.101949	-1183.577537	-1181.848282	-1181.323870	
_alc_40	-1184.101907	-1183.577439	-1181.848379	-1181.323911	
_alc_41	-1184.101730	-1183.577382	-1181.849939	-1181.325591	
_alc_42	-1184.101716	-1183.577265	-1181.849150	-1181.324699	
_alc_43	-1184.101649	-1183.577248	-1181.849562	-1181.325161	

### 8.3 Computational Methods

**Table 8.14.** Continuation.

System	MPW1K/6-31+G(d)		MP2(FC)/G3MP2large//MPW1K/6-31+G(d)		
	E <sub>tot</sub>	H <sub>298</sub>	E <sub>tot</sub>	H <sub>298</sub>	<H <sub>298</sub> >
_alc_44	−1184.101608	−1183.577327	−1181.847861	−1181.323581	
_alc_45	−1184.101582	−1183.577200	−1181.847964	−1181.323581	
_alc_46	−1184.101417	−1183.577008	−1181.848191	−1181.323782	
_alc_47	−1184.101353	−1183.576875	−1181.847717	−1181.323239	
_alc_48	−1184.101308	−1183.576864	−1181.849072	−1181.324628	
_alc_49	−1184.101093	−1183.576928	−1181.847315	−1181.323149	
_alc_50	−1184.101093	−1183.576925	−1181.847316	−1181.323148	
_alc_51	−1184.100993	−1183.576570	−1181.847797	−1181.323374	
_alc_52	−1184.100881	−1183.576414	−1181.847619	−1181.323152	
_alc_53	−1184.100847	−1183.576298	−1181.848959	−1181.324410	
DMNS (4f)					−1000.382069
_pyr_01	−1002.567680	−1002.234660	−1000.715108	−1000.382088	
_pyr_02	−1002.562624	−1002.229625	−1000.709757	−1000.376758	
					−1134.005195
_cat_01	−1136.530815	−1136.117369	−1134.418675	−1134.005229	
_cat_02	−1136.526685	−1136.113276	−1134.414035	−1134.000626	
					−1290.737303
_alc_01	−1293.579954	−1293.130896	−1291.184371	−1290.735312	
_alc_02	−1293.579658	−1293.130574	−1291.187007	−1290.737923	
_alc_03	−1293.579261	−1293.130199	−1291.185245	−1290.736183	
_alc_04	−1293.577853	−1293.128823	−1291.185245	−1290.736214	
_alc_05	−1293.577729	−1293.12881	−1291.183737	−1290.734818	
_alc_06	−1293.576471	−1293.127545	−1291.182770	−1290.733843	
TBDPS (4c)					
_pyr_01	−1158.557013	−1158.123872	−1156.380055	−1155.946914	
_cat_01	−1292.519298	−1292.005895	−1290.083005	−1289.569602	
					−1446.302012
_alc_01	−1449.570057	−1449.013828	−1446.849935	−1446.293706	
_alc_02	−1449.570046	−1449.021171	−1446.849897	−1446.301022	
_alc_03	−1449.569396	−1449.020306	−1446.848296	−1446.299206	
_alc_04	−1449.568806	−1449.019714	−1446.850162	−1446.301070	
_alc_05	−1449.568805	−1449.019713	−1446.850159	−1446.301067	
_alc_06	−1449.568693	−1449.019919	−1446.847979	−1446.299205	
_alc_07	−1449.568470	−1449.019551	−1446.849266	−1446.300347	
_alc_08	−1449.568250	−1449.019189	−1446.849395	−1446.300333	
_alc_09	−1449.568237	−1449.019368	−1446.851279	−1446.302409	
_alc_10	−1449.568018	−1449.019300	−1446.849654	−1446.300936	
_alc_11	−1449.567535	−1449.018398	−1446.852151	−1446.303014	
_alc_12	−1449.568250	−1449.019188	−1446.849397	−1446.300335	
_alc_13	−1449.565970	−1449.017189	−1446.849588	−1446.300807	

Table 8.14. Continuation.

System	MPW1K/6-31+G(d)		MP2(FC)/G3MP2large//MPW1K/6-31+G(d)		
	E <sub>tot</sub>	H <sub>298</sub>	E <sub>tot</sub>	H <sub>298</sub>	<H <sub>298</sub> >
_alc_14	−1449.565724	−1449.016997	−1446.843725	−1446.294998	
_alc_15	−1449.565532	−1449.016510	−1446.847732	−1446.298711	
_alc_16	−1449.564739	−1449.016560	−1446.847858	−1446.299679	
_alc_17	−1449.564169	−1449.015284	−1446.845577	−1446.296691	
_alc_18	−1449.562986	−1449.013828	−1446.848397	−1446.299239	
_alc_19	−1449.562959	−1449.014074	−1446.843762	−1446.294878	
_alc_20	−1449.562939	−1449.013765	−1446.848653	−1446.299479	
-----					
TTMSS (4d)					
_pyr_01	−1765.277994	−1764.803583	−1762.188601	−1761.714190	
_cat_01	−1899.239076	−1898.684149	−1895.890288	−1895.335362	
					−2052.059287
_alc_01	−2056.279568	−2055.689615	−2052.648497	−2052.058544	
_alc_02	−2056.279521	−2055.689499	−2052.649424	−2052.059401	
_alc_03	−2056.278487	−2055.688232	−2052.649022	−2052.058767	
_alc_04	−2056.278078	−2055.688824	−2052.646996	−2052.057742	
_alc_05	−2056.278064	−2055.688054	−2052.649782	−2052.059772	
-----					
BPDMS (4h)					
_pyr_01	−1079.965587	−1079.595532	−1077.952944	−1077.582889	
_cat_01	−1213.928400	−1213.478010	−1211.656071	−1211.205681	
					−1367.925685
_alc_01	−1370.962353	−1370.477879	−1368.407496	−1367.923022	
_alc_02	−1370.962314	−1370.477929	−1368.407383	−1367.922999	
_alc_03	−1370.962202	−1370.477736	−1368.407838	−1367.923372	
_alc_04	−1370.962073	−1370.477675	−1368.407953	−1367.923554	
_alc_05	−1370.961508	−1370.477121	−1368.404893	−1367.920506	
_alc_06	−1370.961444	−1370.47693	−1368.410792	−1367.926278	
_alc_07	−1370.96122	−1370.476766	−1368.410029	−1367.925575	
_alc_08	−1370.96096	−1370.476503	−1368.405699	−1367.921242	
_alc_09	−1370.960896	−1370.476484	−1368.405729	−1367.921318	
_alc_10	−1370.960765	−1370.476406	−1368.405562	−1367.921203	
_alc_11	−1370.960618	−1370.476264	−1368.405295	−1367.920941	
_alc_12	−1370.960353	−1370.475947	−1368.405296	−1367.92089	
_alc_13	−1370.960311	−1370.475791	−1368.405917	−1367.921396	
_alc_14	−1370.960276	−1370.475864	−1368.405193	−1367.920781	
-----					
TPS (4g)					
_pyr_01	−1232.334775	−1231.934668	−1230.048452	−1229.648346	
_pyr_02	−1232.331014	−1231.931738	−1230.044902	−1229.645626	
_cat_01	−1366.297274	−1365.816812	−1363.751340	−1363.270878	
					−1519.999433
_alc_01	−1523.344651	−1522.828636	−1520.514116	−1519.998101	

### 8.3 Computational Methods

**Table 8.14.** Continuation.

System	MPW1K/6-31+G(d)		MP2(FC)/G3MP2large//MPW1K/6-31+G(d)		
	E <sub>tot</sub>	H <sub>298</sub>	E <sub>tot</sub>	H <sub>298</sub>	<H <sub>298</sub> >
_alc_02	−1523.343848	−1522.827866	−1520.512507	−1519.996526	
_alc_03	−1523.343537	−1522.827579	−1520.515155	−1519.999197	
_alc_04	−1523.343396	−1522.827501	−1520.515631	−1519.999737	
_alc_05	−1523.343256	−1522.827339	−1520.515677	−1519.999760	
_alc_06	−1523.343162	−1522.827042	−1520.515216	−1519.999096	
_alc_07	−1523.342815	−1522.826690	−1520.513884	−1519.997759	
_alc_08	−1523.342492	−1522.826392	−1520.513553	−1519.997453	
_alc_09	−1523.341418	−1522.825294	−1520.513726	−1519.997602	
_alc_10	−1523.341319	−1522.825297	−1520.516129	−1520.000107	
_alc_11	−1523.338808	−1522.822499	−1520.514254	−1519.997945	
_alc_12	−1523.338232	−1522.821962	−1520.514014	−1519.997743	

**Table 8.15.** Data for several silyl chlorides, the intermediate with DMAP (\_cat) and their adducts with alcohol **5b** (\_alc). Gas phase calculation with additional SMD values in CHCl<sub>3</sub>.

System	MP2(FC)/G3MP2large// MPW1K/6-31+G(d)		SMD/MPW1K/6-31+G(d)	
	E <sub>tot</sub>	ΔG <sub>sol</sub>	ΔH <sub>298</sub>	<H <sub>298</sub> >
Pyridine				
_01	−247.647677	−0.010709	−247.658386	
DMAP ( <b>3a</b> )				
_01	−381.250023	−0.015239	−381.265262	
_H	−381.625632	−0.075723	−381.701355	
<b>5b</b>				−538.370457
_01	−538.352316	−0.018952	−538.371267	
_02	−538.351571	−0.018269	−538.369840	
_03	−538.350495	−0.018890	−538.369385	
_04	−538.350309	−0.018851	−538.369160	
_05	−538.348871	−0.019947	−538.368818	
_06	−538.350044	−0.019521	−538.369565	
_07	−538.348470	−0.020320	−538.368790	
TBS ( <b>1a</b> )				
_py_01	−773.423465	−0.071527	−773.494992	
_cat_01	−907.047378	−0.068278	−907.115656	
				−1063.798615
_alc_01	−1063.778726	−0.020040	−1063.798766	
_alc_02	−1063.779979	−0.019165	−1063.799144	
_alc_03	−1063.778507	−0.019898	−1063.798405	
_alc_04	−1063.778622	−0.019782	−1063.798404	

Table 8.15. Continuation.

System	MP2(FC)/G3MP2large// MPW1K/6-31+G(d)	SMD/MPW1K/6-31+G(d)		
	$E_{\text{tot}}$	$\Delta G_{\text{sol}}$	$\Delta H_{298}$	$\langle H_{298} \rangle$
_alc_05	−1063.777943	−0.019520	−1063.797463	
_alc_06	−1063.777867	−0.019199	−1063.797066	
_alc_07	−1063.774912	−0.020758	−1063.795670	
-----				
TMS (4a)				
_py_01	−655.859595	−0.071026	−655.930621	
				−789.550527
_cat_01	−789.483590	−0.067135	−789.550725	
_cat_02	−789.482925	−0.067245	−789.550170	
				−946.234752
_alc_01	−946.216641	−0.018137	−946.234778	
_alc_02	−946.217786	−0.017299	−946.235086	
_alc_03	−946.216618	−0.017092	−946.233710	
_alc_04	−946.214443	−0.017627	−946.232071	
-----				
TES (4e)				−773.482901
_pyr_01	−773.411169	−0.072401	−773.483570	
_pyr_02	−773.410375	−0.072331	−773.482706	
_pyr_03	−773.408926	−0.072280	−773.481206	
_pyr_04	−773.409310	−0.072348	−773.481658	
_pyr_05	−773.409455	−0.072658	−773.482112	
_pyr_06	−773.408497	−0.072438	−773.480935	
				−907.103165
_cat_01	−907.035000	−0.069246	−907.104246	
_cat_02	−907.034199	−0.068932	−907.103131	
_cat_03	−907.032744	−0.068992	−907.101736	
_cat_04	−907.032746	−0.068982	−907.101727	
_cat_05	−907.032792	−0.068931	−907.101723	
_cat_06	−907.032800	−0.068936	−907.101736	
_cat_07	−907.033063	−0.069055	−907.102118	
_cat_08	−907.033066	−0.069056	−907.102122	
_cat_09	−907.033307	−0.069304	−907.102611	
_cat_10	−907.033321	−0.069311	−907.102632	
_cat_11	−907.033324	−0.069313	−907.1026372	
_cat_12	−907.032370	−0.069151	−907.1015213	
_cat_13	−907.032012	−0.069020	−907.101032	
				−1063.785584
_alc_01	−1063.764248	−0.021183	−1063.785432	
_alc_02	−1063.764637	−0.021036	−1063.785674	
_alc_03	−1063.765037	−0.021093	−1063.786129	

**Table 8.15.** Continuation.

System	MP2(FC)/G3MP2large// MPW1K/6-31+G(d)	SMD/MPW1K/6-31+G(d)		
	$E_{\text{tot}}$	$\Delta G_{\text{sol}}$	$\Delta H_{298}$	$\langle H_{298} \rangle$
_alc_04	−1063.764943	−0.021176	−1063.786119	
_alc_05	−1063.765321	−0.020848	−1063.786169	
_alc_06	−1063.766461	−0.020273	−1063.786734	
_alc_07	−1063.766203	−0.020296	−1063.786499	
_alc_08	−1063.765423	−0.020716	−1063.786139	
_alc_09	−1063.765510	−0.020698	−1063.786209	
_alc_10	−1063.765709	−0.020708	−1063.786417	
_alc_11	−1063.766502	−0.020124	−1063.786626	
_alc_12	−1063.763811	−0.021299	−1063.785110	
_alc_13	−1063.763755	−0.021109	−1063.784864	
_alc_14	−1063.765592	−0.020207	−1063.785799	
_alc_15	−1063.765426	−0.020348	−1063.785775	
_alc_16	−1063.764179	−0.021322	−1063.785501	
_alc_17	−1063.763804	−0.021129	−1063.784933	
_alc_18	−1063.764104	−0.021129	−1063.785234	
_alc_19	−1063.764698	−0.020815	−1063.785512	
_alc_20	−1063.763010	−0.021307	−1063.784316	
_alc_21	−1063.763242	−0.021254	−1063.784496	
_alc_22	−1063.764438	−0.020831	−1063.785269	
_alc_23	−1063.763242	−0.021110	−1063.784352	
_alc_24	−1063.764304	−0.020977	−1063.785281	
_alc_25	−1063.762941	−0.021402	−1063.784344	
_alc_26	−1063.763561	−0.020898	−1063.784459	
_alc_27	−1063.763214	−0.021326	−1063.784540	
_alc_28	−1063.762421	−0.021438	−1063.783858	
_alc_29	−1063.764400	−0.020877	−1063.785278	
_alc_30	−1063.765430	−0.020066	−1063.785496	
_alc_31	−1063.763699	−0.021041	−1063.784740	
_alc_32	−1063.761832	−0.021459	−1063.783289	
_alc_33	−1063.764419	−0.020459	−1063.784878	
_alc_34	−1063.766056	−0.019927	−1063.785983	
_alc_35	−1063.764564	−0.020487	−1063.785051	
_alc_36	−1063.764084	−0.020336	−1063.784421	
_alc_37	−1063.764892	−0.020167	−1063.785059	
_alc_38	−1063.763232	−0.020972	−1063.784204	
_alc_39	−1063.761816	−0.021279	−1063.783095	
_alc_40	−1063.762634	−0.021356	−1063.783991	
_alc_41	−1063.765307	−0.019961	−1063.785268	
_alc_42	−1063.763898	−0.020528	−1063.784426	



Table 8.15. Continuation.

System	MP2(FC)/G3MP2large// MPW1K/6-31+G(d)	SMD/MPW1K/6-31+G(d)		
	$E_{\text{tot}}$	$\Delta G_{\text{sol}}$	$\Delta H_{298}$	$\langle H_{298} \rangle$
_alc_43	−1063.765890	−0.019825	−1063.785714	
_alc_44	−1063.765307	−0.020143	−1063.785450	
_alc_45	−1063.764137	−0.020477	−1063.784614	
_alc_46	−1063.764591	−0.020375	−1063.784966	
_alc_47	−1063.763136	−0.021018	−1063.784154	
_alc_48	−1063.765128	−0.020082	−1063.785210	
_alc_49	−1063.764036	−0.020477	−1063.784513	
_alc_50	−1063.764350	−0.020594	−1063.784944	
_alc_51	−1063.764195	−0.020310	−1063.784505	
_alc_52	−1063.764645	−0.020092	−1063.784737	
_alc_53	−1063.763683	−0.020730	−1063.784413	
_alc_54	−1063.764433	−0.020423	−1063.784856	
_alc_55	−1063.761371	−0.021338	−1063.782709	
_alc_56	−1063.763777	−0.020384	−1063.784161	
_alc_57	−1063.762916	−0.020495	−1063.783411	
_alc_58	−1063.764835	−0.019926	−1063.784760	
_alc_59	−1063.763016	−0.020685	−1063.783700	
_alc_60	−1063.763644	−0.020539	−1063.784183	
_alc_61	−1063.761938	−0.021082	−1063.783020	
_alc_62	−1063.763201	−0.020727	−1063.783928	
_alc_63	−1063.762394	−0.020643	−1063.783036	
_alc_64	−1063.762063	−0.020905	−1063.782968	
_alc_65	−1063.764314	−0.020480	−1063.784794	
_alc_66	−1063.762135	−0.020784	−1063.782919	
_alc_67	−1063.764167	−0.019982	−1063.784149	
_alc_68	−1063.764384	−0.021094	−1063.785479	
_alc_69	−1063.761713	−0.020490	−1063.782203	
_alc_70	−1063.762729	−0.019996	−1063.782726	
_alc_71	−1063.762513	−0.020300	−1063.782814	
_alc_72	−1063.762932	−0.020172	−1063.783104	
_alc_73	−1063.764751	−0.020113	−1063.784865	
_alc_74	−1063.763046	−0.020550	−1063.783596	
_alc_75	−1063.763984	−0.020144	−1063.784127	
_alc_76	−1063.763365	−0.020176	−1063.783541	
_alc_77	−1063.763497	−0.019990	−1063.783487	
_alc_78	−1063.762942	−0.020268	−1063.783210	
_alc_79	−1063.763836	−0.019827	−1063.783664	
_alc_80	−1063.764030	−0.019771	−1063.783802	
_alc_81	−1063.762868	−0.019958	−1063.782826	

**Table 8.15.** Continuation.

System	MP2(FC)/G3MP2large// MPW1K/6-31+G(d)	SMD/MPW1K/6-31+G(d)		
	$E_{\text{tot}}$	$\Delta G_{\text{sol}}$	$\Delta H_{298}$	$\langle H_{298} \rangle$
_alc_82	−1063.762033	−0.020113	−1063.782146	
_alc_83	−1063.762829	−0.020008	−1063.782837	
_alc_84	−1063.762782	−0.020247	−1063.783030	
_alc_85	−1063.762266	−0.020236	−1063.782503	
_alc_86	−1063.761748	−0.020349	−1063.782098	
_alc_87	−1063.762308	−0.020015	−1063.782322	
_alc_88	−1063.762952	−0.019609	−1063.782561	
_alc_89	−1063.761883	−0.020044	−1063.781927	
-----				
TIPS (4b)				−891.044042
_pyr_01	−890.972404	−0.072226	−891.044630	
_pyr_02	−890.970870	−0.072233	−891.043104	
_pyr_03	−890.971136	−0.072114	−891.043250	
_pyr_04	−890.969813	−0.072095	−891.041908	
_pyr_05	−890.968845	−0.071696	−891.040541	
_pyr_06	−890.968524	−0.072196	−891.040720	
				−1024.664499
_cat_01	−1024.595626	−0.069212	−1024.664838	
_cat_02	−1024.595741	−0.069311	−1024.665051	
_cat_03	−1024.594155	−0.069383	−1024.663538	
_cat_04	−1024.594163	−0.069378	−1024.663541	
_cat_05	−1024.594591	−0.069378	−1024.663970	
_cat_06	−1024.593149	−0.069390	−1024.662539	
_cat_07	−1024.592244	−0.069131	−1024.661375	
_cat_08	−1024.591961	−0.069516	−1024.661477	
				−1181.346769
_alc_01	−1181.325794	−0.021609	−1181.347403	
_alc_02	−1181.326110	−0.021519	−1181.347629	
_alc_03	−1181.325192	−0.021834	−1181.347026	
_alc_04	−1181.326493	−0.021524	−1181.348017	
_alc_05	−1181.325244	−0.021887	−1181.347132	
_alc_06	−1181.325033	−0.021794	−1181.346827	
_alc_07	−1181.324608	−0.021946	−1181.346554	
_alc_08	−1181.326674	−0.020909	−1181.347584	
_alc_09	−1181.325171	−0.021395	−1181.346566	
_alc_10	−1181.325001	−0.021663	−1181.346664	
_alc_11	−1181.323447	−0.022064	−1181.345511	
_alc_12	−1181.325748	−0.021373	−1181.347121	
_alc_13	−1181.325958	−0.021269	−1181.347227	
_alc_14	−1181.325592	−0.020983	−1181.346575	

Table 8.15. Continuation.

System	MP2(FC)/G3MP2large// MPW1K/6-31+G(d)	SMD/MPW1K/6-31+G(d)		
	$E_{\text{tot}}$	$\Delta G_{\text{sol}}$	$\Delta H_{298}$	$\langle H_{298} \rangle$
_alc_15	−1181.324997	−0.021699	−1181.346696	
_alc_16	−1181.323586	−0.021988	−1181.345575	
_alc_17	−1181.324978	−0.021172	−1181.346150	
_alc_18	−1181.324034	−0.021740	−1181.345775	
_alc_19	−1181.323772	−0.022028	−1181.345800	
_alc_20	−1181.324156	−0.021590	−1181.345747	
_alc_21	−1181.324154	−0.021591	−1181.345746	
_alc_22	−1181.323456	−0.021842	−1181.345298	
_alc_23	−1181.325693	−0.021036	−1181.346729	
_alc_24	−1181.323842	−0.021592	−1181.345434	
_alc_25	−1181.323159	−0.021853	−1181.345012	
_alc_26	−1181.324227	−0.021159	−1181.345386	
_alc_27	−1181.325422	−0.021073	−1181.346494	
_alc_28	−1181.324385	−0.021313	−1181.345698	
_alc_29	−1181.324381	−0.021176	−1181.345557	
_alc_30	−1181.323435	−0.021812	−1181.345246	
_alc_31	−1181.324097	−0.021436	−1181.345533	
_alc_32	−1181.323862	−0.021785	−1181.345647	
_alc_33	−1181.323867	−0.021785	−1181.345652	
_alc_34	−1181.324751	−0.020860	−1181.345611	
_alc_35	−1181.322762	−0.021882	−1181.344644	
_alc_36	−1181.323967	−0.021331	−1181.345298	
_alc_37	−1181.323511	−0.021697	−1181.345208	
_alc_38	−1181.323701	−0.021594	−1181.345295	
_alc_39	−1181.323870	−0.021539	−1181.345409	
_alc_40	−1181.323911	−0.021437	−1181.345348	
_alc_41	−1181.325591	−0.020829	−1181.346419	
_alc_42	−1181.324699	−0.021042	−1181.345741	
_alc_43	−1181.325161	−0.021141	−1181.346301	
_alc_44	−1181.323581	−0.021543	−1181.345124	
_alc_45	−1181.323581	−0.021588	−1181.345169	
_alc_46	−1181.323782	−0.021559	−1181.345341	
_alc_47	−1181.323239	−0.021623	−1181.344862	
_alc_48	−1181.324628	−0.020809	−1181.345438	
_alc_49	−1181.323149	−0.021486	−1181.344635	
_alc_50	−1181.323148	−0.021486	−1181.344634	
_alc_51	−1181.323374	−0.021297	−1181.344671	
_alc_52	−1181.323152	−0.021481	−1181.344633	

### 8.3 Computational Methods

**Table 8.15.** Continuation.

System	MP2(FC)/G3MP2large// MPW1K/6-31+G(d)	SMD/MPW1K/6-31+G(d)		
	$E_{\text{tot}}$	$\Delta G_{\text{sol}}$	$\Delta H_{298}$	$\langle H_{298} \rangle$
_alc_53	−1181.324410	−0.021153	−1181.345562	
DMNS (4f)				−1000.457710
_pyr_01	−1000.382088	−0.075743	−1000.457831	
_pyr_02	−1000.376758	−0.078093	−1000.454851	
				−1134.078805
_cat_01	−1134.005229	−0.073717	−1134.078947	
_cat_02	−1134.000626	−0.075576	−1134.076202	
				−1290.764919
_alc_01	−1290.735312	−0.028639	−1290.763951	
_alc_02	−1290.737923	−0.027604	−1290.765527	
_alc_03	−1290.736183	−0.028595	−1290.764778	
_alc_04	−1290.736214	−0.028492	−1290.764706	
_alc_05	−1290.734818	−0.028754	−1290.763571	
_alc_06	−1290.733843	−0.028738	−1290.762582	
TBDPS (4c)				
_pyr_01	−1155.946914	−0.075784	−1156.022698	
_cat_01	−1289.569602	−0.074632	−1289.644234	
				−1446.333599
_alc_01	−1446.293706	−0.031377	−1446.325084	
_alc_02	−1446.301022	−0.031587	−1446.332609	
_a3c_03	−1446.299206	−0.031746	−1446.330951	
_alc_04	−1446.301070	−0.031002	−1446.332073	
_alc_05	−1446.301067	−0.031002	−1446.332070	
_alc_06	−1446.299205	−0.031761	−1446.330967	
_alc_07	−1446.300347	−0.031063	−1446.331410	
_alc_08	−1446.300333	−0.030898	−1446.331231	
_alc_09	−1446.302409	−0.032095	−1446.334504	
_alc_10	−1446.300936	−0.031614	−1446.332550	
_alc_11	−1446.303014	−0.031023	−1446.334038	
_alc_12	−1446.300335	−0.030896	−1446.331231	
_alc_13	−1446.300807	−0.031754	−1446.332561	
_alc_14	−1446.294998	−0.032719	−1446.327718	
_alc_15	−1446.298711	−0.032291	−1446.331002	
_alc_16	−1446.299679	−0.030929	−1446.330607	
_alc_17	−1446.296691	−0.031897	−1446.328589	
_alc_18	−1446.299239	−0.030599	−1446.329839	
_alc_19	−1446.294878	−0.032461	−1446.327339	
_alc_20	−1446.299479	−0.030634	−1446.330112	
TTMSS (4d)				

Table 8.15. Continuation.

System	MP2(FC)/G3MP2large// MPW1K/6-31+G(d)	SMD/MPW1K/6-31+G(d)		
	$E_{\text{tot}}$	$\Delta G_{\text{sol}}$	$\Delta H_{298}$	$\langle H_{298} \rangle$
_pyr_01	−1761.714190	−0.065640	−1761.779830	
_cat_01	−1895.335362	−0.063896	−1895.399258	
				<b>−2052.078540</b>
_alc_01	−2052.058544	−0.020019	−2052.078563	
_alc_02	−2052.059401	−0.019479	−2052.078881	
_alc_03	−2052.058767	−0.019263	−2052.07803	
_alc_04	−2052.057742	−0.019927	−2052.077669	
_alc_05	−2052.059772	−0.018884	−2052.078656	
-----				
BPDMS (4h)				
_pyr_01	−1077.582889	−0.078395	−1077.661284	
_cat_01	−1211.205681	−0.076121	−1211.281801	
				<b>−1367.956274</b>
_alc_01	−1367.923022	−0.031075	−1367.954097	
_alc_02	−1367.922999	−0.031022	−1367.954021	
_alc_03	−1367.923372	−0.031033	−1367.954405	
_alc_04	−1367.923554	−0.031057	−1367.954611	
_alc_05	−1367.920506	−0.031535	−1367.95204	
_alc_06	−1367.926278	−0.030672	−1367.95695	
_alc_07	−1367.925575	−0.030820	−1367.956395	
_alc_08	−1367.921242	−0.031340	−1367.952582	
_alc_09	−1367.921318	−0.031359	−1367.952677	
_alc_10	−1367.921203	−0.031357	−1367.95256	
_alc_11	−1367.920941	−0.031531	−1367.952472	
_alc_12	−1367.92089	−0.031451	−1367.952342	
_alc_13	−1367.921396	−0.031572	−1367.952968	
_alc_14	−1367.920781	−0.031390	−1367.952171	
-----				
TPS (4g)				
_pyr_01	−1229.648346	−0.078239	−1229.726585	
_pyr_02	−1229.645626	−0.078626	−1229.724252	
_cat_01	−1363.270878	−0.077419	−1363.348297	
				<b>−1520.035970</b>
_alc_01	−1519.998101	−0.036594	−1520.034696	
_alc_02	−1519.996526	−0.036713	−1520.033239	
_alc_03	−1519.999197	−0.036756	−1520.035953	
_alc_04	−1519.999737	−0.036719	−1520.036456	
_alc_05	−1519.999760	−0.036068	−1520.035828	
_alc_06	−1519.999096	−0.036057	−1520.035153	
_alc_07	−1519.997759	−0.036352	−1520.034111	
_alc_08	−1519.997453	−0.036183	−1520.033636	

### 8.3 Computational Methods

**Table 8.15.** Continuation.

System	MP2(FC)/G3MP2large// MPW1K/6-31+G(d)	SMD/MPW1K/6-31+G(d)		
	$E_{\text{tot}}$	$\Delta G_{\text{sol}}$	$\Delta H_{298}$	$\langle H_{298} \rangle$
_alc_09	−1519.997602	−0.036987	−1520.03459	
_alc_10	−1520.000107	−0.036536	−1520.036643	
_alc_11	−1519.997945	−0.036124	−1520.034069	
_alc_12	−1519.997743	−0.035852	−1520.033595	

**Table 8.16.** Silyl cation affinities (in  $\text{kJ mol}^{-1}$ ) of various silyl compounds with DMAP relative to pyridine (gas and solution phase data). Reaction enthalpies ( $\Delta H_{\text{Rkt}}$ ) for the transfer to products alcohol (gas and solution phase data)

System	Silyl cation affinities		Reaction Enthalpies	
	$\Delta H_{298}$	$\Delta H_{298} (\text{sol})$	$\Delta H_{298}$	$\Delta H_{298} (\text{sol})$
Pyridine	0	0	n.d.	n.d.
TMS ( <b>4a</b> )	−56.3	−34.2	−20.7	−39.7
TES ( <b>4e</b> )	−55.4	−35.2	−13.8	−35.0
TIPS ( <b>4b</b> )	−55.4	−35.7	−11.0	−34.6
TBS ( <b>1a</b> )	−56.6	−36.2	−15.3	−36.4
TBDPS ( <b>4c</b> )	−53.4	−38.5	−16.7	−53.2
DMNS ( <b>4f</b> )	−54.6	−37.3	−15.9	−44.7
TTMSS ( <b>4d</b> )	−49.4	−33.0	+5.5	−26.7
BPDMS ( <b>4h</b> )	−53.7	−35.8	+15.8	−14.1
TPS ( <b>4g</b> )	−53.4	−39.4	−4.9	−46.6

**Table 8.17.** Data for surface area and cavity volumes for silyl-intermediates with DMAP (**3a**) relative to TBS (**1a**). Data achieved from SMD calculation in  $\text{CHCl}_3$  at SMD/MPW1K/6-31+G(d) level of theory.

System	Surface Area	Cavity Volume	Surf <sub>rel</sub>	Vol <sub>rel</sub>
TBS ( <b>1a</b> )				
_01	296.232	277.119	1.000	1.000
TMS ( <b>4a</b> )				
_01	247.964	229.034	0.837	0.826
_02	247.385	228.697	0.835	0.825
Avg.			<b>0.840</b>	<b>0.830</b>
TES ( <b>4e</b> )				
_01	301.932	279.496	1.019	1.009
_02	301.562	279.702	1.018	1.009
_03	302.816	279.326	1.022	1.008

Table 8.17. Continuation.

System	Surface Area	Cavity Volume	Surf <sub>rel</sub>	Vol <sub>rel</sub>
_04	301.232	279.367	1.017	1.008
_05	302.358	278.561	1.021	1.005
_06	304.161	279.695	1.027	1.009
_07	301.222	279.368	1.017	1.008
_08	302.313	278.507	1.021	1.005
_09	302.902	279.417	1.023	1.008
_10	301.691	279.592	1.018	1.009
_11	302.064	279.153	1.020	1.007
_12	301.782	279.369	1.019	1.008
_13	301.951	279.513	1.019	1.009
Avg.			<b>1.020</b>	<b>1.008</b>
-----				
TIPS (4b)				
_01	349.193	329.623	1.179	1.189
_02	349.265	329.656	1.179	1.190
_03	345.508	329.601	1.166	1.189
_04	345.540	329.342	1.166	1.188
_05	345.787	329.294	1.167	1.188
_06	349.164	329.120	1.179	1.188
_07	347.854	328.582	1.174	1.186
_08	345.132	328.784	1.165	1.186
Avg.			<b>1.172</b>	<b>1.188</b>
-----				
DMNS (4f)				
_01	345.030	334.525	1.165	1.129
_02	345.510	334.826	1.166	1.130
Avg.			<b>1.166</b>	<b>1.130</b>
-----				
TBDPS (4c)				
_01	404.063	398.836	1.364	1.346
Avg.			<b>1.364</b>	<b>1.346</b>
-----				
TTMSS (4d)				
_01	447.006	440.555	1.509	1.487
Avg.			<b>1.509</b>	<b>1.487</b>
-----				
BPDMS (4i)				
_01	384.612	366.515	1.298	1.237
Avg.			<b>1.298</b>	<b>1.237</b>
-----				
TPS (4g)				
_01	416.759	409.415	1.407	1.477
Avg.			<b>1.407</b>	<b>1.477</b>





## 9 References

- [1] P. J. Kocienski, *Protecting Groups*, 3. Aufl., Thieme, Stuttgart, **2005**.
- [2] P. G. M. Wuts, T. W. Greene, *Protective Groups in Organic Synthesis*, 4. Aufl., John Wiley & Sons, **2006**.
- [3] A. Venkateswarlu, E. J. Corey, *J. Am. Chem. Soc.* **1972**, *94*, 6190–6191.
- [4] S. K. Chaudhary, O. Hernandez, *Tetrahedron Lett.* **1979**, *20*, 99–102.
- [5] S. Kim, H. Chang, *Synth. Commun.* **1984**, *14*, 899–904.
- [6] S. Kim, H. Chang, *Bull. Chem. Soc. Jpn.* **1985**, *58*, 3669–3670.
- [7] M. Lissel, J. Weiffen, *Synth. Commun.* **1981**, *11*, 545–549.
- [8] L. Lombardo, *Tetrahedron Lett.* **1984**, *25*, 227–228.
- [9] T. F. Braish, P. L. Fuchs, *Synth. Commun.* **1986**, *16*, 111–115.
- [10] K.-Y. Akiba, Y. Iseki, M. Wada, *Tetrahedron Lett.* **1982**, *38*, 3935–3936.
- [11] K.-Y. Akiba, Y. Iseki, M. Wada, *Bull. Chem. Soc. Jpn.* **1984**, *57*, 1994–1999.
- [12] I. Held, A. Villinger, H. Zipse, *Synthesis* **2005**, 1425–1426.
- [13] I. Held, E. Larionov, C. Bozler, F. Wagner, H. Zipse, *Synthesis* **2009**, *13*, 2267–2277.
- [14] Y. Wei, I. Held, H. Zipse, *Org. Biomol. Chem.* **2006**, *4*, 4223–4230.
- [15] S. Xu, I. Held, B. Kempf, H. Mayr, W. Steglich, H. Zipse, *Chem. Eur. J.* **2005**, *11*, 4751–4757.
- [16] N. D. Rycke, G. Berionni, F. Couty, H. Mayr, R. Goumont, O. R. P. David, *Org. Lett.* **2011**, *13*, 530–533.
- [17] E. Larionov, F. Achrainer, J. Humin, H. Zipse, *ChemCatChem* **2012**, *4*, 559–566.
- [18] M. R. Heinrich, H. S. Klisa, H. Mayr, W. Steglich, H. Zipse, *Angew. Chem. Int. Ed.* **2003**, *42*, 4826–4828.
- [19] C. E. Müller, P. R. Schreiner, *Angew. Chem. Int. Ed.* **2011**, *50*, 6012–6042.
- [20] R. P. Wurz, *Chem. Rev.* **2007**, *107*, 5570–5595.
- [21] J. A. Birrell, J.-N. Desrosiers, E. N. Jacobsen, *J. Am. Chem. Soc.* **2011**, *133*, 13872–13875.
- [22] A. C. Spivey, S. Arseniyadis, *Top. Curr. Chem.* **2009**, *291*, 233–280.
- [23] H. Liang, L. Hu, E. J. Corey, *Org. Lett.* **2011**, *13*, 4120–4123.
- [24] R. D. Crouch, *Tetrahedron* **2004**, *60*, 5833–5871.
- [25] R. D. Crouch, *Synthetic Communications* **2013**, *43*, 2265–2279.
- [26] G. Sartori, R. Ballini, F. Bigi, G. Bosica, R. Maggi, P. Righi, *Chem. Rev.* **2004**, *104*, 199–250.
- [27] G. M. Cooper, R. E. Hausman, *The Cell: A Molecular Approach*, Vol. 6, Sinauer Associates, **2013**.
- [28] D. W. C. MacMillan, *Nature* **2008**, *455*, 304–308.
- [29] C. Grondal, M. Jeanty, D. Enders, *Nature Chemistry* **2010**, *2*, 167–178.
- [30] J. Seayad, B. List, *Org. Biomol. Chem.* **2005**, *3*, 719–724.

- [31] C. Lindner, R. Tandon, B. Maryasin, E. Larionov, H. Zipse, *Beilstein J. Org. Chem.* **2012**, 8, 1406–1442.
- [32] S. W. Smith, G. C. Fu, *J. Am. Chem. Soc.* **2009**, 131, 14231–14233.
- [33] Y. Wei, M. Shi, *Acc. Chem. Res.* **2010**, 43, 1005–1018.
- [34] S. L. Riches, C. Saha, N. F. Filgueira, E. Grange, E. M. McGarrigle, V. K. Aggarwal, *J. Am. Chem. Soc.* **2010**, 132, 7626–7630.
- [35] O. Illa, M. Arshad, A. Ros, E. M. McGarrigle, V. K. Aggarwal, *J. Am. Chem. Soc.* **2010**, 132, 1828–1830.
- [36] W. Steglich, G. Höfle, *Angew. Chem. Int. Ed.* **1969**, 8, 981.
- [37] M. R. Heinrich, H. S. Klisa, H. Mayr, W. Steglich, H. Zipse, *Angew. Chem. Int. Ed.* **2003**, 42, 4826–4828.
- [38] I. Held, S. Xu, H. Zipse, *Synthesis* **2007**, 8, 1185–1196.
- [39] R. Tandon, T. Unzner, T. A. Nigst, N. D. Rycke, P. Mayer, B. Wendt, O. R. P. David, H. Zipse, *Chem. Eur. J.* **2013**, 19, 6435–6442.
- [40] S. E. Denmark, G. L. Beutner, *Angew. Chem. Int. Ed.* **2008**, 47, 1560–1638.
- [41] W. Steglich, G. Höfle, *Tetrahedron Lett.* **1970**, 54, 4727–4730.
- [42] H. Vorbrüggen, *Angew. Chem. Int. Ed. Engl.* **1972**, 11, 305.
- [43] S. Singh, G. Das, O. V. Singh, H. Han, *Tetrahedron Lett.* **2007**, 48, 1983–1986.
- [44] E. J. Corey, C. U. Kim, *J. Org. Chem.* **1973**, 6, 1233–1234.
- [45] S. Hanessian, P. Lavalley, *Can. J. Chem.* **1975**, 53, 2975–2977.
- [46] T. W. Hart, D. A. Metcalfe, F. Scheinman, *J. Chem. Soc., Chem. Commun.* **1979**, 156–157.
- [47] R. F. Cunico, L. Bedell, *J. Org. Chem.* **1980**, 45, 4797–4798.
- [48] A. F. Janzen, G. N. . Lypka, R. E. Wasylishen, *Can. J. Chem.* 58,60(1980). **1980**, 58, 60–64.
- [49] E. J. Corey, H. Oho, C. Ruecker, D. H. Hua, *Tetrahedron Lett.* **1981**, 36, 3455–3458.
- [50] A. R. Bassindale, T. Stout, *Tetrahedron Lett.* **1985**, 26, 3403–3406.
- [51] K. Mai, G. Patil, *J. Org. Chem.* **1986**, 51, 3545–3548.
- [52] C. Moreau, F. Rouessac, J. M. Conia, *Tetrahedron Lett.* **1970**, 40, 3527–3528.
- [53] T. D. Nelson, R. D. Crouch, *Synthesis* **1996**, 9, 1031–1069.
- [54] H. Emde, D. Domsch, H. Feger, U. Frick, A. Goetz, H. H. Hergott, K. Hofmann, W. Kober, K. Kraegeloh, T. Oesterle, W. Steppan, W. West, G. Simchen, *Synthesis* **1982**, 1, 1–26.
- [55] J. R. Bowser, J. F. Bringley, *Synth. React. Inorg. Met.-Org. Chem.* **1985**, 7, 897–905.
- [56] T. P. Mawhinney, M. A. Madson, *J. Org. Chem.* **1982**, 47, 3336–3339.
- [57] K. Sukata, *J. Org. Chem.* **1988**, 53, 4867–4869.
- [58] Y. Tanabe, M. Murakami, K. Kitaichi, Y. Yoshida, *Tetrahedron Lett.* **1994**, 35, 8409–8412.
- [59] S. Pawlenko, *Methoden der Organischen Chemie*, Vol. XIII/5, (Hrsg.: O. Bayer, E. Mueller), Thieme, **1980**.

- [60] G. Simons, M. E. Zandler, E. R. Talaty, *J. Am. Chem. Soc.* **1976**, *24*, 7870–7879.
- [61] R. D. Crouch, *Tetrahedron* **2013**, *69*, 2383–2417.
- [62] Y. Hatanaka, T. Hiyama, *J. Org. Chem.* **1988**, *53*, 918–920.
- [63] S. E. Denmark, R. F. Sweis, *Acc. Chem. Res.* **2002**, *35*, 835–846.
- [64] S. E. Denmark, R. F. Sweis, *J. Am. Chem. Soc.* **2004**, *126*, 4876–4882.
- [65] S. E. Denmark, S. A. Tymonko, *J. Org. Chem.* **2003**, *68*, 9151–9154.
- [66] S. E. Denmark, R. C. Smith, W.-T. T. Chang, J. M. Muhuhi, *J. Am. Chem. Soc.* **2009**, *131*, 3104–3118.
- [67] S. A. Tymonko, R. C. Smith, A. Ambrosi, M. H. Ober, H. Wang, S. E. Denmark, *J. Am. Chem. Soc.* **2015**, *137*, 6200–6218.
- [68] B. Marciniec, *Hydrosilylation: A Comprehensive Review on Recent Advances (Advances in Silicon Science)*, Springer, **2009**.
- [69] M. Pagliaro, R. Ciriminna, V. Pandarus, F. Beland, *Eur. J. Org. Chem.* **2013**, *28*, 6227–6235.
- [70] Y. Nakajima, S. Shimada, *RSC Adv.* **2015**, *5*, 20603–20616.
- [71] C. Cheng, J. F. Hartwig, *J. Am. Chem. Soc.* **2015**, *137*, 592–595.
- [72] B. Li, M. Driess, J. F. Hartwig, *J. Am. Chem. Soc.* **2014**, *136*, 6586–6589.
- [73] P. B. Glaser, T. D. Tilley, *J. Am. Chem. Soc.* **2003**, *125*, 13640–13641.
- [74] M. E. Fasulo, M. C. Lipke, T. D. Tilley, *Chem. Sci.* **2013**, *4*, 3382–3387.
- [75] V. Mandadapu, F. Wu, A. I. Day, *Org. Lett.* **2014**, *16*, 1275–1277.
- [76] A. M. Tondreau, C. C. Hojill, A. K. J. Weller, S. A. Nye, K. M. Lewis, J. G. P. Delis, P. J. Chirik, *Science* **2012**, *335*, 567–570.
- [77] M. D. Greenhalgh, D. J. Frank, S. P. Thomas, *Adv. Synth. Catal.* **2014**, *356*, 584–590.
- [78] A. L. Liberman-Martin, R. G. Bergman, T. D. Tilley, *J. Am. Chem. Soc.* **2015**, *137*, 5328–5331.
- [79] E. Buitrago, L. Zani, H. Adolfsson, *Appl. Organometal. Chem.* **2011**, *25*, 748–752.
- [80] C. Huang, B. Chattopadhyay, V. Gevorgyan, *J. Am. Chem. Soc.* **2011**, *133*, 12406–12409.
- [81] J. F. Hartwig, *Acc. Chem. Res.* **2011**, *45*, 864–873.
- [82] K. K. Ogilvie, E. A. Thompson, M. A. Quilliam, J. B. Westmore, *Tetrahedron Lett.* **1974**, *33*, 2865–2868.
- [83] E. Larionov, M. Mahesh, A. C. Spivey, Y. Wei, H. Zipse, *J. Am. Chem. Soc.* **2012**, *134*, 9390–9399.
- [84] Y. Zhao, J. Rodrigo, A. H. Hoveyda, M. L. Snapper, *Nature* **2006**, *443*, 67–70.
- [85] J. M. Rodrigo, Y. Zhao, A. H. Hoveyda, M. L. Snapper, *Org. Lett.* **2011**, *13*, 3778–3781.
- [86] N. Manville, H. Alite, F. Haeffner, A. H. Hoveyda, M. L. Snapper, *Nature Chemistry* **2013**, *5*, 768–774.
- [87] H. B. Kagan, J. C. Fiaud, *Top. Stereochem.* **1988**, *18*, 249–330.
- [88] E. Vedejs, M. Jure, *Angew. Chem. Int. Ed.* **2005**, *44*, 3974–4001.

- [89] Y. Zhao, A. M. Mitra, A. H. Hoveyda, M. L. Snapper, *Angew. Chem. Int. Ed.* **2007**, *46*, 8471–8474.
- [90] I. Shiina, K. Nakata, Y. Onda, *Eur. J. Org. Chem.* **2008**, 5887–5890.
- [91] S. Rendler, M. Oestreich, *Angew. Chem. Int. Ed.* **2008**, *47*, 248–250.
- [92] I. Shiina, K. Nakata, K. Ono, Y. Onda, M. Itagaki, *J. Am. Chem. Soc.* **2010**, *132*, 11629–11641.
- [93] Z. You, A. H. Hoveyda, M. L. Snapper, *Angew. Chem. Int. Ed.* **2009**, *48*, 547–550.
- [94] A. D. Worthy, X. Sun, K. L. Tan, *J. Am. Chem. Soc.* **2012**, *134*, 7321–7324.
- [95] X. Sun, A. D. Worthy, K. L. Tan, *Angew. Chem. Int. Ed.* **2011**, *50*, 8167–8171.
- [96] C. I. Sheppard, J. L. Taylor, S. L. Wiskur, *Org. Lett.* **2011**, *13*, 3794–3797.
- [97] R. K. Akhani, M. I. Moore, J. G. Pribyl, S. L. Wiskur, *J. Org. Chem.* **2014**, *79*, 2384–2396.
- [98] L. Wang, R. K. Akhani, S. L. Wiskur, *Org. Lett.* **2015**, *17*, 2408–2411.
- [99] S. Rendler, O. Plefka, B. Karatas, G. Auer, R. Froehlich, C. Mück-Lichtenfeld, S. Grimme, M. Oestreich, *Chem. Eur. J.* **2008**, *14*, 11512–11528.
- [100] H. Klare, M. Oestreich, *Angew. Chem. Int. Ed.* **2007**, *46*, 9335–9338.
- [101] S. Rendler, G. Auer, M. Oestreich, *Angew. Chem. Int. Ed.* **2005**, *44*, 7620–7624.
- [102] G. A. Olah, T. Bach, G. K. S. Prakash, *J. Org. Chem.* **1989**, *54*, 3770–3771.
- [103] G. H. Hakimelahi, Z. A. Proba, K. K. Ogilvie, *Tetrahedron Lett.* **1981**, *52*, 5243–5246.
- [104] R. W. Alder, N. C. Goode, N. Miller, *J. Chem. Soc., Chem. Commun.* **1978**, *3*, 89–90.
- [105] M. Baidya, S. Kobayashi, F. Brotzel, U. Schmidhammer, E. Riedle, H. Mayr, *Angew. Chem. Int. Ed.* **2007**, *46*, 6176–6179.
- [106] L. Soovaeli, T. Rodima, L. Kaljurand, A. Kuett, I. Koppel, I. Leito, *Org. Biomol. Chem.* **2006**, *4*, 2100–2105.
- [107] I. T. Ibrahim, A. J. Williams, *J. Chem. Soc., Perkin Trans. 2* **1982**, 1459–1466.
- [108] B. J. Mayer, T. A. Spencer, K. D. Onan, *J. Am. Chem. Soc.* **1984**, *106*, 6342–6348.
- [109] Z. Pawelka, T. Zeegers-Huyskens, *Can. J. Chem.* **2003**, *81*, 1012–1018.
- [110] T. Fujii, H. Nishida, Y. Abiru, M. Yamamoto, M. Kise, *Chem. Pharm. Bull.* **1995**, *43*, 1872–1877.
- [111] N. Virtanen, L. Polari, M. Vällilä, S. Mikkola, *J. Phys. Org. Chem.* **2005**, *18*, 385–397.
- [112] F. Hibbert, K. P. P. Hunte, *J. Chem. Soc., Perkin Trans. 2* **1983**, 1895–1899.
- [113] C. B. Fischer, S. Xu, H. Zipse, *Chem. Eur. J.* **2006**, *12*, 5779–5784.
- [114] C. Lindner, R. Tandon, Y. Liu, B. Maryasin, H. Zipse, *Org. Biomol. Chem.* **2012**, *10*, 3210–3218.
- [115] E. Vedejs, O. Daugulis, L. A. Harper, J. A. MacKay, D. R. Powell, *J. Org. Chem.* **2003**, *68*, 5020–2027.
- [116] T. Watahiki, M. Matsuzaki, T. Oriyama, *Green Chem.* **2003**, *5*, 82–84.
- [117] F. L. Cabirol, A. E. C. Lim, U. Hanefeld, R. A. Sheldon, I. M. Lyapkalo, *J. Org. Chem.* **2007**, *73*, 2446–2449.

- [118] C. Reichardt, *Chem. Rev.* **1994**, 94, 2319–2358.
- [119] V. Gutmann, *Coord. Chem. Rev.* **1976**, 18, 225–255.
- [120] T. Kawabata, W. Muramatsu, T. Nishio, T. Shibata, H. Schedel, *J. Am. Chem. Soc.* **2007**, 129, 12890–12895.
- [121] A. R. Bassindale, T. Stout, *J. Chem. Soc., Perkin Trans. 2* **1986**, 221–225.
- [122] C. Zhang, PhD thesis, LMU München, **2014**.
- [123] J. Lambert, Y. Zhao, S. M. Zhang, *J. Phys. Org. Chem.* **2001**, 14, 370–379.
- [124] C. Chult, R. J. P. Corriu, C. Reye, J. C. Young, *Chem. Rev.* **1993**, 93, 1371–1448.
- [125] A. D. Dilman, L. Ioffe, *Chem. Rev.* **2003**, 103, 733–772.
- [126] M. Arshadi, D. Johnels, U. Edlund, C.-H. Ottosson, D. Cremer, *J. Am. Chem. Soc.* **1996**, 118, 5120–5131.
- [127] C. A. Reed, *Acc. Chem. Res.* **1998**, 6, 325–332.
- [128] S. D. Kinrade, E. W. Deguns, A.-M. E. Gillson, C. T. G. Knight, *Dalton Trans.* **2003**, 3713–3716.
- [129] R. R. Holmes, *Chem. Rev.* **1996**, 96, 927–950.
- [130] C. Hansch, A. Leo, R. W. Taft, *Chem. Rev.* **1991**, 91, 165–195.
- [131] A. Bose, P. Mal, *Tetrahedron Lett.* **2014**, 55, 2154–2156.
- [132] A. Krasovskiy, P. Knochel, *Angew. Chem.* **2004**, 116, 3396–3399.
- [133] L. Friedman, H. Shechter, *J. Org. Chem.* **1961**, 26, 2522–2524.
- [134] C. Lindner, Y. Liu, K. Karaghiosoff, B. Maryasin, H. Zipse, *Chem. Eur. J.* **2013**, 19, 6429–6434.
- [135] X. Liu, J. G. Verkade, *Heteroat. Chem.* **2001**, 12, 21–26.
- [136] K. Yoshida, K. Takao, *Tetrahedron Lett.* **2014**, 55, 6861–6863.
- [137] R. G. Pearson, *J. Am. Chem. Soc.* **1963**, 85, 3533–3539.
- [138] E. Vedejs, X. Chen, *J. Am. Chem. Soc.* **1996**, 118, 1809–1810.
- [139] J. G. Seitzberg, C. Dissing, I. Sotofte, P.-O. Norrby, M. Johannsen, *J. Org. Chem.* **2005**, 70, 8332–8337.
- [140] E. Vedejs, X. Chen, *J. Am. Chem. Soc.* **1997**, 119, 2584–2585.
- [141] C. B. Fischer, S. Xu, H. Zipse, *Chem. Eur. J.* **2006**, 12, 5779–5784.
- [142] P. M. Treichel, D. B. J. Shaw, *Organomet. Chem.* **1977**, 139, 21–30.
- [143] A. Renzetti, N. Koga, H. Nakazawa, *Bull. Chem. Soc. Jpn.* **2014**, 87, 59–68.
- [144] C. S. Chen, Y. Fujimoto, G. Girdaukas, C. J. Sih, *J. Am. Chem. Soc.* **1982**, 104, 7294–7299.
- [145] S. Hoops, S. Sahle, R. G. C. Lee, J. Pahle, N. S. M. Singhal, L. Xu, P. Mendes, U. Kummer, *Bioinformatics* **2006**, 22, 3067–3074.
- [146] H. Mayr, A. Ofial, *Angew. Chem. Int. Ed.* **2006**, 45, 1844–1854.

- [147] T. J. Barton, C. R. Tully, *J. Org. Chem.* **1978**, *43*, 3649–3653.
- [148] E. Larionov, H. Zipse, *WIREs Comput. Mol. Sci.* **2011**, *1*, 601–619.
- [149] C. A. Deakyne, M. Meot-Ner, *J. Phys. Chem.* **1990**, *94*, 232–239.
- [150] Y. Wei, T. Singer, H. Mayr, G. N. Sastry, H. Zipse, *J. Comput. Chem.* **2007**, *130*, 3473–3477.
- [151] Y. Wei, G. N. Sastry, H. Zipse, *J. Am. Chem. Soc.* **2008**, *130*, 3473–3477.
- [152] P. Hommes, C. Fischer, C. Lindner, H. Zipse, H.-U. Reissig, *Angew. Chem. Int. Ed.* **2014**, *53*, 7647–7651.
- [153] R. Tandon, T. A. Nigst, H. Zipse, *Chem. Eur. J.* **2013**, 5423–5430.
- [154] Maestro, version 9.7, Schrödinger, LLC, New York, NY, **2014**.
- [155] B. J. Lynch, P. L. Fast, M. Harris, D. G. Truhlar, *J. Phys. Chem.* **2000**, *104*, 4811–4815.
- [156] M. J. Frisch, G. W. Trucks, H. B. Schlegel, G. E. Scuseria, M. A. Robb, J. R. Cheeseman, J. A. Montgomery, Jr., T. Vreven, K. N. Kudin, J. C. Burant, J. M. Millam, S. S. Iyengar, J. Tomasi, V. Barone, B. Mennucci, M. Cossi, G. Scalmani, N. Rega, G. A. Petersson, H. Nakatsuji, M. Hada, M. Ehara, K. Toyota, R. Fukuda, J. Hasegawa, M. Ishida, T. Nakajima, Y. Honda, O. Kitao, H. Nakai, M. Klene, X. Li, J. E. Knox, H. P. Hratchian, J. B. Cross, V. Bakken, C. Adamo, J. Jaramillo, R. Gomperts, R. E. Stratmann, O. Yazyev, A. J. Austin, R. Cammi, C. Pomelli, J. W. Ochterski, P. Y. Ayala, K. Morokuma, G. A. Voth, P. Salvador, J. J. Dannenberg, V. G. Zakrzewski, S. Dapprich, A. D. Daniels, M. C. Strain, O. Farkas, D. K. Malick, A. D. Rabuck, K. Raghavachari, J. B. Foresman, J. V. Ortiz, Q. Cui, A. G. Baboul, S. Clifford, J. Cioslowski, B. B. Stefanov, G. Liu, A. Liashenko, P. Piskorz, I. Komaromi, R. L. Martin, D. J. Fox, T. Keith, M. A. Al-Laham, C. Y. Peng, A. Nanayakkara, M. Challacombe, P. M. W. Gill, B. Johnson, W. Chen, M. W. Wong, C. Gonzalez, J. A. Pople, Gaussian 03, Revision C.02, Gaussian, Inc., Wallingford, CT, **2004**.
- [157] J. Tomasi, B. Mennucci, R. Cammi, *Chem. Rev.* **2005**, *105*, 2999–3093.
- [158] H.-J. Schneider, *Angew. Chem. Int. Ed.* **2009**, *48*, 3924–3977.
- [159] X. Shu, J. Fan, J. Li, X. Wang, W. Chen, X. Jia, C. Li, *Org. Biomol. Chem.* **2012**, *10*, 3393–3397.
- [160] F. London, *Trans. Faraday Soc.* **1937**, *33*, 8–26.
- [161] K. E. Riley, M. Pitonak, P. Jurecka, P. Hobza, *Chem. Rev.* **2010**, *110*, 5023–5063.
- [162] S. Grimme, P. R. Schreiner, *Angew. Chem. Int. Ed.* **2011**, *50*, 12639–12642.
- [163] J. Haslmayr, T. Renger, *J. Chem. Phys.* **2013**, *139*, 044103.
- [164] P. Lazar, F. Karlicky, P. Jurecka, M. Kocman, E. Otyepkova, K. Safarova, M. Otyepka, *J. Am. Chem. Soc.* **2013**, *135*, 6372–6377.
- [165] J. R. Premkumar, D. Umadevi, N. Sastry, *Indian J. Chem.* **2014**, *53A*, 985–991.
- [166] T. Risthaus, S. Grimme, *J. Chem. Theory Comput.* **2013**, *9*, 1580–1591.
- [167] E. Lyngvi, I. A. Sanhueza, F. Schoenebeck, *Organometallics* **2015**, *34*, 805–812.
- [168] A. V. Marenich, C. J. Cramer, D. G. Truhlar, *J. Phys. Chem. B* **2009**, *113*, 6378–6396.
- [169] A. Tkatchenko, R. A. D. Jr., M. Head-Gordon, M. Scheffler, *J. Chem. Phys.* **2009**, *131*, 094106.

- [170] A. Fischli, *Helv. Chim. Acta* **1979**, 62, 882–893.
- [171] A. R. Katritzky, M. L. Lopez-Rodriguez, J. G. Keay, R. W. King, *J. Chem. Soc., Perkin Trans. 2* **1985**, 165–170.
- [172] T. Werner, A. G. M. Barrett, *J. Org. Chem.* **2006**, 71, 4302–4304.
- [173] K. Lam, I. E. Marko, *Org. Lett.* **2011**, 13, 406–409.
- [174] E. D. Skakovskii, S. A. Lamotkin, S. I. Shpak, L. Y. Tychinskaya, O. A. Gaidukevich, A. I. Lamotkin, *J. Appl. Spectrosc.* **2006**, 73, 275–279.
- [175] E. M. Kaiser, R. A. Woodruff, *J. Org. Chem.* **1970**, 35, 1198–1199.
- [176] M. Päviö, D. Mavrynsky, R. Leino, L. T. Kanerva, *Eur. J. Org. Chem* **2011**, 8, 1452–1457.
- [177] S. V. Slungard, T.-A. Krakeli, T. H. K. Thvedt, E. Fuglseth, E. Sundby, B. H. Hoff, *Tetrahedron* **2011**, 67, 5642–5650.
- [178] A. D. P. M. Espindola, R. Crouch, J. R. D. Bergh, J. M. Ready, J. B. MacMillan, *J. Am. Chem. Soc.* **2009**, 131, 15995–15995.
- [179] M. Hatano, Y. Furuya, T. Shimmura, K. M. amd S. Kamiya, T. Maki, K. Ishihara, *Org. Lett.* **2011**, 13, 426–429.
- [180] V. Diemer, H. Chaumeil, A. Defoin, *Eur. J. Org. Chem* **2006**, 12, 2727–2738.